

# ResearchOnline@JCU

This file is part of the following reference:

**Wormald, Peter John (1993) *Geology of the Mt. Leyshon gold deposit, Australia: a study of breccia pipe formation, facies and brecciation mechanisms*. PhD thesis, James Cook University of North Queensland.**

Access to this file is available from:

**<http://researchonline.jcu.edu.au/47307/>**

*If you believe that this work constitutes a copyright infringement, please contact*  
*[ResearchOnline@jcu.edu.au](mailto:ResearchOnline@jcu.edu.au) and quote*  
**<http://researchonline.jcu.edu.au/47307/>**

Geology of the Mt. Leyshon gold deposit, Australia : A  
study of breccia pipe formation, facies and brecciation  
mechanisms

Thesis submitted by

Peter John WORMALD BSc (Hons) Kingston, London

in August 1993

For the degree of Doctor of Philosophy in the Department of Geology  
at James Cook University.

## DECLARATION

I declare that this thesis is my own work and has not been submitted in any form for another degree or diploma at any university or other institution of tertiary education. Information derived from the published or unpublished work of others has been acknowledged in the text and a list of references is given.

P J Wormald

23 August 1993

I, the undersigned, the author of this thesis, understand that the following restriction placed by me on access to this thesis will not extend beyond three years from the date on which the thesis is submitted to the University.

I wish to place restriction on access to this thesis as follows:

Access not to be permitted for a period of two (2) years.

After this period has elapsed I understand that James Cook University of North Queensland will make it available for use within the University Library and, by microfilm or other photograph means, allow access to users in other approved libraries. All users consulting this thesis will have to sign the following statement:

“In consulting this thesis I agree not to copy or closely paraphrase it in whole or in part without the written consent of the author; and to make proper written acknowledgement for any assistance which I have obtained from it.”

(signature)

23<sup>rd</sup> August 1993.

(date)

## Abstract

The facies architecture of the Mt. Leyshon breccia complex is reinterpreted as a subvolcanic intrusive breccia and igneous complex. The main pipe breccia defines the margins of the complex, which also contains a number of smaller breccia pipes and dykes, associated with porphyritic intrusives. The grossly rhombohedral shaped main pipe breccia has antler-like geometries with inter-fingering, intrusive host rock contacts. The faulted granite-metasediment contact, controlled the location of the complex within a regional wrench system.

The main pipe breccia is composed of distinctive fine and coarse variants with steeply dipping, gradational contacts. Localised zones of accretionary pellets are interpreted to result from particle accretion during brecciation and gaseous fluid transfer, and are therefore not necessarily diagnostic of pyroclastic lithologies. A juvenile igneous component has not been identified, although the rare presence of cognate igneous fragments suggest the prior existence of a magma system.

An interactive period followed, where smaller breccia bodies are characterised by the presence of cognate and juvenile igneous fragments and the digestion of a fragmental component by the magma. The Mt. Leyshon breccia pipe (the main gold-bearing unit) formed first, followed closely by emplacement of the fragmental component of porphyry unit II, the Mt. Hope breccia, and felsic igneous intrusions (porphyry unit II-IV). The latter partly engulfs and reworks the last two breccia units. Finally, late breccia bodies formed as steeply and gently dipping units containing abundant cognate and juvenile igneous particles (tuffsite breccia dykes and late breccia dykes).

The mobile/transported components of breccia units have characteristics suggesting forceful injection into host rocks. No unambiguous evidence for pyroclastic lithologies exists, nor is there evidence that the complex vented. Facies characteristics suggest the main pipe breccia resulted from prolonged mobilisation and upwards transport of fragments in the presence of a gaseous fluid phase, combined with pervasive host rock extension of basement. Subsequent pipe forming events have characteristics dominantly suggesting processes of localised host rock extension, in conjunction with minor to moderate gaseous fluid release. Strike slip reactivation of ductile basement structures is implicated in brittle extension in the complex. Facies characteristics of the final breccia dykes suggest they resulted from processes of prolonged fragment mobility/transport, as a consequence of gaseous fluid release.

Four main episodes of igneous emplacement, breccia generation and hydrothermal evolution are defined by the geological and paragenetic studies on the Mt. Leyshon breccia complex. In the first episode, extensional quartz veins formed in host rock and emplacement of a magmatic system at depth probably contributed to main pipe breccia formation. Episode II began with argillic I alteration of the main pipe breccia, suggesting a significant time interval between breccia formation and high temperature fluid flow resulting in later potassic and propylitic alteration. In the latter part of episode II, the emplacement of intermediate then felsic dykes preceded sericitic I alteration and quartz-molybdenite vein formation.

Repeated breccia formation and (intermediate and felsic) igneous emplacement, beginning with the Mt. Leyshon breccia, characterises episode III (interactive magma/breccia sequence). Argillic II alteration affecting the episode III sequence, suggests a time break between rock unit formation and high temperature (episode IV) fluid flow through vein and fault style re-brecciation of rock, in the absence of igneous emplacement. The bulk of gold mineralisation in the Mt. Leyshon ore body, is concentrated within re-break zones (secondary porosity) in breccia cavities and veins.

The breccia pipe is divided into six facies, based on fragmentation characteristics, the proportion of mixed fragment zones and fragment types. The six facies are interpreted to reflect variations in three fundamental mechanisms of pipe formation: (1) Host rock fragmentation. (2) Host rock expansion. (3) Fragment transport/mobility. Facies characteristics suggest the presence of a fluid phase during brecciation.

A pre-pipe host rock stratigraphy is defined by variably *in situ* fragmented host rock and change of dominant fragment type. Portions of the pipe dominated by fragmentation progressions are merely *in situ* fragmented host rock, and probably formed by fault induced fragmentation. Regions of the pipe dominated by jigsaw fit textures and highly expanded fragments in matrix indicate horizontal and vertical extension of the host rock during pipe formation. As the degree of host rock fragmentation, expansion and transport/mobility increases in a given portion of the pipe, jigsaw fit textures and mixed fragment zones become dominant over fragmentation progressions reflecting stages in the progressive evolution of the breccia pipe. Zones of fragment transport occur in narrow regions of maximum extension throughout the pipe and in a steeply dipping irregular region at the northern end of the pipe; the probable focus of fluid release.

An early association of magma with the main pipe is implied by cognate igneous fragments within the main pipe breccia. Subsequent, early igneous intrusion was associated with relatively closed system behaviour (culminating in quartz-molybdenite mineralisation). In a later interactive period of tectonically induced extension, intrusion of igneous bodies were genetically related to and partially consumed breccia units. Current models for magmatic evolution associated with porphyry-style (Cu, Au) mineralised systems require modification to reflect this more realistic geologic situation.

The magnetite bearing Mt. Leyshon igneous units are divided into a felsic and intermediate group based on petrography and geochemistry. A late stage petrogenetic model for the Mt. Leyshon igneous units, proposes fractional crystallisation of the observed phenocryst phases controlled their evolution. Periodic input of more basic magma into the system occurred, inducing minor magma mingling (implying volatile transfer), and during extension, resulted in periodic igneous emplacement and volatile loss into the Mt. Leyshon complex.

Brecciation in the Mt. Leyshon complex is related to a repeated magmatic cycle: (1) Recharge of more basic magma and volatile transfer to the felsic magma system. (2) Fractionation to felsic magma compositions. (3) Intrusive breccia generation during vapour release. The Mt. Leyshon

igneous rocks have characteristics (e.g. K-feldspar megacrysts in felsic units genetically related to brecciation) implying they were not saturated with an aqueous fluid phase at the time of emplacement. Instead, a vapour phase with significant non-aqueous species (CO<sub>2</sub>, HCl, SO<sub>2</sub>, etc.) is favoured for brecciation.

Wide variation in breccia types can be produced by changing the rate and duration of structural, fluid phase and magmatic processes. A dynamic model for the Mt. Leyshon breccia complex proposes five breccia forming events linked to four geological cycles. Brecciation results from variable coupling of: (1) Brittle host rock extension, interpreted to result from seismic rupture perturbation at dilational strike slip fault irregularities, as a consequence of the earthquake (crustal/fluid pressure) cycle. (2) Vapour evolution as a consequence of periodic recharge of basic magma and vapour, combined with fractional crystallisation. (3) Explosively driven hydrofracture as a consequence of rapid magmatic vapour decompression (first boiling), evolving to time dependent vapour discharge, and as a result, fragment transport/mobilisation in breccia pipes and dykes. (4) Fluid redistribution in conjunction with after shock activity.

The Mt. Leyshon breccia complex records the passage of a magmatic system through the upper crust during transcurrent faulting. Three general mechanisms of brecciation are envisaged within this time-space framework: (1) Tectonic extension dominant (eg. main pipe, and Mt. Leyshon breccias). (2) Magma recharge and vapour evolution dominant (e.g. tuffsite breccia dykes). (3) A complex regime where both mechanisms interact (e.g. "porphyry" unit II).

Gold mineralisation postdates all coeval igneous emplacement and occurs late in the hydrothermal evolution. Gold occurs in three principal sites within the host rocks: (1) Primary porosity reflecting the breccia characteristics. (2) Secondary porosity resulting from re-break zones cutting across rock units. (3) Tertiary porosity resulting from dissolution of rock and alteration minerals. The characteristics of the ore body (geometry, timing and gold distribution) suggest gold mineralisation was controlled by fault reactivation under high fluid pressure conditions.

The steeply dipping and bulbous geometry of the Mt. Leyshon ore body is consistent with control by the irregular nature of porosity and permeability on gold deposition. At lower levels the ore body consists of linear NE and SE trending en-echelon segments; interpreted to result from movement on strike slip faults. Upper levels of the ore body are expanded, probably resulting from an upward branching fault geometry and/or rheological contrast between host rocks to the ore body.

These characteristics suggest that at the regional scale the Mt. Leyshon ore body was controlled by secondary porosity, resulting from the intersection of strike slip fault segments linked to the Mt. Leyshon and Mt. Dean corridors. The geological model suggests hydrothermal fluid evolution resulted from complex mixing of diffusing fluid into dilated regions of the complex, with trapped magmatic vapour released during after shocks.

## Acknowledgements

This project was made possible through the conviction of Ian Hodgkinson and Tom Orr of Mt. Leyshon Gold Mines Ltd. I am particularly grateful for their encouragement and assistance with many aspects of the study.

The thesis was supervised by Associate Professor Roger Taylor and Dr John Wright. I would like to thank Roger for encouraging me to come to Australia in the first place, and his friendship and advice during the project. John is thanked for his ideas and direction at the outset of the project. His enthusiastic support as the project progressed and work on thesis drafts are especially appreciated.

Mt. Leyshon Gold Mines Ltd. of the Normandy-Poseidon Group is thanked for providing a three year scholarship, technical support, and access to mine data. The receipt of a partial W C Lacy Scholarship from the department of Geology, James Cook University is also acknowledged. A portion of the analytical expenses for this thesis were provided by the World Gold '88 Endowment Fund.

Several people were of great help with the project: Liz Coumbis, Glen Mennie and Sandy Thomson, for drafting figures; the staff of the James Cook University photography unit; Peter Whitehead for frequent computer assistance; Rocio Andrews for typing some references; technical and administrative staff of the Geology department for their support. A number of people are thanked for comments on draft chapters in this thesis: Pat Williams, Neil Adshead, Paul Gamson, Kaylene Camuti, Gordon Saul and Neil Phillips. Discussion with Bill Laing on structural mapping and data analysis is also appreciated.

Life saving assistance with final thesis preparation from my friends, especially Geoffrey De Jong, Bill Harmsworth, Shirley Sorokin and Randi Larsen is greatly appreciated. The support and friendship of Hiromi Shigehara will always be remembered. A special thanks to my friends David and Rocio Andrews for their kind support in difficult times.

*Abstract**Acknowledgements**List of Figures**List of plates**List of Tables*

## CHAPTER 1

## INTRODUCTION

1.1 Regional setting	1
1.2 Background	1
1.3 Aims	3
1.4 Approach	3

## CHAPTER 2

## GEOLOGY AND FACIES ARCHITECTURE OF THE MT. LEYSHON BRECCIA COMPLEX

2.1 Introduction	5
2.2 Facies characteristics of the Mt. Leyshon breccia complex	6
2.2.1 Basement units	6
2.2.2 Main pipe breccia	8
2.2.3 Interactive magma / breccia sequence	9
2.2.3.1 Breccia units	9
2.2.3.2 Igneous units of the Mt. Leyshon breccia complex	12
2.3 Time relationships between the facies of the Mt. Leyshon complex	15
2.4 Discussion of facies relationships in the Mt. Leyshon breccia complex	15
2.4.1 Implications of the basement / main pipe breccia relationships	16
2.4.2 Magma / breccia interaction: evidence for breccia generation during igneous emplacement	20
2.4.3 A facies model for the Mt. Leyshon breccia complex	25

## CHAPTER 3

## STRUCTURAL SETTING OF THE MT. LEYSHON BRECCIA COMPLEX

3.1 Introduction	37
3.2 Regional structural framework	38
3.3 Structural elements of the Mt. Leyshon breccia complex	39
3.3.1 Pre-complex structures	39
3.3.2 Early syn-complex structures	41
3.3.3 Later syn-complex structures	43
3.3.4 Post-Mt. Leyshon breccia structures	45
3.4 Preferred orientation of breccia and igneous facies	48

3.4.1 Breccia units	48
3.4.2 Igneous units	49
3.5 Rheological control on brecciation	50
3.6 The structural development of the Mt. Leyshon breccia complex	50
3.6.1 Early basement structural history	51
3.6.2 Late Palaeozoic to Mesozoic history	52
3.6.3. Summary structural model	59

## CHAPTER 4

### MINERAL PARAGENESIS AND HYDROTHERMAL ALTERATION STUDIES OF THE MT. LEYSHON ORE BODY

4.1 Introduction	67
4.2 Stages of alteration and mineralisation within the Mt. Leyshon breccia complex	69
4.2.1 Pre-main pipe breccia veins (Episode I, stage I)	69
4.2.2 Pre-Mt. Leyshon breccia alteration (episode II)	70
4.2.3 Post-Mt. Leyshon breccia alteration (episode III)	72
4.2.4 Alteration and mineralisation within igneous units	78
4.3 Clay alteration in the Mt. Leyshon complex	80
4.4 Spatial distribution of alteration types	80
4.5 Problems with interpretation of the Mt. Leyshon hydrothermal system	82
4.6 Integrated paragenesis of igneous emplacement, breccia formation and hydrothermal evolution in the Mt. Leyshon breccia complex	85

## CHAPTER 5

### FACIES ANALYSIS OF THE MT. LEYSHON BRECCIA PIPE

5.1 Introduction	95
5.2 Methodology	96
5.2.1 Open cut investigation	96
5.2.2 Graphic analysis system for the subvolcanic environment	97
5.3 Facies characteristics of the Mt. Leyshon breccia pipe	98
5.3.1 Fragment size variation	98
5.3.2 Fragment types and degree of mixing	98
5.3.3 Fragment shape and matrix proportion	99
5.3.4 Fragmentation characteristics	100
5.4 Facies and facies geometry of the Mt. Leyshon breccia pipe	101
5.5 Interpretation of breccia facies characteristics and facies distribution in the Mt. Leyshon pipe	104
5.6 Facies model for the Mt. Leyshon breccia pipe	109

## CHAPTER 6

### PETROGRAPHIC AND GEOCHEMICAL CHARACTERISTICS OF THE MT.

#### LEYSHON IGNEOUS ROCKS

6.1 Introduction	119
6.2 The Mt. Leyshon igneous rocks	121
6.2.1 Petrography of the Mt. Leyshon igneous rocks	121
6.2.2 Chemical effects of the post-crystallisation changes	124
6.3 The regional igneous units	128
6.3.1 Field and petrographic relationships of the regional igneous units	128
6.4 Chemical Analyses	129
6.4.1 Major elements	129
6.4.2 Trace elements	129
6.5 Classification of the Mt. Leyshon igneous rocks	130
6.6 A comparison of the Mt. Leyshon and regional igneous rocks	131
6.7 Petrogenesis of the Permo-Carboniferous igneous rocks	133
6.7.1 Petrogenesis of the Mt. Leyshon Igneous Rocks	133
6.7.2 Petrogenesis of the regional igneous rocks	135
6.7.3 Towards a trace element model for Mt. Leyshon igneous rocks	136
6.8 Summary	138

## CHAPTER 7

### BRECCIA MECHANISMS AND MAGMATIC PROCESSES WITHIN THE MT.

#### LEYSHON BRECCIA COMPLEX

7.1 Introduction	141
7.2 Regional crustal setting and evidence for depth of emplacement	141
7.3 The role of structure in breccia complex formation	143
7.3.1 The role of structure in brecciation	143
7.3.2 The role of structure in igneous emplacement	148
7.4 The role of a fluid phase in brecciation	149
7.4.1 Source and nature of the fluid phase	150
7.4.2 Non-explosive processes resulting from high fluid and magma pressure	151
7.4.3 Explosively driven hydrofracture and time dependent gas discharge	153
7.5 The role of the magmatic system in brecciation	158
7.5.1 Geologic constraints on physical processes in the magmatic system	158
7.5.2 Volatiles in the magmatic system	160
7.6 Discussion of brecciation mechanisms	166
7.7 A dynamic model for breccia complex formation	168

## CHAPTER 6

### PETROGRAPHIC AND GEOCHEMICAL CHARACTERISTICS OF THE MT.

#### LEYSHON IGNEOUS ROCKS

6.1 Introduction	119
6.2 The Mt. Leyshon igneous rocks	121
6.2.1 Petrography of the Mt. Leyshon igneous rocks	121
6.2.2 Chemical effects of the post-crystallisation changes	124
6.3 The regional igneous units	128
6.3.1 Field and petrographic relationships of the regional igneous units	128
6.4 Chemical Analyses	129
6.4.1 Major elements	129
6.4.2 Trace elements	129
6.5 Classification of the Mt. Leyshon igneous rocks	130
6.6 A comparison of the Mt. Leyshon and regional igneous rocks	131
6.7 Petrogenesis of the Permo-Carboniferous igneous rocks	133
6.7.1 Petrogenesis of the Mt. Leyshon Igneous Rocks	133
6.7.2 Petrogenesis of the regional igneous rocks	135
6.7.3 Towards a trace element model for Mt. Leyshon igneous rocks	136
6.8 Summary	138

## CHAPTER 7

### BRECCIA MECHANISMS AND MAGMATIC PROCESSES WITHIN THE MT.

#### LEYSHON BRECCIA COMPLEX

7.1 Introduction	141
7.2 Regional crustal setting and evidence for depth of emplacement	141
7.3 The role of structure in breccia complex formation	143
7.3.1 The role of structure in brecciation	143
7.3.2 The role of structure in igneous emplacement	148
7.4 The role of a fluid phase in brecciation	149
7.4.1 Source and nature of the fluid phase	150
7.4.2 Non-explosive processes resulting from high fluid and magma pressure	151
7.4.3 Explosively driven hydrofracture and time dependent gas discharge	153
7.5 The role of the magmatic system in brecciation	158
7.5.1 Geologic constraints on physical processes in the magmatic system	158
7.5.2 Volatiles in the magmatic system	160
7.6 Discussion of brecciation mechanisms	166
7.7 A dynamic model for breccia complex formation	168

## CHAPTER 8

### GOLD DISTRIBUTION AND CONTROLS IN THE MT. LEYSHON BRECCIA COMPLEX

8.1 Introduction	171
8.2 Distribution of gold mineralisation	172
8.3 Geometry of gold bearing zones and relationship to facies distribution	174
8.4 Structural control on gold mineralisation	175
8.5 Implications of the dynamic geological model for gold mineralisation	176
8.6 Model for gold mineralisation at Mt. Leyshon	177

## CHAPTER 9

### CONCLUSIONS

9.1 Facies model of an intrusive breccia and igneous complex	181
9.2 Structural setting of the breccia complex	182
9.3 Integrated geologic and hydrothermal fluid evolution	183
9.4 Facies model of the Mt. Leyshon breccia pipe	183
9.5 Evolution of the magmatic system	184
9.6 Breccia mechanisms	185
9.7 Model for gold mineralisation	186
9.8 Recommendations for future work	187

REFERENCES	189
------------	-----

### APPENDICES

following 201

Appendix 1: Selected microprobe mineral analyses

Appendix 2: Geochemical analysis of the Mt. Leyshon igneous rocks

Appendix 3: CIPW norm data

Appendix 4: Igneous unit geochemistry expressed as atomic %

Appendix 5: Regional unit analyses

Appendix 6: Methods appendix

Appendix 7: Sample catalogue

### ENCLOSURES

Enclosure 1: Geological map of the Mt. Leyshon breccia complex

Enclosure 2-5: Graphic analysis of the Mt. Leyshon breccia pipe (sections 5800 N, 5925 N, 6025 N and 6125 N).

## LIST OF FIGURES

Following page no.

Figure 1.1a: Regional geological setting of the Mt. Leyshon breccia complex.	2
Figure 1.1b: Main structural elements of NE Queensland.	3
Figure 2.1: Geological map of the Mt. Leyshon breccia complex.	6
Figure 2.2a: Lithofacies geometry (plan) in the Mt. Leyshon breccia complex.	8
Figure 2.2b: Lithofacies geometry (section) in the Mt. Leyshon breccia complex.	8
Figure 2.3: Facies relationships of the Mt. Leyshon igneous units.	14
Figure 2.4: Facies timing within the Mt. Leyshon breccia complex.	16
Figure 2.5: Derivative map to illustrate the sequential development of the main components within the Mt. Leyshon breccia complex.	18
Figure 2.6: Facies model for the Mt. Leyshon breccia complex (lithofacies cross section).	26
Figure 3.1: Regional aerial linear pattern around the Mt. Leyshon breccia complex.	38
Figure 3.2: Structure of the Mt. Leyshon breccia complex.	40
Figure 3.3: Poles to bedding/cleavage orientations in metasediment.	42
Figure 3.4: Inter-breccia shear zone near the western margin of the Mt. Leyshon breccia pipe (line drawing of Plate 3.7).	62
Figure 3.5: Trend of dyke, vein and small scale brecciation directions in the Mt. Leyshon breccia complex.	44
Figure 3.6: Movement lineations on fault surfaces in the Mt. Leyshon breccia complex.	46
Figure 3.7: Rebrecciation zone at late dyke /main pipe breccia contact (line drawing of Plate 3.13).	66
Figure 3.8: Fault orientations within Mt. Leyshon breccia complex.	48
Figure 3.9: Joint orientations within basement, main pipe breccia and igneous units of the main pipe breccia.	50
Figure 3.10: Structural evolution of the Mt. Leyshon breccia complex.	56
Figure 4.1: Textural evidence for the paragenesis of pre-Mt. Leyshon breccia alteration.	70
Figure 4.2: Textural evidence for the paragenesis of post-Mt. Leyshon breccia alteration.	72
Figure 4.3: Large scale distribution of major alteration events in the Mt. Leyshon breccia complex.	80
Figure 4.4: Integrated paragenesis of igneous emplacement, breccia generation and hydrothermal evolution.	86
Figure 5.1: Explanation of the graphic logging system.	96

Figure 5.2: Location of drill holes used for graphic logging.	98
Figure 5.3: Cross-sections through the Mt. Leyshon breccia pipe.	102
Figure 5.4: Plans through the Mt. Leyshon breccia pipe.	104
Figure 5.5: Subdivision of the Mt. Leyshon breccia pipe based of the relative proportions of three facies characteristics.	106
Figure 5.6: Simplified breccia facies of the Mt. Leyshon breccia pipe.	106
Figure 5.7: Isometric view of the Mt. Leyshon breccia pipe (100-480 RL).	108
Figure 5.8: Isometric geometry of the Mt. Leyshon breccia pipe facies.	108
Figure 5.9: Facies model for the Mt. Leyshon breccia pipe depicted as a cross-section.	110
Figure 6.1: Total alkali versus silica diagram for the Mt. Leyshon and regional igneous rocks.	122
Figure 6.2: Alteration effects on the chemistry of the Mt. Leyshon igneous rocks.	124
Figure 6.3: Selected major element variation diagrams comparing the Mt. Leyshon and regional igneous rocks.	126
Figure 6.4: Zr, Nb and Y characteristics of the Mt. Leyshon and regional igneous rocks.	130
Figure 6.5: SiO <sub>2</sub> versus FeO and FeO/MgO characteristics of the the Mt. Leyshon and regional igneous rocks.	132
Figure 6.6: SiO <sub>2</sub> versus Nb/Y variation diagram comparing the Mt. Leyshon and regional igneous rocks.	132
Figure 6.7: K <sub>2</sub> O versus SiO <sub>2</sub> variation for the Mt. Leyshon and regional igneous rocks.	134
Figure 6.8: Evolution of the concentrations C <sub>1</sub> and C <sub>2</sub> for two elements 1 and 2 having bulk distribution coefficients D <sub>1</sub> and D <sub>2</sub> respectively equal to 5 and 0.1.	138
Figure 6.9: Trace element model for the Mt. Leyshon igneous units.	138
Figure 7.1: Dynamic geological model for the Mt. Leyshon breccia complex.	170
Figure 8.1: Orthographic projection of the Mt. Leyshon ore body.	172
Figure 8.2: Perspective model of the Mt. Leyshon ore body.	174
Figure 8.3: Comparison between gold distribution and breccia facies in the Mt. Leyshon pipe (400 RL).	176
Figure 8.4: Comparison between gold distribution and breccia facies in the Mt. Leyshon pipe (200 RL).	178

LIST OF PLATES	Following page
Plate 2.1: Crackle to rubble breccia texture in a basement rhyolite body.	28
Plate 2.2: Rubble textured metasediment (inside main pipe breccia).	28
Plate 2.3: Main pipe breccia / basement contact in drill core.	28
Plate 2.4: Characteristics of coarse main pipe breccia.	28
Plate 2.5: Characteristics of fine main pipe breccia.	28
Plate 2.6: Cognate felsic igneous fragment in the fine main pipe breccia.	30
Plate 2.7: Rare outcrop contact between coarse and fine variants of the main pipe breccia.	30
Plate 2.8: Common drill core contact between coarse and fine variants of the main pipe breccia.	30
Plate 2.9: Internal form of accretionary structures.	30
Plate 2.10: Porphyry unit IV intruding the Mt. Hope breccia.	30
Plate 2.11: Characteristics of the Mt. Hope breccia.	32
Plate 2.12: Fine tuffisite breccia dyke intruding Mt. Leyshon breccia.	32
Plate 2.13: Tuffisite breccia dyke characteristics (coarse and fine variants).	32
Plate 2.14: Weakly altered fine tuffisite dyke.	32
Plate 2.15: Typical late breccia dyke.	32
Plate 2.16: Time relations between Mt. Leyshon breccia and porphyry unit II-IV	34
Plate 2.17: Porphyry unit II intruding crackle brecciated metasediment in outcrop.	34
Plate 2.18: Porphyry unit II outcropping in the main igneous centre.	34
Plate 2.19: Local matrix rich zone of a late breccia dyke.	36
Plate 2.20: Porphyry unit IV networks invading porphyry unit III.	36
Plate 2.21: False-pyroclastic textures in altered porphyry unit IV.	36
Plate 3.1: Bedding and cleavage in crackle brecciated metasediment within the breccia complex.	36
Plate 3.2: North trending mylonite zone deforming metasediment at the margin of the complex.	36
Plate 3.3: Intense zone of penetrative cleavage in a ductile fault zone.	36
Plate 3.4: Fault and fracture mesh in metasediment block inside the main pipe breccia.	60
Plate 3.5: Crackle brecciated metasediment subparallel to cleavage.	60
Plate 3.6: Quartz-molybdenite vein cutting basement rhyolite.	60
Plate 3.7: Inter-breccia shear zone.	62
Plate 3.8: Oblique-slip normal fault zone in metasediment.	64
Plate 3.9: Sharp contact of the Mt. Leyshon breccia and marginal crush zone.	64
Plate 3.10: En-echelon extensional shear (chlorite-pyrite) veins cutting a granite fragment in the Mt. Leyshon breccia.	64
Plate 3.11: Linear zone of calcite cemented extensional fault breccia, cutting the Mt. Leyshon breccia.	64

Plate 3.12: Late strike slip fault cutting main pipe breccia.	64
Plate 3.13: Rebrecciation zone developed at late dyke / main pipe breccia contact.	66
Plate 3.14: Late strike-slip fault zone reactivating the margin of a vein.	64
Plate 4.1: Transition from argillic I alteration to potassic alteration in main pipe breccia.	88
Plate 4.2: Propylitic I alteration overprinting argillic I alteration in main pipe breccia.	88
Plate 4.3: Potassic alteration overprinting argillic I alteration in main pipe breccia.	88
Plate 4.4: Main pipe breccia, close-up of Plate 4.3.	88
Plate 4.5: Main pipe breccia, biotite alteration of breccia fragments and matrix.	88
Plate 4.6: Main pipe breccia. Quartz-molybdenite veins crosscutting sericitic I alteration.	88
Plate 4.7: Mt. Leyshon breccia. Contact between fragmental component and main pipe breccia block.	90
Plate 4.8: Fine tuffisite breccia dyke, weakly altered.	90
Plate 4.9: Re-brecciation zone in fine tuffisite breccia dyke (shown in Plate 4.8).	90
Plate 4.10: Mt. Leyshon breccia, weakly altered.	90
Plate 4.11: Infill sequence in the Mt. Leyshon breccia.	90
Plate 4.12: Infill sequence in the Mt. Leyshon breccia.	92
Plate 4.13: Infill sequence in a microcavity in a tuffisite breccia dyke.	92
Plate 4.14: Sequential rebrecciation of the Mt. Leyshon breccia.	92
Plate 4.15: Large gold grains in a Mt. Leyshon breccia cavity.	92
Plate 4.16: Large gold grains in high grade vein (shown in Plate 8.1).	92
Plate 4.17: Small gold inclusion within pyrite grain in a Mt. Leyshon breccia cavity.	94
Plate 4.18: Infilled cavities in highly altered porphyry unit IV (mine porphyry).	94
Plate 5.1: Zone 1, Mt. Leyshon breccia - partially fragmented main pipe breccia.	94
Plate 5.2: Zone 2A, Mt. Leyshon breccia, intact host rock block in breccia.	94
Plate 5.3: Zone 2B, Mt. Leyshon breccia.	112
Plate 5.4: Zone 2B, Mt. Leyshon breccia (close-up of Plate 5.3).	112
Plate 5.5: Zone 3, Mt. Leyshon breccia.	112
Plate 5.6: Zone 3, Mt. Leyshon breccia - abundant jigsaw fit textures.	114
Plate 5.7: Zone 4A, Mt. Leyshon breccia - well packed polymict breccia.	114
Plate 5.8: Zone 4A, Mt. Leyshon breccia.	114
Plate 5.9: Small scale dilational region (zone 4A), Mt. Leyshon breccia.	116
Plate 5.10: Contact between zone 4A and zone 3, Mt. Leyshon breccia.	116

Plate 5.11: High matrix zone in transitional region between zones 4A and 3 (close-up of Plate 5.10).	116
Plate 5.12: Well developed high matrix zone in drill core, Mt. Leyshon breccia.	118
Plate 5.13: Fragmentation progressions in Mt. Leyshon breccia, Zone 2B.	118
Plate 6.1: Intermediate igneous unit (porphyry unit I).	140
Plate 6.2: Felsic igneous unit (2-2 dyke).	140
Plate 6.3: Broken K-feldspar xenocryst in enclave bearing zone of porphyry unit I (detail of Plate 6.1).	140
Plate 6.4: Felsic igneous unit (Porphyry unit IV).	140
Plate 6.5: Felsic igneous unit (1-2 dyke).	140
Plate 6.6: Granophyric patches and acicular apatite needles in microgranitoid enclave.	140
Plate 6.7: Petrographic texture of basalt dyke.	179
Plate 8.1: Polymetallic (sp-cpy-ga-gold) vein cutting DG dyke within Mt. Leyshon breccia pipe.	179
Plate 8.2: Scanning electron microscope image of gold particles on a pyrite grain in fine tuffisite breccia dyke.	179
Plate 8.3: Detail of composite gold/illite particle inside pocket on pyrite surface shown in Plate 8.2.	179

## LIST OF TABLES

Following page no.

Table 2.1: Facies characteristics of the Mt. Leyshon breccia units.	10
Table 2.2: Facies characteristics of the Mt. Leyshon igneous units.	12
Table 3.1: Structural elements of the Mt. Leyshon breccia complex.	52
Table 4.1: Mineral paragenesis stages of the Mt. Leyshon hydrothermal system.	68
Table 4.2: Mineralogical and textural changes to the Mt. Leyshon igneous rocks.	78
Table 5.1: Internal facies characteristics of the Mt. Leyshon breccia pipe.	100
Table 6.1: Petrography of the Mt. Leyshon igneous rocks.	120
Table 6.2: Classification of the Mt. Leyshon igneous rocks.	page 131
Table 7.1: Brecciation processes in the Mt. Leyshon breccia complex.	164

# Chapter 1

## INTRODUCTION

---

This project is primarily an investigation of the geology and genesis of the Mt. Leyshon breccia complex, a multiphase intrusive system hosting the Mt. Leyshon gold mine (Australia). As a consequence of the detailed geologic investigations undertaken in this thesis, this study also has implications for breccia forming mechanisms and magmatic processes in actively deforming upper crust.

### 1.1 REGIONAL SETTING

The Mt. Leyshon complex, hosting one of two world class breccia-hosted gold deposits in North Queensland, is situated approximately 25 kilometres south of Charters Towers, near the western edge of the New England Fold Belt (Figure 1.1a; Johnson and Henderson, 1991). The Mt. Leyshon mine has a published resource of 40.01 Mt at 1.73 g/t gold (at a 0.7 g/t cut-off; company report, June, 1992), associated with poly-metallic mineralisation. The region occurs in the major east-trending Lolworth-Ravenswood (Charters Towers) block (Henderson, 1980; Peters, 1990), predominantly composed of Ordovician to Permian granitoids, and is flanked by the Drummond, Bowen, Galilee and Burdekin basins (Figure 1.1b). The geologic evolution of this area is complex and includes multiple igneous intrusions (Hartley et al., 1989). Meta-volcano-sedimentary inliers, forming part of a Lower Palaeozoic active continental margin extending the full length of eastern Australia (Henderson, 1986), occur within the syn-tectonic to post-tectonic batholithic rocks (Hutton et al., 1990). The breccia complex is located at the contact between one such inlier and the Mt. Leyshon granite (Figure 1.1a), within the Mt. Leyshon Corridor (Figure 3.1; Peters, 1987). There are numerous gold deposits in the area, including Charters Towers, Ravenswood, Pajingo and Mt. Wright (Figure 1.1a). Regional structural aspects are discussed in Chapter 3.

### 1.2 BACKGROUND

Prior to the early 1980s, the Mt. Leyshon area had been extensively explored by several mining companies (Paull et al., 1990), though little was known of the detailed geology. The discovery of a significant reserve by 1983 and subsequent decision to mine in 1986, provided the impetus for several studies on the deposit (Morrison et al., 1987, 1988; Paull et al., 1990). These workers suggested that the Mt. Leyshon complex is the remnants of a high level diatreme which vented at surface with a maar type crater lake. Drill hole data interpreted by mine staff early in 1989 raised doubts on this earlier work. Wright (unpublished report, 1989) further questioned these models which implied the presence of pyroclastic deposits in the succession and the operation of pyroclastic fragmentation processes, and instead suggested hydrothermal brecciation was the dominant mode of fragmentation.

These conflicts arise because the interpretation of fragmental rocks is problematic, particularly in the subvolcanic and ore forming environments, which have been outside the focus of much

sedimentary and volcanic breccia research. Although of restricted aerial extent, breccias occur throughout the geological record and are present in most geological environments (surface, subsurface and mixed subsurface-surface). Present classification and terminology of breccias is confused and in non-sedimentary breccias is largely unsatisfactory.

There are two aspects to the problem of breccia interpretation in the subvolcanic and ore forming environment:

- (1) The interpretation of the fragmental rocks.
- (2) The nature, timing and controls of hydrothermal alteration and mineralisation accompanying the breccias.

Concerning the first aspect, an integral part of this problem is the approach used by breccia researchers in recent times. As pointed out by Laznika (1988), early workers used extensive descriptions and detailed sketches to make interpretations of breccias (eg. Judd, 1873; Geikie, 1902). Subsequent attempts at breccia classification adopted a genetic breccia terminology (Norton, 1917; Reynolds, 1928). Such genetic emphasis on breccia research has persisted and most subsequent researchers have followed this approach. This is especially true for most existing work of direct relevance to the present study, namely for breccia pipes or bodies (any breccia body, regardless of shape, enclosed in host rocks) associated with magmatic activity and hydrothermal mineralisation (cf. Bryner, 1961; Wright and Bowes, 1963; Kents, 1964; Bryner, 1968). Sillitoe (1985) provides an excellent overview of breccias but similarly his classification is genetic and is based on the inferred mode of fragmentation combined with the relationship to accompanying ore deposition. These classifications are difficult to apply because little objective work exists on the interpretation of fragmentation mode in the subvolcanic environment.

In sedimentary (cf. Eyles et al., 1983; Walker, 1984) and volcanic (extrusive) systems (cf. Cas and Wright, 1987), detailed facies analysis forms the basis for most genetic interpretation. Sillitoe (1985) notes that in a similar way the interpretation of breccia genesis could be based on descriptive criteria, but this has proved impossible in the case of ore related breccias. It is important to appreciate that most existing work is based on isolated interpretation of general breccia features rather than the establishment of breccia facies based on the systematic analysis of descriptive characteristics. For example, some workers have noted variation of breccia characteristics (eg. Gates, 1959; Kents, 1964) but did not describe the fragmentation characteristics in detail, their relationship to host rock, nor the contact relations with texturally different breccia units. More recently, interpretation of breccia pipes has been based on fluid inclusion and isotope studies (eg. Norman and Sawkins, 1985). The fundamental question remains (Locke, 1926): "Why was the rock broken into small, angular pieces, with such lavish expenditure of energy rather than along a few principal planes of movement?"

The second aspect to the problem is the nature and timing of the associated mineralisation. Many workers (eg. Bryner, 1961; Perry, 1961; Kents, 1964; Sawkins, 1969; Norton and Cathles, 1973; Sillitoe, 1985) assume hydrothermal alteration is genetically linked to the breccia pipe forming

process, but provide little direct evidence to support this claim. As a consequence they have developed breccia mechanisms based on the release of this fluid, either during magma withdrawal or advance. However, the classification of Bryner (1961) notes pre-hydrothermal and co-hydrothermal breccias, exposing the questionable basis for this assumption. Several other workers have noted the minimal to absent alteration and mineralisation associated with breccia pipes (Gates, 1959; Bryant, 1968; Sillitoe, 1985), further suggesting that fluid release resulting in hydrothermal alteration is not an essential process in breccia formation. In addition to the problem of interpreting fragmentation mode noted above, this last possibly leads to further difficulty in applying a classification based on style of mineralisation (Sillitoe, 1985).

On a more practical note, the hydrothermal alteration associated with brecciation, especially in conjunction with porphyry intrusives can lead to further difficulty of breccia interpretation. This alteration may also produce false clastic or pyroclastic textures.

Resolution of these conflicts is critical to exploration models, understanding brecciation mechanisms and controls on gold mineralisation within the Mt. Leyshon breccia complex. For example, in a diatreme setting (ie. a vent produced by volcanic explosion), gold mineralisation may be expected to occur in a particular pyroclastic unit, marginal ring fractures or in extensional faults formed by block collapse into the diatreme. It may also relate to the boiling zone in epithermal systems. In deeper level systems mineralisation may have a more consistent structural control or spatial relationship to igneous intrusions. It is for these reasons, that the facies architecture and structural setting of the Mt. Leyshon complex were investigated, which together comprise the geological framework to understand controls on gold mineralisation.

### 1.3 AIMS

Existing work on the Mt. Leyshon breccia complex is contradictory and, as discussed above, provides the possibility for several significantly different exploration models. Therefore, the primary aim of this project is to resolve such geological and genetic conflicts by developing a rigorous facies model based on systematic analysis of facies and structural architecture in relation to the regional geological setting. A secondary aim is to combine the geological data from the Mt. Leyshon breccia complex with what is currently known of crustal processes, to derive a dynamic model for breccia formation in the upper crust.

### 1.4 APPROACH

Facies analysis formed the basis of the approach adopted in this study. Initially, the rock relations were analysed by detailed logging of 18 drill core (including a 600 metre long, north plunging core) and a well outcropping test area mapped (Mt. Hope; 1:1000 scale). Close attention was paid to establishing basement units and understanding the effects of alteration on masking and altering rock unit textures. Once the basic rock units (facies) were established, their characteristics were summarised and lithofacies drill-sections constructed (four, 25 m spaced cross-sections and one plan-150 metres below ground) to illustrate their geometry and relation to ore zones.

Subsequently the whole breccia complex was mapped in detail using the previously established facies. The complex comprises five prominent hills, surrounded by creek dissected, gently sloping ground (elevation 510–400 m.s.l). Outcrop is good in the complex, allowing mapping at a spacing of generally less than twenty metres (except for the northern area between Mt. Leyshon and Mt. Mawe). Emphasis was on outcrop distribution, unit geometry, contact relations, relationship to basement units and the extent and style of basement fragmentation. New units were established in the main igneous centre and their characteristics defined. Structural data from all units within the complex were collected routinely in conjunction with outcrop mapping. Essential aspects of the study were distilled and a facies model was constructed for the whole breccia complex in conjunction with assessment of additional drill hole data (10 drill core logged in detail).

The partially resolved mineral paragenesis and alteration studies from earlier phases of the research were detailed in an extensive drill core, polished slab, and thin section study. This study constrained the timing of mineralisation in the complex, and the relationship between igneous emplacement, breccia generation and hydrothermal fluid evolution. The broad distribution of major alteration styles was compiled from mapping and limited drill core data. In addition to timing, the distribution, geometry and structural control on gold mineralisation were partially investigated.

A system facilitating graphic logging of breccia units in the subvolcanic environment was established. Detailed facies analysis of the Mt. Leyshon breccia pipe was undertaken based on graphic/textural analysis in drill core (and open pit). The breccia pipe was divided into several facies and their internal and external characteristics were defined. A facies model for the Mt. Leyshon breccia pipe was constructed based on the variation and geometry of these characteristics.

Igneous petrogenesis associated with the breccia complex was investigated by examining the petrographic and geochemical characteristics of the Mt. Leyshon igneous units, and by comparison to regional igneous units. Sample selection of the Mt. Leyshon igneous units was based on the facies analysis in the complex.

Analysis and synthesis of this data was combined with what is presently known of physical processes in the upper crust, to construct a dynamic model for breccia mechanisms in the Mt. Leyshon complex. As a consequence this model has implications for general breccia mechanisms in continental crust.

This conceptual framework was integrated with the investigation of controls on gold mineralisation in the Mt. Leyshon complex, to propose a model for gold mineralisation.



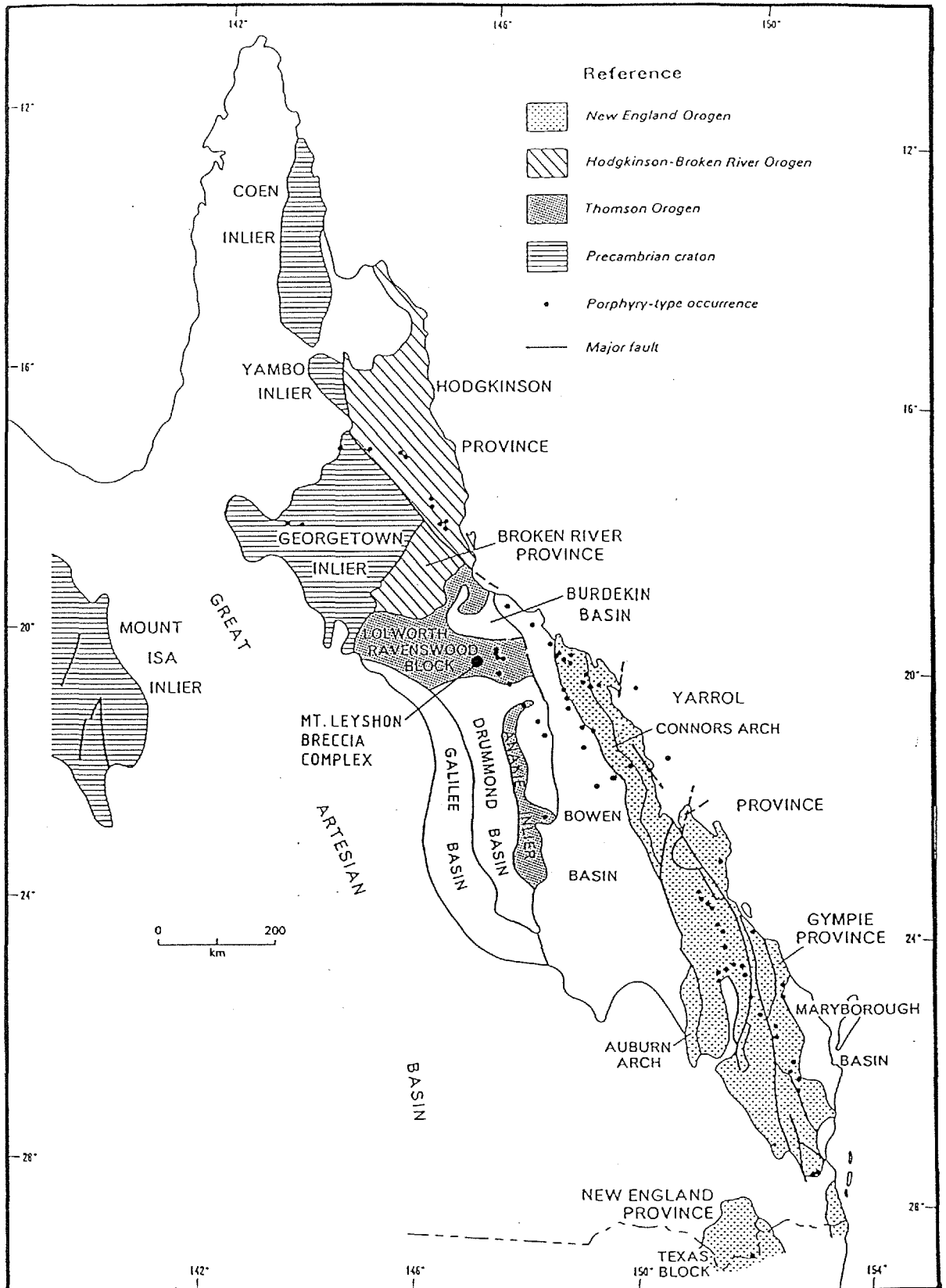


Figure 1.1b: The main structural elements of NE Queensland (modified from Horton, 1982).

## CHAPTER 2

# GEOLOGY AND FACIES ARCHITECTURE OF THE MT. LEYSHON BRECCIA COMPLEX

---

### 2.1 INTRODUCTION

There is now overwhelming evidence that intrusive breccia pipes are genetically related to magmatic systems. In volcanic and near surface environments eruptions which result in breccia pipe vents generally form by phreatic (geothermal heating of groundwater) or phreatomagmatic (water / magma interaction) explosions. These near surface eruptions have been observed several times (eg. Wolfe, 1980). As a result the detailed facies architecture of the fragmental rocks formed by these processes are fairly well documented (eg. Hedenquist and Henley, 1985; Cas and Wright, 1987). Providing the alteration is not too intense, fossilised volcanic breccia pipes can generally be recognised by careful comparison with the facies characteristics of documented recent examples.

The formation of subvolcanic or hypabyssal breccia pipes cannot be observed and the products of breccia pipe formation cannot be directly related to present day processes. There is a paucity of well documented facies models for hypabyssal intrusive breccia complexes and those presently proposed are not based on a systematic facies analysis of the whole system. As a result, misinterpretation of the rocks in these complexes has occurred. Early intrusive breccia investigations (Kents, 1964), which attempted to define a genetic terminology based on an isolated breccia texture, met with limited success because breccias formed by different processes can have similar textures. More recent workers have tended to resort to theoretical consideration of breccia mechanisms (Norton and Cathles, 1973; Burnham, 1985), and breccia research has typically focused on fluid inclusion and isotope studies to infer magmatic processes responsible for brecciation (eg. Norman and Sawkins, 1985; Porter and Ripley, 1985).

The Mt. Leyshon breccia complex has previously been interpreted as a near surface diatreme (Morrison et al., 1987, 1988) and a maar-type volcanic centre (Paull et al., 1990). These workers describe extrusive volcanic units which, as discussed by Wright (unpublished report, 1989), imply the breccia complex resulted from phreatomagmatic fragmentation processes. The Mt. Leyshon breccia complex has recently been re-interpreted as an intrusive breccia and igneous complex (Wormald et al., 1991). Independent geochemical evidence (Morrison et al., 1987), suggesting that the early stages of the hydrothermal system were dominantly derived from magmatic fluids, is consistent with this interpretation.

Documentation of facies characteristics and unit geometry presented in this Chapter, together with an understanding of the structural evolution of the breccia complex (Chapter 3), provide new information to examine these conflicts. This work also provides a comprehensive facies model for comparison with other fossilised breccia complexes which are suspected of being intrusive.

Detailed facies analysis initially concentrated on characterising basement, the suite of igneous unit types in the complex and igneous fragments present in the breccia units. Basement was used to define the bounding geometry of the first breccia unit. The characteristics and geometry of subsequent breccia units were defined by their relationship to basement and the first breccia unit. Polymict breccias have been subdivided according to fragment types, texture, spatial association and sequence of intrusion.

Finally, the work has implications for the magmatic evolution resulting in brecciation in the Mt. Leyshon complex. When the timing of brecciation with respect to igneous emplacement is integrated with the hydrothermal evolution examined in Chapter 4, it has important implications for both the nature and timing of fluid evolution in porphyry-style magmatic systems.

The aims of Chapter 2 are to:

- (1) Document the detailed facies characteristics of units in the Mt. Leyshon breccia complex.
- (2) Examine the field based evidence for the relationship between the emplacement of igneous and breccia units in the complex.
- (3) Form a facies model for the Mt. Leyshon breccia complex based on the observed facies characteristics.

Three terms are used to describe igneous fragments which occur in breccia and igneous units described in this and subsequent Chapters; namely, juvenile, cognate and accidental. *Juvenile* fragments are considered to be pieces of igneous melt fragmented during brecciation. *Cognate* fragments are considered to have been derived from an earlier episode of intrusion from the Mt. Leyshon magmatic system. *Accidental* fragments are considered to be unrelated to the magmatic system and represent basement. Evidence to support these interpretations is provided.

## **2.2 FACIES CHARACTERISTICS OF THE MT. LEYSHON BRECCIA COMPLEX**

Units of the Mt. Leyshon breccia complex have been divided into three main elements (Enclosure 1; Figures 2.1 and 2.4):

- (1) Basement.
- (2) Main pipe breccia.
- (3) Interactive magma / breccia sequence.

Facies characteristics of these three elements are described in this section and are used to construct a facies model for the breccia complex in section 2.4. The tendency for breccia and igneous units to follow a preferred orientation is described in section 3.4.

### **2.2.1 Basement units**

Pre-breccia basement is composed of four units; namely Puddler Creek Metasediment, Mt. Leyshon granite, porphyritic rhyolite and dolerite dykes (Enclosure 1; Figures 2.1 and 2.4). The complex is mostly developed in metasediment (and the dykes), although granite is brecciated at the northern and eastern contacts. The metasediment unit consists of a monotonous sequence of

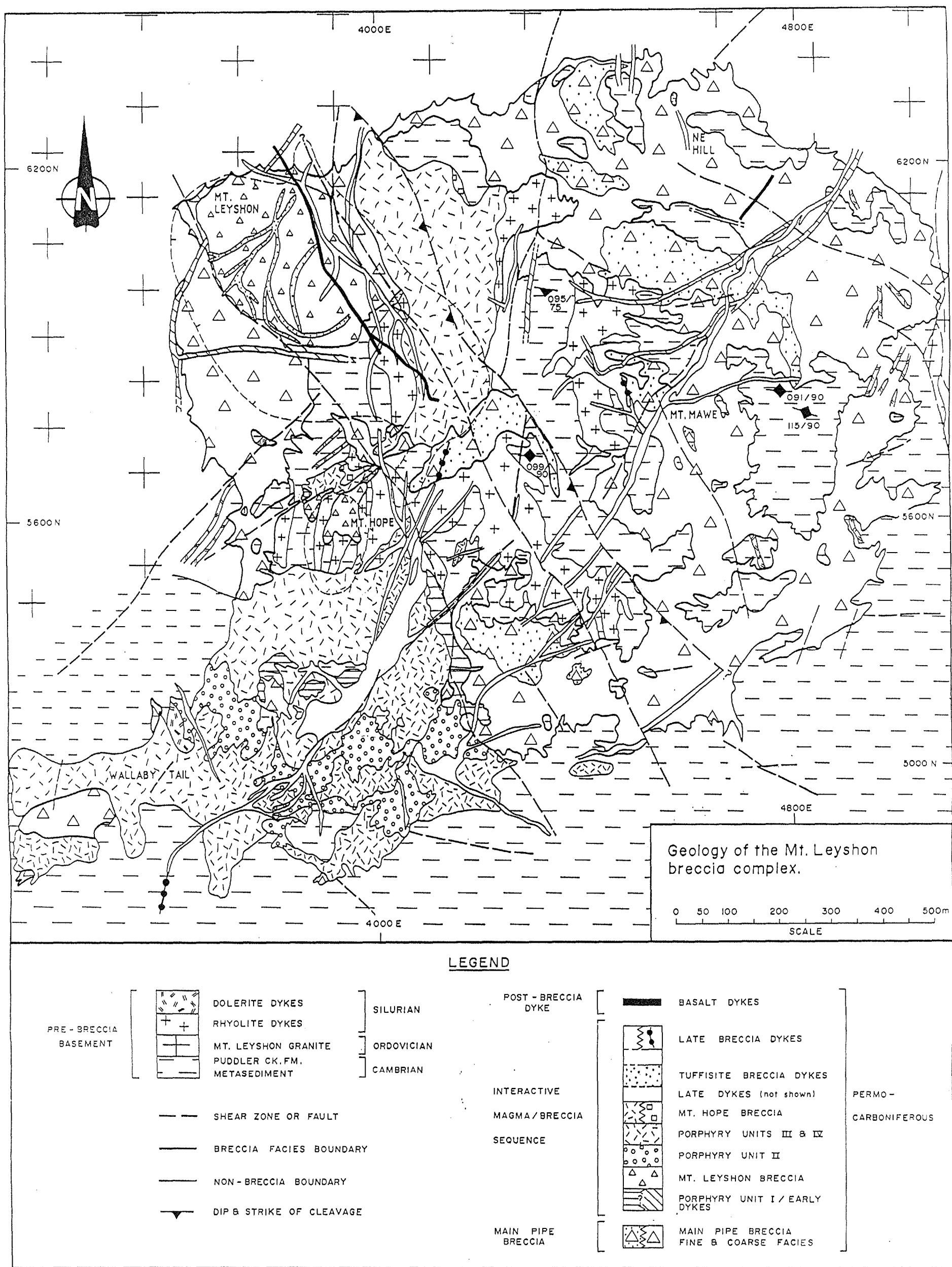


Figure 2.1: Geological map of the Mt. Leyshon breccia complex. Map is based on outcrop mapping at 1 : 2000 scale (conducted by the author, except as shown in the key to Enclosure 1). Pit outline is shown as a dashed/ticked line. Geology on Mt. Leyshon is projected to the 410 RL. The majority of basement rhyolite dykes and dolerite dykes have been omitted for clarity.

Note: (1) the three main elements of the breccia complex (see legend), (2) the intrusive, interfingering geometry of the main pipe breccia, (3) the location of the main igneous centre, (4) the orientation of metasediment cleavage within the little rotated basement blocks, and (5) the preferred orientation of breccia and igneous units.

metamorphosed (greenschist facies) sandstones, siltstones and greywackes (Henderson, 1986). In the complex the metasediment is thickly bedded and preserves a prolonged structural history (see Chapter 3). The Mt. Leyshon granite consists of the following approximate modal proportions: 35% plagioclase, 35% quartz, 27% K-feldspar and 3% biotite, and varies from coarse grained to aplitic textures. In the area of the breccia complex the contact between metasediment and granite is embayed, although the actual contact was poorly exposed at only one locality (Figure 2.1). Outcrop mapping east of Mt. Hope indicates that the granite / metasediment contact has been offset by faulting (see Chapter 3) but emplacement of the main pipe breccia has obscured the relationships. The embayed geometry of the gross granite / metasediment contact is therefore considered to be due to fault offset. Additional characteristics of this metasediment / granite contact are discussed in Chapter 5. Both metasediment and granite are intruded by numerous pre-complex intrusions with earlier porphyritic rhyolite dykes and bodies, cross-cut by dolerite dykes. Basement rhyolite dykes vary in texture from porphyritic with an aphanitic groundmass to a crowded porphyritic texture with rounded quartz megacrysts. Dolerite dykes have a medium grained equigranular texture and alteration can produce a similar looking lithology to the metasediment. The majority of these dykes have been omitted for clarity in Figure 2.1. The larger basement rhyolite bodies in the complex appear to have inhibited main pipe breccia development (see section 3.5).

Large basement blocks are preserved in the breccia complex (Figure 2.1) and show various degrees of partial to complete fragmentation, with crackle, mosaic or rubble textures (Plate 2.1). Despite this brecciation, the blocks generally maintain their pre-breccia integrity, illustrated by the continuity of porphyritic rhyolite and dolerite dykes in outcrop (see Mt. Hope; GR 3825 5450, Figure 2.1). Bedding and cleavage orientations were also measured in brecciated metasediment blocks (see Chapter 3). For example, laminated siltstone units are interbedded with massive fine sandstone units at GR 4730 5240 (Plate 2.2; Figure 2.1) and the units are still traceable in outcrop, despite the rubble textured brecciation (which has resulted in expansion and local rotation).

During mapping, partially brecciated basement outcrops were systematically rated according to their degree of brecciation (crackle, mosaic or rubble) to examine whether there is a spatial relationship between basement fracture intensity and distribution of the main pipe breccia. No systematic pattern of basement outcrop breccia texture was found and the degree of basement brecciation was found to be independent of distance from the main pipe breccia. Furthermore, zones of crackle or mosaic textured basement locally occur as isolated zones in rubble textured basement (Plates 2.1 and 3.5). The trend of fractures in the less deformed regions may be oblique to the dominant fabric in the rubble textured zones. Finally, basement units contain a complex network of highly expanded regions which may contain small fragments that are equant to splinter shaped. These observations suggest that two basement fragmentation events occurred during main pipe breccia formation.

### 2.2.2 Main pipe breccia

The first breccia event recognised in the complex resulted in the most volumetrically significant unit referred to here as the main pipe breccia (Enclosure 1; Figure 2.1). The facies characteristics of this and subsequent breccia units are summarised in Table 2.1. The main pipe breccia occurs throughout the breccia complex (over an area of approximately 2 by 1.5 kilometres) and its margins effectively define the boundary of the complex. Outcrop mapping (Figure 2.1), drill core logging and lithofacies sections (eg. Figures 2.2a and 2.2b) indicate that the main pipe breccia is a steeply dipping body with an inter-fingering, antler-like geometry.

Contacts between main pipe breccia and basement are generally sharp, although they are commonly irregular and inter-fingering as indicated in Plate 2.3. At the hand-lens-scale, polymict main pipe breccia passes either sharply into weakly (crackle) brecciated basement or into expanded but little transported host rock which commonly contains a fine clastic inter-fragment component. Thin section observations indicate that this clastic component is dominated by quartz chips, and forms a fine complex network (10's of microns to millimetres wide) within these host rock regions, but links with the main pipe breccia outside the host rock blocks. During the investigation of more than 30 thin sections and several kilometres of drill core, no breccia cavities were found in the polymict main pipe breccia (with the possible exception of one biotite filled cavity in thin section). Hence, fragments in the polymict main pipe breccia are either supported in a rock flour matrix or where the proportion of inter- fragment contact is high the space is filled by matrix.

Two distinct subfacies are distinguished on the basis of average fragment size and proportion of matrix; namely coarse and fine main pipe breccia (Table 2.1, Figures 2.1, 2.2a and 2.2b, Plates 2.4 and 2.5). In some areas, it is possible to define a third subfacies which is a gradational medium variant (fragment dominated, fragments < 1 cm). However, drill core observations indicate it is a minor component and has an irregular distribution thus no attempt has been made to separately map the intermediate subfacies. Both coarse and fine subfacies consist of fragments which are almost exclusively derived from basement units (section 2.2.1). However, two types of igneous fragments occur in the main pipe breccia which are unlike any basement unit. Firstly, uncommon fragments which have a flow aligned texture (in thin section) characteristic of later intermediate igneous units. Secondly, a single four centimetre fragment (Plate 2.6) occurs in the fine main pipe breccia which is texturally very similar to later felsic units. Both types are considered to be cognate because brittle fracture of the fragments suggests that they were solid at the time of emplacement. Breccia matrix (< 2 mm fragment size) consists of angular to subrounded basement fragments and quartz and feldspar grains. Similar cognate fragments (or juvenile fragments) do not form part of the breccia matrix in thirty thin sections from coarse and fine main pipe breccia. This suggests that both the coarse and fine main pipe breccia (> 70% matrix) are almost completely composed of basement units; the rare cognate igneous fragments indicate minor coeval pre-complex igneous emplacement.

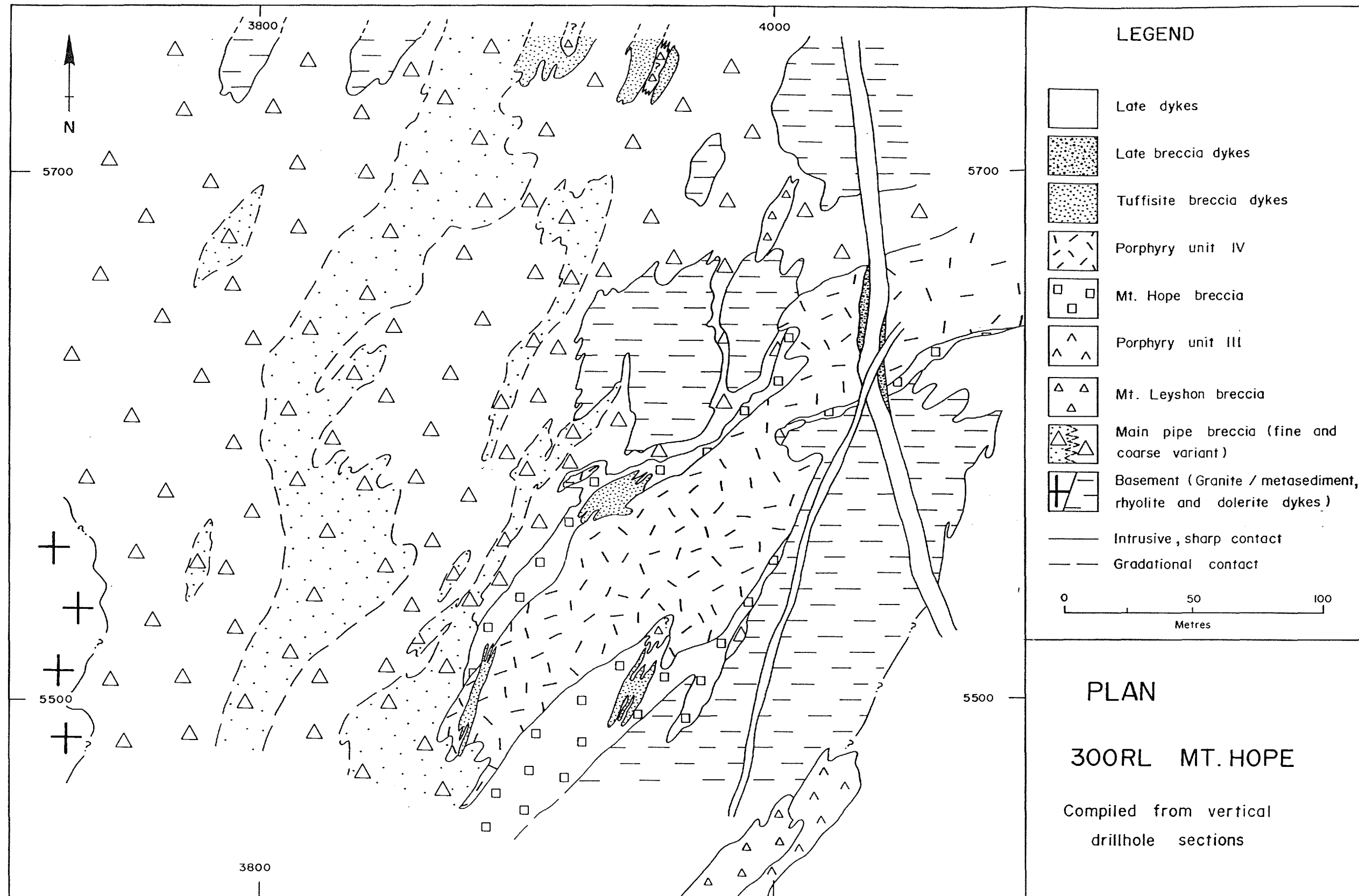


Figure 2.2a: Plan section to illustrate the lithofacies relationships between units of the Mt. Leyshon breccia complex. Granite / main pipe breccia contact, and Mt. Leyshon breccia / porphyry unit III zone are projected from mapping at the surface. Note: (1) the intrusive, inter-fingering geometry of the main pipe breccia, (2) the linear zones of fine main pipe breccia within the coarse variant, (3) the sheath-like geometry of the Mt. Hope breccia around porphyry unit IV, (4) the linear nature of the poorly developed Mt. Leyshon breccia and tuffisite breccia dykes, and (5) the spatial relationship between late breccia dykes and late dykes.

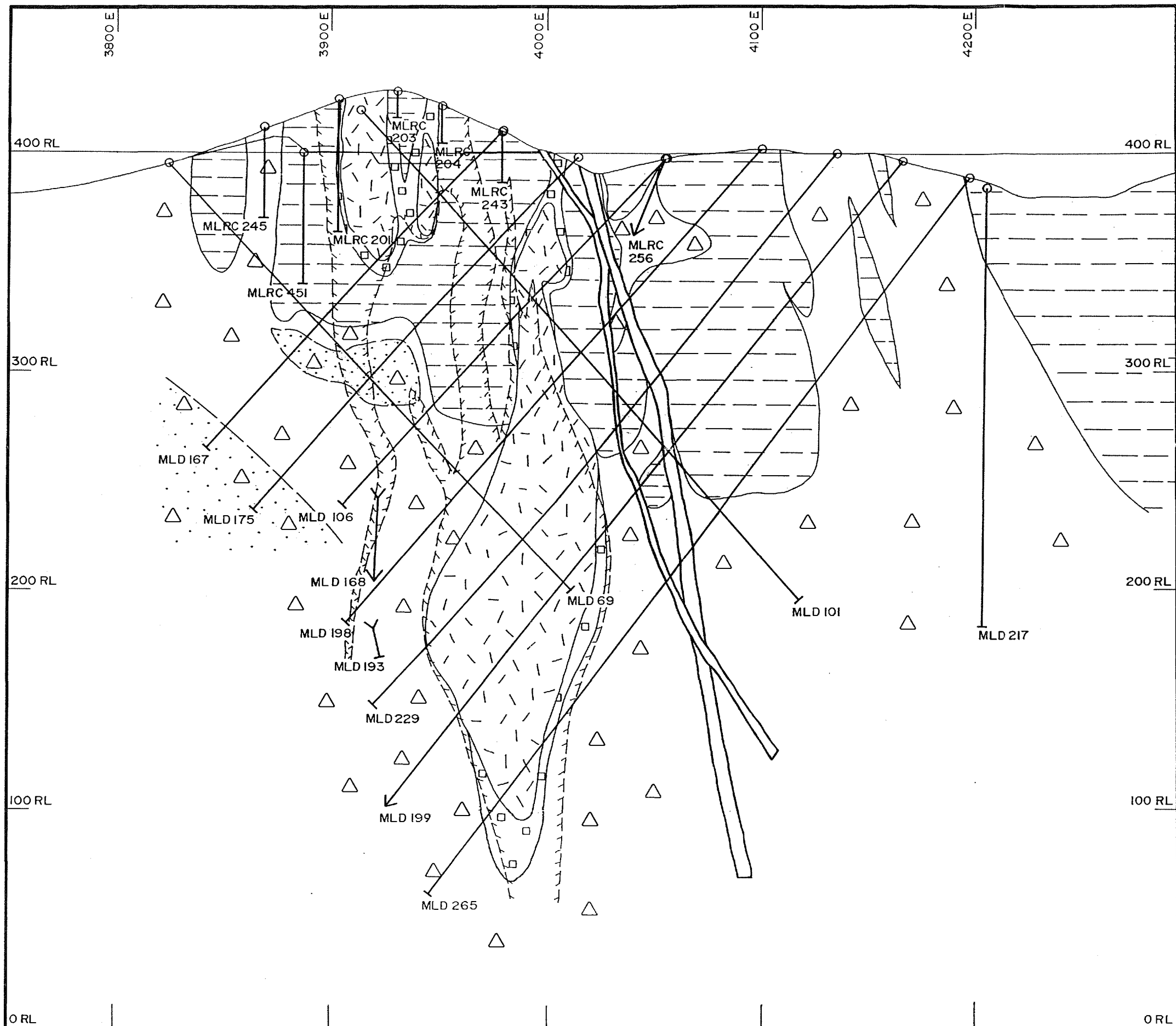


Figure 2.2b: Cross section to illustrate the lithofacies relationships in the Mt. Leyshon complex. See Figure 2.2a for key and notes. MLRC = R.C drill hole, MLD = diamond drill hole. Dashed hatched line = mineralisation envelope. Adapted from Wormald (unpublished data, 1990) and Orr (unpublished data, 1991).

Both coarse and fine subfacies map out as distinct units (Figures 2.1, 2.2a and 2.2b) although each may include a minor element of the other unit. These units correspond to vent breccia and lapilli tuff, respectively of Morrison et al. (1987) and Paull et al. (1990). However, contacts between the two subfacies are gradational and steeply dipping (Plates 2.7 and 2.8). The fine variant typically forms linear zones within the more voluminous coarse variant (Figure 2.1, 2.2a and 2.2b) and as already noted the whole unit has an intrusive, inter-fingering geometry. Textural and fragment size characteristics (eg. grading or sorting) in each subfacies are typically constant or change gradually over metres to 10's of metres. In contrast, uncommon zones occur in drill core (eg. MLD 104) which oscillate between fine and coarse variants over intervals of as little as 5 - 50 centimetres. The coarse unit has a weak fabric defined by an alignment of the fragment long axes (Plate 2.4), though the fragments are internally undeformed. In the context of the facies relations of this breccia unit, this fabric is interpreted to result from the flow alignment of fragments. Both facies types have a very low permeability when sealed up by early alteration (Chapter 4).

Fine main pipe breccia commonly contains accretionary structures or pellets (up to 10 mm in diameter) which may be flattened, broken, or which occur in steeply dipping layers (Plate 2.5). These structures also locally occur in the coarse variant. They are confined to the main pipe breccia unit which, as noted above, has a steeply dipping inter-fingering contact with basement. Thin section observation reveals that the accretionary structures are composed of a nucleus of fine rock fragments and matrix which is coated in a finer grained material (very small rock fragments, clay and silica; Plate 2.9). In addition, partial or complete shells, composed of coarser grained material, occur within the fine rim. Long aspect ratio fragments bound up in this fine rim typically have their long axes tangential to the rim margin which suggests that they are not a product of alteration (see section 2.4.1 for interpretation of their mode of formation).

### **2.2.3 Interactive magma / breccia sequence**

Following the development of the main pipe breccia and the early hydrothermal events (Chapter 4) a sequence of igneous and breccia units was emplaced into the complex, collectively referred to here as the interactive magma / breccia sequence. The facies characteristics of these units are described below and summarised in Tables 2.1 and 2.2. A discussion of the evidence for facies timing is delayed until section 2.3. To aid the description of this interactive sequence, the breccia and igneous units are described separately. The evidence for their interaction is examined in section 2.4.

#### **2.2.3.1 BRECCIA UNITS**

Breccia formation which occurred after main pipe breccia is mainly confined to the NW corner of the complex. However, late breccia dykes occur in several parts of the complex (Figures 2.1, 2.2a and b) and there is abundant small scale crackle to rubble textured brecciation of main pipe breccia and basement. The discussion of breccia unit characteristics presented in this and the previous section is divorced from observations of hydrothermal alteration for clarity. However, it is important to note that the definition and investigation of the breccia units within the Mt. Leyshon

complex was only possible through an understanding of the hydrothermal alteration accompanying the breccias (see Chapter 4).

### Mt. Leyshon breccia

General facies characteristics of the Mt. Leyshon breccia are described in this section, although a detailed facies analysis of the Mt. Leyshon breccia pipe is presented in Chapter 5. The Mt. Leyshon breccia, which is volumetrically the second most important breccia unit of the complex, occurs in three localities (Enclosure 1, Figure 2.1):

- (1) A breccia pipe on Mt. Leyshon proper.
- (2) A smaller pipe on Mt. Hope.
- (3) As NE trending breccia dykes to the SE of Mt. Hope (80 metres by 10 metres). The Mt. Leyshon breccia pipe has vertical dimensions of at least 660 m and is a crude rhombohedron in plan (425 by 225 metres) at the 400 RL (metres above sea level; Figure 5.4). Pre-mine mapping by Morrison (unpublished report, 1986) indicates that the breccia body narrowed upwards to dimensions of 240 by 170 metres at the top of Mt. Leyshon (summit RL 520). The detailed geometry of the Mt. Leyshon breccia pipe is presented in Chapter 5. The geometry of the Mt. Leyshon breccia pipe on Mt. Hope is less well known. It has dimensions of 100 by 60 metres in plan at the 400 RL (Figure 2.1, Enclosure 1). However, on Mt. Hope it appears that the Mt. Leyshon breccia is intruded and removed by a zone of porphyry unit IV and Mt. Hope breccia (compare Figures 2.1 and 2.2a).

The Mt. Leyshon breccia consists of two main components; zones of intact to weakly brecciated pre-existing stratigraphy and polymict zones (see Chapter 5). Polymict Mt. Leyshon breccia is generally fragment supported with angular to rounded fragments between 20 - 100 mm in size (e.g. Plate 5.8). In contrast to the main pipe breccia the Mt. Leyshon breccia has a low matrix proportion, although matrix rich zones occur locally (see Chapter 5). The breccia generally contains significant void space and cavity-fill mineralisation, however the linear dyke like zones SE of Mt. Hope are almost unaltered (Plate 4.10). Where polymict, the Mt. Leyshon breccia can contain fragments of all previous units (ie. basement, main pipe breccia, porphyry phase I and early dyke) and rare fragments which are texturally similar to porphyry unit IV. The detailed facies characteristics and subfacies of the Mt. Leyshon breccia are considered in Chapter 5.

### Mt. Hope breccia

The Mt. Hope breccia represents a further contraction in the area affected by brecciation. It is restricted to three areas: (1) a main zone on Mt. Hope (where it was defined during this work), (2) small zones at the southern end of the mine porphyry, and (3) a small zone at the northern end of the mine porphyry (Enclosure 1, Figure 2.1). Facies characteristics of Mt. Hope breccia are summarised in Table 2.1.

The main Mt. Hope breccia body forms a steeply dipping, elliptical sheath zone around an elongate body of porphyry unit IV (Figure 2.2a and b), and has dimensions of 290 by 100 metres at 300 RL. Breccia contacts are generally sharp, however locally they are irregular where they pass

BRECCIA CHARACTERISTIC	MAIN PIPE BRECCIA (MPB)	MT. LEYSHON BRECCIA (MLB)	MT. HOPE BRECCIA (MHB)	TUFFISITE BRECCIA DYKES (TBD)	LATE BRECCIA DYKES (LBD)
<b>External facies characteristics</b>					
PRESENT DISTRIBUTION	Occurs throughout the breccia complex between the basm. blocks and defines the complex boundaries.	Restricted to the NW corner of the complex in 3 locations: (1) the Mt. Leyshon breccia pipe, (2) a small pipe on Mt. Hope, and (3) narrow breccia dykes SE of Mt. Hope.	As a breccia body on Mt. Hope and as small zones at the southern and ?northern end of the mine porphyry (porphyry unit IV).	Generally restricted to Mt. Leyshon; rare on Mt. Hope; unknown elsewhere.	Throughout the breccia complex, where late dykes occur.
SIZE of main body	Partially occupies an area of approximately 2 by 1.5 kilometres; vertical extent of at least 660 metres.	Approximately 400 by 300 metres in plan; vertical extent of at least 660 metres.	Occurs partially over an area of 150 by 75 metre on Mt. Hope.	From 0.01 to >15 metres thick with a strike length of upto 200 metres.	Upto 1.5 metre thick with a strike length of atleast ?120 metres.
GEOMETRY / ATTITUDE / CONTACTS	Outline of complex defined by a crude rhombohedron. Intricate, interfingering and generally steeply dipping contacts. Linear zones make up this pattern.	A crude rhombohedron in plan which narrows upwards and downwards. Generally sharp, steeply dipping contacts which are bound to the E and W by strike slip faults.	Forms an elliptical sheath zone around PU IV. Steeply dipping irregular contacts.	Steeply dipping to flat lying, linear to curved dykes. contacts commonly sharp. Smaller breccia dykes have irregular and interfingering contacts.	Generally steeply dipping dyke like form with sharp contacts.

Table 2.1: Facies characteristics of breccia units within the Mt. Leyshon breccia complex.

BRECCIA CHARACTERISTIC	MAIN PIPE BRECCIA (MPB)	MT. LEYSHON BRECCIA (MLB)	MT. HOPE BRECCIA (MHB)	TUFFISITE BRECCIA DYKES (TBD)	LATE BRECCIA DYKES (LBD)
<b>Internal facies characteristics</b>					
SUB - FACIES TYPES	Coarse and fine variants; coarse dominant.	Three variants due to frag. type and texture: (1) Granite rich, (2) MPB rich, and (3) exclusively MPB.	None recognised.	Three variants due to frag. size: coarse, medium and fine variants.	Local matrix rich zones.
APPROX. MATRIX PROPORTION	Coarse MPB: 1 - 20%, locally 30%. Fine MPB: 70 - 100%.	Generally <1% - 5%, rarely >15%.	<1% - ? 5%; masked by alteration.	Coarse and medium TBD: 5 - 15%; fine TBD: 99 - 100%.	Typically < 5%; locally grades into zones with >90%.
FRAGMENT TYPES	Basm. and rare cognate igneous frag.s.	Basm., MPB, ED, PU I, cognate igneous frag.s.	Basm., MPB, ED, cognate frag.s texturally identical to PU IV.	Coarse and medium TBD: basm., MPB, ED, cognate igneous frag.s. Fine TBD: Mostly composed of ?juvenile igneous material.	Basm., MPB, cognate and juvenile igneous frag.s. Cognate/juvenile fragments may dominate.
FRAGMENT SIZE/ SORTING	Coarse MPB: Generally between 10 - 50 mm, locally up to 1000 mm; blocks 1 m - >500 m. Fine MPB: generally <5 mm. Moderately to well sorted.	Commonly 20 - 100 mm, up to 500 mm; blocks ≥ 1 m - 15 m. Poorly to locally moderately sorted.	Generally 20 - 50 mm. Upto 500 mm. Local blocks of several metres. Moderately to well sorted.	Coarse: >10 mm; medium: 2 - 10 mm; Fine <2 mm. Very well sorted.	Generally 20 - 50 mm; local zones <2 mm. Moderately sorted, local well sorted regions.
FRAGMENT ANGULARITY	Subangular to subrounded.	Angular to subrounded.	Sub angular to rounded.	Well rounded (matrix angular).	subangular to subrounded.

Table 2.1: Facies characteristics of breccia units within the Mt. Leyshon breccia complex.

BRECCIA CHARACTERISTIC	MAIN PIPE BRECCIA (MPB)	MT. LEYSHON BRECCIA (MLB)	MT. HOPE BRECCIA (MHB)	TUFFISITE BRECCIA DYKES (TBD)	LATE BRECCIA DYKES (LBD)
FABRICS	Shows frag. size layering and/or grading. Uncommon flow fabric defined by long axis of fragments.	Generally absent. Rare, weak frag. size grading. Rare flow fabric defined by aligned long aspect ratio frag.s and matrix.		Common 1 - 10 mm layering and frag. size grading. Less common diffuse flow fabric.	Strong flow fabric in local matrix rich zones.
OTHER	Fine MPB commonly contains accretionary structures, very rare in coarse MPB.	Numerous host rock blocks of $\geq 1$ m separate zones of smaller fragments.	Uncommon preexisting blocks separate polymict zones.	Three types can occur separately or together with gradational to sharp contacts. Rarely reworks MLB.	Spatially associated with late dyke varieties.
POROSITY / PERMEABILITY <sup>†</sup>	Very low.	Moderate to high.	High	Very high.	Moderate.

Notes: Basm. - prebreccia complex units: metasediment, granite, rhyolite and dolerite dykes. See Chapter 5 for the detailed facies characteristics of the Mt. Leyshon breccia.

† - porosity / permeability at time of mineralising fluids.

MPB-main pipe breccia, ED-early dyke, PU IV-porphyry unit IV, TBD-tuffisite breccia dyke.

Table 2.1: Facies characteristics of breccia units within the Mt. Leyshon breccia complex.

into rubble to crackle textured basement or main pipe breccia. Porphyry unit IV occupies a central position to the Mt. Hope breccia and intrudes the margins of the breccia (Plate 2.10).

The Mt. Hope breccia is broadly similar to the Mt. Leyshon breccia in texture (ie. a fragment supported breccia with void space and cavity fill mineralisation). However, in contrast to the Mt. Leyshon breccia, the Mt. Hope breccia is predominantly polymict with a high degree of fragment roundness. Narrow, weakly developed zones do contain partially brecciated main pipe breccia and basement units. Interpretation of the Mt. Hope breccia is complicated by the intensity of alteration. However, it contains fragments which include; basement, main pipe breccia, early dyke and fragments which are texturally identical to porphyry unit IV (Plate 2.11).

#### Tuffisite breccia dykes

Tuffisite breccia dykes are restricted to the NW corner of the complex on Mt. Leyshon proper and the northern end of Mt. Hope (Figures 2.1, 2.2a and b, 5.3 and 5.4). They are susceptible to weathering and were only observed in open pit exposure and drill core during this study. Morrison et al. (1987) indicate they cropped out on the pre-mine summit of Mt. Leyshon. Numerous tuffisite dykes intrude the Mt. Leyshon breccia pipe as tabular bodies between 0.01 - >15 metres thick. The larger bodies have a strike length of over 200 metres and they are both steep and gently dipping. Their contacts are obviously intrusive and sharp (Plate 2.12), although they locally display gradational contacts where the tuffisite dykes appear to rework the Mt. Leyshon breccia. Three types of tuffisite dyke have been defined according to their average fragment size, namely, fine, medium and coarse (see Table 2.1). These three types are well sorted and occur independently or as composite bodies with gradational to sharp contacts between each type. More diffuse contact relationships rarely occur where the coarse tuffisite dykes intrude basement, resulting in a region of *in situ* expanded basement injected by clastic matrix. Some coarse tuffisite breccia dykes are poorly sorted and have a higher proportion of matrix. Tuffisite dykes commonly show grading or fine layering (1-10 mm; Plate 2.13). Fine tuffisite dykes rarely display convoluted flow textures in areas where they pass around obstructions.

The fragment composition varies for subfacies type. Coarse and medium tuffisite breccia dykes contain fragments of all previously described rock types, and cognate igneous fragments. The igneous fragments do not match any igneous unit type, although they have some textural affinity with porphyry unit IV. The nature of the matrix component commonly present in coarse and medium tuffisite dykes is strongly altered and consequently its composition is obscured.

Likewise, fine tuffisite dykes are generally strongly altered. However, one fine tuffisite breccia dyke located in a deep drill hole (MLD 236; Plate 4.8) is relatively fresh and the nature of the fragments are clearly visible in thin section (Plate 2.14). This fine tuffisite breccia dyke consists of K-feldspar, biotite and quartz phenocryst fragments interspersed between larger sub-angular to rounded fragments of a felsic igneous rock. Phenocryst fragments are the same type and size as those in the igneous fragments, suggesting that they formed by break up of the igneous material. Greater than 99% of the fragments consist of this igneous material (the remaining types are earlier

cognate or accidental fragments). Furthermore, the groundmass and phenocryst texture of these fragments is very similar to the igneous "2-2 dykes" (Table 6.1) which tuffisite dykes precede in the intrusive sequence. Trace element geochemistry of the weakly altered fine tuffisite breccia dyke consistently groups it with that for 2-2 dykes, in contrast to other igneous units (see Appendix 2). Altered fine tuffisite breccia dykes are texturally similar to this weakly altered example.

### Late breccia dykes

The last major episode of brecciation was responsible for the late breccia dykes which occur throughout the complex. The late breccia dykes are narrow (generally <1.5 metres), discrete dyke-like bodies with sharp contacts and are always steeply dipping (Figure 2.2a and 2.2b). Late breccia dykes in the complex are spatially (and almost certainly genetically, see section 2.4.2) related to at least two late igneous dykes which intrude this breccia unit. They commonly contain <5% fragmental matrix but are locally gradational to zones with up to 99% matrix. Typical breccia dykes are dominantly fragment supported (Plate 2.15).

Fragments are composed of basement, previous breccia complex lithologies and abundant cognate igneous fragments which are similar to the late dyke associated with the breccia dykes. Matrix typically comprises < 10% of the breccia dyke and is composed of a fine grained material (now altered to clay) and chips of quartz and feldspar phenocryst fragments. At least some of the igneous fragments are juvenile because they have a chilled margin against the groundmass. Likewise, the following thin section observations indicate that the local matrix rich zones (Plate 2.19) are predominantly juvenile. The matrix consists of two parts:

- (1) Vermicular, lenticular fragments generally < 2 mm across (approximately 60%) with chilled margins, irregular swirling flow banding and abundant evidence for disintegration (Plate 2.19).
- (2) Small angular phenocryst fragments which are identical to phenocrysts in the lenticular igneous fragments.

### 2.2.3.2 IGNEOUS UNITS OF THE MT. LEYSHON BRECCIA COMPLEX

Igneous units predominantly occur in the western half of the Mt. Leyshon breccia complex, with the greatest density located in the main igneous centre at the SW of the complex (Figure 2.1). The map scale geometry and relationships of the igneous units are shown in Figure 2.3. Mapping at an outcrop spacing of ten metres or less was undertaken to illustrate the particularly intricate relationships of units in the main igneous centre (Figure 2.3b). Evidence for the timing of igneous units, both relative to each other and to the breccia units of the interactive magma / breccia sequence, is presented in section 2.3. Igneous units commonly contain cognate xenoliths and locally the late dykes contain microgranitoid enclaves. The features of these igneous fragments are described in Chapter 6.

IGNEOUS UNIT	DISTRIBUTION	GEOMETRY / ATTITUDE / SIZE	TEXTURE / FABRIC	OTHER
Porphyry unit I (intermediate)	Eastern margin of magmatic centre; isolated zones within later units.	Narrow, elongate unit 300 by 40 m. Steeply dipping.	Sparsely porphyritic with weak flowbanding.	Contains rare xenolith bearing zones.
EP dyke (intermediate)	Only one occurrence known from MLD 166.	Dyke of unknown orientation. Few metres thick.	Moderately porphyritic with weak flowbanding. Strongly altered	
Early dykes (felsic)	Restricted to northern half of the complex where they are common.	Steeply dipping dykes, up to 5 m thick with a strike length of >500 m.	Moderately porphyritic, commonly strongly altered.	
Porphyry unit II (felsic)	Middle of the magmatic centre.	Originally as steeply dipping linear zones upto 250 by 60 m in plan. Now partially removed by PU IV.	Has the appearance of a breccia; contains >70% upto 98% mixed frags. (commonly 2 - 5 cm in size). Sparsely porphyritic groundmass with igneous microstructures.	Contains cognate igneous frags.; rare clastic textured groundmass. Reworked by porphyry unit IV. Transitional to brecciated basement.
Porphyry unit III (felsic)	Northern and eastern edge of the magmatic centre.	Elongate, linear zones, originally atleast 350 by 60 m in plan, now partially invaded and removed by PU IV.	Sparsely porphyritic with well developed flow banding.	Diachronous with PU IV.
Porphyry unit IV (felsic)	Makes up >50% of the magmatic centre; forms Walaby Tail and the mine porphyry.	Elongate bodies >500 by 130 m in plan plus smaller bodies.	Crowded porphyritic texture with weakly developed flowbanding. Commonly strongly altered which has increased phenocryst angularity and resulted in pseudopyroclastic textures.	Networks of PU IV intrude PU I - III. Spatial and temporal relationship to Mt. Hope breccia.

Table 2.2: Facies characteristics of the Mt. Leyshon igneous units.

IGNEOUS UNIT	DISTRIBUTION	GEOMETRY / ATTITUDE / SIZE	TEXTURE / FABRIC	OTHER
Sills (intermediate)	Presently restricted to Mt. Leyshon proper.	Gently dipping sills commonly upto 5 m thick.	Moderately porphyritic with rounded quartz phenocrysts.	
2-2 dykes (felsic)	Presently restricted to Mt. Leyshon proper.	Steeply dipping dykes upto 20 m thick. Strike length of at least 70 m.	Moderately porphyritic.	Commonly contains microgranitoid enclaves.
1-2 dykes (felsic)	Abundant in the western half of the complex, rare in the eastern half. Occur outside the complex.	Steeply dipping dykes upto 55 m thick. Strike length of > 1 km.	Moderately to crowded porphyritic texture. Glomerocrystic feldspar phenocrysts.	Commonly contains microgranitoid enclaves.
DG dykes (intermediate)	Restricted to Mt. Leyshon proper.	Steeply dipping dykes typically 1 - 2 m thick and as a larger body under Mt. Hope. Also as irregular fingers <0.5 m intruding the Mt. Leyshon and Mt. Hope breccias.	Moderately porphyritic with a fine grained to aphanitic texture. Commonly strongly altered and hence dark green in colour.	Rarely contains basic ?enclaves.
Fine late dykes (felsic)	Common on Mt. hope, rare on Mt. Leyshon or elsewhere.	steeply dipping narrow dykes typically <1 m thick.	Moderately porphyritic with 1mm sized phenocrysts, sometimes weakly flowbanded.	Spatially and temporally associated with late breccia dykes.
Basalt dykes (basic)	Unknown due to poor outcrop. Common on Mt. Leyshon, rare elsewhere.	Steeply dipping dykes, typically 0.5 - 1m thick.	Fine grained, sparsely porphyritic.	Post dates all brecciation and gold mineralisation

Notes: (1) Igneous units have an aphanitic groundmass unless otherwise stated.

Table 2.2: Facies characteristics of the Mt. Leyshon igneous units.

### Porphyry unit I / early dykes

Porphyry unit I forms the eastern margin of the main igneous centre and also occurs as remnant zones in porphyry unit IV defining a linear SE trending zone (Figure 2.3). Porphyry unit I is a fairly massive unit with low outcrop relief, and is more resistant to alteration than felsic units. It contains rare xenolith bearing zones up to 0.5 metres wide, but their maximum size and distribution are unknown. Porphyry unit I shows extensive evidence for network invasion by later units, particularly porphyry unit IV.

Early dykes appear to be restricted to the northern half of the breccia complex (Figure 2.3). Individual dykes are up to five metres thick, extend for a strike length of > 500 metres and are strongly altered. In addition, one other early type of igneous dyke is recognised and is referred to in this study as the EP dyke. The EP dyke was located in drill core only and no outcrop is known.

### Porphyry unit II

Porphyry unit II crops out as irregular masses within the main igneous centre (Figure 2.3) and is intruded by porphyry unit IV, consequently their precise distribution is partly obscured. Nevertheless, porphyry unit II defines linear zones which intersect near the mid point of the main igneous centre. Porphyry unit II crops out as hummocky masses of breccia (Plate 2.18) and typically contains >70% fragments. However, thin sections and polished slabs indicate that this unit has an igneous groundmass between the fragments (Plate 2.16). Fragment types consist of all previously formed lithologies and a number of additional cognate igneous fragments (with a texture suggesting they are coeval with the igneous complex, although they do not obviously relate to mapped igneous units). In contrast to the typical igneous groundmass of porphyry unit II, which commonly shows flow alignment of feldspar phenocrysts, rare clastic textured zones are preserved within swirls in the igneous groundmass. In drill core, rare cavities between fragments are infilled by epidote and calcite and these minerals also alter the igneous groundmass.

In a few outcrops of porphyry unit II (eg. GR 4004 5075) the fragmental unit contains a phenocryst crowded groundmass and is gradational to porphyry unit IV. Because fragment crowded zones with a groundmass of porphyry unit IV do not occur elsewhere, porphyry unit II is probably being reworked by porphyry unit IV in this zone. Likewise, strongly altered and isolated fragmental zones (which have a fine grained matrix) within porphyry unit IV are considered to be digested zones of porphyry unit II.

Where porphyry unit II intrudes basement or main pipe breccia, this fragment crowded unit passes gradationally into basement, with abundant jigsaw fit textures and networks of igneous groundmass (over  $\leq$  three metres; Plate 2.17), and finally into crackle brecciated basement. The fragment shapes in this transitional zone are more cusped than the rectangular fragment pattern elsewhere in the basement blocks, suggesting that local basement fragmentation occurred during intrusion of porphyry unit II.

### Porphyry unit III and IV

Porphyry unit III occurs as narrow linear zones along the northern and eastern margin of the main igneous centre (Figure 2.3). Porphyry unit IV forms greater than 50% of the main igneous centre, the whole of Wallaby Tail, and also occurs as a separate large body to the east of the Mt. Leyshon breccia (Figure 2.3).

Both units are distinctive due to the difference in their phenocryst proportion (Tables 2.2 and 6.1) and good outcrop, although porphyry unit III appears to show "diachronous" relationships. The northern zone of porphyry unit III occurs as blocks in porphyry unit IV (Figure 2.3b), and flow banding in unit IV is oblique to and truncates unit III. For example, at GR 3775 5300, flow banding in porphyry unit III, which trends 005 / 80E, is truncated by porphyry unit IV which trends 167 / 75W. At this locality, these relationships suggest that porphyry unit III was essentially solid during invasion by porphyry unit IV. However, in outcrop of the eastern zone, which is only 60 metres lower in elevation (eg. GR 4100 5170; Figure 2.3b), narrow fingers of porphyry unit IV (typically 5 - 20 millimetres thick), network into porphyry unit III along and oblique to flow banding. Elsewhere in the eastern zone (eg. GR 4080 5305), both units have a sharp but unchilled contact, subparallel flow banding.

These field observations were subsequently confirmed by a cored intersection (MLD 230) through an intricate zone of igneous units. Both units occur as separate bodies in this zone and also as an interconnected region, where unit IV networks into unit III, causing mixing of phenocrysts at the inter-fingering contact only (Plate 2.20). Therefore, in the eastern zone the relationships between the two units suggest that their period of emplacement overlapped.

Finally, thermal effects associated with igneous intrusion in the complex are minimal to non-existent. At GR 3785 4868, a baked and disrupted zone adjacent to porphyry unit IV extends only 1.5 metres into the metasediment country rock.

### Late igneous dykes

Five late igneous dyke types are recognised here (Table 2.2, see Table 6.1 for details of their petrography), namely:

- (1) "sills".
- (2) "2 - 2 dykes".
- (3) "1 - 2 dykes".
- (4) "DG dykes".
- (5) "fine late dykes".

Only 1 - 2 dykes are recognised outside the north east corner of the complex (Figure 2.3; except for one fine late dyke which occurs at GR 4095 5500). At least two types of late dyke are spatially associated with breccia dykes and they usually intrude the breccia dyke or occupy a structure parallel to it. On Mt. Hope, fine late dykes are typically associated with breccia dykes and are texturally similar to igneous fragments which occur in the breccia dyke (see Plate 2.15).

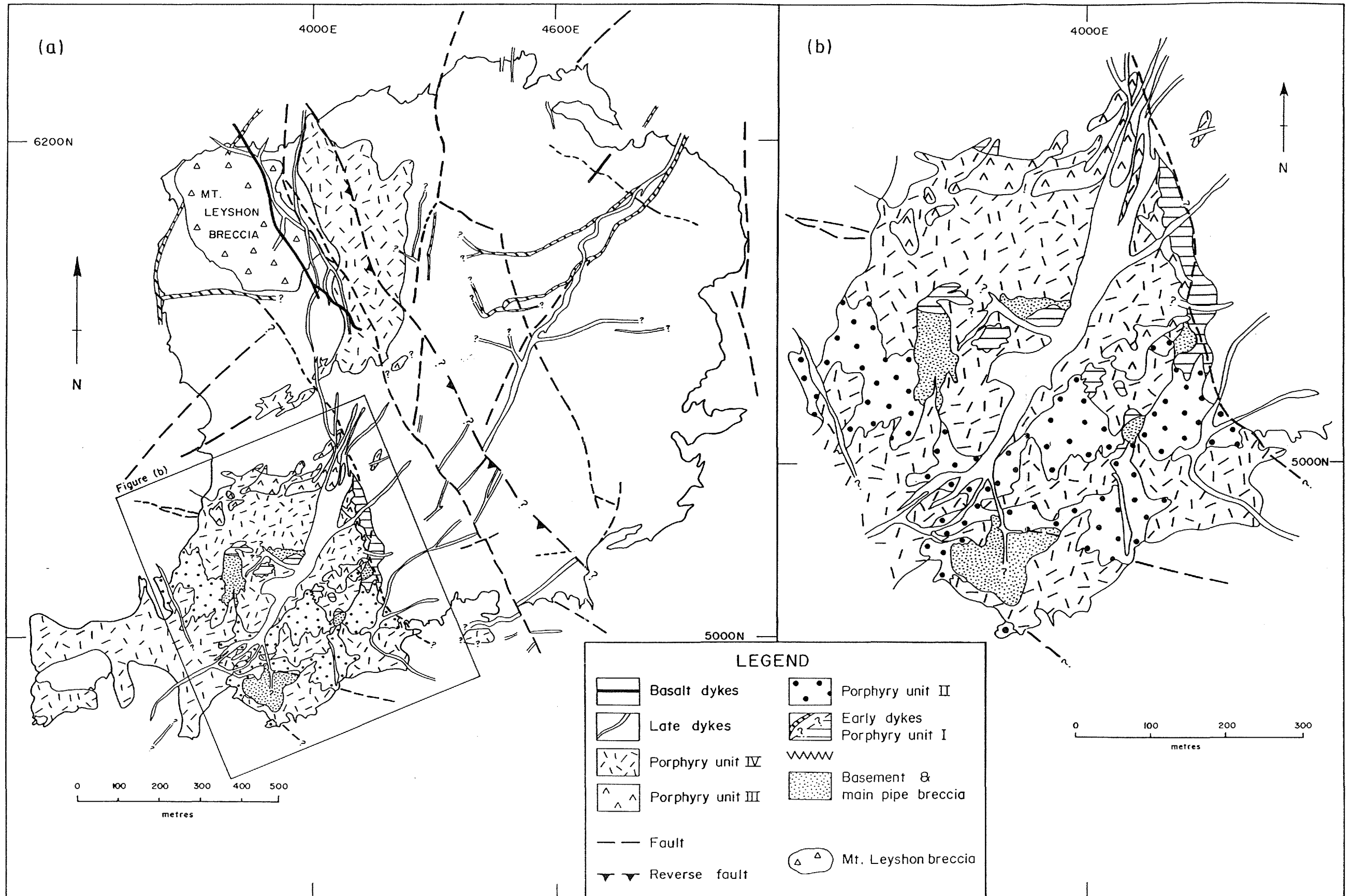


Figure 2.3: Facies relationships of the Mt. Leyshon igneous units within: (a) the whole complex, (b) an enlargement of the main igneous centre. The remaining area of the complex largely represents basement and main pipe breccia components. Note: (1) the concentration of the igneous units in the western half of the breccia complex, (2) the reverse fault which has thrust the western side of the complex up to the east, (3) the preferred orientation of the igneous units, and (4) the complex nature of the igneous facies contacts in the main igneous centre both with each other and basement.

### 2.3 TIME RELATIONSHIPS BETWEEN THE FACIES OF THE MT. LEYSHON COMPLEX

The time relations between units of the Mt. Leyshon breccia complex are presented in Figure 2.4. These relationships are based on cross-cutting contacts or the occurrence of breccia fragments of one unit in a later brecciation event. However, the timing of a few units cannot be fully resolved, and these are discussed in this section.

Porphyry unit I and early dykes both intrude main pipe breccia and predate the Mt. Leyshon breccia (in which they occur as fragments). The inferred time relationship between these two igneous units is based on the textural affinity of early dykes to later igneous units, in contrast to porphyry unit I. Geochemical characteristics of the two units discussed in Chapter 6 are consistent with this interpretation. The EP dyke intrudes the main pipe breccia and evidence from the mineral paragenesis (section 4.6) suggests that the EP dyke predates the early dykes. The EP dyke is inferred to predate porphyry unit I, based on the textural affinity of EP dyke to other intermediate igneous units, whereas porphyry unit I has no textural affinity.

Porphyry unit II and III both intrude porphyry unit I and are in turn intruded by porphyry unit IV, although, as described earlier, the emplacement history of unit III and IV overlap. The main body of porphyry unit IV is not seen to intrude the Mt. Leyshon breccia pipe because they are separated by a wedge of basement, and a reverse fault displaces the contact beneath this wedge down to the west (Chapter 3). However, detailed graphic logging (Chapter 5) located small zones of porphyry unit IV which intrude the Mt. Leyshon breccia. In addition, porphyry unit II, III and IV intrude the dyke-like zones of Mt. Leyshon breccia, SE of Mt. Hope (Plates 2.16 and 4.10).

A contact between the Mt. Hope and Mt. Leyshon breccias has not been observed. Despite the texturally distinct nature of these breccia units they may be contemporaneous. However, the facies characteristics of the Mt. Hope breccia strongly suggests it formed during the emplacement of porphyry unit IV (section 2.4). Sections and plans compiled from drill core beneath Mt. Hope (Figures 2.2a and 2.2b), suggest that the Mt. Leyshon breccia is intruded by the Mt. Hope breccia and porphyry unit IV. The sills subsequently intrude the Mt. Leyshon breccia and porphyry unit IV and are cross cut by tuffisite dykes. All other igneous late dykes postdate the tuffisite dykes but both predate and postdate late breccia dykes.

### 2.4 DISCUSSION OF FACIES RELATIONSHIPS IN THE MT. LEYSHON BRECCIA COMPLEX

In this section, a facies model is constructed for the Mt. Leyshon breccia complex. Aspects of this model are in disagreement with two previous descriptions of the Mt. Leyshon breccia complex geology. A derivative map indicating the sequential map scale development of the breccia complex is shown in Figure 2.5. The evolution of breccia and igneous units in the complex is divided into two main periods:

- (1) A period prior to and including main pipe breccia formation (Figures 2.5 A and B).

(2) A post-main pipe breccia period (Figures 2.5 C to F).

The facies relationships are illustrated in Figure 2.6, which represents an idealised and condensed east - west cross section across the breccia complex.

#### **2.4.1 Implications of the basement / main pipe breccia relationships**

Blocks of basement in the complex are extensively brecciated (to a crackle, mosaic or rubble texture), but display only limited rotation. Laznika (1988) described the common occurrence of a fragmentation progression (crackle to mixed breccia) when approaching a body of polymict breccia. This progression which is applicable to the Mt. Leyshon breccia complex in a general sense, has four textural types:

- (1) Crackle brecciated host (1 - 5% expansion, fracture mesh only).
- (2) Mosaic textured breccia (5 - 20% expansion, some fragment separation).
- (3) Rubble textured breccia (20 - 50% expansion, expanded in-situ breccia).
- (4) Mixed breccia (which results from fragment transportation).

The ubiquitous occurrence of these textures in host rock within the complex suggests considerable expansion (extension) of the basement units. However, a progression between the three host rock breccia textures and the main pipe breccia (mixed breccia), is only rarely seen in outcrop or drill core, and the degree of basement fragmentation in the complex is independent of distance from the main pipe breccia. Furthermore, the occurrence of weakly brecciated zones in rubble textured basement, which have geometrically different fracture systems, suggests at least two basement fracturing events occurred during the formation of the main pipe breccia. Further fragmentation occurred during formation of the polymict breccia. Therefore, three styles of host rock fragmentation are defined in the complex, based on outcrop mapping and the detailed facies analysis in Chapter 5:

- (1) First order - extensive areas of only partially fragmented basement containing fault and fracture meshes (Chapter 3).
- (2) Second order - erratic zones of expanded basement, commonly with splinter shaped fragments.
- (3) Third order - further host rock fragmentation and attrition of fragments during transport, resulting in a polymict breccia.

These observations imply a large region of crackle to rubble brecciated rock (2 by 1.5 kilometres at the present level) existed prior to the emplacement of the main pipe breccia. The Amargosa Chaos, a megabreccia in the Death Valley region, U.S.A., may have a similar configuration to the first order basement fracturing in the Mt. Leyshon complex. Noble (1941) described this megabreccia as consisting of large (mostly over 60 metres and up to 800 metres long), tightly packed, disordered blocks, with no fine matrix. Each fault bounded block is extensively fractured, yet the original bedding is clearly visible in each block.

The main pipe breccia forms a large complex body with inter-fingering and intrusive contacts to basement (Figures 2.5B and 2.6) rather than having margins defined by steep normal faults as

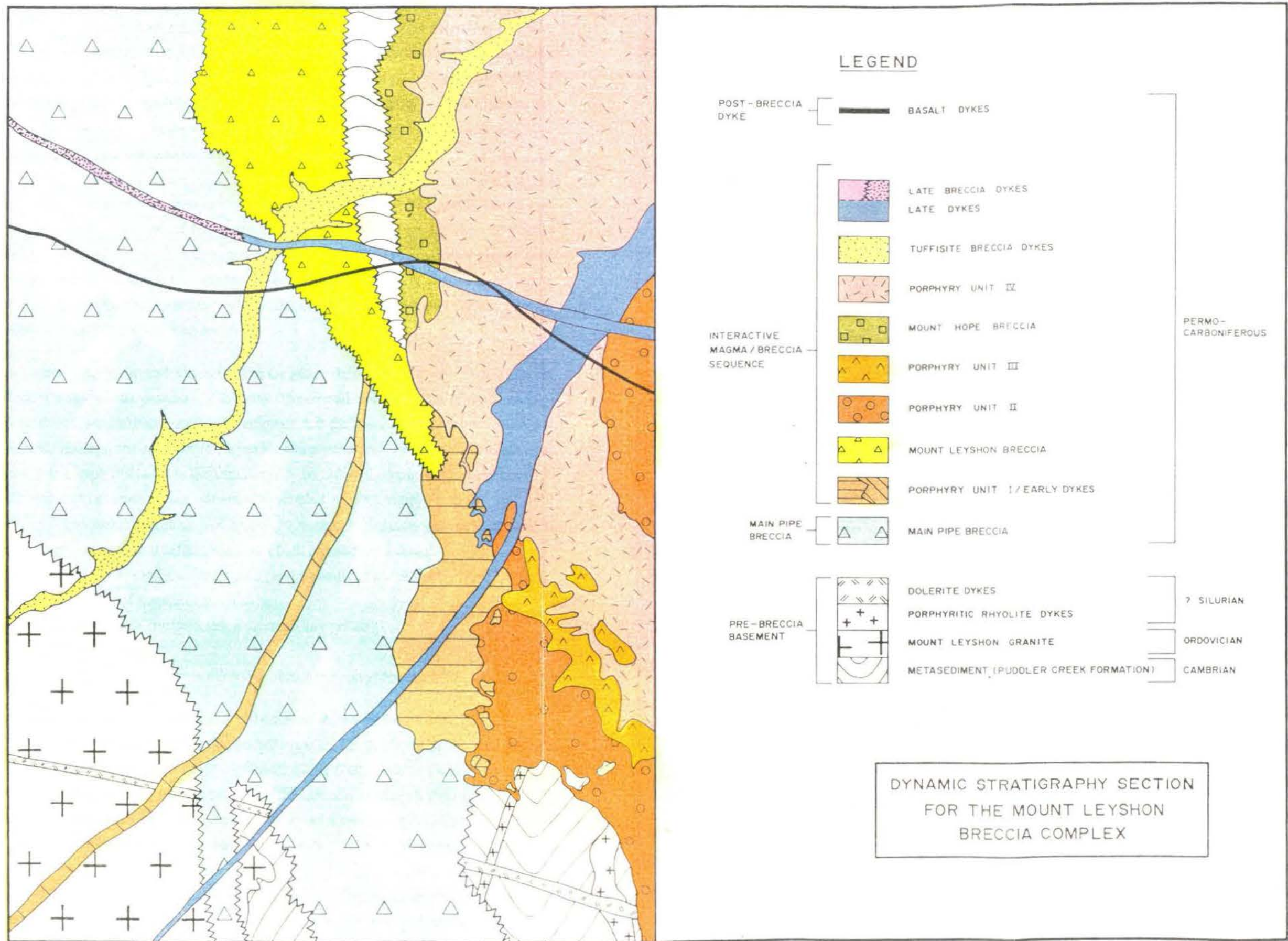


Figure 2.4: Facies timing within the Mt. Leyshon breccia complex. The diagram illustrates the cross cutting and crude spatial relationships between units in a cross section form and is not to scale. The late (igneous) sills which precede tuffisite breccia dykes are not shown on this diagram.

suggested by previous workers (Morrison et al., 1987 and 1988; Paull et al., 1990). The coarse and fine main pipe breccia facies have gradational and steeply dipping contacts indicating that they represent one unit, not separate vent breccia and lapilli tuff units of the previous interpretations. These observations preclude a pyroclastic mode of origin for the fine fragmental unit. With the exception of rare cognate igneous fragments, no other cognate or juvenile igneous material has been found in the main pipe breccia. A sparse rhyolite porphyry unit and sparse porphyry fragments in the main pipe breccia were interpreted by Morrison et al. (1987) to be the first stage of a coeval magmatic system. However, a pre-complex age for this unit is indicated here because the "sparse porphyry" is shown to form part of the basement (Figure 2.5A) and is cut by pre-complex dolerite dykes. Fragments of this sparse porphyry in the main pipe breccia obviously relate to this basement unit and are therefore accidental fragments. The provenance of granodiorite fragments in the main pipe breccia is unknown, though they are texturally similar to basement units which crop out four kilometres to the N of the complex and are presumably derived from an extension of this unit underlying the complex.

The intricate nature of the facies characteristics, and the geometry of the main pipe breccia (Figure 2.6) do not allow a simple interpretation of this unit. The overall characteristics of the main pipe breccia and its relationship to basement blocks suggests that the breccia resulted from sustained fragment mobility and upward transport of fragments along structures. Because the breccia does not have a juvenile component but is notably matrix rich, considerable disintegration and abrasion of host rock probably occurred during intrusion. A number of observations indicate that fluid dynamic processes operated during main pipe breccia formation, brecciation was accomplished in the presence of a fluid phase, and this fluid was under high pressure, as follows:

- (1) The presence of steeply dipping grading, layering and a possible flow fabric.
- (2) Moderate to high sorting of fragments and matrix.
- (3) Possible particle accretion during brecciation (accretionary pellets).
- (4) The absence of breccia cavities.
- (5) The presence of a fine clastic matrix in expanded but untransported basement.

Cloos (1941) describes the pervasive intrusion of host rock blocks by forceful injection of tuff to form the Schwabischen tuff slots (pipes; Western Germany). Large blocks of the well layered sedimentary host rock have been pervasively infiltrated along faults, fractures and fissures to the finest scale ("tuffified"), although the stratigraphy of the layers is preserved. According to Cloos (1941), the *in situ* infiltration represents the early stage in a dynamic progression, and as the process continues there is a gradual loosening of the infiltrated host rock, and passage of the passive components into the active (mobile) components. The observations of Cloos (1941) provide a classic description of the fragmentation characteristics formed by injection of a gas / tuff mixture into extensively deformed host rock. The tuff slots at Schwabischen are at an obviously higher crustal level to that inferred for the main pipe breccia, and all evidence indicates their formation involved a clastic juvenile magma / host rock mixture propelled by volcanic gas. In contrast, the clastic matrix injected into the host rock blocks and between the fragments in the

main pipe breccia is almost exclusively derived from break-up of the host rock. Nevertheless, the similarity in infiltration textures between the two systems supports the above observations, suggesting the main pipe breccia was partly the result of forceful injection of a fluid phase into basement. Such expanded and injected regions of host rock occur in the Mt. Leyshon breccia (Chapter 5) and locally at the margin of tuffisite breccia dykes (section 2.2.3.1), which despite their gross facies differences, provide a common thread between the origin of breccia units in the Mt. Leyshon complex.

Accretionary structures (pellets; Plates 2.5 and 2.9) present in the main pipe breccia have a questionable mode of formation. A pyroclastic mode of origin is precluded by:

- (1) The facies characteristics and relations documented here; specifically their occurrence within one gradational unit that has steeply dipping, intrusive contacts to basement.
- (2) Field outcrop suggests irregular circular surface distributions; drill core correlation also suggests they may be confined to slot-like features (<1 - >20 metres wide).
- (3) Drill core indicates the pellets occur over 400 metres of continuous "vertical stratigraphy" which is far too thick to have a simple pyroclastic mode of origin.

Figure 2.5: Derivative map based on Figure 2.1, to illustrate the sequential development of the main components within the Mt. Leyshon breccia complex.

**A. Basement relationships.** Note: (1) the orientation of early shear zones (see Chapter 3) and the position of the large basement rhyolite dyke body (compiled from its preserved distribution), and (2) the embayed nature of the granite / metasediment contact.

**B. Main pipe breccia generation.** The margin of the complex is shown as a dotted line. Close spaced dashes indicate blocks of basement. Note: (1) the distribution of the main pipe breccia with respect to the units shown in A, (2) the inter fingering nature of the main pipe breccia / basement contacts, and (3) the weakly brecciated (crackle to rubble texture) basement blocks.

**C. Pre Mt. Leyshon breccia igneous units.** Note the preferred orientation of these igneous units.

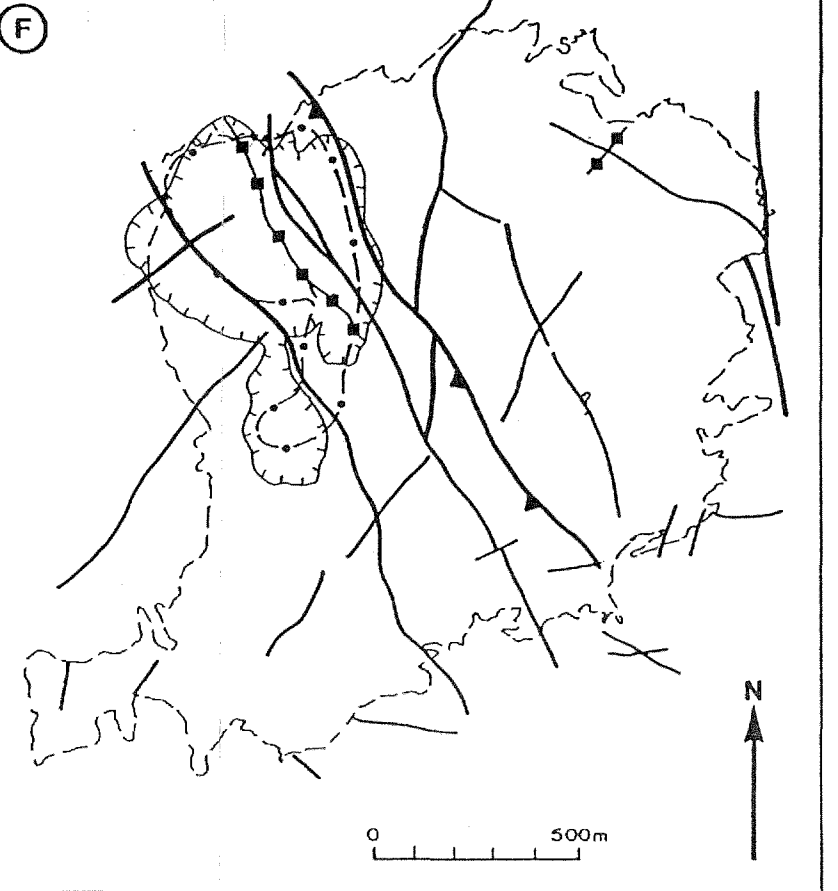
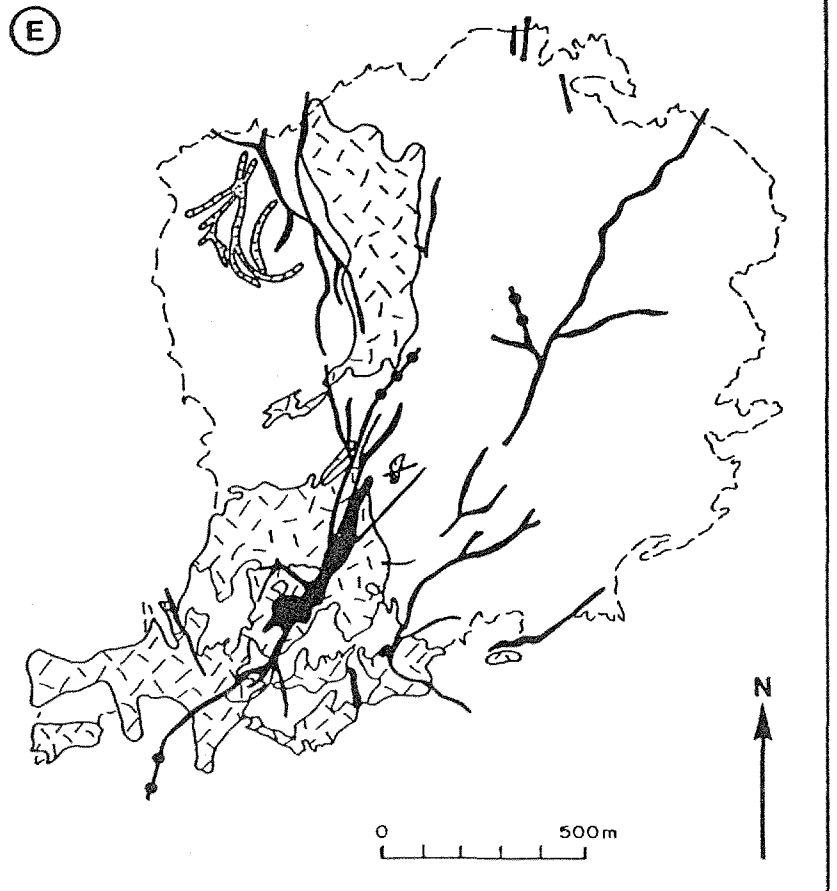
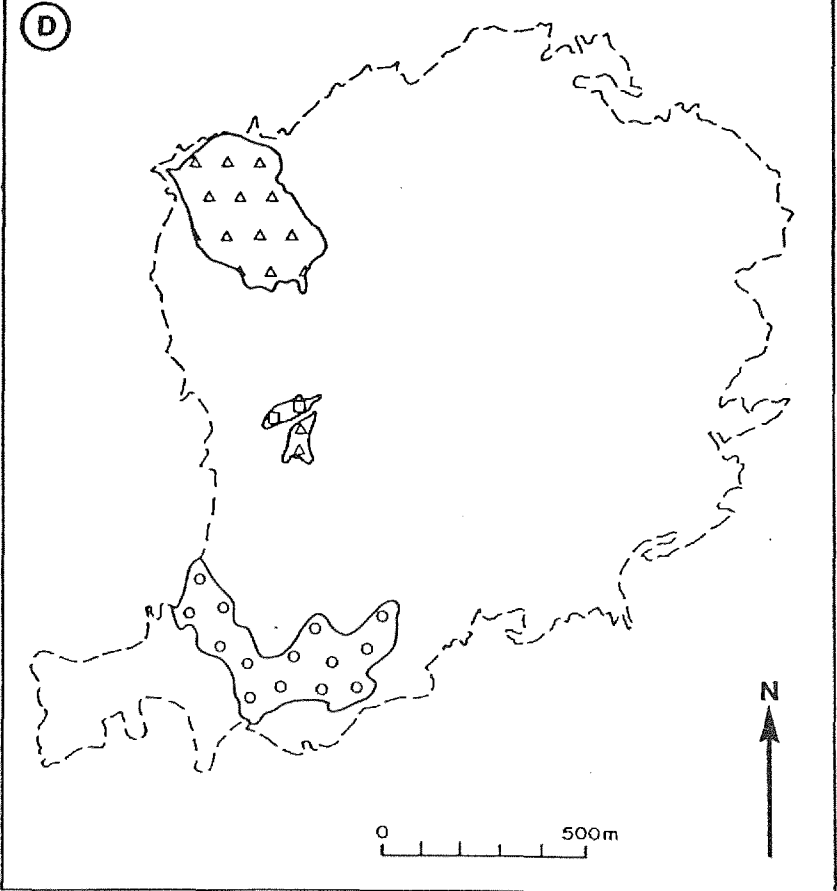
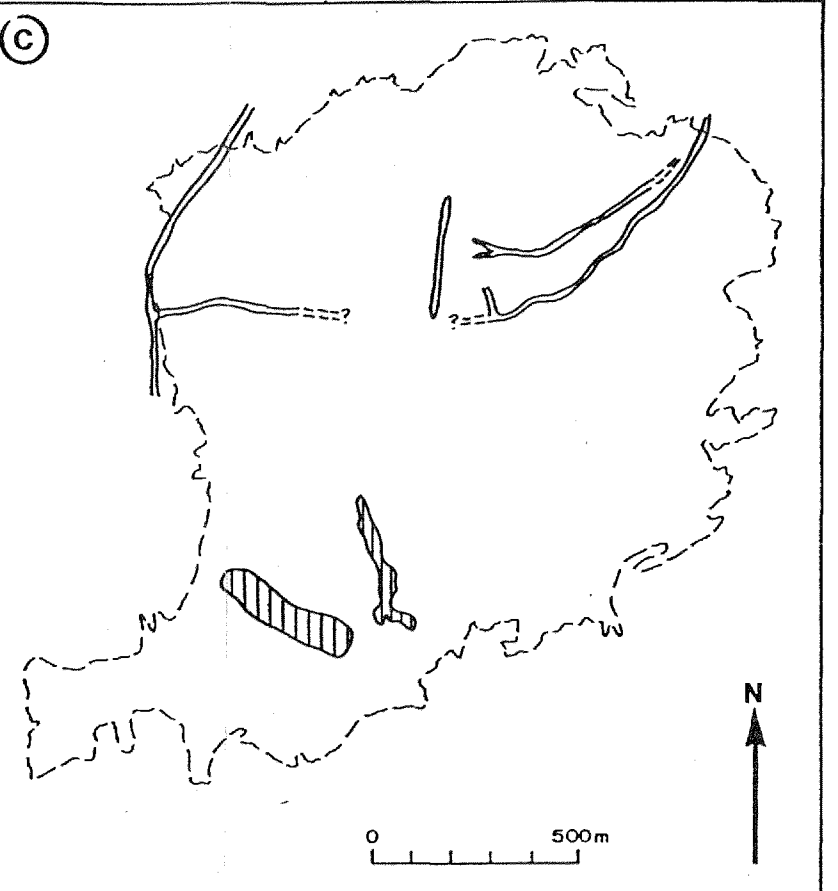
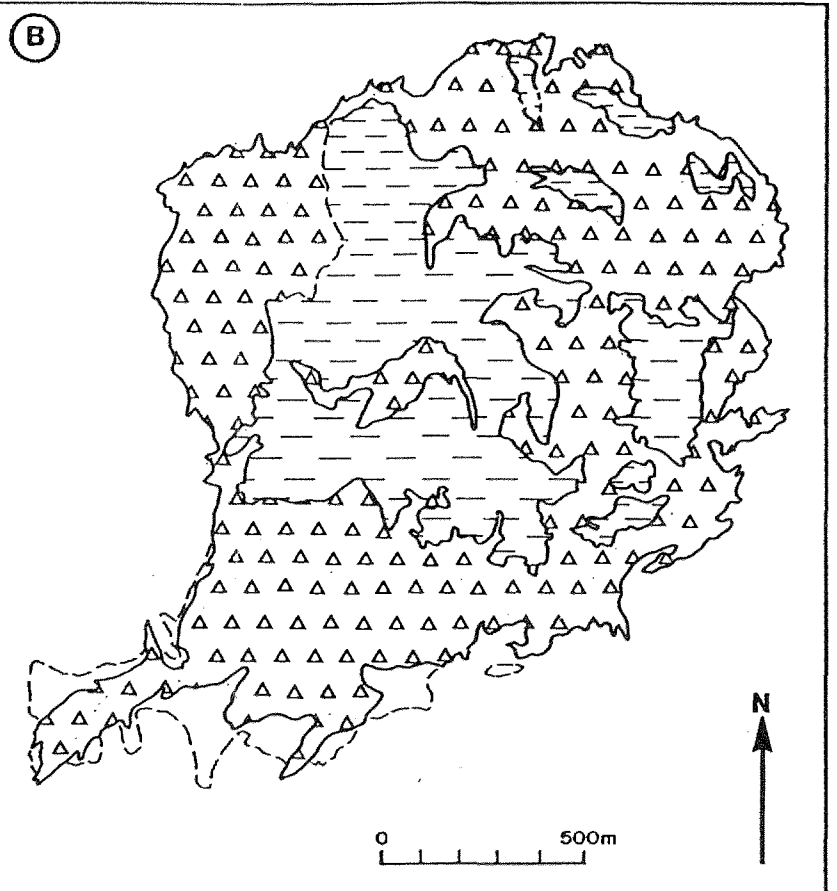
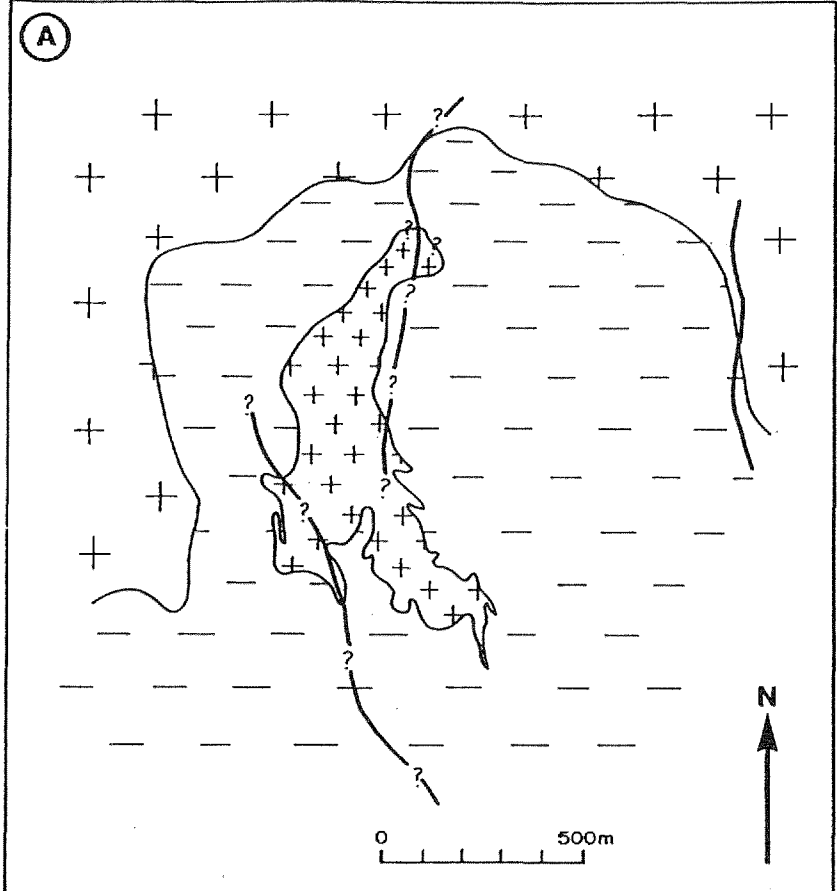
**D. Major interactive breccia units.** Note that the surface expression of these breccia units is confined to the western half of the breccia complex.

**E. Interactive igneous units.** Porphyry units II, III and IV show close spatial and temporal relationships to interactive breccia units. Also shown are the tuffisite breccia dykes, late igneous dykes and late breccia dykes. Note the change in igneous unit trend from predominantly N and E to NE.

**F. Syn to post breccia structures (see Chapter 3).** The post breccia basalt dykes are also shown. The open pit outline and the approximate limit of gold mineralisation is also shown.

#### LEGEND (Fig.2-5)

	MAIN PIPE BRECCIA		MT. HOPE BRECCIA		BASALT DYKES
	LARGE RHYOLITE DYKE BODY		PORPHYRY UNITS II, III & IV		LATE BRECCIA DYKES
	GRANITE		FRAGMENTAL COMPONENT OF PORPHYRY UNIT II		LATE DYKES
	METASEDIMENT (Rhyolite and dolerite dykes not shown)		MT. LEYSHON BRECCIA		TUFFISITE BRECCIA DYKES
			EARLY DYKES/PORPHYRY UNIT I		LATE DYKES
	FAULTS & SHEAR ZONES		PIT OUTLINE		APPROX. LIMIT OF THE GOLD MINERALIZATION



Observations presented in section 2.2.2 suggest they are not a product of alteration and instead formed by a process of particle accretion. Within the context of the facies relationships described in this Chapter, accretionary structures are interpreted to form during upward transport of fragmental material. The formation of accretionary structures in gas escape pipes from the base of ignimbrite sheets (Cas and Wright, 1987) and experimental modelling of gas streaming in pipes by McCallum (1985; which produced numerous accretionary pellets) supports this interpretation. Their occurrence in the main pipe breccia indicates their presence within a rock unit is not necessarily diagnostic of pyroclastic processes.

The following discussion is provided to suggest that the present geometry and characteristics of the main pipe breccia represent a frozen picture (time slice) of a rapidly changing dynamic system, resulting from high pressure fluid release. Despite the geometric complexity and textural diversity of the main pipe breccia, a given zone typically displays remarkable internal consistency. Furthermore, the geometry and characteristics of the main pipe breccia are consistently repeated at a number of scales (finger, outcrop, subfacies and whole body), suggesting its characteristics are scale invariant. Some understanding of how these characteristics relate to natural processes can be gained by considering recent work on other dynamic natural systems (Middleton, 1990). Scale invariant patterns of this type have been described by many workers investigating natural systems (eg. weather patterns and turbulent fluid flow) and the behaviour of these systems is found to be governed by non-linear partial differential equations (chaos theory; see Gleick, 1987). Recently, geoscientists have suggested that some geological phenomena are governed by the principles of non-linear dynamics. For example, Shaw (1988) has suggested that volcanic eruptions and their associated seismic tremors are non-linear dynamic systems.

Such non-linear systems have characteristics which help explain the geometry and facies characteristics of the main pipe breccia; these are:

- (1) They are very sensitive to the initial conditions, so that at a given instant their future behaviour cannot be predicted accurately far into the future or traced far into the past.
- (2) parts of a map produced by the system have regular, and other parts, highly irregular behaviour.
- (3) a small variation in a dynamic variable can push a meta-stable system into chaotic behaviour.

Thus, if the main pipe breccia was controlled by non-linear dynamics as is inferred here, then its geological expression is best understood by considering the characteristics of the whole system, rather than attempting to relate individual facies components to the evolution between the onset of catastrophic behaviour and the observed static distribution. These considerations help explain why some characteristics of the main pipe breccia are regular (fine or coarse variant), whereas other characteristics are highly irregular (overall chaotic geometry of the whole unit). Furthermore, the textural diversity within the main pipe breccia may be the result of non-linear dynamic behaviour of the controlling variables, which probably include the rate of energy (fluid) release and the energy distribution. Zones of main pipe breccia which oscillate between coarse and fine variants

over short distances may represent chaotic boundary conditions between regions of regular energy release. The processes responsible for this energy release are discussed in Chapter 7.

#### **2.4.2 Magma / breccia interaction: evidence for breccia generation during igneous emplacement**

The second major period of breccia complex evolution resulted in a contracted facies system (Figures 2.5C to E). Breccia and igneous units which postdate the main pipe breccia were predominantly emplaced in the western half of the complex, after the inter-breccia (later syn-complex) structures and early hydrothermal alteration (Chapters 3 and 4).

Porphyry unit I, EP dyke and early dykes were the first events of the second period of breccia formation, and the first igneous units emplaced into the complex; none were associated with an intrusive breccia forming event (Figure 2.5C). However, the early dykes immediately preceded an episode of quartz-molybdenite vein development (see Chapters 3 and 4). Subsequent igneous activity is closely associated with brecciation (Figures 2.5D and E). Porphyry unit II (fragment crowded) is distinct from xenolith bearing margins of other units, and is in part intruded by porphyry units III and IV. The interpretation of porphyry unit II facies relationships is questionable because breccias comprising fragments in an igneous matrix can have a number of origins. Igneous breccias have been reported in the literature from many localities, but few workers have considered their origin in detail. Sillitoe et al. (1975) reported polymict igneous breccias from the giant Llallagua tin deposit in Bolivia but their origin was not investigated. Sharp (1978) described monolithologic igneous breccias, consisting of blocks of feldspar in a swirl textured mass of feldspar matrix, from the Redwell Basin mineralised (Mo) complex in Colorado. He interpreted them as forming by the brecciation of an earlier intrusion by a later one, but the mechanism for this was not considered.

Goodspeed (1953) subdivided the various types of igneous breccias into three groups:

- (1) Igneous plutonic breccias.
- (2) Replacement breccias.
- (3) Rheomorphic breccias.

Many of his examples were from deeper levels in the crust than the Mt. Leyshon breccia complex, at depths where anatexis occur. He described igneous breccias as those consisting of fragments in a typical igneous matrix that may be chilled. Replacement and rheomorphic (when flowage appears to have occurred) breccias are formed by the progressive metamorphic replacement and feldspathisation of country rocks (groundmass microstructures typically have a crystalloblastic texture). The characteristics of porphyry unit II are similar to the igneous breccias described by Goodspeed (1953), however the origin of fragmentation in these breccias was not directly considered. Fragments in replacement and rheomorphic breccias were considered to have formed by replacement of a pre-existing cataclasite (fault) breccia. The chilled nature of porphyry unit II, the polymict nature of the fragments (many of which are subrounded), the rare zones of clastic

textured groundmass and inter-fragment cavities, suggest that porphyry unit II originally developed as a polymict intrusive breccia and was subsequently engulfed by the igneous groundmass. It is not known whether cataclasis played an early role in fragmentation. These observations imply that the clastic breccia was formed as a first stage to porphyry unit II emplacement and was subsequently reworked by the magmatic system, causing further fragmentation during the emplacement of the igneous material. Myers (1975) suggested that similar reduction in fragment size and rounding of fragments in igneous breccias within the coastal batholith of Peru was the result of turbulent gas flow and mechanical abrasion in the magma.

The Mt. Leyshon breccia (Figure 2.5D) and the fragmental component of porphyry unit II possibly formed contemporaneously because both the Mt. Leyshon breccia and porphyry unit II postdate porphyry unit I. However, the major textural differences between these fragmental units suggest that the porphyry unit II fragmental component does not represent zones of Mt. Leyshon breccia engulfed by the igneous component. Rather, the characteristics of the fragments in porphyry unit II suggest they resulted from a high degree of mixing and transport. The implications of the Mt. Leyshon breccia facies characteristics are discussed in Chapter 5.

Both the Mt. Leyshon breccia and porphyry unit II contain cognate igneous fragments indicating igneous emplacement prior to both these units. They are texturally similar to the later igneous units (including porphyry unit IV) but represent solidified igneous material which formed prior to the Mt. Leyshon breccia (but are not recognised as separate units). These fragments may be the result of failed, small scale intrusive igneous events which were rebrecciated and subsequently incorporated into the breccia units and ultimately porphyry unit II (as it reworked the breccia). Further local reworking of porphyry unit II has occurred where it is intruded by porphyry unit IV (and probably III). This has produced a complex zone which networks and grades into unit II (and small remnants of basement, main pipe breccia and porphyry unit I).

As described previously (section 2.2.3.2), porphyry unit III shows “diachronous” relationships suggesting porphyry units III and IV were simultaneously molten. Whether porphyry unit III was intruded as two pulses (northern and eastern zones), or merely cooled more slowly in the eastern zone, is unknown. Whatever the case, these relationships suggest that porphyry unit III coexisted with porphyry unit IV in a magma system and that both units generally remained separate from each other even during mutual intrusion. The igneous groundmass of porphyry unit II is similar in texture and mineralogy to unit III but contains smaller phenocrysts. This similarity and an earlier time of emplacement, suggests that the igneous material forming the groundmass of unit II possibly coexisted with units III and IV, if all three units resided in a magma chamber. These observations could be used to support a zoned magma chamber beneath the breccia complex consisting of chilled units (porphyry units II and III) transitional to the crowded porphyry unit IV. Similar complex magmatic behaviour to the Mt. Leyshon system is described by Carter (1969) in a classic paper on the Cloudy Pass batholith, North Cascade Mountains, Washington. The batholith has associated porphyry plugs, intrusive and igneous breccias and a chilled porphyry complex

comprising separately injected and contrasting layers of porphyry. These layers are fluidly intermixed, but at higher levels have sharp contacts and behave as dyke like bodies. The chilled complex has both sharp and gradational contacts with the main granodiorite batholith. Intrusive and igneous breccias in both the Mt. Leyshon and Cloudy Pass complexes appear to be closely related to the emplacement of a chilled complex. It is unlikely that this chilling occurred by heat loss to the wall rocks alone, hence the development of chilled facies provides evidence for brecciation processes in the Mt. Leyshon complex as discussed in Chapter 7.

The following facies characteristics imply that the Mt. Hope breccia (Figure 2.5D) formed during the emplacement of porphyry unit IV:

- (1) The occurrence of fragments texturally identical to porphyry unit IV within the Mt. Hope breccia.
- (2) The sheath - like geometry of Mt. Hope breccia around porphyry unit IV.
- (3) the intrusion of the Mt. Hope breccia by porphyry unit IV.

The Mt. Hope breccia facies characteristics suggest material transport and mixing in an expanded, elliptically shaped zone. These relationships could indicate the Mt. Hope breccia developed as an intrusive breccia, driven by a fluid phase, released from porphyry unit IV as it was emplaced.

Considered together, these observations on the second period of the complex suggest a close relationship between igneous emplacement and breccia generation. The data (section 2.2.3.2) also indicates that igneous units have a fairly uniform internal character and texture but with complex external facies relationships to other igneous and breccia units. This is in contrast to the description of Morrison et al. (1987) who envisaged a series of zoned porphyry plugs passing from a crowded core through normal porphyry, then fragmental and tuffaceous porphyry, and to a sparse porphyry margin. Furthermore, the facies relationships allude to the chaotic nature of the magmatic system and indicate the short period of time separating the emplacement of the Mt. Leyshon breccia, porphyry unit II, III and IV, and the Mt. Hope breccia. The possibility that the Mt. Leyshon magma chamber was zoned has implications for the igneous unit geochemistry discussed in Chapter 6. In addition, these observations provide important constraints on possible magmatic processes during brecciation discussed in Chapter 7.

The final period of breccia and igneous emplacement in the complex was confined to dyke- or sill-like bodies. A period of subhorizontal igneous sill emplacement was followed by the formation of a series of irregular tuffisite breccia dykes. Tuffisite breccia dykes have facies characteristics strongly suggesting they resulted from a gas / solids mobilisation process because of the similarities with those produced by the gas streaming experiments of McCallum (1985). Similar facies characteristics (grading and layering in well sorted units injected into host rock) to the tuffisite breccia dykes were described by Cloos (1941), in the Schwabischen tuff pipes (western Germany). Likewise, he interpreted "tuffisite" (literally any mixed rock) to have formed at least in part by a gas / solids mobilisation process. It is in this sense that the term tuffisite dyke has been used here, and it is not intended to infer a tuff or pyroclastic origin or mode of fragmentation.

The fine tuffisite dykes are extraordinary because they are composed of > 99% igneous material which is geochemically and texturally similar to 2 - 2 dykes and thus is at least cognate. However, the interpretation of the origin of the fine tuffisite material is questionable because, despite the chilled nature of the fine particles, plastic deformation indicative of active magma quenching during disintegration, are absent. The presence of juvenile igneous material (plastically deformed fragments) in late breccia dykes strongly suggests they formed by gas release and magma fragmentation during late igneous dyke emplacement. Several workers (eg. Hazlitt and Thompson, 1980; Sillitoe, 1985) have suggested a similar origin for plastically deformed fragments in other breccias. Coarse and medium tuffisites are dominated by earlier (basement and cognate) fragments but the texture of the fine matrix material (despite the alteration) suggests that at least part is derived from fine tuffisite dykes. Most fragments are derived from their host rocks, yet they are well rounded and graded, suggesting transport of material in the coarse or medium tuffisite dykes is restricted. In contrast, fine tuffisite material was implicitly derived from the Mt. Leyshon magma chamber beneath the complex, with magma and gas travelling together during brecciation and intrusion. Consequently, coarse and medium tuffisite dykes may represent the first stages of tuffisite dyke development resulting from the early stages of gas / solids mobilisation (fixed bed agitation), whereas fine tuffisite dykes probably represent transported (fluidised) breccias.

Before a facies model is presented for the Mt. Leyshon breccia complex, two further aspects of the facies relationships require attention:

- (1) The facies evidence for the depth of emplacement.
- (2) The nature of false pyroclastic textures in the complex which have previously resulted in misinterpretation.

There is no unambiguous evidence for pyroclastic lithologies in the Mt. Leyshon breccia complex. In Chapter 7 several independent lines of evidence are presented which suggest that the breccia complex formed at depths of at least two to three kilometres. At the present level of exposure there is no evidence that the breccia complex vented during the main pipe breccia event, although it is likely that at least volatiles may have escaped from the extensive fault and fracture system which was active during the formation of the complex. In diatremes, "a vent produced by volcanic explosion", as defined by Daubree (1891; eg. Wau, Papua New Guinea; Sillitoe et al, 1984), fragmentation is by phreatomagmatic or phreatic processes, and blocks of pre-existing lithologies in such breccias have commonly rotated and collapsed into the pipe (Cloos, 1941; Lorenz, 1975; Sillitoe et al., 1984). Juvenile igneous material is abundant in these diatreme breccias and may be represented by variably vesiculated and shard-like debris indicating fragmentation and explosion was the result of water/magma interaction (Cas and Wright, 1987; Laznika, 1988; White, 1991). In addition, diatremes commonly have an upward flaring geometry and smooth striated walls (Novikov and Slobodskoy, 1979). No evidence for these facies characteristics or processes have been found in the Mt. Leyshon complex.

Later breccia units in the complex are unlikely to have reached the surface for the following reasons. A minimum amount of erosion can be estimated above the Mt. Leyshon breccia pipe by using the sill (Figure 5.3) to reconstruct Mt. Leyshon relative to Mt. Mawe (ie. removing the effect of the reverse fault described in Chapter 3). The reconstructed elevation difference is approximately 180 metres. If the dip of the western and eastern pipe margins are projected upwards (and the apex is rounded off) then the pipe closes off approximately 170 metres above its present level (T. Orr, written communication). It is far more likely that since the Carboniferous erosion was in excess of the minimum indicated by the fault offset, and therefore it is postulated the Mt. Leyshon breccia did not reach the surface. Fine tuffisite breccia dykes have facies characteristics indicative of fluidisation processes (restricted definition of Wolfe, 1980). As noted by Wolfe (1980), fluidisation in industrial applications is only achieved under certain boundary conditions. These conditions require that the system is essentially closed to material transfer. Assuming these conditions are also required for fluidisation in natural systems, these characteristics would not have been developed if the fine tuffisite dykes had reached the surface.

Previous workers established several pyroclastic units within the Mt. Leyshon complex, in addition to lapilli tuff (fine main pipe breccia) discussed previously. These units justified the interpretation of the complex as a near surface diatreme with a pyroclastic apron. This is contrary to the field mapping and drill core observations presented in Wormald et al. (1991) and this Chapter. Critical evidence indicating other pyroclastic units previously identified at Mt. Leyshon represent intrusive igneous and breccia units (with textures modified by hydrothermal alteration) is summarised below:

- (1) The apron breccia of Morrison et al. (1987) has a pipe-like geometry and abundant fragmentation progressions and jigsaw fit textures (Mt. Leyshon breccia, detailed in Chapter 5).
- (2) The rocks previously described as ash tuff and lithic lapilli tuff (Paull et al., 1990) commonly grade into crackle brecciated metasediment. The bleached "tuffaceous" nature of these zones results from strong sericite alteration of brecciated metasediment.
- (3) Paul et al. (1990) describe extensive areas of crystal tuff in the Mt. Leyshon breccia complex. However, this unit has steeply dipping intrusive contacts with chilled and xenolith bearing margins. The false pyroclastic texture of this unit (Plate 2.21) results from primary igneous resorption and strong differential alteration (sericite, carbonate, clay). Similar textures have been reinterpreted as altered coherent igneous units rather than pyroclastic units elsewhere in Australia (eg. Benambra, NSW; Allen, 1988).

These observations suggest the possibility that other units in some ore forming environments, which are presently considered to have a volcanic (pyroclastic) origin, may represent intrusive igneous and breccia units. Elsewhere in NE Queensland, many of the rocks previously considered to be pyroclastic at Pajingo Gold Mine have characteristics of brecciated and altered porphyry intrusives (J. V. Wright and P. J. Wormald, pers. observations, 1990).

### 2.4.3 A facies model for the Mt. Leyshon breccia complex

A facies model for the formation of the breccia complex is based on the following points (Figure 2.6):

- Zones of basement within the complex are brecciated with a crackle to rubble texture, although they are commonly internally consistent (as indicated by the continuity of dolerite and rhyolite dykes). Cleavage orientations indicate blocks have undergone only limited rotation (see Chapter 3).
- The preservation of two geometrically different fracture networks (in basement), suggests at least two stages of fragmentation occurred prior to the emplacement of the main pipe breccia. Considerable expansion of basement occurred during these two episodes and fragmentation was concentrated in metasediment. The rheology of the metasediment, and the presence of abundant discontinuities in this unit favoured brecciation.
- The main pipe breccia has intrusive, inter-fingering contacts to both the margins of the complex and basement blocks within the complex. Overall the unit has an antler-like geometry.
- The overall facies characteristics of the main pipe breccia suggest it resulted from prolonged and complex energy release involving a fluid phase. This fluid both mobilised and transported fragments upwards along structures.
- The two subfacies of the main pipe breccia (fine and coarse variants) are distinct units but have gradational, steeply dipping and intrusive contacts. Commonly they are uniform zones or gradually change over tens to hundreds of metres but locally the main pipe breccia oscillates between fine and coarse variants over short distances.
- Rare non-vesiculated cognate igneous fragments in the main pipe breccia suggest a well established magma chamber existed prior to the formation of the main pipe breccia. A juvenile igneous component has not been identified in the main pipe breccia.
- Accretionary structures which occur predominantly in the fine facies variant of the main pipe breccia suggest particle accretion during breccia formation. Their presence in the main pipe breccia indicates that they are not necessarily diagnostic of pyroclastic lithologies.
  - Subsequent to main pipe breccia formation, the facies system contracted and magma was emplaced higher in the crust. Both igneous emplacement and brecciation were concentrated in the western half of the complex.
- An initially quiescent magmatic stage was followed by a dynamic and interactive stage in which there was a close link between igneous emplacement and breccia generation. Evidence for magma / breccia interaction is provided by a progressive increase in cognate and juvenile fragments in breccia units and the implied invasion of the fragmental component of porphyry unit II by the groundmass.
- The first brecciation events of this interactive stage (Mt. Leyshon and Mt. Hope breccias and the fragmental component of porphyry unit II) resulted in breccia pipes and breccia dykes. These were subsequently partly engulfed and reworked by the magmatic system.

- The facies relationships of the main igneous centre indicate textural diversity and simultaneously molten units, and suggest the possible existence of a zoned magma chamber during the interactive stage.
- The final breccia (tuffisite breccia dykes, late breccia dykes) and igneous events (sills, 2-2, 1-2, DG and fine late dykes) were focused into dyke- and sill-like bodies. The facies characteristics of the final breccia units suggest processes of gas / solids mobilisation and fluidisation controlled their formation.
- No unambiguous evidence for pyroclastic lithologies occurs in the complex, nor is there evidence that the complex vented. However, during brecciation volatile and energy loss presumably occurred through interaction with both the active fault and groundwater systems.
- Breccia units of the Mt. Leyshon complex invade host rock, resulting in a continuum of fragment sizes down to matrix. This invasion utilised fractures, faults, cleavage/bedding planes and, vein and dyke contacts (see Chapter 3). These characteristics and the presence of rounded and transported cognate igneous fragments indicate that the breccias are intrusive to host rock lithologies. Their combined features suggest the breccias formed during high pressure fluid discharge, rather than low pressure free discharge to the surface (see Chapter 7).
- Post cooling recrystallisation and alteration (see Chapter 4) formed false pyroclastic textures in the igneous units and resulted in misinterpretation of breccia complex units. Such textures are being increasingly recognised in global ore forming environments, and demand cautious interpretation of igneous and fragmental facies.

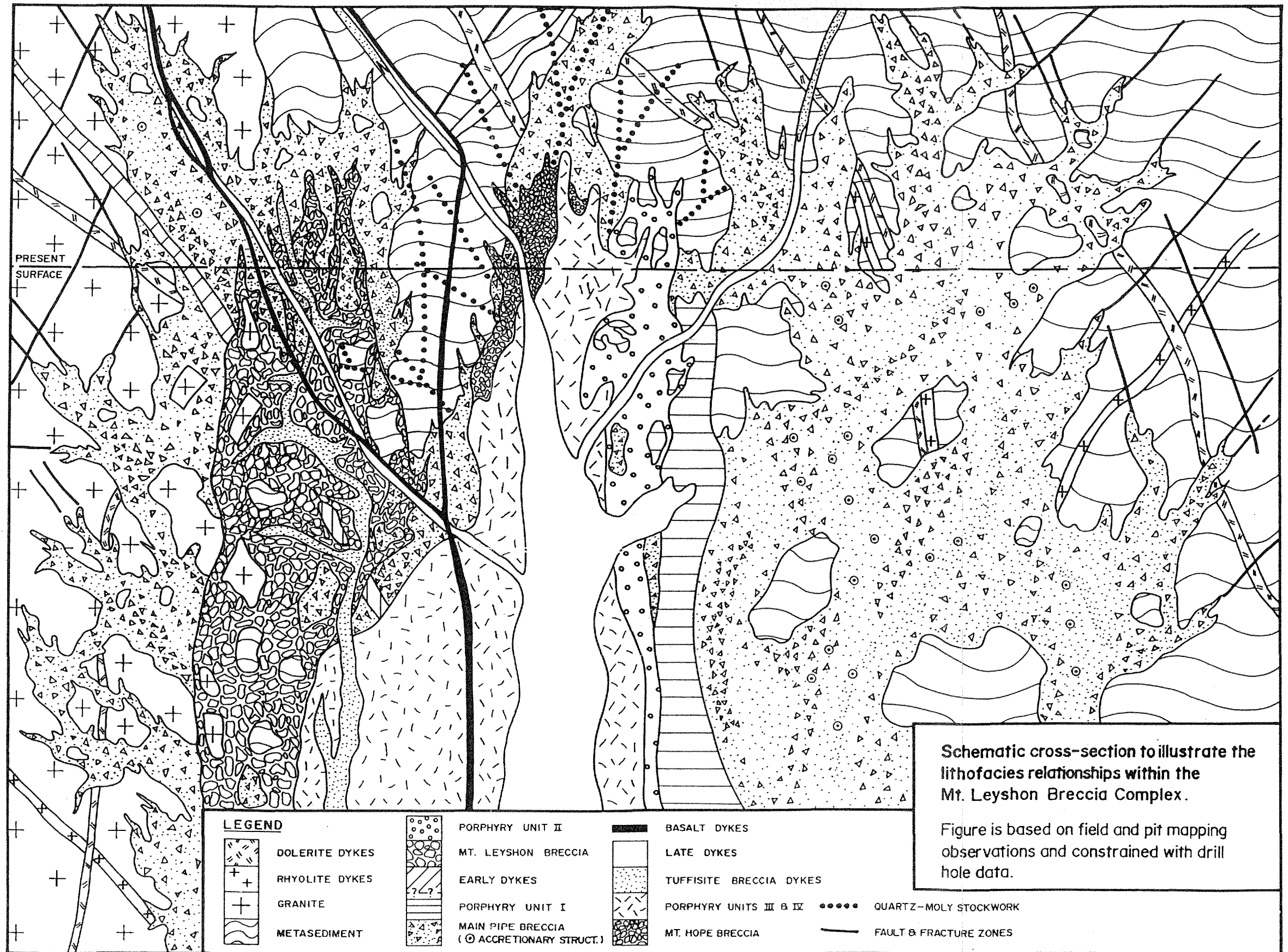


Figure 2.6: Lithofacies cross section. Syn to post complex faults are not shown for clarity. Note: (1) the little rotated basement blocks in the complex, (2) the steeply dipping, chaotic antler-like geometry of the main pipe breccia, (3) complex variation and gradation between main pipe breccia sub facies, (4) steeply dipping, interfingering porphyry contacts (true complexity of the igneous facies system is not depicted, see figure 3b), (5) spatial relationship between Mt. Hope breccia and porphyry unit IV, (6) gross textural difference between each of the main pipe, Mt. Leyshon and Mt. Hope breccias, and (7) the interfingering and intrusive nature of the tuffisite breccia dykes.



Plate 2.1: Crackle to rubble breccia texture in a basement rhyolite body . Crackle breccia (A) consists of a suborthogonal fracture pattern with only minor expansion. Irregular zones of mosaic breccia (at point of pen) show increased expansion and cuts across the crackle breccia. Rubble breccia (bottom left) forms irregular zones of highly fragmented and expanded rhyolite linking with the mosaic breccia.(GR. 4400 5550.)

Plate 2.2: Rubble textured metasediment (inside main pipe breccia). Note that despite brecciation and limited fragment mobilisation, siltstone layer (bottom, bedding visible in fragments) and sandstone layer have remained separate. Outcrop is 75 cm from top to bottom, looking due north. (GR. 4730 5240.)

Plate 2.3: Main pipe breccia / basement contact. Note that outside the main pipe breccia granite and dolerite are crackle brecciated (top of plate) but the original intrusive dolerite contact (at arrow) is preserved. A zone of rubble brecciated (expanded) granite and poorly developed main pipe breccia occur at the down hole contact of the dolerite dyke (A), and grade into well mixed coarse main pipe breccia (B). (MLD 177, 169.70 - 181.80 m.)

Plate 2.4: Coarse main pipe breccia (cut polished slab, western pit wall). Low matrix and tightly packed variant. Note the weak flow fabric defined by the long aspect ratio fragments (at a low angle to the photo base). Biotite / silica alteration imparts a black colouration to fragments and masked the breccia matrix. (Slab no. ST1)

Plate 2.5: Fine main pipe breccia . Note: (1) the gradational fragment size grading and layering (approx. 45° to core axis), and (2) the layers of flattened accretionary structures, predominantly in the higher matrix component (LHS).(MLD 156, 207.50 m.)



2.1



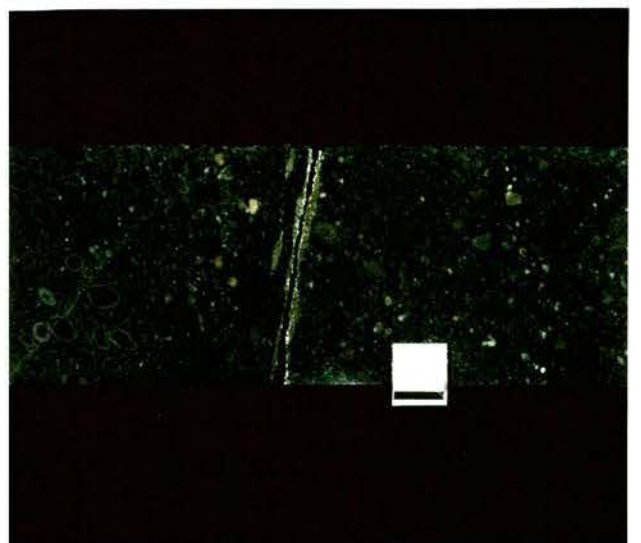
2.2



2.3



2.4



2.5



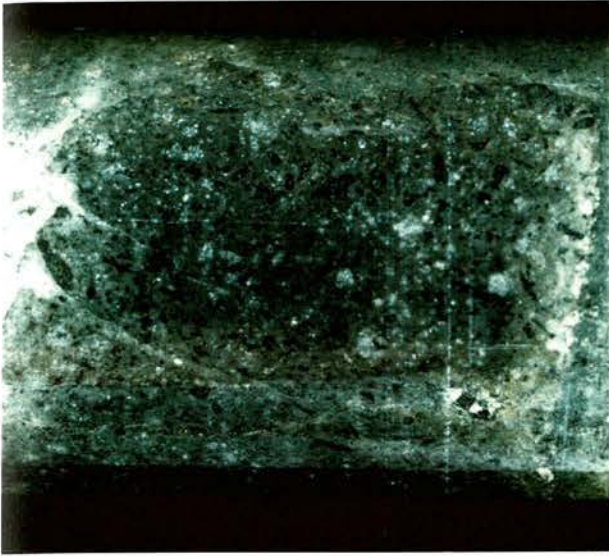
Plate 2.6: Cognate felsic igneous fragment in the fine main pipe breccia. Note the dark chlorite pseudomorphs which are after mafic phenocrysts, and the angular to embayed quartz phenocrysts which are similar to those in porphyry unit IV. (MLD 231, 224.3 m; back of core.)

Plate 2.7: Rare outcrop contact between coarse and fine variants of the main pipe breccia. Note: (1) abundant subangular to subrounded fragments in the coarse variant, which are absent from the fine variant (LHS), (2) steeply dipping and gradational nature of contact. (GR. 4670 5790.)

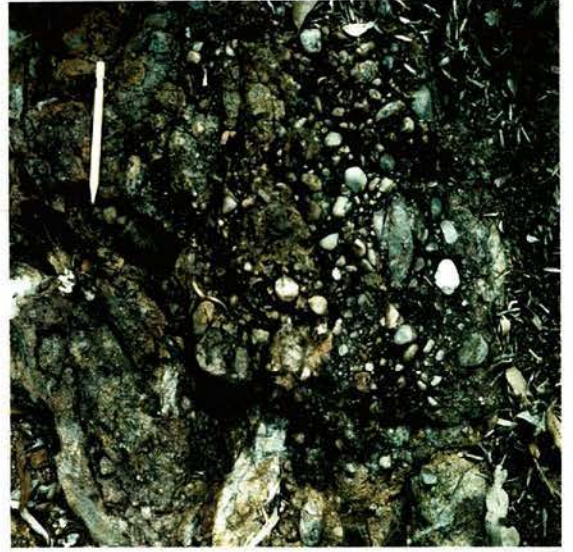
Plate 2.8: Common drill core contact between coarse and fine variants of the main pipe breccia . Note the fragment crowded nature of the coarse variant and the absence of large fragments and high matrix proportion in the fine variant. The gradational contact between the two variants occurs at the point where the large fragments cease (at arrow). (MLD 192, 196.80 - 202.30 m.)

Plate 2.9: Internal form of accretionary structures. Note: (1) the coarse grained nucleus (centre and lower left) is similar in composition to the breccia matrix outside the structure (top RHS), (2) the fine grained rim which contains small particles that are tangential to the circumference of the structure, and (3) the partial coarser grained layer in the rim (RHS). (photomicrograph, XPL, photo base = 8 mm, sample No. T/156/34)

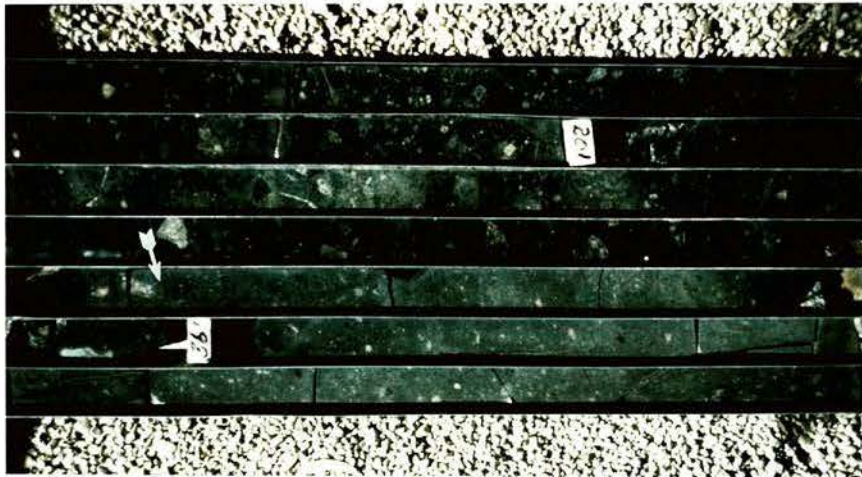
Plate 2.10: Porphyry unit IV intruding the Mt. Hope breccia. Note the inter-fingering nature of the porphyry unit IV contact and the false pyroclastic textures induced in the igneous unit by differential alteration. (MLD 153, 87.90 m.)



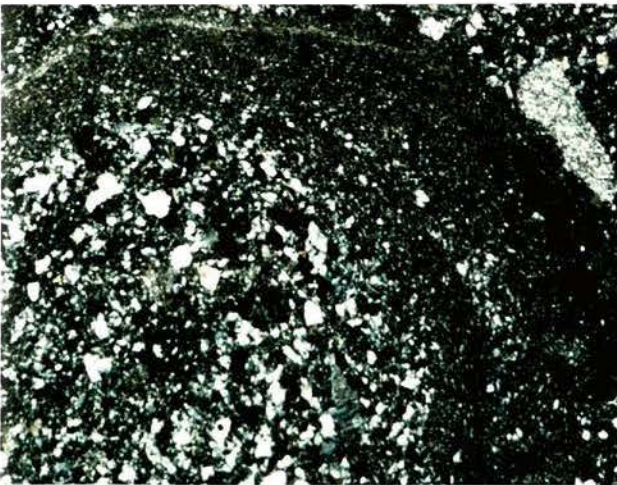
2.6



2.7



2.8



2.9



2.10



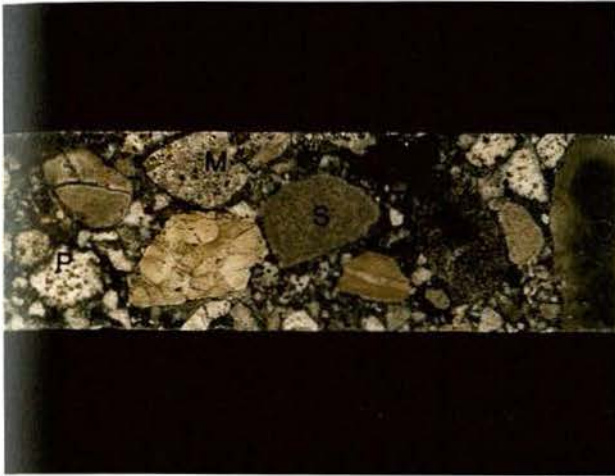
Plate 2.11: Mt. Hope breccia (polished drill core sample, MLD 232, 215 m). Note the subrounded to rounded fragments of metasediment (S), dolerite (D), main pipe breccia (M) and fragments texturally identical to porphyry unit IV (P; compare with Plate 2.10). The breccia matrix and fragments are altered and cemented by minerals which include, quartz, muscovite, pyrite, chlorite, siderite, sphalerite.

Plate 2.12: Fine tuffisite breccia dyke intruding Mt. Leyshon breccia (in the open pit). Note the steeply dipping intrusive contacts of the tuffisite breccia dyke. The RHS of the dyke has subsequently been reactivated during brittle faulting. Bench height is 10 metres. (Photograph courtesy of T. H. Orr.)

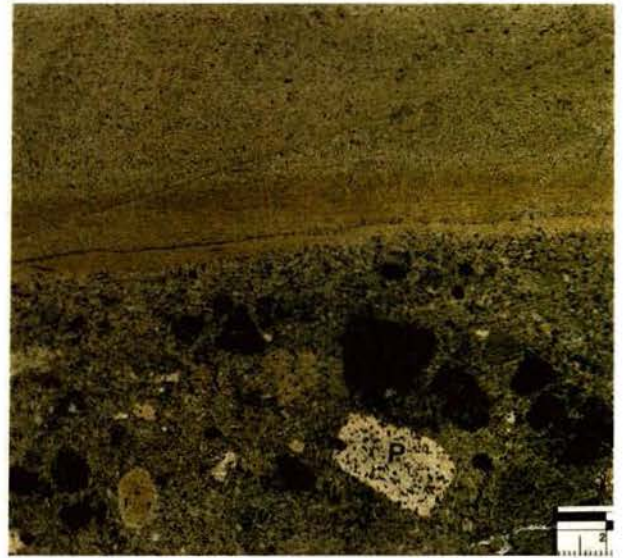
Plate 2.13: Tuffisite breccia dyke (coarse and fine variant; cut pit sample). The coarse variant consists of dolerite, metasediment, main pipe breccia and cognate igneous fragments (P) in a fine clastic matrix. The fine variant is composed almost entirely of igneous particles. Note: (1) the sharp, irregular contact between coarse and fine variants, (2) the fragment size grading of the coarse variant (and increase in sorting) towards the contact, and (3) the fine particulate nature and diffuse layering of the fine variant. (The line at 30° to layering is a saw-blade mark.)

Plate 2.14: Weakly altered fine tuffisite dyke . Note that the fine tuffisite dyke is composed of porphyritic igneous textured particles (P) and inter-particle phenocryst fragments (derived from the particles); quartz (Q), Kfeldspar (K) and biotite (B). (Photomicrograph, XPL, photo base = 5.2 mm, sample No. T/236/16.)

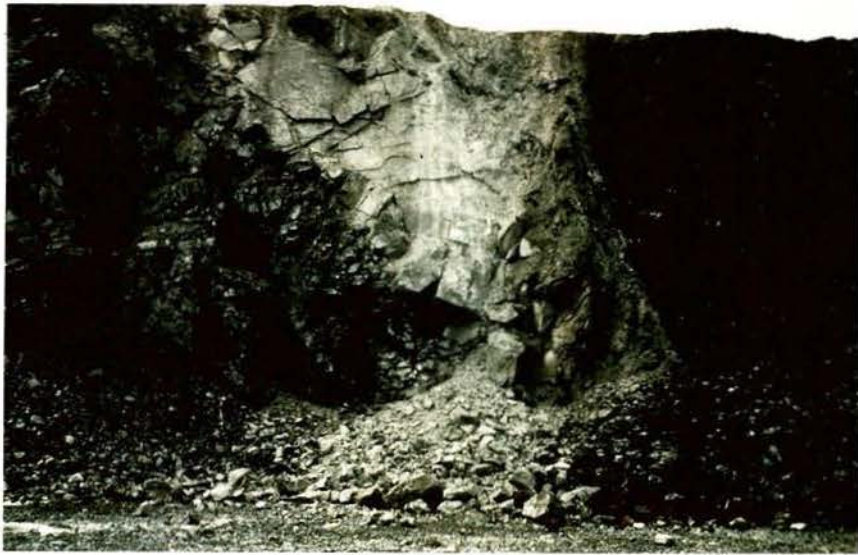
Plate 2.15: Typical late breccia dyke composed of dolerite, cognate and juvenile (J) igneous fragments. Note the ragged nature of the juvenile igneous fragment. Small networks (A) of a spatially and genetically associated late igneous dyke (strongly altered) intrude the breccia. (MLD 101, 172.50 m.)



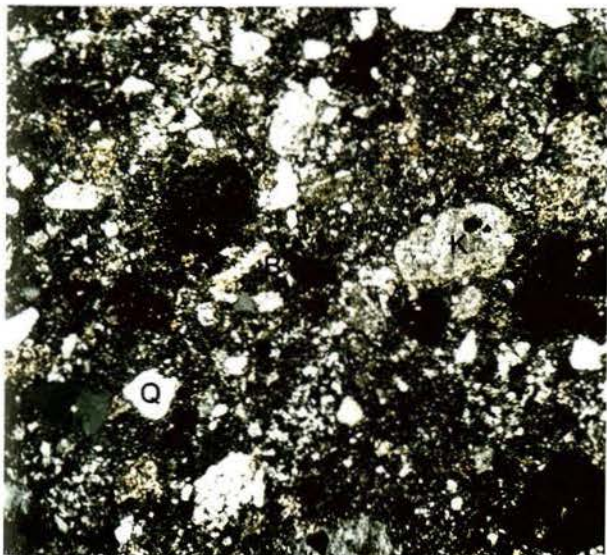
2.11



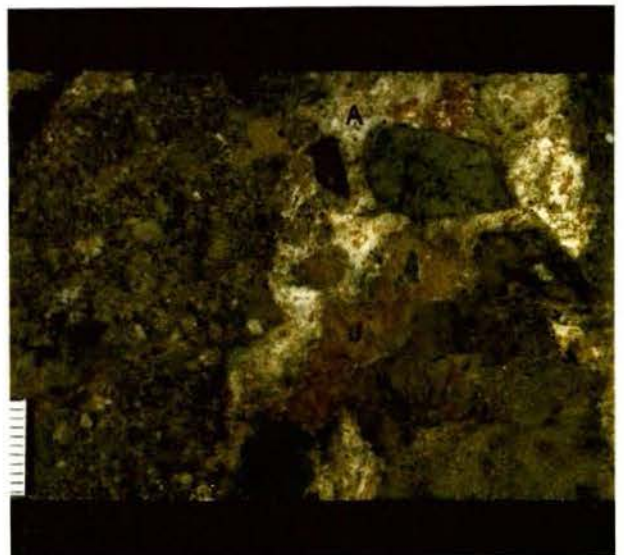
2.13



2.12



2.14



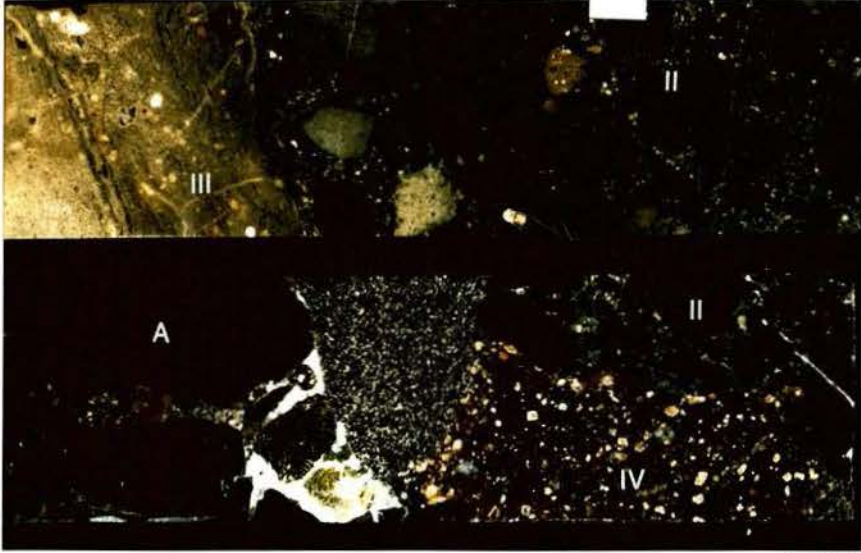
2.15



Plate 2.16: Time relations between Mt. Leyshon breccia and porphyry unit II-IV. Note: (1) Weakly altered Mt. Leyshon breccia (A) composed of dolerite and metasediment fragments, with epidote and calcite breccia infill. (2) Porphyry unit II (II), composed of crowded fragments in a phenocryst bearing igneous groundmass (arrow), partially invades Mt. Leyshon breccia. (3) Porphyry unit III (III) intrudes porphyry unit II with a sharp contact. (4) Porphyry unit IV (IV) intrudes Mt. Leyshon breccia and porphyry unit II. (MLD 230, top-102.75 m, bottom-130 m.)

Plate 2.17: Porphyry unit II intruding crackle brecciated metasediment. Note the following zones: (1) crackle brecciated metasediment with no igneous groundmass (A), (2) mosaic textured metasediment with minor expansion and igneous invasion (B) and, (3) rubble textured metasediment with a high degree of expansion in an igneous matrix (C). The fracture pattern in the crackle brecciated metasediment is angular in contrast to the subrounded fragmentation pattern present in the mosaic to rubble textured zones. (GR 4030 5015.)

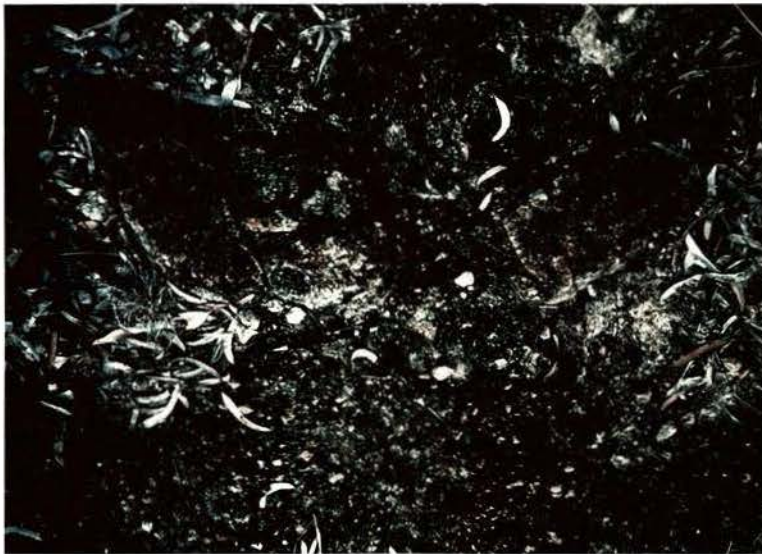
Plate 2.18: Porphyry unit II in the main igneous centre. Note: (1) The unit is fragment crowded and crops out as a breccia, and (2) larger cognate igneous fragments in the unit. Pen is 12 cm long. (GR. 4035 5000.)



2.16



2.17



2.18



Plate 2.19: Local matrix rich zone of a late breccia dyke. Note: (1) The lenticular, juvenile magma fragments (J) with chilled margins that are disintegrating in the breccia stream. (2) Phenocryst fragments (A) derived from the juvenile magma. (Photomicrograph, PPL, photo base = 4 mm, sample no. T/161/3.)

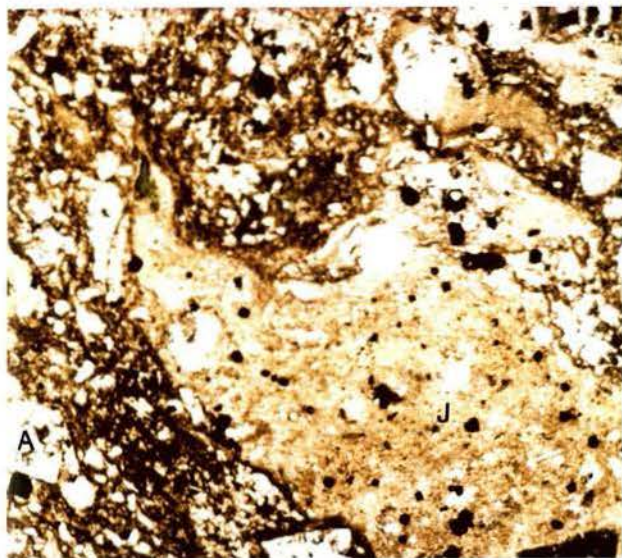
Plate 2.20: Porphyry unit IV networks invading porphyry unit III. Note: the highly irregular contacts between separate regions of unit III and IV, and local phenocryst mixing at contacts, suggesting they were simultaneously molten. (MLD 230, 148.70 m.)

Plate 2.21: False-pyroclastic textures in altered porphyry unit IV. Note: (1) Differential alteration (LHS) results in pseudofragmental texture, but porphyritic texture is partially preserved. (2) Uniform, intense alteration (RHS) produces fine “tuffaceous” appearance. (3) False unit contact resulting from alteration front separating textural styles. (MLD 156, 59.50 m.)

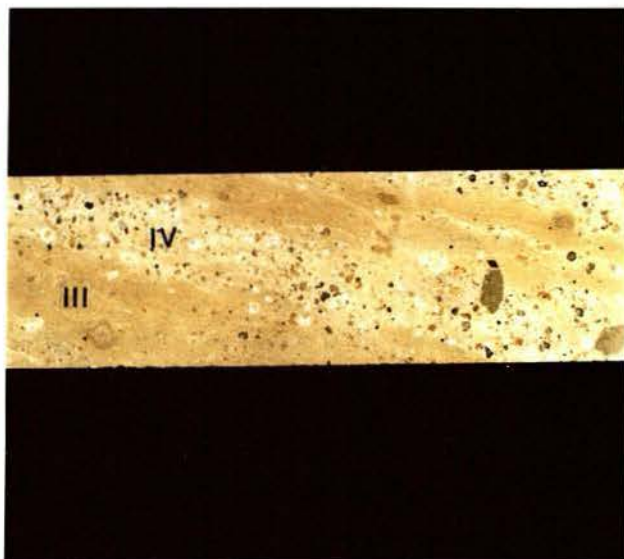
Plate 3.1: Bedding ( $S_0$ ) and cleavage ( $S_1$ ; subparallel to bedding) in crackle brecciated metasediment within the breccia complex. Bedding is visible in fragments at the base of the outcrop, and cleavage forms a penetrative fabric throughout the rock. (GR. 4750 5750.)

Plate 3.2: North trending mylonite zone deforming metasediment. This mylonite occurs at, and is parallel to, the eastern edge of the breccia complex. It has been reactivated in a brittle manner further to the north and controls main pipe breccia emplacement. (GR. 5075 5875.)

Plate 3.3: Intense zone of penetrative cleavage in the bank of a creek bed. Note that the intensity of cleavage formation increases towards the creek centre (RHS). A carbonate replaced cataclasite occupies the centre of the creek (not shown) and indicates that this ductile fault zone has been reactivated by brittle faulting. (GR. 4165 5135.)



2.19



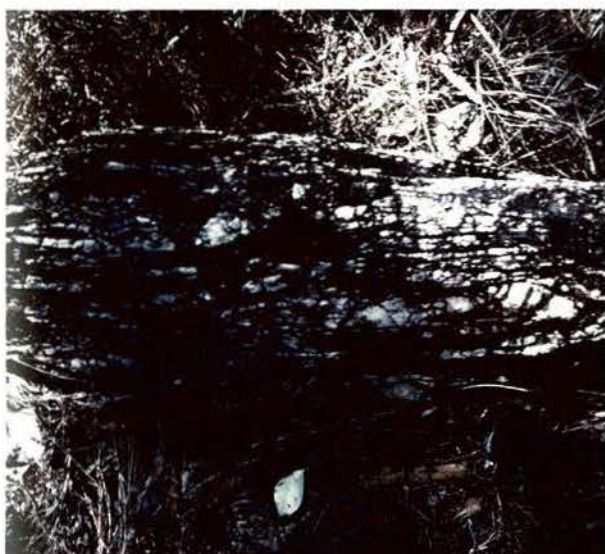
2.20



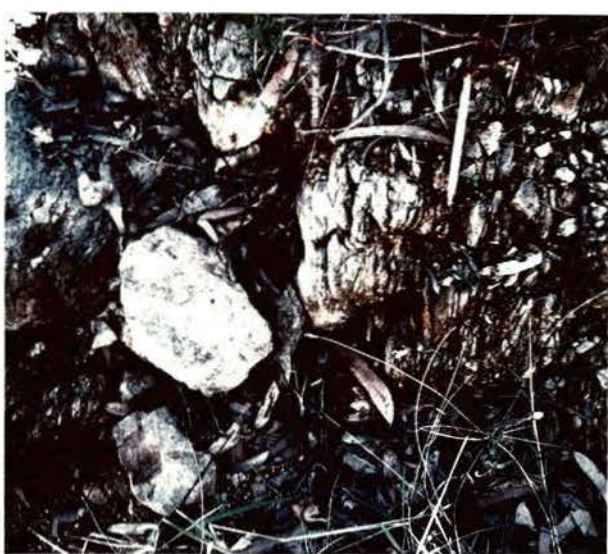
2.21



3.1



3.2



3.3

## Chapter 3

# STRUCTURAL SETTING OF THE MT. LEYSHON BRECCIA COMPLEX

---

### 3.1 INTRODUCTION

There are significant differences of opinion concerning the role of structure in the formation of breccia systems. Historically, most workers have considered that structures associated with breccia pipes are produced by igneous emplacement processes, rather than during regional deformation. Alternatively, faults are considered to act only as a pre-existing weakness for breccia pipe location. For example, in a classic paper describing the breccia pipe complex in the Redwell Basin, Colorado, Sharp (1978) noted the special relationship of steeply dipping normal faults which intersect at the location of the breccia pipe. Sharp (1978) however, emphasised the role of the magmatic system in the formation of the breccia pipe complex, and considered the faults only localised the complex. More recently, Sillitoe (1985) discounted the production of dilatant zones on major faults as a general mechanism of breccia pipe formation because fault control could not account for the ubiquitous association of alteration and mineralisation associated with breccia pipes. However, Lacy (1990) noted the importance of stress induced microfracturing along both high and low angle faults, and stated that this microfracturing was the first step in the formation of most breccias.

Indeed, there is some evidence in the literature that structure plays an inter-active role in the development of breccia pipes, in addition to fault breccias. In a study of more than one hundred intrusive breccia bodies associated with ore in the Warren mining district, Arizona, Bryant (1968) concluded that most breccias were controlled by movement along sinuous faults (including strike slip faults) which produced extensive regions of crackled and sheared ground. Mitcham (1974) emphasised the classic "room problem" in the formation of breccia pipes and proposed that many intrusive breccia pipes were produced as dilational zones on faults. The Olympic Dam breccia complex is of particular interest from the Australian perspective; major structural control is suggested for the formation of this breccia complex, which is interpreted to have resulted from the multi-phase interaction of faulting, dyke injection, and hydrothermal fluid flow (Sugden, 1989). A number of other workers have also emphasised the importance of faults and fault zones in the location and formation of breccia pipes (Kuhn, 1941; Novikov and Slobodskoy, 1979). The study by Sugden and Cross (1989) of the Olympic Dam breccia complex is the only published structural synthesis of a breccia complex known to the author in the available literature. This study clearly demonstrates structural control can have a bearing on the location and mechanism of breccia formation, and on the location of mineralisation within breccia pipes.

No previous work has been done on the structure of the Mt. Leyshon Breccia complex, although Wright (1990) speculated that the breccia complex was controlled by a dilational jog on a strike slip fault system. In this study structural data were collected on basement cleavages, faults, veins,

joints, preferred directions of both brecciation and igneous emplacement, from outcrop, pit mapping and oriented drill core logging within the Mt. Leyshon breccia complex. All directions quoted in this Chapter are in relation to true north. At the same time the author initiated a field based Masters project (Clayton, 1992) investigating basement structure around the Mt. Leyshon complex.

The aims of this chapter are to:

- (1) Place the Mt. Leyshon breccia complex within its regional structural framework.
- (2) Document the structures present within the Mt. Leyshon breccia complex.
- (3) Assess the role of structure on breccia complex formation.
- (4) Present a summary structural model.

The structural data presented in this Chapter have implications for breccia mechanisms (Chapter 7) and controls on gold mineralisation (Chapter 8), both within the complex and the surrounding region. They also have wider implications for the development of upper crustal intrusive breccia and igneous complexes in actively deforming crust.

### 3.2 REGIONAL STRUCTURAL FRAMEWORK

The main structural elements of NE Queensland are shown in Figure 1.1b and discussed in Murray et al. (1987). In this section, aerial photography is used to infer the regional structural framework around the Mt. Leyshon complex.

The aerial photograph interpretation (approximately 1 : 85 000 scale black and white photos) shown in Figure 3.1 stretches from the Gregory Development road in the west, to east of Seventy Mile Mount. The interpretation was based on observations that major topographic depressions and linear creek sections, commonly reflect fault zones (including those within the Mt. Leyshon breccia complex).

The regional linears fall largely into two populations - those greater than four kilometres, and those less than two kilometres. Generally only structures greater than four kilometres have been considered. Major linear features occurring in the region around the breccia complex have been divided into four groups based on their dominant orientation (Figure 3.1):

- (1) The northeast group - this group is dominant throughout the surveyed area and comprises linear features with two distinct orientations. The dominant and (typically longest) features in this group trend 045°. A second less abundant group of linear features trend 070°.
- (2) The southeast group - southeast oriented linear features typically trend 130°, although a number of shorter features trend between 150° and 160°. Southeast trending linears are not as common as the northeast linear features.
- (3) The north to north northeast group - this is the third most common orientation and the NNE linear features generally trend between 000° and 020°.
- (4) East to east southeast group - Linear features with this orientation are only poorly developed, are typically shorter than other linears ( $\leq 3$  kilometres) and trend between 090° and 110°.

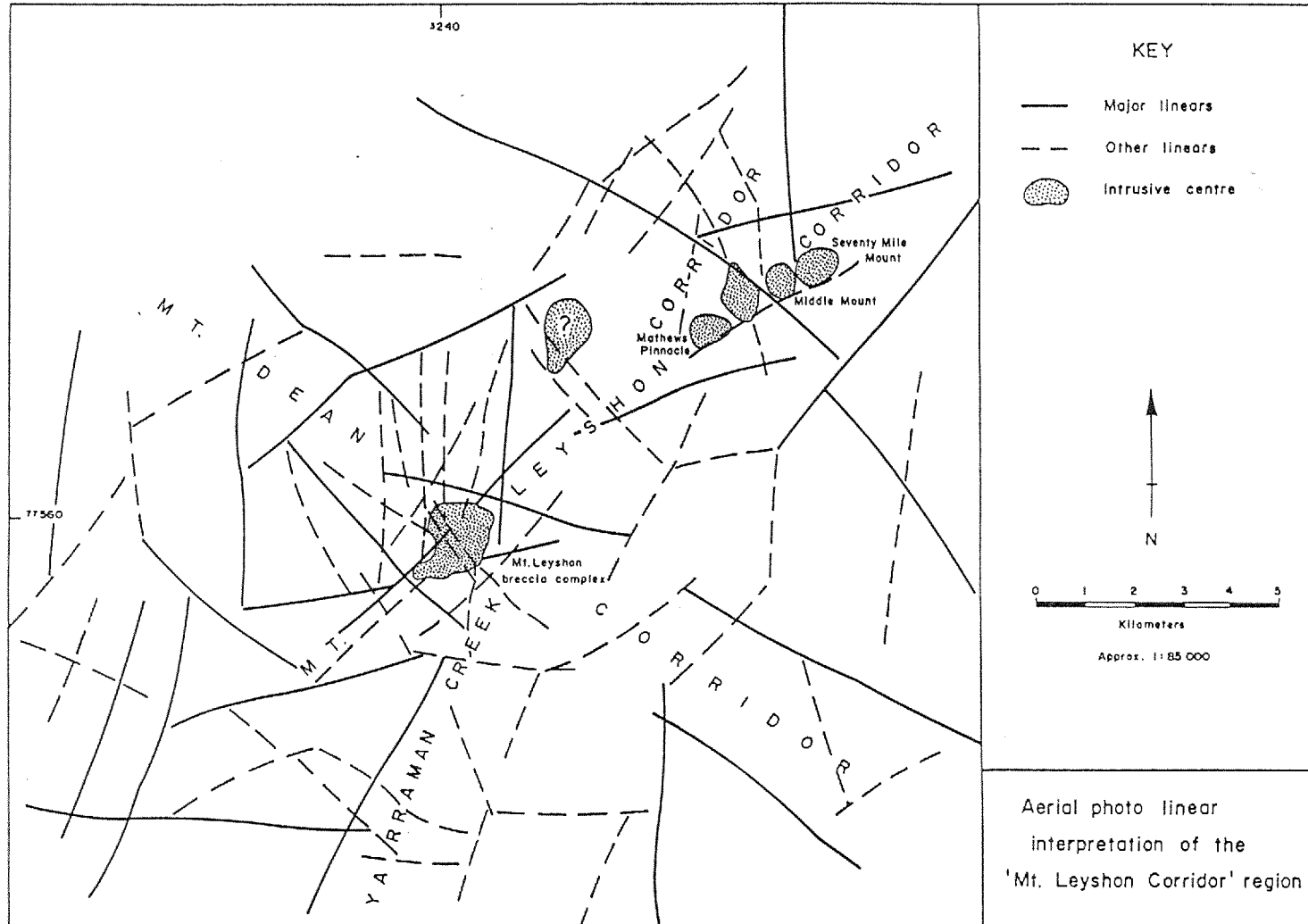


Figure 3.1: Regional aerial linear pattern around the Mt. Leyshon breccia complex. Note: (1) the dominant NE and SE orientation of linears in the area, (2) the increased density of linears which define the Mt. Leyshon and Mt. Dean corridors, (3) the local significance of N trending linears around intrusive centres, and (4) that only major linears are shown (generally > 4 kilometres in length).

A number of further observations are made concerning the regional linear pattern. An increase in density of NE, SE and NNE linears defines three main corridors (Figure 3.1). These are referred to here as the Mt. Leyshon corridor (NE), Mt. Dean corridor (SE) and the Yarraman Creek corridor (NNE). In addition, a second poorly defined SE trending aerial linear corridor probably straddles Mathews Pinnacle, and a second NNE trending linear corridor probably incorporates the Black Knob inlier (western limit of interpretation), although regional linears are less well developed in these areas. At the local scale a marked increase in the density of linears occurs around the Mt. Leyshon breccia complex, and less so around the Mathews Pinnacle - Seventy Mile Mt. complex. In these areas orientations which are uncommon elsewhere take on a local significance. In particular, 000° trending linears are well developed, as are linears trending 160°. The 000° trending linears are generally confined to the north of the complex and are rare to the south.

The Mt. Leyshon breccia complex occurs at the intersection of the Mt. Dean and Mt. Leyshon corridors, and the Yarraman Creek corridor bounds the eastern margin of the breccia complex. The Mathews Pinnacle - Seventy Mile Mount complex is localised at the intersection of the Mt. Leyshon corridor and the poorly defined second SE trending corridor noted above.

### 3.3 STRUCTURAL ELEMENTS OF THE MT. LEYSHON BRECCIA COMPLEX

The Mt. Leyshon breccia complex hosts a multi-age array of structures and generally lacks appropriate marker horizons. As a consequence a rigorous structural time scale cannot easily be developed. However, the Mt. Leyshon complex structures can be divided into the following groups, based on their indicated or suggested stage of development (as discussed below):

- (1) Pre-complex structures.
- (2) Early syn-complex structures.
- (3) Late syn-complex structures.

#### 3.3.1 Pre-complex structures

Structural elements described in this section developed before the formation of the breccia complex and are preserved both in the basement at the margin of the complex and in blocks within the complex. Hence, they provide evidence of the Palaeozoic deformation history prior to breccia complex development.

##### 3.3.1.1 BEDDING / CLEAVAGE

Bedding occurs in the Puddler Creek metasediments as a fissile parting in the rock, although in several outcrops thinly bedded mudstone layers (2 - 20 cm thick) are interbedded with massive siltstone layers (20 - 100 cm thick). The dominant cleavage preserved in the metasediments within the complex is a penetrative to spaced cleavage ( $S_1$ ) which is sub-parallel to bedding (Plate 3.1). Alteration and brecciation of the metasediments commonly prevents distinction between bedding and the subparallel cleavage  $S_1$ . Consequently they are considered together here. Excluding the NW domain, bedding and cleavage in the breccia complex have a dominant 090 - 100° orientation (Figure 3.3B and C), although with some scatter. In contrast, cleavage and bedding orientations in

the NW domain are widely scattered (Figure 3.3A), and do not show a dominant trend. In addition to bedding and  $S_1$ , a well developed fracture cleavage is present in several outcrops, the orientation of which is shown in Figure 3.3D. These fracture cleavages generally trend between  $015^\circ$  and  $050^\circ$ , although one outcrop displays a  $150^\circ$  trending cleavage. Where both  $S_1$  and a fracture cleavage are present in the same outcrop, the fracture cleavage overprints  $S_1$ .

#### 3.3.1.2 FOLDS

Two types of folds were observed within the Puddler Creek metasediments in the complex. Firstly, one occurrence of an isoclinal fold (half wavelength = 5 cm) with an axial plane generally parallel to bedding and  $S_1$  (fold axis plunging  $73^\circ$  towards  $091^\circ$ ). Secondly, two occurrences of kink folds (half wavelength = 50 cm) which fold  $S_1$  (fold axes plunge  $45^\circ$  towards  $210^\circ$ , and  $39^\circ$  towards  $276^\circ$ ; Plate 3.5).

#### 3.3.1.3 SHEAR ZONES

Few faults have been timed as pre-complex with certainty, although the multi-age nature of faulting in the complex has probably obscured several pre-complex faults. Nevertheless, in addition to cleavage formation and folding, some evidence for pre-complex deformation exists in the form of shear zones within metasediment. A 25 centimetre wide banded mylonite (dip and strike  $003^\circ / 84^\circ W$ ), which is shown in Plate 3.2 outcrops at the edge of the complex (GR. 5060 5880, Figure 3.2). This mylonite has been intruded by a pre-complex dolerite dyke, and by a post-main pipe breccia ED dyke (trending  $017^\circ$ ). Approximately 150 metres north along strike from the mylonite outcrop, a carbonate cemented fault breccia (dip and strike  $176^\circ / 70^\circ W$ ) brecciates granite (see section 3.3.4.2 for a description of these late fault zones). Both these structures form part of a major north trending linear zone (Yarraman Creek corridor) which crudely defines the eastern margin of the breccia complex. These outcrops provide evidence of early north trending ductile structures and their subsequent reactivation during later tectonic events before formation of the breccia complex, and during its development.

Elsewhere, on the contacts between dolerite and basement rhyolite dykes and the surrounding metasediment a steeply plunging stretching lineation is developed on a penetrative cleavage in the metasediment. For example, a strongly cleaved 0.5 metre wide zone of metasediment, incorporated at the margin of a basement rhyolite dyke (GR. 4260 5500), has a stretching lineation plunging  $60^\circ$  towards  $005^\circ$  on a cleavage face oriented  $005^\circ / 90^\circ$ . Significantly, this ductile fabric is roughly coincident with the southern mapped extent of a NNE trending fault zone that cuts the breccia complex, and forms a major NNE trending linear to the north of the complex. Extensive brittle fracturing and hydrothermal alteration along this NNE trending fault zone indicate subsequent reactivation during development of the breccia complex.

Penetrative fabrics which are confined to narrow zones, and have steeply dipping mineral lineations in outcrop, indicate the presence of early ductile fault zones prior to the development of the breccia complex. For example, a well developed steeply dipping cleavage (Plate 3.3) occurs on two metasediment outcrops (GR. 4165 5135 and 4170 5360; Figure 3.2) exposed in a fault



zone which trends 150 - 160°. This fault zone also exposes a vertical cleavage which trends 025° with a fine vertical mineral lineation. Brittle strike slip faults (see section 3.3.4.2) have reactivated this ductile fault zone after emplacement of the main pipe breccia, and the fault zone now defines the western margin of the Mt. Leyshon breccia pipe (Figure 3.2). At the regional scale this structure is confined to the breccia complex, although a parallel structure (which bounds the eastern margin of the Mt. Leyshon breccia pipe) forms a four kilometre linear feature within the Mt. Dean corridor. In addition, at the southwest corner of the breccia complex (GR. 3460 4815) a small scale shear surface with a dip and strike of 056° / 70 N shows a fine mineral lineation plunging 62° towards 013°. This small shear provides an indication of the early fault style on a parallel regional linear which intersects the breccia complex approximately 200 metres to the west (although it is not exposed).

Drill-core observations reveal later more discrete brittle-ductile fault zones within dolerite dykes and at dolerite - granite contacts. Narrow dolerite dykes (< 0.5 metres) are locally strongly deformed in contrast to the granite host, indicating strain was partitioned into narrow dykes.

#### 3.3.1.4 MUTUALLY INTERSECTING QUARTZ VEINS

Quartz veins (2 to 30 centimetres wide) occur in two areas of granite cropping out below the NW flanks of Mt. Hope (GR. 3710 5440). The steeply dipping vein sets have formed dominantly along a 120° trend, with a less well developed set on a 045° trend, approximately parallel to the Mt. Dean and Mt. Leyshon corridors, respectively. The veins comprise fine grained white quartz and fragments of granite. The granite fragments show jigsaw fit textures and are floating in the quartz. Replacement of the granite at the vein margin is minimal. Together these features suggest that the quartz infilled the veins at a time of extension, and that extension on both vein sets was simultaneous. These quartz veins are overprinted by crackle brecciation probably related to main pipe breccia development. The pre-complex age assigned to these structures is based on their restriction to a single area of outcrop (in contrast to later quartz veins), and vein textures suggesting one episode of open space fill, rather than the development of an incremental fibrous texture.

### 3.3.2 Early syn-complex structures

Structural elements described in this section are considered to have formed early in the development of the breccia complex. These structures are overprinted by the main pipe breccia although, for reasons discussed in section 3.6.2, they have special significance because they formed prior to, and synchronously with, the development of the breccia complex.

#### 3.3.2.1 QUARTZ VEINS

Quartz veins from 1 to 20 millimetres thick occur in metasediment and granite fragments within the main pipe breccia, and within preserved basement outcrop at several points in the complex. These are designated as stage I in the hydrothermal evolution documented in Chapter 4. Microscope examination reveals these veins have a fibrous texture, and that fibres commonly

cause minor replacement of metasediment in the wall rock. Their orientation is unknown as subsequent brecciation results in vein disruption and minor rotation.

### 3.3.2.2 BRITTLE FAULT AND FRACTURE MESHES

In the eastern half of the breccia complex large areas of basement metasediment show extensive brittle deformation, although the individual fragments are commonly only slightly separated or expanded. This brittle deformation provides important constraints on the early development of the complex, and is particularly well illustrated by a large sub-horizontal surface in a creek section (GR. 4855 5665). At the SE of the outcrop a small scale cataclasite fault (one - two centimetres wide) trends approximately  $140^\circ$ , and contains brecciated silica vein material indicative of cohesive brittle faulting. Approximately three metres to the NW this structure splits into a suborthogonal network of smaller vertical faults which trend  $147^\circ$  and  $058^\circ$  (Plate 3.4). These smaller faults define fragmentation domains composed of a "patchwork" of rectangular metasediment fragments, whose bounding fractures commonly mirror the orientation of the small scale domain faults. Elsewhere on the outcrop the orientation of these small scale faults is more irregular and the fragmentation results in a more chaotic rubble texture. These fragmentation textures are overprinted and destroyed by the transition to strongly expanded rubble textured metasediment (see section 3.3.2.3) and the formation of the main pipe breccia. These fracture meshes are also observed in areas of basement rhyolite, although outcrop is generally less continuous and it is not known if these meshes in the basement rhyolite also relate to small scale faults.

### 3.3.2.3 REACTIVATION OF BEDDING / CLEAVAGE

Metasediment cropping out in the complex generally shows an intense brittle deformation, developed preferentially along irregular zones subparallel to cleavage and bedding, where present. Erratic second order fragmentation and expansion both overprints and exploits this cleavage parallel deformation (Plate 3.5). In expanded (rubble textured) metasediment this brittle fabric is sometimes preserved in the regions of less intense fragmentation as a ghost fabric, suggesting this deformation predates the emplacement of main pipe breccia. In addition, phyllosilicates are developed on less competent mudstone layers (2 - 10 centimetres thick) in several areas of metasediment, which indicating strain parallel to bedding. Thus bedding parallel fault zones in metasediment appear to combine ductile shearing in thin incompetent beds with brittle fracturing in competent beds.

The age of small scale brittle faults which commonly occur in preserved regions of basement lithologies is ambiguous. Some certainly cut the main pipe breccia and are described below, whereas other faults in basement could not be traced across main pipe breccia outcrops, and pre-date or are synchronous with the formation of the breccia complex.

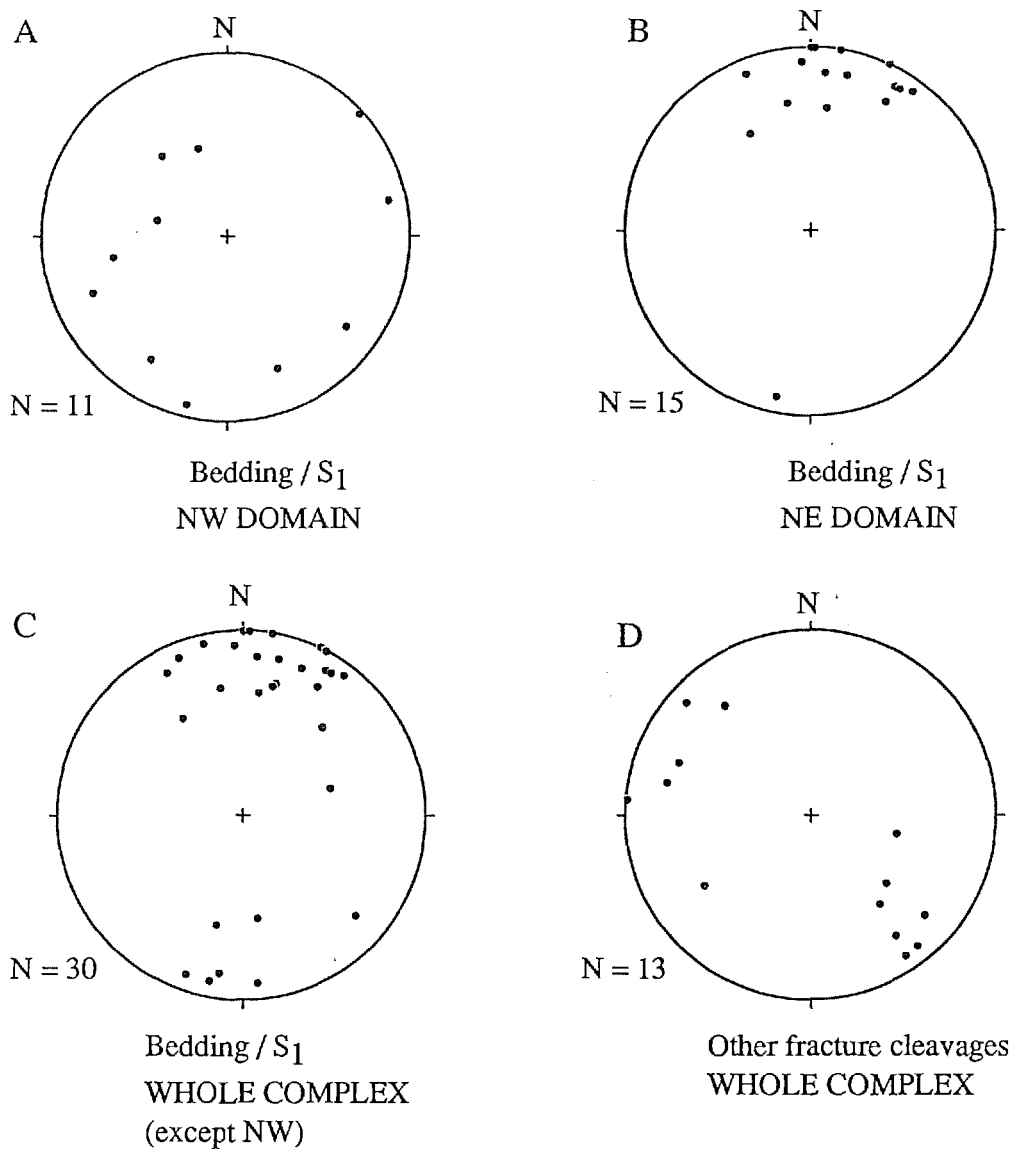


FIGURE 3.3: Poles to bedding / cleavage orientations within the Mt. Leyshon breccia complex, (A) NW domain, (B) NE domain, and (C) whole complex (except NW). (D) Other fracture cleavages. Note: (1) the marked scatter of data in the NW domain compared to the whole complex, (2) the scattered but dominantly  $100^\circ$  trending bedding and cleavage orientation of the complex.

### 3.3.3 Later syn-complex structures

Structures which cut the main pipe breccia are described in this section. These structures are multi-phase and commonly show signs of reactivation by later faults or veins. Structures of this group span the second half of the breccia complex evolution.

#### 3.3.3.1 QUARTZ-MOLYBDENITE VEIN SYSTEM

Quartz-molybdenite veins have an irregular inter-connected character, and are generally less than two centimetres wide (Plate 3.6), although veins with a thickness of up to 15 centimetres rarely occur. These lilac coloured veins consist of alternating bands of inter-connecting quartz crystals and thin molybdenite layers. Slivers of wall-rock are interleaved between the bands, and thin section observation reveals that the quartz crystals contain bands of inclusions parallel to the vein margin, suggesting incremental growth. Quartz crystals which parallel the plane of the thin-section demonstrate unidirectional growth across the veins. Thin-sections oblique to the long axis of the quartz crystals reveal inter-locking and sutured crystal boundaries (Plate 4.6). In places the crystals nucleate within the wall-rock and grow back towards the vein. Replacement of wall-rock and slivers is clearly demonstrable, although rare open spaces have been observed within the veins.

Collectively, these textures have many similarities with the features of extensional fibre veins or "crack seal" veins (Ramsay and Huber, 1983). The presence of molybdenite (and pyrite?), together with a replacement quartz component in the vein, indicates that fluid in the vein was not in equilibrium with the wall rocks at the time of formation. Hence the fluid is likely to have been derived from an external source. Only fifteen quartz-molybdenite veins were located in the open pit and outcrop. These veins strike from 067° to 125° (most often between 080° and 100°) with a steep dip. They are confined to a crudely north trending zone on Mt. Leyshon proper, extending to the east and west of the region, subsequently intruded by porphyry unit IV (Figure 4.3). The veins are therefore spatially related to a regional SSE trending strike slip fault (see section 3.3.4.2) which bounds the eastern margin of the Mt. Leyshon breccia. Other evidence for extensional fibre vein development occurs within rare veins that cut metasediment fragments within the Mt. Hope breccia. These veins are up to 0.5 centimetres thick and have an irregular branching geometry, but lack the molybdenite or pyrite mineralisation.

#### 3.3.3.2 INTER-BRECCIA SHEAR ZONES

Three minor shear zones were observed during graphic logging (see Chapter 5) of drill core from the Mt. Leyshon breccia pipe. Although two of these shear zones were partially destroyed during the Mt. Leyshon brecciation event, a third which is largely preserved is shown in Figure 3.4 and Plate 3.7. The preserved shear zone occurs approximately 15 metres inside the western margin of the Mt. Leyshon breccia pipe, at the edge of a six metre granite block. The granite block is brecciated to a crackle or mosaic texture and passes into a six centimetre wide zone of deformation and alteration. The following features indicate these shear zones postdate the main pipe breccia, but predate the Mt. Leyshon breccia. The crackle brecciated granite passes through a

sharp contact into a three to four centimetre wide zone of cohesive cataclasite. The cataclasite is dominantly composed of granite (zone A, Figure 3.4) but includes a 0.5 to 1.5 centimetre region of main pipe breccia (zone B, Figure 3.4). Deformation is most intense at the transition between the comminuted granite and main pipe breccia; only small granite fragments and quartz phenocrysts remain here. In contrast to the deformed granite, deformation in the more competent main pipe breccia occurs in discrete zones. The deformed main pipe breccia and granite are replaced by silica, although a one centimetre wide zone of only weakly deformed main pipe breccia exists outside the intensely sheared region (zone C, Figure 3.4). A 0.5 centimetre region of deformed main pipe breccia (zone D, Figure 3.4) forms the lower margin of this pre-Mt. Leyshon breccia shear zone. This region has been replaced by chlorite and pyrite, as have small re-break zones elsewhere in the deformation zone. Sheared and chlorite - pyrite altered main pipe breccia from zone D occurs as fragments in the Mt. Leyshon breccia near the margin (zone E; Figure 3.4). Because chlorite and pyrite obviously replace and crosscut fragments in the Mt. Leyshon breccia, identical alteration in zone D is considered to be the same age as that which effects the Mt. Leyshon breccia. A laminated and fibrous calcite vein (zone F, Figure 3.4) postdates the Mt. Leyshon breccia and reactivates the shear zone at the Mt. Leyshon breccia contact. Slivers of zone E separate individual bands of the calcite vein and suggest crack-seal processes operated during vein formation.

#### 3.3.3.3 OBLIQUE-SLIP NORMAL FAULTS

On the north east flank of Mt. Hope (around GR. 3850 5650) extensively fractured and faulted metasediment passes into "tongues" of main pipe breccia trending approximately ESE. Here bedding, which has previously been deformed in a ductile manner sub parallel to layering, is further disrupted (Plate 3.8; Figure 3.4) and has been rotated to  $013^\circ / 32^\circ$  E and  $157^\circ / 68^\circ$  E either side of a small scale fault oriented  $104^\circ / 72^\circ$  S. This fault, and a parallel structure, show minor oblique normal (extensional) displacement of the metasediment layers. Four faults of this type are mapped on Mt. Hope and trend between  $104^\circ$  and  $127^\circ$ . They are cut by 1-2 dykes, but their relationship to the main pipe breccia is only implied, based on the local shearing of main pipe breccia along strike from the fault outcrop.

#### 3.3.3.4 MT. LEYSHON BRECCIA MARGIN CRUSH ZONE

The long margins of the Mt. Leyshon breccia pipe are bounded by two strike slip faults which trend approximately  $150^\circ$ , and show evidence for post-Mt. Leyshon breccia movement (Figure 3.2). Outside the Mt. Leyshon breccia contacts, extensive brittle deformation of the main pipe breccia, basement, and porphyry unit IV lithologies occurs along all but the north western margin. This deformation consists of fractures, faults and veins and terminates sharply at the Mt. Leyshon breccia boundary (Plate 3.9). For example, in the zone of brittle deformation outside the north east contact three dominant fracture and fault directions occur which have the following approximate orientations:  $100^\circ$ -steep dip to south;  $015^\circ$ -subvertical; and  $035^\circ$ -moderate dip to south. Minor strike slip movement in this zone is indicated by subhorizontal movement lineations on many of these fractures and at the margin of fault breccia. Some of this deformation obviously postdates

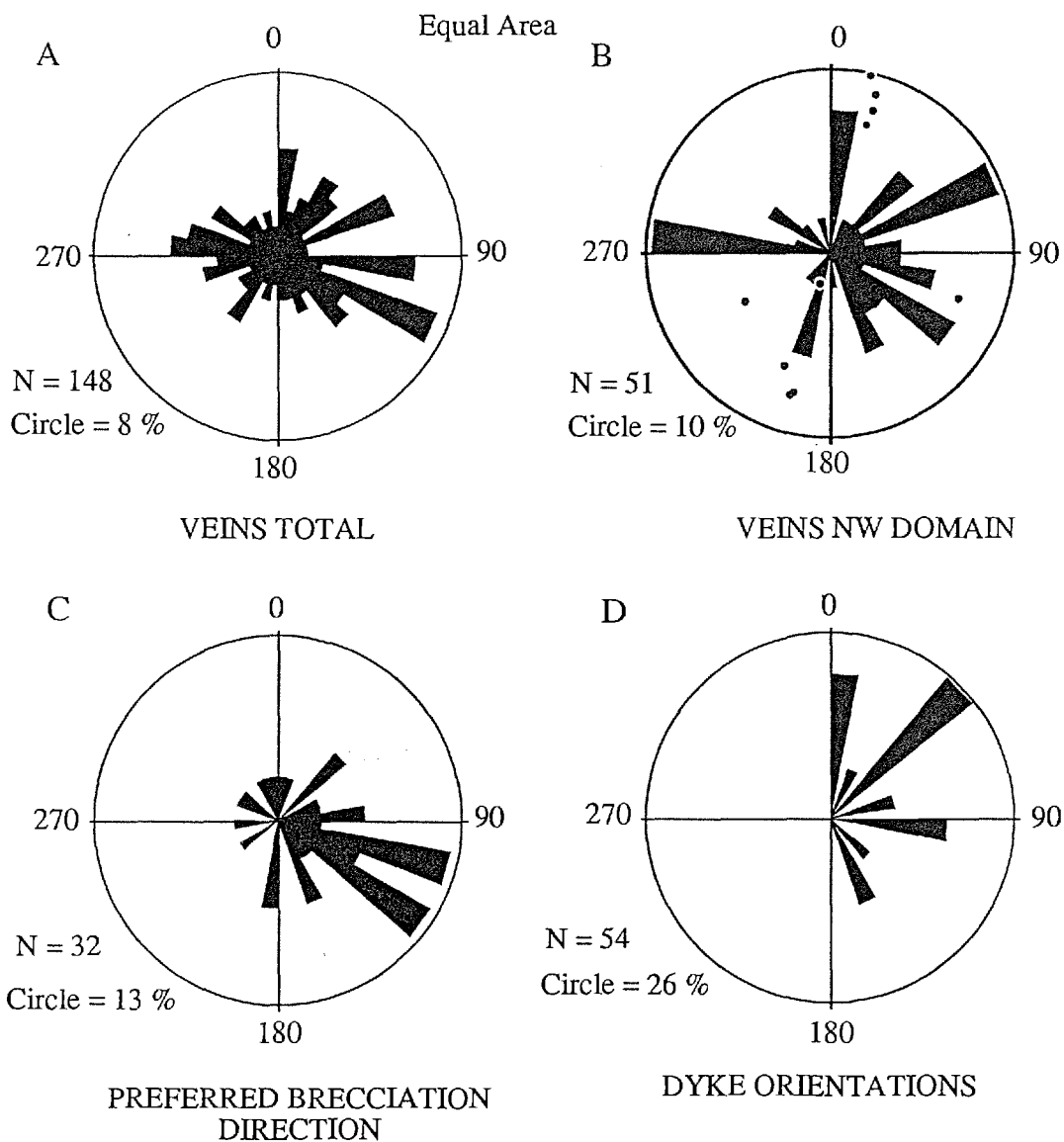


Figure 3.5: Orientation of: (A) All veins, (B) veins and shear veins in the NW domain (• plunge and plunge direction of slickensides), (C) preferred brecciation direction, and (D) dykes (plotted as a strike between 0-180°) in the Mt. Leyshon breccia complex. N = number of measurements and the circle radius represents the percentage of data in the largest petal. In A, B and C planes which dip N through to SSE plot in the upper half circle, those planes which dip S through to NNW plot below. Shear fibres in B are plotted as though the circle is a stereonet. Note: the multidirectional nature of vein, preferred brecciation and dyke orientations; although all veins and preferred brecciation directions have a dominantly 115° trend, whereas dyke orientations dominantly have an 045° trend and less dominant 000°, 090° and 160° trends.

the Mt. Leyshon breccia. However, zones of weakly re-brecciated main pipe breccia within the Mt. Leyshon breccia have a suborthogonal fracture pattern which is not present in regions of mixed Mt. Leyshon breccia that surround these blocks. The preservation of this fracture pattern in blocks within the Mt. Leyshon breccia indicates that at least some brittle deformation predates the development of the Mt. Leyshon breccia.

The north western contact of the Mt. Leyshon breccia was not observed in the open pit, although drill hole MLD 227 passes through this contact. In contrast to other Mt. Leyshon breccia contacts, the north western contact passes from polymict Mt. Leyshon breccia into weakly jointed granite.

### 3.3.4 Post-Mt. Leyshon breccia structures

#### 3.3.4.1 LATE VEINS

Numerous veins cut igneous and breccia units in the Mt. Leyshon breccia complex, and are particularly common in the NW corner of the complex. Veins are from 0.1 to > 50 centimetres in thickness, although most are less than 2 centimetres thick, and veins less than 0.5 centimetres thick are abundant. Veins are multi-phase and vary from mono-mineralic pyrite or calcite veins, to complex intergrowths resulting from successive reactivation of the same vein. For example, chlorite-pyrite veins are commonly reactivated by base metal veins which may be re-used by calcite veins. Likewise, the quartz-molybdenite veins described in section 3.3.3.1 are commonly reactivated by all or some of the following vein types: pyrite, pyrite-chlorite, sphalerite-chalcopyrite and calcite. Veins exist for many of the hydrothermal stages outlined in Chapter 4.

Repeated small scale re-brecciation (of earlier sealed breccia cavities and fragments) in the Mt. Leyshon breccia generated irregular, transient permeability for successive stages of hydrothermal fluid flow. Several types of vein and vein-breccia occur in breccias and basement, and these are listed below.

- (1) Polymineralic veins composed of crystals (e.g. quartz, pyrite-chlorite, base metals, etc.) which suggest growth into open space, but with complexly overprinting textures suggesting repeated reactivation and replacement during a number of stages (Plate 8.1; Chapter 4).
- (2) Small scale veins consisting of overlapping shear fibres of calcite, pyrite or pyrite-chlorite.
- (3) Numerous small scale (commonly 1-5 millimetres thick) irregular en-echelon veins which have formed in minor faults in granite and breccia units (Plate 3.10). These en-echelon veins may be composed of quartz, pyrite-chlorite or calcite.
- (4) Minor extensional vein-breccias that are infilled by calcite (Plate 3.11).
- (5) Crack-seal textured calcite veins (Plate 3.7).

The weathered nature of veins outcropping in the complex prevented discrimination and classification of the veins based on their mineralogy. Consequently, vein orientation data for the whole complex are plotted collectively. Veins are multi-directional although the most commonly orientation is at 115° trend, with less common maxima trending 000°, 040° and 070° (Figure 3.5A). In the NW domain many veins occur, observed in unoriented drill core, although veins are

difficult to locate in the open pit. Nevertheless, limited vein orientations could be measured, both in the open pit and in oriented drill core. Veins in the NW domain are also multi-directional, but veins and shear veins show preferred trends of 45°- 65°, 090°, 115° and 000° - 015° (Figure 3.5B). Only ten shear veins had measurable slickenside orientations, although fibres generally plunge between 0° and 30° (seven veins) but steeper plunges of 30° to 50° (two veins) and greater than 50° (one vein) also occur. Fibres dominantly plunge shallowly to the NNE (Figure 3.5B).

#### 3.3.4.2 LATE FAULTS

Extensive evidence for post-main pipe breccia faults occurs in the breccia complex (Figure 3.2), although the faults are poorly exposed and generally only crop out in creeks or topographic depressions which are subparallel to the fault strike. Most faults are actually fault zones, which are commonly from one to three metres wide, but locally up to fifteen metres wide. Because of their discontinuous nature and poor outcrop, many of the faults in the complex cannot be traced for more than a few tens of metres. However, several larger and more continuous faults do occur in the complex, as shown in Figure 3.2, and many of these link with regional scale faults (compare Figures 3.1 and 3.2).

Three periods of late faulting are discriminated within the Mt. Leyshon breccia complex, and are listed from oldest to youngest below.

- (1) A period of cataclasite formation (in the sense of Sibson, 1986).
- (2) An extended period of dominantly strike slip faulting.
- (3) A period of reverse faulting.

Fragments of cohesive fault rocks, interpreted to be cataclasite, are preserved in carbonate cemented strike slip fault breccias. Their presence suggests that in the first period strike slip faults formed initially as cataclasites, although their age relative to the Mt. Leyshon breccia is unknown (they may be equivalent in age to the inter-breccia shear zones). These cataclasites were subsequently reactivated after the formation of the Mt. Leyshon breccia, and the resulting fault breccias were infilled and replaced by calcite.

Faults of the second period produced cohesionless breccia and gouge which cross-cut the calcite cemented faults and postdate all lithologies. Slivers and regions of undeformed rock occur in the fault zones, and narrow seams (1-2 centimetres wide) of ultracrushing and slip accommodate most deformation. In competent lithologies such as the main pipe breccia and Mt. Leyshon breccia, the fault zones are typically around one metre wide (Plate 3.12). In contrast, within porphyry units (particularly porphyry unit IV) the fault zones splay out into wide crush zones. These late fault zones commonly have an upward branching and curved geometry (as observed in the open pit) and gently plunging movement lineations (Figure 3.6).

Fault movement during the second period, and the consequent brecciation, are commonly focused along previously formed faults (ductile or brittle), dykes and veins. A wide zone of strike slip faulting extends from the eastern margin of the Mt. Leyshon breccia pipe and into the contact

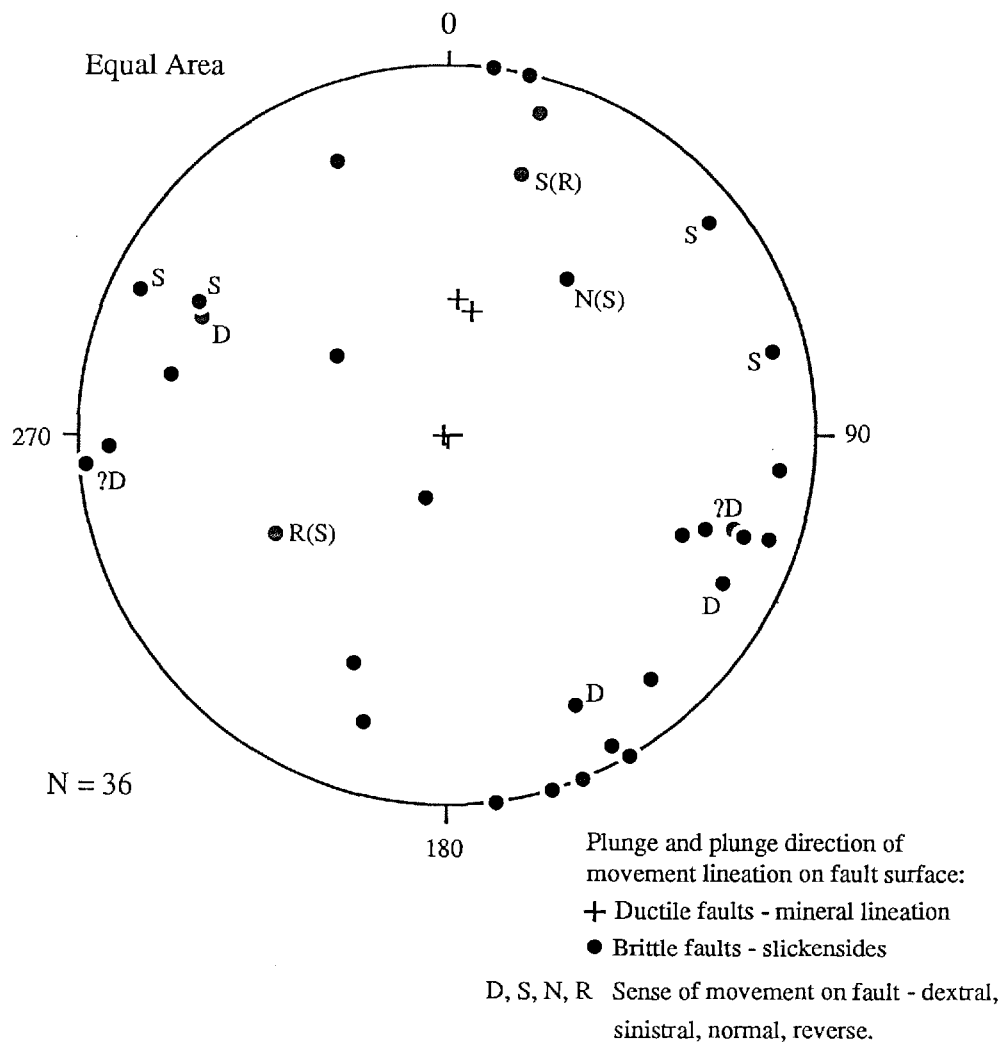


Figure 3.6: Movement lineations on fault surfaces within the Mt. Leyshon breccia complex. Sense of movement estimated from rough smooth criteria on slickensides is indicated where possible. Note: (1) that most lineations have a plunge of  $\leq 30^\circ$ , (2) a small group of lineations plunge moderately to steeply, and (3) that the sense of movement on lineations with a similar plunge is not consistent.

zone of porphyry unit IV (see section 3.3.4.2). In this fault zone, gently plunging movement lineations are exposed in the open pit on a steeply dipping shear surface. The rough smooth character of calcite fibres (Ramsay and Huber, 1987) on this fault surface suggests a sinistral sense of movement. In the south of the complex the continuation of this fault zone (GR. 4500 5040; Figure 3.2) shows a sinistral offset on a steeply dipping late dyke, consistent with this interpreted sense of movement.

Syn-complex igneous dykes commonly show evidence for brittle and brittle-ductile movement along their contacts or flow banding, also formed in the second period. For example, at the SE corner of the complex (GR. 4220 4930) a contact is exposed between porphyry unit IV and a later 1-2 dyke. Here an anastomosing cleavage (110 / 80W) has developed on the margin of the 1-2 dyke subparallel to the dyke-porphry contact. On Mt. Mawe (GR. 4800 5785) a lozenge shaped breccia zone, trending 040°, is formed at a strike change in a late dyke which intrudes the main pipe breccia (Plate 3.13). For the most part the dyke trends approximately 020°, but a strike change to 040° and back to 020°, over approximately five metres, localises a breccia zone which fragments both the dyke and main pipe breccia (with a crackle to rubble texture) as shown in Figure 3.7. Brecciation occurs mainly as the result of the intersection of fractures trending approximately 045° / 50°W and 142° / 90° and the new breccia zone is altered and iron stained. The SW end of the new breccia zone pinches out sharply at the inflection point in the original dyke-main pipe breccia contact, and is cut by sulphide veins which postdate the brecciation. The NE breccia termination is not exposed. In addition, the thick pyrite - quartz - muscovite vein shown in Plate 3.14 has a strike slip fault developed along its margins.

The third period of late faulting in the complex produced a reverse fault zone striking approximately 160° and dipping 50° to the west (Figure 3.2). The position of this fault is known accurately in the pit area, although its position to the south east is inferred on the basis of the lack of late dyke outcrop either side of the reverse fault. Additional smaller reverse faults occur nearby in the pit, but are of an unknown extent. The main reverse fault cuts the post-mineralisation basalt dykes, consistently offsets the "sill" and 1-2 dyke units with west block up (see Enclosure 3), and has rare, steeply plunging slicken-sides. The dip slip offset on the sill, 1-2 dyke, and the ore body is approximately 220 metres (based on mine drill hole data), and the shape of the northern contact of porphyry unit IV suggests a dextral offset of approximately 90 metres. Brecciated pyrite vein material in the reverse fault indicates multiple fault movement in this zone.

Faults in the breccia complex are multi-directional with four dominant orientations (Figure 3.8A): (1) N to NNE, (2) NE to ENE, (3) E to ESE, and (4) SSE. These orientations are identical to the regional linear groups established in section 3.2. Two further observations are made concerning the orientations of the fault sets within the complex. Firstly, faults of the western domain (Figure 3.8B) are dominantly west dipping, and in this domain E trending faults are poorly developed. Secondly, in the eastern domain fault dips are less consistent (Figure 3.8C), although east dipping faults are dominant, and 150° trending faults are poorly developed.

The irregular nature of the basement units (poorly bedded metasediment intruded by numerous dolerite and rhyolite dykes), and the disrupting effect of the main pipe breccia, have resulted in the loss of any basement marker units. Subvertical igneous dykes generally provide the only possible marker horizon. Where these dykes have been offset, the horizontal displacement is generally only up to a few metres, and in one case, twenty metres (excluding the late reverse fault, see below). In addition, sense of movement criteria on fault surfaces are poorly developed and ambiguous. Of 135 faults recorded in the breccia complex (Figure 3.8A), movement lineations were recorded on only 36 fault surfaces (Figure 3.6). The majority of these lineations ( $n = 29$ ) plunge between 0 and 30° suggesting faulting in the breccia complex was dominantly strike slip in nature. In contrast, a separate group of dominantly dip slip faults also occurs ( $n = 7$ ), which includes movement lineations on ductile pre complex faults. Overall, kinematic indicators are rare on faults in the complex and an estimate of relative movement was possible on only 20 faults (Figure 3.8A), based mainly on rough-smooth criteria on shear fibres or slickensides (Ramsay and Huber, 1987) and also on apparent offsets on steeply dipping dykes. These data indicate a complex movement history on the faults, and suggest some faults with the same orientation had opposing relative movement. Nevertheless, the 150° trending strike slip fault which bisects the breccia complex, and controls the eastern margin of the Mt. Leyshon breccia, shows consistent sinistral offset—both at the south of the complex, and in the irregular splayed fault zone outside the eastern margin of the Mt. Leyshon breccia.

#### 3.3.3.6 JOINTS

A systematic collection of joint data was made from units in the breccia complex. A joint is defined here as any planer discontinuity without evidence for displacement. Joints were subdivided, for the purpose of data collection and plotting (Figure 3.9), into those which cut basement, main pipe breccia and igneous units. Joints in basement and main pipe breccia units are multi-directional, although there is a slight predominance of joints which trend N and ESE in basement and N, ESE and SSE in the main pipe breccia. Joints in igneous units have two preferred orientations which are NE and SSE.

### 3.4 PREFERRED ORIENTATION OF BRECCIA AND IGNEOUS FACIES

This section describes the strong preferred orientation of breccia and igneous units in the complex, and highlights the significance of these orientations in relation to the regional scale linears.

#### 3.4.1 Breccia units

The boundary of the breccia complex is defined by the main pipe breccia, although the overall geometry of the complex is polygonal (Figure 3.2). The boundaries of the complex can be approximated by linear elements which have the following orientation:

- (1) Lines trending 000° for the western and eastern margins.
- (2) Lines trending 070° for the north western and south eastern margins.
- (3) A line trending 125° for the north east contact.

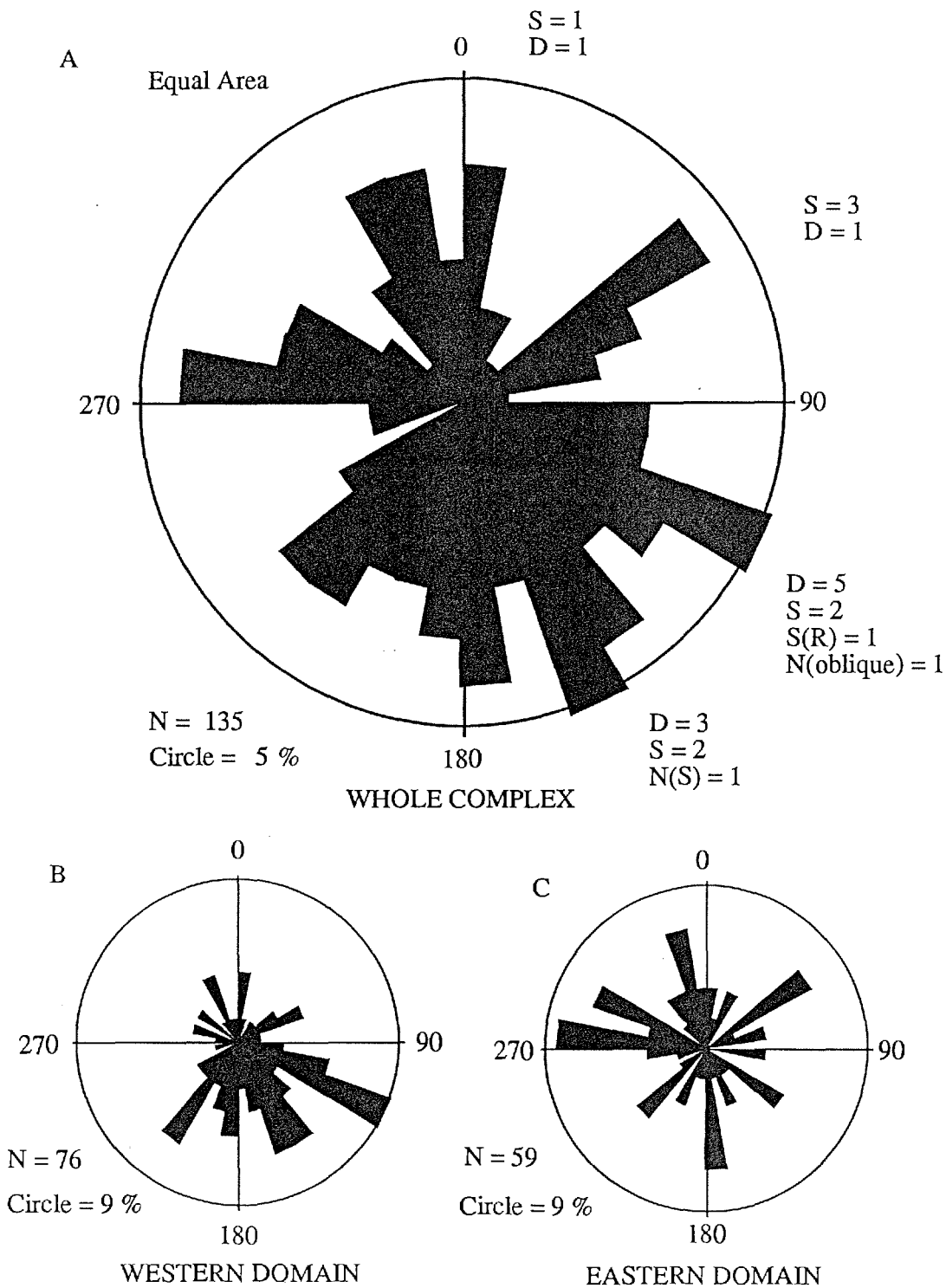


Figure 3.8: Fault orientations within the Mt. Leyshon breccia complex. (A) Whole complex, (B) western domain, and (C) eastern domain. Faults which dip N through to SSE plot in the upper half circle, those faults which dip S through to NNW plot in the lower half circle. D, S, N, R refer to the sense of movement on faults of a given orientation (number = frequency). Percentage of data represented by the circle radius is indicated. Note: (1) that faults in the Mt. Leyshon breccia complex are multidirectional, (2) dominant orientations are N(-NNE), NE(-ENE), ESE(-E) and SSE, and (3) sense of movement on similarly orientated faults is conflicting.

Overprinting of the southwestern margin of the complex by several igneous units (see section 3.4.2) obscures the margin geometry in this region. Within the complex, the main pipe breccia has an irregular geometry, although there are a number of preferred orientations, trending approximately 000°, 070° and 125°, together with a minor 045° trending zone (Figure 2.5B). Thus these main pipe breccia zones, and the linear trending contacts, coincide with regional linears.

The Mt. Leyshon breccia pipe has a different shape to the complex as a whole. It is elongate in a SSE orientation, parallel to the two strike-slip fault zones which now bound its east and west margin, as discussed above (Figure 3.2). The northern contacts consist of intersecting surfaces trending 115° and 045°, and the southern margins trend approximately 090° and 045°. Orientations of the Mt. Leyshon breccia margins shown in Figure 3.2 are those measured during pit mapping on the 380, 390 and 400 RL benches. The approximately 045° trending contacts of the Mt. Leyshon breccia was not observed during this study, and is based on mapping by mine geologists.

The smaller breccia units also show preferred orientation. The Mt. Hope breccia forms a NE trending zone, coinciding with a marked topographic depression immediately to the southwest (compare Figure 2.1 and Figure 3.2). This topographic depression is parallel to a regional NE trending linear which intersects the complex 100 metres to the west. The orientation of three breccia dykes have been mapped in the complex, two along 020° trends and one on a 150° trend. In contrast to other breccia units, tuffisite breccia dykes have a more variable orientation, although they do show a preferred NE trend (Figure 2.1).

During mapping of the breccia complex directions of preferred brecciation were noted at the outcrop scale. These include tongues of main pipe breccia intruding into basement as breccia dykes and regions of later brecciation. Although brecciation is multi-directional, the dominant orientation of small scale preferred brecciation is ESE (Figure 3.5C).

### 3.4.2 Igneous units

Igneous porphyry units (I - IV) and dykes also show a strong preferred trend. In the main igneous centre the orientation and original distribution of the earliest igneous units is partly obscured by later igneous units. Preferred orientation of porphyry units is as follows (Figure 2.3):

- (1) 130° and 150° for porphyry unit I.
- (2) 070° and 130° for porphyry unit II.
- (3) 070° and 150° for porphyry unit III.
- (4) 000°, 090° and, minor 045° and 070° for porphyry unit IV.

In addition, the numerous dykes which intrude the breccia complex show preferred orientation. The dominant trend of dykes in the complex is 045° (Figure 3.5D) in contrast to the trend of larger porphyry units, although smaller groups occur which trend 000°, 090° and 150°.

### 3.5 RHEOLOGICAL CONTROL ON BRECCIATION

The style and extent of brecciation of basement units is controlled by the strength of the rock, and the nature of its crystalline structure. For example, granite and dolerite dykes commonly form spherical fracture patterns as a result of brecciation. Similarly, post-main pipe breccia porphyry units deform with a spherical to elliptical fracture pattern, whereas metasediment and basement rhyolite dykes form angular fragments with planer surfaces. This fracture style is also reflected in the rubble textured (expanded but mostly untransported) host rock. Dolerite dykes were apparently more resistant than metasediment to main pipe brecciation, as in areas where the metasediment unit was completely destroyed, dolerite outcrops can be traced through polymictic main pipe breccia. In addition, contacts between metasediment and dolerite dykes are rarely preserved in outcrop within areas of less intense main pipe breccia formation. In these areas the metasediment has a rubble texture, whereas the dolerite dykes are only weakly brecciated. This contrast in the mechanical behaviour of dolerite and metasediment was also observed in drill core.

Silicification and sealing-up of the main pipe breccia (Chapter 4) resulted in the formation of an homogenous and brittle region in the NW corner of the breccia complex (Figure 4.3), and deformation occurs by brittle fracture. This brittle region grades out to a weakly altered and less competent region of main pipe breccia in the eastern half of the complex, where deformation results in anastomosing diffuse shear zones. This contrasting fragmentation behaviour appears to be important in Mt. Leyshon breccia formation.

Units within the breccia complex also show contrasting mechanical behaviour during vein formation. Competent units such as granite and silicified main pipe breccia commonly form planar veins, whereas the Mt. Leyshon breccia and porphyry units generally form an anastomosing mass of irregular discontinuous veins (see also sections 3.3.4.1 and 4.5).

The contact between weakly deformed granite and highly deformed metasediment (fault offset) acted as a gross rheological contrast during breccia complex formation (Figures 2.5A., 2.5B and 3.2 insert). In addition, the basement rhyolite body to the south of this contact generally inhibited main pipe breccia formation (Figure 2.5A and B). The rheological control is a product of a strength-mechanical contrast between the granite and metasediment, and may also reflect a much larger number of dislocation points within the highly deformed metasediment. The location of the Mt. Leyshon breccia pipe was similarly controlled, in part, by the rheological contrast between granite to the north, and main pipe breccia to the south (Chapter 5).

### 3.6 THE STRUCTURAL DEVELOPMENT OF THE MT. LEYSHON BRECCIA COMPLEX

Structures in the Mt. Leyshon breccia complex show evidence for both ductile and brittle deformation, and correlate with regional scale structures. These pre-, syn- and post-complex structures link with and form linears that are part of the regional structural framework. For these reasons it is important to view the structural evolution of the breccia complex as part of the

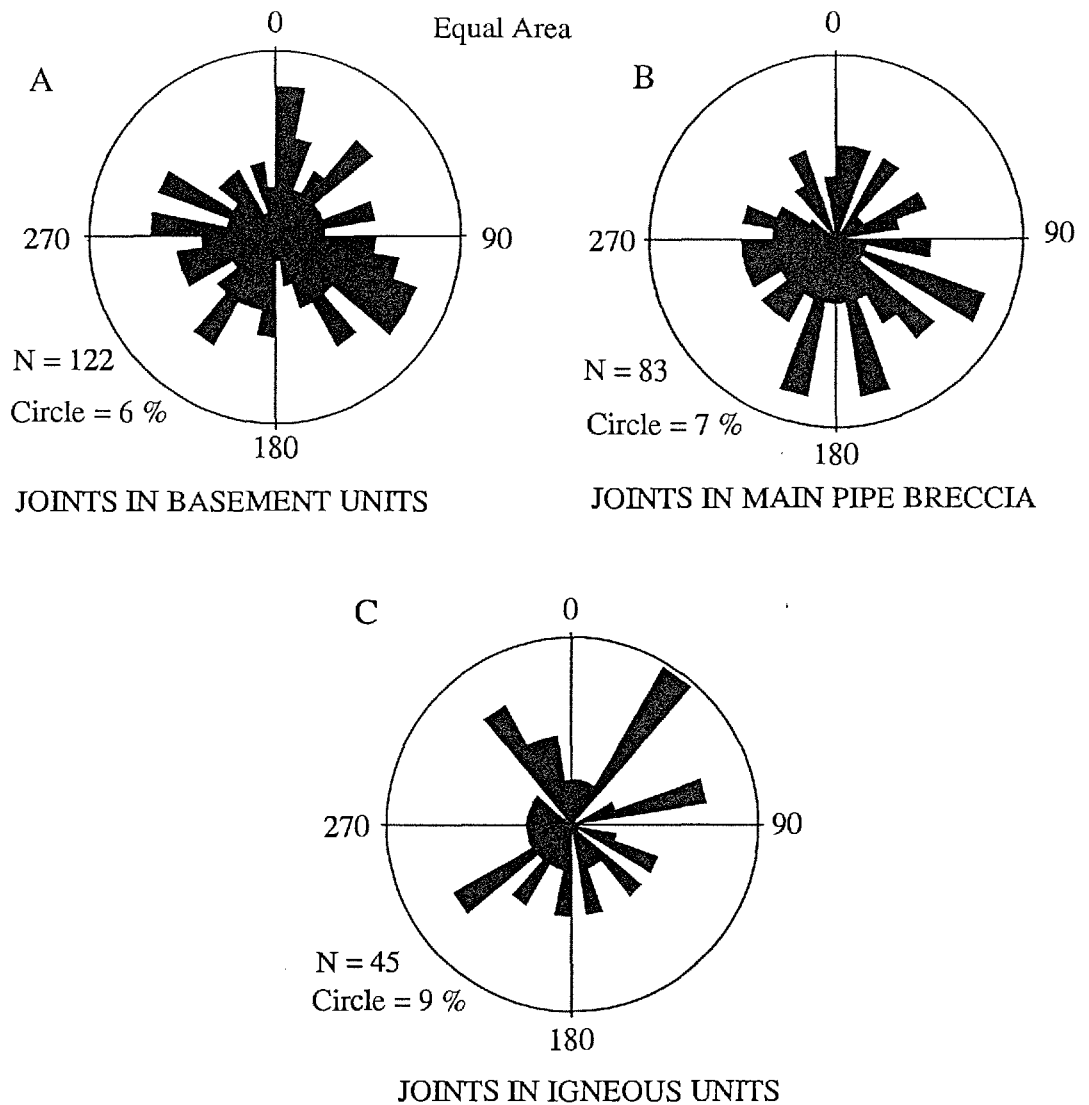


Figure 3.9: Joint orientations within basement (A), main pipe breccia (B), and igneous units (C) of the Mt. Leyshon breccia complex. Planes which dip N through to SSE plot in the upper half circle, those planes which dip S through to NNW plot below. N = number of measurements and the circle radius represents the percentage of data in the largest petal. Joints in the main pipe breccia and basement show nearly a random trend, whereas joints in igneous units show weakly preferred NE and SE trends.

Palaeozoic deformation history of north east Queensland, and in particular that of the Charters Towers Block (Lolworth-Ravenswood block; Figure 3.10A). The previous sections document a prolonged structural history preserved in units within the breccia complex. These structures are summarised in Table 3.1, and their significance in terms of local and regional structural evolution is assessed below.

### 3.6.1 Early basement structural history

Bedding and  $S_1$  cleavage in metasediment are the earliest structures preserved in the complex and have a variable trend, with maxima at  $100^\circ$  (excluding the NW domain). Clayton (1992), described a similar pattern for bedding and  $S_1$  cleavage around the complex, and reported a dominant trend of  $080^\circ$  to  $090^\circ$ , suggesting that bedding and cleavage within the complex have undergone limited rotation. Henderson (1986) suggested this cleavage was formed in response to destruction of a Lower Palaeozoic basin by the emplacement of the Lolworth - Ravenswood batholith. West of the breccia complex, Clayton (1992) describes erratic bedding orientations and suggests this results from  $F_1$  and  $F_2$  fold interference in this zone. Likewise, bedding and cleavage orientations in the NW domain of the breccia complex are erratic. This scatter may either result from  $F_1$  and  $F_2$  fold interference (both folds occur in the complex) or the rotation of bedding across faults (as indicated at Mt. Hope; section 3.3.3.3).

Other ductile structures cropping out in the complex provide further evidence of the early regional strain history. The north trending mylonite that forms part of the eastern margin of the breccia complex is parallel to the Puddler Creek Mylonite zone, which crops out three kilometres further to the east. Here, the Puddler Creek Mylonite is intruded by a north trending mafic unit and the Ordovician Merriland Tonalite (Hartley et al., 1989) indicating at least an Ordovician age for both these structures. Elsewhere in the Charters Towers Block, mylonite foliations are also believed to be Ordovician in age (Peters, 1990).

Fracture cleavages also occur in the breccia complex. These trend from  $015^\circ$  to  $050^\circ$  (in addition to the  $S_1$  cleavage), although their significance is uncertain. Clayton (1992), reports a NNE trending cleavage in metasediments around the complex which he correlates with the Policeman Creek Fault zone. The  $020^\circ$  trending cleavage in the complex ( $S_2$ ) is probably equivalent to this. The Policeman Creek Fault zone is the largest of a broad region of NNE trending faults which has effected much of the Seventy Mile Range Group to the south of the breccia complex (Henderson, 1986). According to Henderson (1986) these fault zones show phyllosilicate cleavage development, subhorizontally stretched clasts, and produced strike slip offset of Seventy Mile Range Group formations. Clayton (1992) was unable to trace the effect of these fault zones into the area around the breccia complex due to poor outcrop and lack of marker horizons. However, the NNE trending cleavage implies the early development of such fault zones parallel to the Yarraman Creek corridor.

Zones of intense penetrative cleavage (within metasediment), which outcrop in fault zones in the breccia complex, define the map trace of early ductile structures. These zones occur in faults.

trending 005°, 025°, 056° and 150°, and also as rare zones parallel to bedding (090°). Because these cleavage zones have steeply plunging mineral lineations, and they commonly control dolerite and rhyolite dykes (particularly in N and NNE trending faults), it is suggested these structures were produced in response to early E - W extension. However, the timing of these events is uncertain. Henderson (1986), describes predominantly N trending dolerite sills and dykes, and later quartz feldspar porphyry dykes, as being restricted to the basal formation of the Seventy Mile Range Group and predating the Ravenswood batholith. He suggests they were emplaced during an early Palaeozoic basin forming event. In contrast, in the breccia complex (this study) and the surrounding area (Hartley et al., 1989; Clayton, 1992), dolerite dykes are younger than the porphyritic rhyolite dykes, and both intrude the Mt. Leyshon granite of the Ravenswood complex. A Silurian age has been assigned to these dykes (Hartley et al., 1989) and for this reason the period of early extension in the Charters Towers terrain is assigned a Silurian age.

### 3.6.2 Late Palaeozoic to Mesozoic history

Thus, by the Devonian an array of ductile structures was present in the Charters Towers Province. The Late Palaeozoic deformation history of the Charters Towers Block remains unclear, although the presence of weakly developed foliations in the Devonian granitoids (Clayton, 1992) implies that the block was tectonically active in the Devonian. In addition, Hartley et al. (1989) suggested the brittle east dipping faults in the Charters Towers area were of Devonian age. Work on the eastern margin (Burdekin sub-province) and particularly to the south in the Drummond and Bowen basins is also beginning to clarify tectonic development of the Charters Towers Province. The significance of brittle structures developed in the breccia complex is now discussed and their relationship to the regional tectonic events to the east and south is assessed.

Structural analysis in brittle terrains is often more difficult than ductile terrains, where it is generally possible to erect a structural history on the basis of overprinting cleavages. Much of the evidence for brittle faulting prior to and/or synchronous with the formation of the breccia complex was probably overprinted by intrusion of the main pipe breccia, and by the later brittle strike slip fault system. In addition, some of the fracturing observed in basement was probably generated during igneous emplacement and breccia generation. The scatter of joints and fault orientations in basement and main pipe breccia is probably due to such an effect. Clayton (1992) could find only limited outcrop of brittle faults in the basement around the complex (though their presence is also indicated by outcrop inside the complex, by the regional aerial photo pattern, section 3.2, and by the aeromagnetic linear pattern, Laing, unpublished report, 1991). Claytons data, however, indicates the presence of brittle-ductile structures within basement dykes, and suggests ductile structures were commonly reactivated by brittle faulting. The early brittle-ductile structures at the northern margin of the complex are tentatively correlated with those of Clayton (1992). The pre-main pipe breccia mutually intersecting quartz vein sets occur in two linear zones parallel to the Mt. Dean and Mt. Leyshon Corridors, in contrast to later veins in the Mt. Leyshon breccia complex which are multi-directional. These pre-main pipe veins provide evidence for pre-complex extension parallel to both corridors.

STRUCTURAL TYPE	DESCRIPTION	ORIENTATION
<b>PRE-COMPLEX STRUCTURES</b>		
Bedding (S <sub>0</sub> )	Poorly bedded sequence with a fissile parting.	Variable (070° - 120°), maxima 100°, steep to moderate dip.
<b>Ductile structures</b>		
F <sub>1</sub> folds	Isoclinal folds. One occurrence only.	Plunges 73° towards 091°
S <sub>1</sub> cleavage	Axial planar to F <sub>1</sub> folds. Penetrative or fracture cleavage.	Variable, parallel to bedding.
F <sub>2</sub> folds	F <sub>2</sub> folds effect S <sub>0</sub> and S <sub>1</sub> . Two occurrences only.	Plunge 45° towards 210° and 39° towards 276°.
(1) Mylonite.	One occurrence at the eastern margin of the breccia complex.	North trending, steep dip to west.
(2) Zones of penetrative cleavage	Cleavage crops out as remnants within major fault zones in the complex.	005°, 025°, 056° and 150° trend; steeply plunging mineral lineations.
(3) Reactivation of bedding	Zones of phyllosilicate development in mudstone metasediment layers (1 - 10 cm thick)	Parallel to bedding.
S <sub>2</sub> Cleavage	Fracture cleavage in metasediment, poorly developed.	Approximately 020°, steep dip.
Brittle-ductile shearing	Shearing within dolerite dykes and at dolerite-granite contacts.	Unknown, unoriented drill core (regionally NE and NW)
<b>Brittle structures</b>		
Mutually intersecting quartz veins	Mutually intersecting infill veins with floating fragments in granite east of Mt. Hope. Age relative to other pre-complex brittle structures is conjectural.	120° and 045°, steep dip.
<b>EARLY SYN-COMPLEX STRUCTURES</b>		
Quartz veins	Common small scale replacement type in basement lithologies.	Unknown
Fault and fracture meshes	Extensive brittle deformation of basement units. Preserved in metasediment zones and probably also in basement rhyolite within main pipe breccia.	147° and 058°, steep dip.
Brittle reactivation of bedding	Dense fracturing of metasediment. Rarely preserved as a ghost fabric in rubble textured zones.	Sub parallel to bedding.

Table 3.1: Structural elements of the Mt. Leyshon breccia complex.

STRUCTURAL TYPE	DESCRIPTION	ORIENTATION
<b>LATER SYN-COMPLEX STRUCTURES (POST-MAIN PIPE BRECCIA)</b>		
Quartz molybdenite veins	Laminated veins with fibrous textured crystals which contain inclusions. Veins contain abundant wall rock slivers.	Steeply dipping veins which strike from 067° to 125°.
Inter breccia shear zones	Brittle / ductile shearing of main pipe breccia and granite prior to the formation of the Mt. Leyshon breccia.	unknown (unoriented drill core).
Oblique slip normal faults	Offset of deformed mudstone horizons in extensively fragmented metasediment on Mt. Hope.	104° - 127°, steep dip
Mt. Leyshon margin crush zone	Zone of brittle deformation marginal to the Mt. Leyshon breccia. (Post-Mt. Leyshon breccia strike slip movement occurs on the fractures.)	Three dominant fracture orientations (NE contact): 100° steep dip to south, 015° subvertical, 035° moderate dip.
<b>POST-MT. LEYSHON BRECCIA STRUCTURES</b>		
Late veins	Veins consisting of many of the hydrothermal stages outlined in Chapter 4. Both open space veins and shear fibre veins (commonly with shallow dipping movement fibres).	Multidirectional, maxima trending 115° but also at 000°, 040° and 070°.
Late faults	Strike slip faults developed throughout the complex: (1) Cataclasites (subsequently reactivated, infilled and replaced by carbonate). (2) fault breccia and gouge. Reverse faults consisting of fault breccia and gouge, postdate basalt dykes, and offset the ore body by approximately 200 metres.	Four dominant directions: N to NNE, NE to ENE, E to ESE and SSE, generally steeply dipping.  Approximately 150° strike, moderate dip to the west.
Joints	Abundant within units of the breccia complex, particularly basement. Probably multi-stage.	Multidirectional. Joints in igneous units dominantly trend NE and SSE.

Table 3.1: Structural elements of the Mt. Leyshon breccia complex.

Figure 3.10: Structural evolution of the Mt. Leyshon breccia complex. Large arrows indicate inferred regional (solid) and local (dashed) principle compression / extension directions. B - F shows sequential evolution; numbers refer to Figure caption.

A Regional structural setting. Note: The location of the Mt. Leyshon breccia complex (MLBC) at the intersection between the Mt. Dean and Mt. Leyshon corridors, the other NE trending transfer faults (double lines), and the extensional structural grain of the Drummond Basin (dashed lines; Johnston and Henderson, 1991)

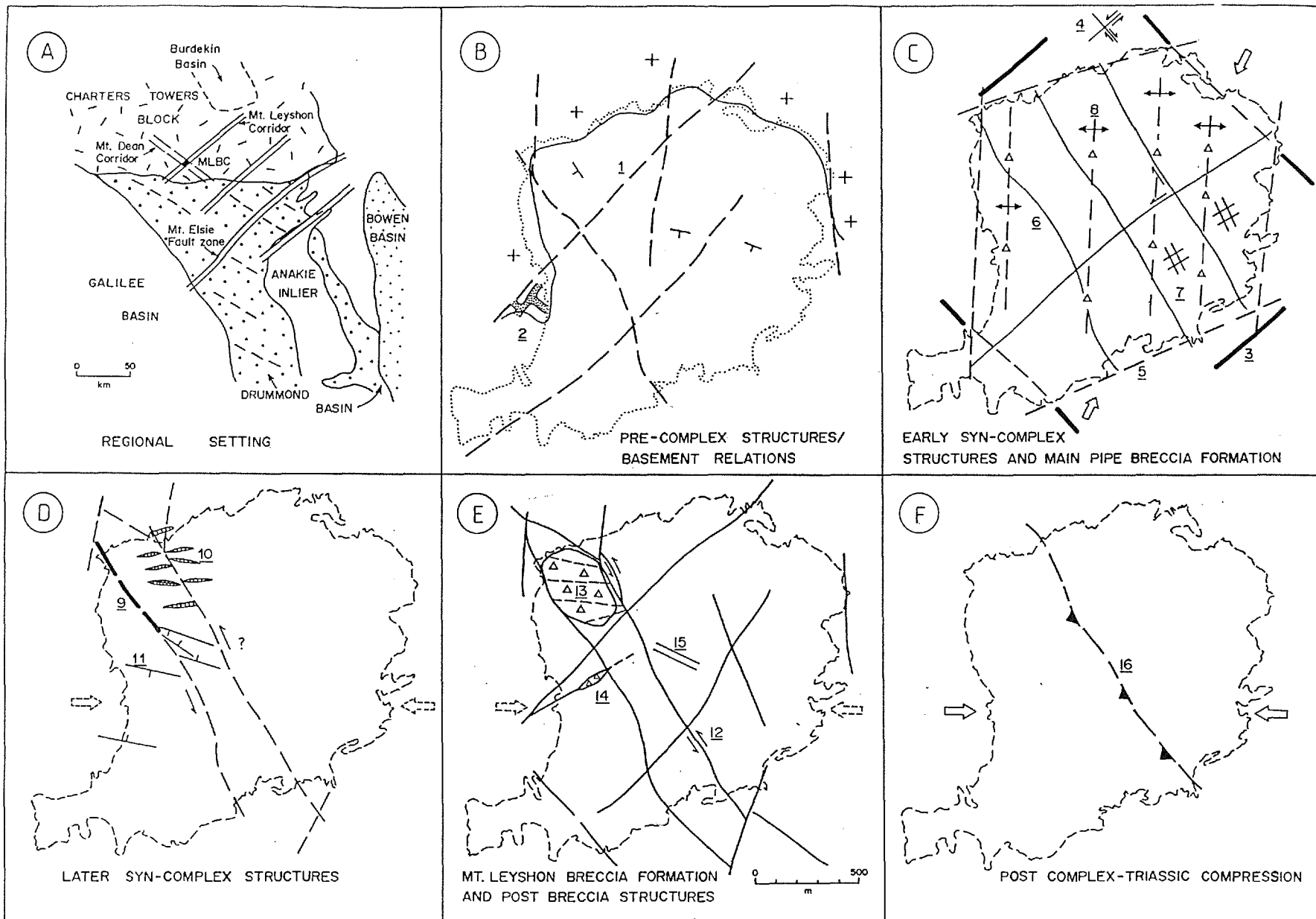
B Pre-complex structures and basement relations. Note: The fault offset granite / metasediment contact (solid line) which influences the subsequent development of the breccia complex (dotted line), the location of pre-complex ductile faults (observed in preserved basement blocks) which are reactivated during the formation of the breccia complex (1), the mutually intersecting extensional quartz veins (2) both of which are sub-parallel to the Mt. Leyshon and Mt. Dean Corridors, and N trending ductile faults which are parallel to ductile structures in the Anakie Inlier (Johnston and Henderson, 1991).

C Early syn-complex structures and main pipe breccia formation. Note: The orientation of the regional structural corridors with respect to the breccia complex (3), the sense of movement on brittle / ductile shear zones probably active during this time (4; Clayton, 1992), the approximately linear boundaries of the breccia complex which probably represent basement faults (5), brittle reactivation of basement structures (6) resulting in extensive basement fragmentation by fault and fracture meshes (7), and inferred extensional reactivation of N trending basement faults during main pipe breccia formation (8).

D Later syn-complex structures. Note: The inter-breccia shear zones (9) and their inferred location in the complex (thin dashed lines), the orientation of quartz molybdenite veins (10) and their relationship to the inter-breccia shear zones, and the orientation of the oblique-slip normal faults (11).

E Mt. Leyshon breccia formation and post-Mt. Leyshon breccia structures. Note: The configuration of late strike slip faults and the consistent sense of movement on one of the faults (12), the location of the Mt. Leyshon breccia (13) with respect to these faults and the possible extensional fractures (dashed lines) in the pipe, the location of the Mt. Hope breccia on a subsidiary fault (14), and the orientation maxima for the late veins and preferred direction of brecciation (15).

F Post complex Triassic compression. The orientation of the late reverse fault zone which cuts the ore body and all lithologies in the complex is shown (16).



Early syn-complex brittle fault and fracture meshes in metasediment zones have an orthogonal pattern (again parallel to the Mt. Dean and Mt. Leyshon corridors) but pass into zones of acute intersection in more intense areas of shear strain. These observations suggest weakly extensional strike slip faulting at an early stage in the formation of the breccia complex. The N-trending zones of main pipe breccia, are consistent with (?hydraulic) reactivation of N - S trending ductile fault zones, localising main pipe breccia emplacement.

Structural elements which developed between formation of the main pipe and Mt. Leyshon breccia comprise:

- (1) Quartz-molybdenite veins.
- (2) Inter-breccia shear zones.
- (3) Oblique-slip normal fault.
- (4) Mt. Leyshon breccia crush zones.

The significance of the quartz-molybdenite veins to the local stress system is only partially resolved because data collection was hampered by poor outcrop. The quartz-molybdenite vein textures suggest incremental extension, although a more complete understanding of their relationship awaits the collection of further vein data. The fifteen measured veins (067° and 125° orientation) probably formed as en-echelon vein arrays in conjugate shear zones, or as a single set of veins which show a scatter due to pre-existing fabrics (eg. bedding) and/or rotation during later faulting. As en-echelon shear veins commonly have a sigmoidal shape (Ramsay and Huber, 1987) and the Mt. Leyshon veins are planar, formation due to the second case is favoured. The veins may represent extensional veins formed during sinistral strike slip on 150° in response to broadly east - west compression. This interpretation is consistent with the suggested sense of displacement of the subsequent late strike slip fault which bounds the eastern margin of the Mt. Leyshon breccia (see below). Likewise, small scale oblique normal faults which trend 104° to 127°, suggest oblique sinistral extension in the complex prior to intrusion of the Mt. Leyshon breccia.

Inter-breccia shear zones have been observed in unoriented drill core and, consequently, their geometric significance is unknown. They do however, provide evidence for brittle-ductile deformation of granite and main pipe breccia in the area which subsequently became the Mt. Leyshon breccia. The earliest deformation in the crush zone around the Mt. Leyshon breccia pipe predates the formation of the pipe, and movement on the inter-breccia shear zones may have been responsible for this earliest deformation. If this is true, the inter-breccia shear zones fragmented and prepared the ground for the Mt. Leyshon breccia pipe formation. However, structural analysis of the crush zone outside the Mt. Leyshon breccia has been prevented by the complexity resulting from the late strike slip fault system. Post-Mt. Leyshon breccia fractures and faults in this crush zone are approximately parallel to regional faults and indicate continued movement on the regional structures. One possible mechanism for producing this crush zone involves refraction of shear strain, from regional Mt. Dean Corridor faults, onto the 160° trending strike slip faults which bisect the complex (and link with SE trending faults). In this scenario, sinistral reactivation of the

inter-breccia shear zones combined with E trending extension fractures, could act as a triggering mechanism for the Mt. Leyshon breccia pipe formation (see section 7.3.1). The presence of E trending (080°) high dilation breccia zones in metasediment at the SE corner of the Mt. Leyshon breccia (390 RL, noted in pit mapping and cut slabs), is consistent with this interpretation.

Hydrothermal fluids flowed through the Mt. Leyshon breccia after its formation, cementing fragments and reducing permeability (see Chapter 4). The numerous late veins in the NW domain are important as they allowed repeated fluid access to the Mt. Leyshon breccia. Discrete veins formed around the Mt. Leyshon breccia, in the isotropic lithologies which have a low porosity (main pipe breccia and basement). Irregular inter-connected veins and zones of diffuse fracturing formed in the more anisotropic and porous Mt. Leyshon breccia. Discontinuous veins formed in igneous and tuffsite breccia dykes which cut the breccia. This repeated vein formation and reactivation of pre-existing veins is important to the controls on the gold mineralisation within the Mt. Leyshon breccia (see Chapter 8).

An understanding of the mechanism responsible for vein formation requires a knowledge of vein timing and a study of successive vein textures (constrained by the mineral paragenesis). A number of features provide evidence for the possible mechanism of vein formation. Firstly, pre-existing structures are commonly the site for vein formation and vein textures are generally of the infill type. Secondly, the presence of strike slip shear-fibre veins of the same paragenetic stage, particularly in the more isotropic lithologies, indicates that wrench faulting was also active during this period. Furthermore, limited data indicate these fibres commonly have a NNE or SSW plunge suggesting NNE trending strike slip faults were active during vein formation.

The above observations are consistent with the work of Segall and Pollard (1983), in granitoid rocks of Sierra Nevada (California), who suggested strike slip faults nucleated on earlier formed extensional mineral filled joints (veins). Adjacent fault segments did not propagate into intact rock in their own plane, rather the faults were linked together by secondary dilational fractures. In contrast to the study of Segall and Pollard (1983), the Mt. Leyshon extensional veins are multi-directional and, as discussed in Chapter 7, suggest that abnormally high fluid pressures existed during their formation. However, the dominant 115° trend of both veins and preferred direction of brecciation in the breccia complex is consistent with their combined formation due to SSW - NNE directed extension.

The presence of both infill (open space, tension veins) and shear veins for a number of paragenetic stages suggests that fluctuations in normal and shear stress occurred during vein formation. These fluctuations may result from variations in fluid pressure accompanying seismic faulting, in the manner suggested by Sibson (1989a; see section 7.4.2). If this is true both the formation of new veins and reactivation of pre-existing structures in unfavourable orientations would have occurred in response to high fluid pressure. Thus, although the regional stress system was active during vein formation, the changing local stress conditions induced by (?fluctuating) high fluid pressure prevent the use of the veins to define the orientation of the regional stress field. A similar

limitation may apply to the use of igneous dyke orientations in the breccia complex to investigate temporal variations in the regional stress field.

Late structural activity resulted in the formation of abundant faults within the Mt. Leyshon breccia complex. Early strike slip faults formed cohesive cataclasites, and a later period of carbonate fault breccias was superseded by cohesionless fault gouge and breccia. In a crude way, the type of fault breccia or gouge produced can be related to the depth of formation. At shallow crustal levels (brittle deformation zone), Sibson (1989a) suggested that below approximately three kilometres cataclasite fault rocks are dominant. This is consistent with the present erosion level originally representing a depth of 2-3 kilometres, as discussed previously (section 2.4.2). The transition to non-cohesive faults (dominated by breccia and gouge) possibly occurred due to uplift and erosion, as the complex moved to shallower depths. The timing of this deformation is partly constrained by the later reverse faulting which has affected the breccia complex. This compressional event may be correlated with the widespread compression of eastern Queensland during the early to mid Triassic, which produced inversion and thrusting in the Bowen and Drummond basins (Hammond, 1990; Johnson and Henderson, 1991).

Faults in the breccia complex are multi-directional, although four dominant orientations occur. These orientations match those at the regional scale deduced from aerial photography in this study and major structures of the Charters Towers Block (Peters, 1987), indicating that the regional fault pattern is repeated at the complex scale. Such a pattern of self similarity for faults at a number of scales has been reported by several workers (eg. Velde et al., 1991). Furthermore, ductile fabrics preserved in brittle fault zones, which form part of the regional fault network, indicate later strike slip faults formed by brittle reactivation of pre-complex basement structures. Similarly, the orientation of igneous and breccia units in the complex, together with the presence of brittle-ductile cleavage and fault zones at dyke margins, suggests they were emplaced during repeated reactivation of basement structures. Similar reactivation tectonics have been documented for a number of wrench systems.

The data presented here suggests the breccia complex formed at the intersection of two regional scale orthogonal corridors, one trending NE and the other trending SE (Mt. Leyshon and Mt. Dean corridors, respectively). A third, locally developed, N trending corridor (Yarraman Creek corridor) was also reactivated to form the complex. At the breccia complex scale, two dominant suborthogonal conjugate fault sets are present, one set striking NE and the other striking SSE. These breccia complex faults link with SE, NE and N trending regional faults which form the corridors, although the stress systems which produced the structures in the Mt. Leyshon breccia complex is problematic.

The orientation of both the regional and local fault pattern is not that predicted by conventional theory of strike slip faulting. Conventional mohr - coulomb fault theory (Anderson, 1951; Jaeger and Cook, 1979) which is generally applied to brittle fault analysis, combined with laboratory derived rock friction coefficients (Byerlee, 1978), suggests that conjugate fault planes will form at

an angle of approximately 50°-60° to  $\sigma_1$  (maximum principle stress), rather than approximately 90° as for the Mt. Leyshon and regional faults. However, a recent survey of currently active regions of strike slip faulting (Thatcher and Hill, 1991) has highlighted the common occurrence of mutually perpendicular conjugate strike slip faults. Thatcher and Hill (1991) suggest orthogonal conjugate faults are typical of active strike slip faulting rather than exceptional, and they are developed, in particular, in regions of relatively extensional strike slip faulting characterised by elevated heat flow and recent volcanism (eg. Izu, Japan; Salton trough, USA). The work of Thatcher and Hill (1991) may require a major refinement in conventional fault analysis.

A normal Riedel Analysis has not been attempted on the fault sets defined in this Chapter for the following reasons:

- (1) The orientations of Mt. Leyshon and regional strike slip faults are geometrically consistent with the observations of Thatcher and Hill (1991).
- (2) The rarity of kinematic indicators, and the available data does not indicate a simple kinematic pattern, as parallel faults have conflicting sense of movement, suggesting slip reversals.
- (3) Brittle faults formed over an extended period with only certain fault blocks or fault segments active at any given time.
- (4) Transpressional movement due to the crustal shortening, and resulting formation of the late reverse faults in the breccia complex, may have reactivated Permian strike slip faults during the early Triassic. Such reactivation may be partly responsible for the conflicting sense of movement on faults in the breccia complex.

Some evidence for the stress history is available from regional work around the breccia complex. Clayton (1992) suggested that brittle-ductile deformation in granitoid and metasediment lithologies around the breccia complex represents a conjugate strike slip fault system. Brittle-ductile structures cut dykes interpreted by Hartley et al. (1989) as Carboniferous, suggesting some of this deformation is probably Late Carboniferous in age.

The deformation due to the conjugate fault system is most simply defined in the Mt. Leyshon granite where it occurs as foliation and brecciation of dykes. Displacements on dykes are consistently sinistral on NE and dextral on NW trending shears, according to Clayton, 1992. He further suggests the regional structural pattern formed in response to N-S directed compressive stress, and the Mt. Leyshon corridor acted as a sinistral strike slip system. Clayton (1992) presents only limited data to suggest conjugate shearing on faults trending 038° and 140° (ie. with a 60° acute angle between the conjugate faults). However, the data of Clayton (1992) are better interpreted as representing orthogonal conjugate fault sets which trend approximately 050° and 135°. In this interpretation the data also suggest N-S directed compression (E-W extension), although the conjugate strike slip faults are now geometrically consistent with the regional and complex scale data presented in this thesis.

Laing (unpublished report, 1991) interpreted the regional fault pattern based on an aeromagnetic data set, and used the inferred faults to identify a number of structural corridors. These corridors

generally coincide with the aerial photographic linear corridors identified in this study (Figure 3.1), although the Mt. Dean corridor was not identified by Laing. He suggested two dominant orthogonal strike slip corridors controlled Permo-Carboniferous regional structural evolution in the area around the breccia complex. These corridors, which he interpreted to have formed during E-W compression, are the dextral Mt. Leyshon corridor, and the sinistral Merri Monarch corridor (which is equivalent to the second SE trending linear corridor noted in section 3.2). Despite the complicated history of the Mt. Leyshon complex faults, the sense of displacement on the SE trending strike slip fault which bisects the breccia complex (and bounds the eastern margin of the Mt. Leyshon breccia pipe) is in agreement with this interpretation by Laing (1991). However, these interpretations have the opposite sense of movement for the Mt. Leyshon corridor to that proposed by Clayton (1992). The apparent conflict between the two interpretations may result from the tendency for the aeromagnetic data to reflect the later Permian or Triassic stress system, as offset on magnetic marker units would also have occurred at these later times. In contrast, the veins and brittle-ductile fault zones reported by Clayton (1992) are likely to reflect pre- to early-complex structures (? latest Carboniferous to early Permian). If this is true, then the data suggests an earlier period of N - S compression followed by a change to E - W compression.

It is now important to consider the Mt. Leyshon complex in the wider context of what is presently understood of the Late Palaeozoic regional deformation history of NE Queensland. The Drummond Basin, which formed in an active margin setting during the Late Devonian to Early Carboniferous (Henderson, 1980), abuts and onlaps the southern margin of the Charters Towers Province (Figure 3.10A). Johnson and Henderson (1991) interpret the Drummond Basin to have formed from NE-SW directed extension on NW-SE trending structures, although local wrench faulting is reported. Accommodation of these extensional structures was enabled by major NE trending transfer faults (Gibbs, 1984); structures which also extend north into the Charters Towers Block. During folding and inversion of the Drummond Basin (largely considered to be of Late Carboniferous age; McPhie et al., 1990) the transfer faults were reactivated, particularly along the northern margin with the Anakie Inlier and the Charters Towers Block, where a major transfer fault (Mt. Elsie Fault Zone, Figure 3.10A) is reactivated as a zone of dextral megashear during compression (Johnson and Henderson, 1991). Significantly, these transfer structures were active after inversion of the Drummond Basin as indicated by their control on Permo-Carboniferous igneous intrusives both at the northern Drummond Basin margin and into the Charters Towers block. Furthermore, Lang et al. (1990) proposed Late Devonian to Early Carboniferous extension of the Lolworth-Ravenswood block for formation of the Burdekin Basin (possibly as a result of dextral transtension). Once again the NW trending faults and NE trending (?transfer) faults were reactivated in the Late Carboniferous, and also controlled Permo-Carboniferous intrusives.

The age of the Mt. Leyshon breccia complex is only partially resolved. The age at onset of breccia complex formation is unknown, although the extensive history of hydrothermal and structural events documented in this thesis, raises the possibility that associated activity spanned several million years. Indeed, Warnaars et al. (1985) report a period of batholith emplacement, cooling

and hydrothermal alteration spanning at least 15.2 Ma in the Mio-Pliocene Los Bronces-Rio Blanco porphyry copper and tourmaline breccia complex. Radiometric ages of  $280 \pm 2$  Ma on late (sericite) alteration (Paull et al., 1990) and a  $280 \pm 20$  Ma Pb-isochron mineralisation age (Dean and Carr, unpublished CSIRO report, 1988) suggest that related intrusive activity in the Mt. Leyshon complex had ceased by the Permo-Carboniferous boundary (Figure 4.4). A Rb - Sr isochron age of  $283 \pm 19$  Ma (Uemoto et al., 1992) for porphyry unit IV is consistent with this interpretation.

An evolution only slightly longer than that indicated by Warnaars et al. (1985), would indicate the breccia complex was initiated at the end of the Drummond Basin inversion. There is independent evidence (J. V. Wright, unpublished regional data) suggesting NE-SW compression active during mid-late Carboniferous which also caused Drummond Basin inversion. The stress configuration inferred for the breccia complex is consistent with this compression direction. The post-mineralisation basalt dykes (which are probably geochemically unrelated to other Mt. Leyshon igneous units, Chapter 6) have been dated at  $278 \pm 2$  Ma in this study (in conjunction with A. Webb), which is synchronous with extension in the Bowen basin. This implies that hydrothermal activity in the complex overlapped with the onset of extension in the Bowen Basin (E-W extension). Thus, although it is possible that the Mt. Leyshon complex is as old as the final inversion of the Drummond Basin, it is more likely to have been entirely synchronous with the onset of extension in the Bowen Basin, and possibly also the formation of the Lizzie Creek Volcanics, both of which are considered to be earliest Permian (Hammond, 1990). Bowen Basin architecture is considered to have been controlled by the linking of extensional structures with transfer faults in a similar way to the older basins, and once again transfer structures also controlled igneous emplacement (Hammond, 1990).

One further aspect of the link between regional deformation and the local structural evolution of the breccia complex requires attention. From the above discussion, late igneous and breccia emplacement and hydrothermal alteration in the complex probably overlapped with regional E-W extension. However, the orientation of later syn-complex structures (Figure 3.10D) and the post-Mt. Leyshon breccia structures (Figure 3.10E) is more consistent with local E-W compression. Given the small scale of the area within the complex, and the dynamic fluctuations in the local stress field likely to have accompanied high pore fluid pressure, gas and magma pressure (Chapter 7), the later syn- to post-complex structures probably represent a local aberration of the regional stress field.

The transfer faults have played an important role in the structural development of sedimentary basins in the region, and in controlling igneous emplacement. They are unlikely to be simple accommodation structures confined to sedimentary basins (as originally defined by Gibbs, 1984), and probably represent reworking of more fundamental basement structures (as proposed by Wright, 1990). In the Drummond Basin their importance in controlling gold mineralisation has also been identified (Bimurra, Wirralie, Yandan; Henley and Adams, 1992). The Mt. Leyshon

corridor (which has the same orientation as the regional transfer faults) is interpreted here as a transfer zone as it is composed of a number of strike slip faults, and has localised a number of intrusive igneous and breccia complexes in addition to the Mt. Leyshon complex (eg. Tuckers Igneous Complex, Seventy Mile Mount).

### 3.6.3. Summary structural model

In summary (Figure 3.10), the data, analysis and discussion presented in this Chapter indicates:

- Complex-scale faults link with the regional scale structures suggesting that the regional stress system controlled structural development in the complex.
- Late Devonian to Permian deformation in the Burdekin Basin of the Charters Towers Block, and in the basins to the south, is explained by the linking of NE trending transfer faults with extensional, compressional and strike slip faults.
- During this period transfer faults played a central role in locating igneous emplacement and, possibly, gold mineralisation.
- The breccia complex is localised at the intersection of two regional orthogonal strike slip corridors; a third local NNE trending corridor also seems important. These corridors are defined by groups of linears and faults (Figure 3.1).
- Brittle reactivation of the ductile basement structures controlled the dominantly brittle strike slip system (Figure 3.10B).
- The pre-complex brittle strike slip faulting, which occurred prior to main pipe breccia emplacement (Figure 3.10C), was weakly extensional in nature. Limited regional data suggests a fault system consistent with E-W extension.
- Laminated quartz-molybdenite veins and oblique slip normal faults suggest a local change to E-W compression prior to Mt. Leyshon breccia formation (Figure 3.10D).
- The presence of inter-breccia shear zones implies the strike slip fault system remained active during this time (Figure 3.10D). These shear zones possibly produced the brittle deformation which occurred between the main pipe and Mt. Leyshon breccia events. The orientation of quartz-molybdenite veins and oblique normal faults, that also occurred at this time, is consistent with sinistral strike slip movement on inter-breccia shear zones during E-W compression.
- The preferred orientation of breccia and igneous units (Figure 2.5) is similar to the dominant fault orientations, and strike slip faults reactivated earlier formed dyke margins, veins and faults. These data suggest the wrench system remained active during all periods of breccia complex development.
- During hydrothermal activity which postdates the Mt. Leyshon breccia, the strike slip faults remained active during a period of fluctuating high fluid pressure.
- The late strike slip faults of the breccia complex have a complicated movement history but consistent sinistral offset on one of the main complex scale strike slip faults (Figure 3.10E) implies E-W compression controlled the fault pattern.
- Development of late reverse faults in the breccia complex indicate a change to dominantly compressional tectonics (Figure 3.10F). This seems regionally related to general E-W

compression and Triassic inversion of the Bowen Basin. It is likely that this change in the stress system resulted in the complicated movement history of the breccia complex strike slip faults.

---

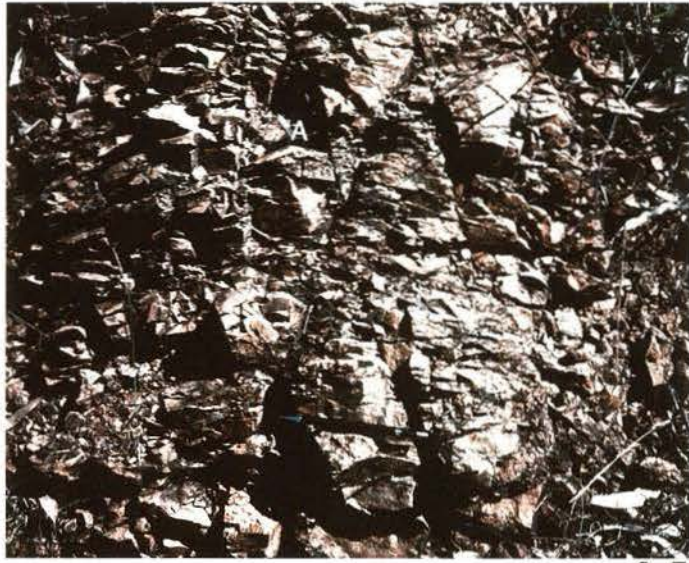
Plate 3.4: Fault and fracture mesh in metasediment block inside the main pipe breccia. Note the suborthogonal mesh of small scale fractures bounded by larger scale faults, defining fragmentation domains within the basement block. Second order fragmentation described elsewhere in basement blocks is almost absent. (GR. 4855 5665.)

Plate 3.5: Crackle brecciated metasediment subparallel to cleavage. Note the kink fold closure (A) preserved through the brecciation. Second order fragmentation and expansion (B) forms erratic zones overprinting the cleavage parallel brittle fabric. (GR. 3500 4825.)

Plate 3.6: Quartz-molybdenite vein cutting basement rhyolite. Note: (1) Extension resulting in vein formation occurred in two directions, (2) slivers of wall rock are interleaved between the vein increments, (3) the fine parallel banding in the quartz layers, and (4) the parallel bands of molybdenite occurring in the vein. (Sample no. 31561.)



3.4



3.5



3.6



Plate 3.7: Inter-breccia shear zone. See Figure 3.4 (below) for explanation. (MLD 277, 132 m.)

Figure 3.4: Line drawing of the inter-breccia shear zone shown in Plate 3.7:

Zone A - comminuted granite.

Zone B - comminuted main pipe breccia.

Zone C - weakly deformed main pipe breccia (note the visible fragments in the breccia, the textural and colour difference between this zone and strongly comminuted main pipe breccia, zone B).

Zone D - strongly deformed main pipe breccia replaced by chlorite and pyrite alteration.

Zone E - crack seal type calcite vein containing slivers of chlorite altered zone D.

Zone F - Mt. Leyshon breccia which is dominated by main pipe breccia fragments-also note the fragments of altered zone D in the breccia..



3.7

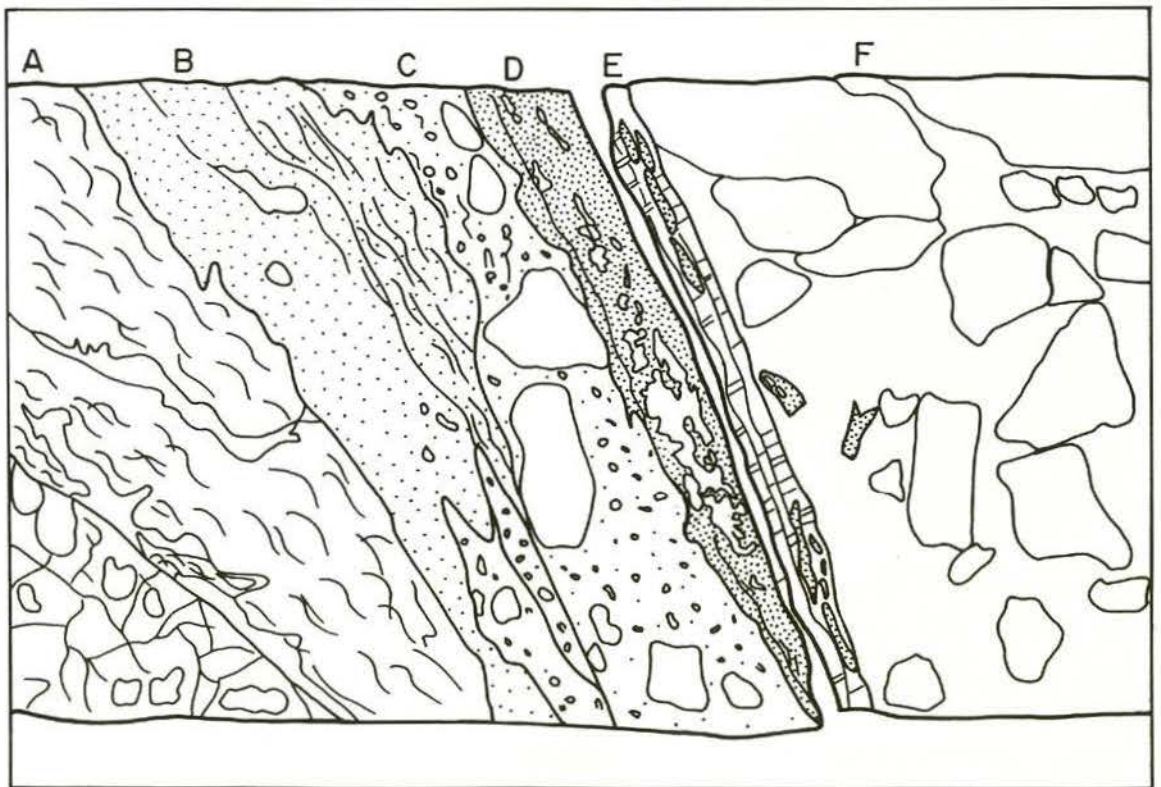


Figure 3.4



Plate 3.8: Oblique-slip normal fault zone in metasediment on western flank of Mt. Hope. Although the outcrop is extensively fractured, note a siltstone horizon (A) occurs in the more massive sandstone unit (B) and is down-thrown to the north by approximately 70 cm across the fault zone (at hammer). (GR. 3830 5600.)

Plate 3.9: Sharp contact of the Mt. Leyshon breccia and marginal crush zone. Note: the knobbly massive texture of the Mt. Leyshon breccia (A), in contrast to the strongly fractured main pipe breccia (B), and the sharp contact of the Mt. Leyshon breccia (at the grid peg). (Open pit, GR. 3900-6150.)

Plate 3.10: En-echelon extensional shear (chlorite-pyrite) veins cutting a granite fragment in the Mt. Leyshon breccia. Note that these veinlets cut an earlier diffuse network of silica and sericite alteration (scale = 1 cm). (MLD 277, 132 m).

Plate 3.11: Linear zone of calcite cemented extensional fault breccia, cutting the Mt. Leyshon breccia. Note jigsaw fit of fragments and floating clasts (scale = 1 cm). (MLD 380, 427 m.)

Plate 3.12: Late strike slip fault cutting main pipe breccia. Slickensides on fault surfaces plunge  $16^\circ$  towards  $109^\circ$ . Note: (1) one metre wide central zone of crushing and slip (at hammer); (2) discrete anastomosing zones of gouge; (3) wide crush zone (fracture surfaces are subparallel to gouge principle slip surfaces) overprinted by this fault zone. (Open cut, GR. 3915 6160.)

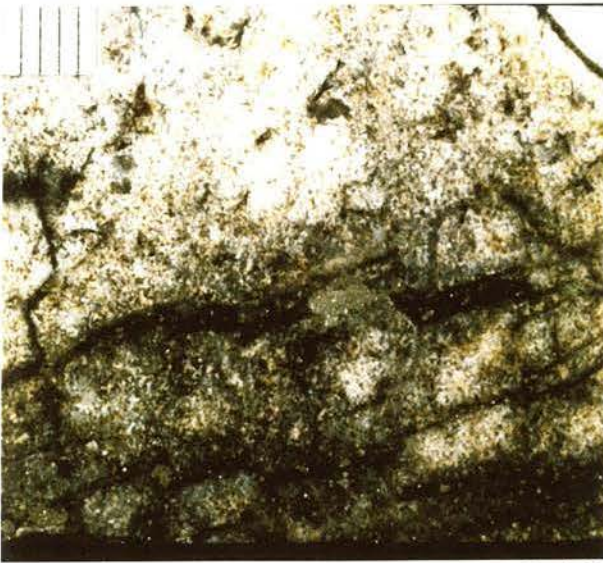
Plate 3.14: Late strike-slip fault zone cutting the main pipe breccia and reactivating the margin of a pyrite-quartz-muscovite vein (A; stages VII-IX, Chapter 4). Dip and strike of fault zone  $102^\circ / 73^\circ$ , slickensides plunge  $17^\circ$  towards  $100^\circ$ . (Open cut, GR. 3710 6200.)



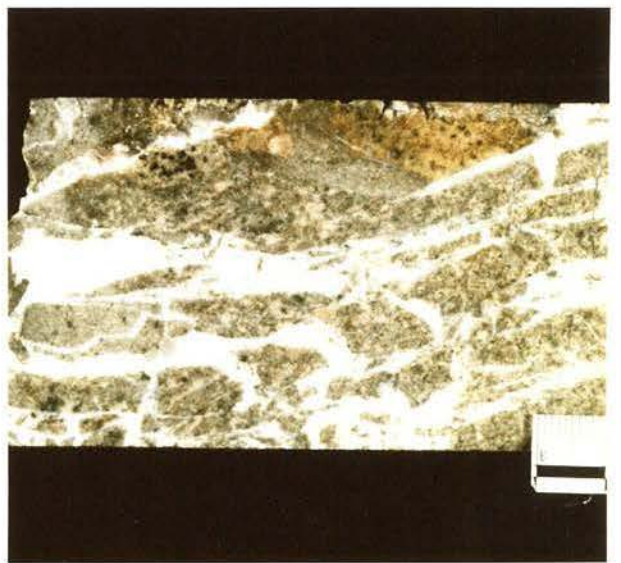
3.8



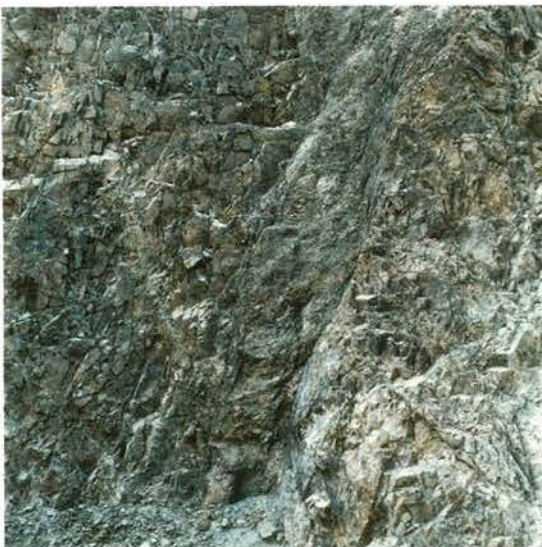
3.9



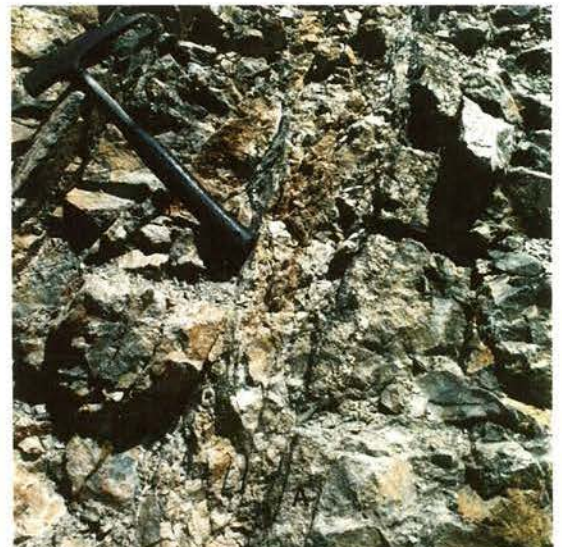
3.10



3.11



3.12



3.14



Plate 3.13: Rebrecciation zone developed at late dyke-main pipe breccia contact. See Figure 3.7 for explanation. (GR. 4800 5785.)

Figure 3.7: Line drawing of Plate 3.13 showing the outcrop relations of a rebrecciation zone at a late dyke / main pipe breccia contact. Note pen for scale.



3.13

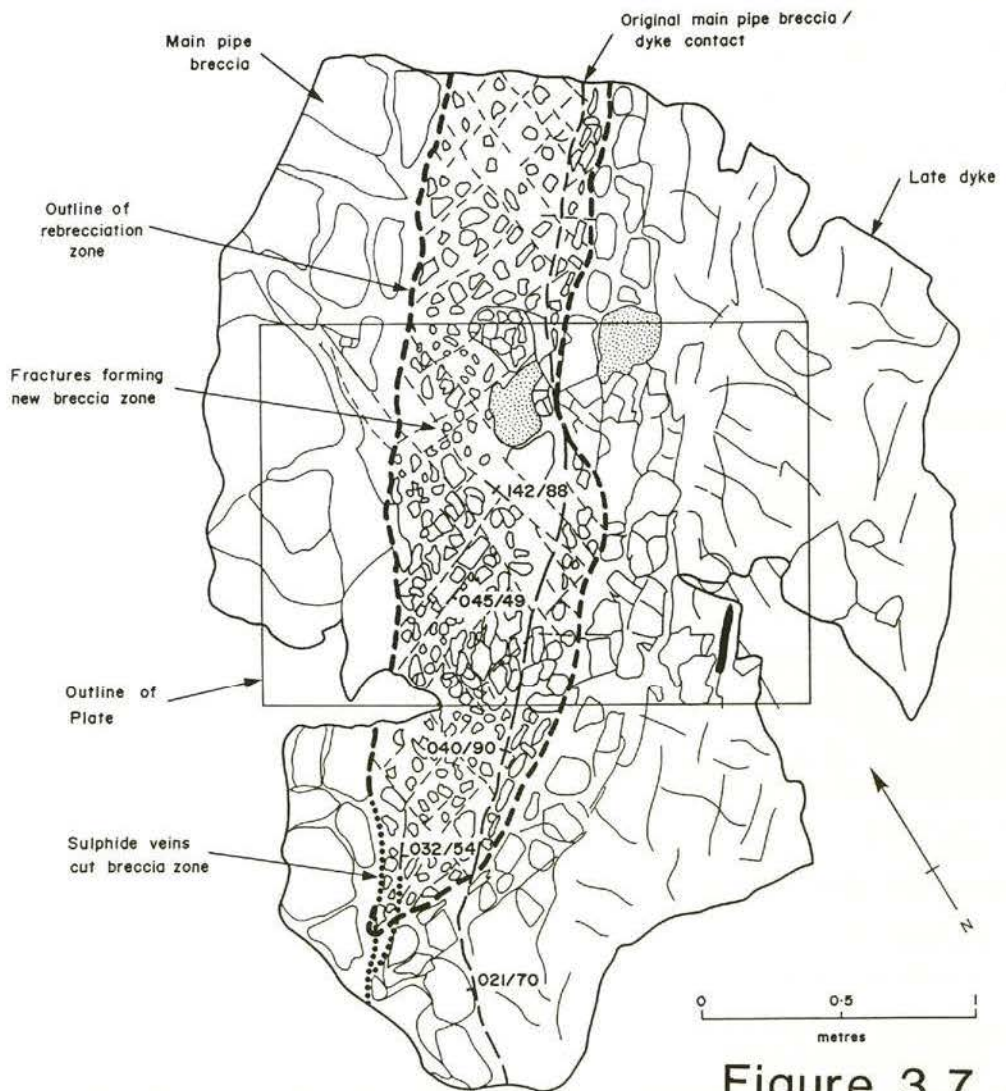


Figure 3.7

## Chapter 4

# MINERAL PARAGENESIS AND HYDROTHERMAL ALTERATION STUDIES OF THE MT. LEYSHON ORE BODY

---

### 4.1 INTRODUCTION

Mineralisation studies aim to understand the processes leading to ore body formation and when the mineralisation formed. Comparatively few studies of hydrothermal systems are well constrained by a detailed paragenesis of the mineral growth. Often the timing of mineral growth is only substantiated by statements such as "the ore is folded" or "the mineralisation is strata bound", and no detailed textural evidence is presented. Furthermore, an appreciation of the geological environment at the time of ore formation constrains many parameters of the mineralising system (eg. pressure, temperature, oxygen fugacity, etc.). The mineral paragenesis is therefore critical to the understanding of ore genesis providing the link between the geological environment and the local ore forming environment.

Teale (unpublished report, 1987) carried out the first systematic mineralogical description of the alteration and mineralisation associated with the Mt. Leyshon breccia complex. This was mainly based on samples collected from the first 19 diamond drill-holes, and provides a comprehensive record of the mineral phases present, although these observations are not paragenetically constrained. Teale also included a series of photomicrographs on sulphide and gold relationships. Morrison et al. (1987) developed a three stage mineral paragenesis for part of the hydrothermal system; however no documentation of the textural evidence for establishing this paragenesis was presented.

A detailed textural study is presented here to establish the timing and mode of occurrence of mineral development with respect to the rock units investigated in Chapter 2. This has implications for:

- (1) The timing of hydrothermal evolution relative to igneous emplacement and breccia generation.
- (2) The nature and chemistry of the fluid responsible for magmatic related brecciation.
- (3) General temperature, pressure and composition of the evolving hydrothermal fluid.
- (4) Timing and controls on gold mineralisation.
- (5) The minimum number of brecciation episodes.

Samples were collected to examine the alteration and mineralisation of the hydrothermal system in conjunction with core-logging to establish the nature and timing of the breccia phases present. Pit mapping and block sample collection were undertaken largely within and adjacent to the Mt. Leyshon breccia (main host rock for gold mineralisation). Polished slabs (20-30 cm across) were prepared from a representative suite of these blocks. These slabs were used to establish a basic paragenesis which was refined during an extensive microscope study.

An important consideration in studying mineralising system is the recognition of infill versus wall

rock alteration mineral components. The techniques for establishing these components are discussed by Taylor (1992) and Taylor (in prep.). This potentially allows the separation of the hydrothermal system into two components:

- (1) A component precipitated within the fluid filled void space (infill).
- (2) A component derived by reaction with the wall rock (alteration / replacement).

A paragenesis based on cross-cutting relationships between alteration phases is established within the wall rock. This paragenesis is cross-checked with the sequence of infill for each mineral phase within the breccia cavities and/or open space veins. This process is refined until each phase is grouped into a stage, which in turn are arranged in a sequence. Where possible each stage represents a coexisting mineral assemblage which formed from the hydrothermal fluid.

Clearly, in the development of a comprehensive mineral paragenesis of a complex hydrothermal system, the researcher has to overcome a number of difficulties. At Mt. Leyshon these include:

- (1) The need for a wide sampling procedure to take all of the mineral phases into account.
- (2) The possibility that the timing relationship between different phases may not physically occur within the chosen samples.
- (3) The timing relationship of one mineral to other phases may be obscured by one or more later minerals. For example, the paragenetic relationship of epidote is often obscured by a late carbonate which replaces it.
- (4) The occurrence of the same alteration mineral in two separate stages. Phases which occur in more than one stage at Mt. Leyshon include illite, muscovite, clay, carbonate and pyrite.

At the Mt. Leyshon breccia complex two problems warrant special mention. Firstly, many generations of pyrite are suspected although detailed studies of pyrite growth zones have not been made. Secondly, the clay alteration at Mt. Leyshon is particularly complex because of its fine grain size and the presence of several clay alteration phases. The overprinting of hydrothermal clays by both supergene and oxide zone clays at Mt. Leyshon adds further to the problems of clay interpretation.

The following terminology is applied in this chapter and throughout the thesis. Each mineral forming part of the hydrothermal system is referred to as a phase (eg. chlorite, pyrite, etc.) Several phases which have similar timing relationships are grouped together to form a stage. A number of stages which represent a major hydrothermal event are referred to as an episode.

EPISODE	STAGE	ASSEMBLAGE	MODE OF OCCURRENCE
Pre-main pipe breccia alteration	I	Quartz only.	Fine grained, usually narrow, fibrous replacement quartz veins which occur in basement units throughout the breccia complex.
<b>Pre-Mt. Leyshon breccia alteration</b>	II	Illite* - quartz - ?pyrite ± albite - hematite.	Pervasive alteration of main pipe breccia matrix and small fragments throughout the breccia complex (Intense patches in the NW corner of the breccia complex).
	IIIa	Biotite - k-feldspar - pyrite ± chalcopyrite - pyrrhotite.	Biotite - pervasive alteration of main pipe breccia in the NW corner of the breccia complex. K-feldspar - minor replacement veinlets, cutting main pipe breccia; rare infill K-feldspar veins occur in metasediment.
	IIIb	Chlorite - pyrite ± epidote ± albite <sup>†</sup> .	Pervasive alteration of the main pipe breccia outside the NW corner of the complex, particularly dolerite, granite and basement rhyolite fragments.
	IV	Muscovite ± quartz - pyrite.	Replacement zones to fractures which coalesce resulting in strongly altered areas. Some fractures have minute seed quartz crystals at their centre.
	V	Quartz - molybdenite.	Persistent veins which consist of fibrous and laminated quartz crystals with fine seams of molybdenite. Veins are developed in basement and main pipe breccia units to the east and west of porphyry unit IV.
<b>Post-Mt. Leyshon breccia alteration</b>	VI	Illite* - quartz - ?pyrite ± albite ± hematite.◊	Pervasive alteration of matrix and fragments in Mt. Leyshon breccia, tuffisite dykes and late breccia dykes. Also occurs as replacement of feldspar phenocryst and groundmass in igneous units.
	VII	Quartz.	Abundant infill phase and minor replacement of selected fragments in the Mt. Leyshon and Mt. Hope breccias. Minor infill of cavities in igneous and tuffisite dyke units.
	VIII	Chlorite - pyrite ± epidote ± ?albite.	These phases are most intense within dolerite dykes (alteration), the Mt. Leyshon and Mt. Hope breccia (infill and alteration) and intermediate igneous units (alteration).
	IX	Muscovite ± ?quartz - ±pyrite <sup>†</sup> .	Infill of breccia cavities and replacement of stage VIII chlorite, together with complete alteration of small igneous fragments and the formation of narrow selvages to larger fragments in the Mt. Leyshon and Mt. Hope breccias. Selective replacement of the tuffisite dykes, late breccia dykes and the Mt. Leyshon igneous units. Also present in persistent quartz-muscovite-pyrite veins as infill and alteration selvages.
	X	Illite* - ?quartz ± ?pyrite.	Minor retrogression of muscovite (stage IX) breccia infill and extensive alteration in igneous units and tuffisite dykes.
	XI	Kaolinite.	Replacement of groundmass and infill of cavities in tuffisite dykes and igneous units. Minor infill in Mt. Leyshon breccia.
	XII	Manganosiderite - anatase.	Commonly replacing muscovite/illite in igneous units and breccia fragments. Also infilling cavities.
	XIII	Sphalerite - chalcopyrite <sup>†</sup> - galena ± ?pyrite.	Infill to cavities and veins in the Mt. Leyshon, Mt. Hope and tuffisite dyke breccias, and in strongly altered igneous units.
	XIV	<b>Gold</b> - bismuth bearing phases.	Dominantly within the Mt. Leyshon breccia and its partially re-brecciated host rocks, tuffisite dyke breccias and porphyry unit IV. Gold occurs within cavities and in veins.
	XV	Calcite - magnetite <sup>‡</sup> .	White crystalline calcite as vein and breccia infill. Local occurrence of magnetite replacing calcite in veins and cavities.
	XVI	Calcite.	Calcite veins which cut basalt dykes and which occupy faults in the complex.

<sup>‡</sup>See section 4.5. <sup>†</sup>Possible minor gold crystallisation here (see text). \*Variable smectite component (see section 4.3). ◊ Possible prograde muscovite here (see section 4.2.3.1)

Table 4.1: Mineral paragenesis stages of the Mt. Leyshon breccia complex.

## 4.2 STAGES OF ALTERATION AND MINERALISATION WITHIN THE MT. LEYSHON BRECCIA COMPLEX

The alteration and mineralisation of the Mt. Leyshon breccia complex is grouped into pre-main pipe breccia, post-main pipe breccia and post-Mt. Leyshon breccia episodes (Table 4.1). On the basis of cross-cutting relationships and consistent associations the mineral paragenesis is divided into 16 stages which are listed in Table 4.1. An attempt has been made to qualify each stage in terms of a representative mineral assemblage. The detailed textural evidence of mineral replacement and infill which justifies these assemblages is presented in Figures 4.1 and 4.2 and the relationship between the phases is described in the text. Electron micro-probe and XRD analyses confirming selected mineral phases are listed in Appendix 1. Carbonate staining was employed to assist the timing of carbonate introduction. In addition, short wavelength infrared spectra (1300-2500 nm spectral range) were collected (S. Pontual, unpublished report) on thin section off-cuts and drill core samples used to establish the paragenesis in this study. These spectra were collected using the PIMA II portable infrared spectrometer (developed by CSIRO) and assisted in selection of samples with distinct clay mineralogy for petrographic investigation of the late clay alteration.

The investigation of the Mt. Leyshon mineral paragenesis concentrated on the basement and breccia units of the complex. The breccia units provide the best timing constraint on the paragenesis (when phases are separated into infill and alteration components) because the infill minerals are commonly coarser grained in contrast to the igneous units where the minerals are generally fine grained and have complex intergrowth textures. In addition, the Mt. Leyshon igneous units are commonly weakly to strongly altered by clays, which further obscures the timing relationships between alteration phases in these fine grained units. Alteration of the igneous units is discussed separately in section 4.2.4 because it is important in evaluating the effect on the whole rock geochemistry investigated in Chapter 6.

### 4.2.1 Pre-main pipe breccia veins (Episode I, stage I)

Prior to the formation of the main pipe breccia, evidence for hydrothermal alteration is confined to generally narrow replacement type quartz veins. These stage I quartz veins occur within basement outcrop in the breccia complex and within fragments of the main pipe breccia. Three types of quartz vein have been observed:

- (1) Veins of fine quartz crystals up to 2 centimetres wide (but generally < 0.5 cm) within granite and metasediment. Fragments of these are present within the main pipe breccia.
- (2) Micro veinlets of quartz in granite fragments within the main pipe breccia.
- (3) A comb quartz vein with pyrite infilling around euhedral quartz.

Types 1 and 2 are composed of finely interlocking crystals with a preferred orientation. They are texturally similar to the later quartz - molybdenite veins which cut the main pipe breccia (their significance is discussed below). The type 3 vein which occurs in silicified ?granodiorite has only been observed once, and may be accidental and related to an earlier system. The pyrite mineralisation infilling part of this type 3 vein may belong to the later post-main pipe breccia

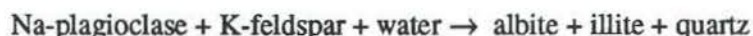
system.

### 4.2.2 Pre-Mt. Leyshon breccia alteration (episode II)

This section of the Chapter presents the evidence for establishing four hydrothermal stages subsequent to the main pipe breccia but prior to the formation of the Mt. Leyshon breccia (II-V; Table 4.1). However, the paragenesis of disseminated and veinlet pyrite in this episode has not been fully resolved.

#### 4.2.2.1 ARGILLIC I ALTERATION (ILLITE - SILICA - ?PYRITE ± ALBITE, STAGE II)

The matrix of the main pipe breccia and fragments generally smaller than 2 millimetres are replaced by illite-silica±albite alteration (Figure 4.1). This fine grained alteration is intense in relict pods preserved in the NW corner of the breccia complex (Plate 4.1), whereas only a weak illite-silica±albite alteration occurs in the bulk of the main pipe breccia examined in drill core (Plate 4.2). This low temperature assemblage probably formed by the break down of K-feldspar fragments in a reaction such as:



The following evidence indicates that the illite, silica and albite phases are the first minerals to replace the main pipe breccia matrix, and that they predate the potassic alteration (stage III):

- (1) Domains of predominantly illite and silica (± albite) alteration in main pipe breccia occur at depth within drill core to the east of the pit and porphyry unit IV, in regions dominated by potassic alteration (see below). The illite - silica domains pass gradationally through a colour transition into the black colour characteristic of the potassic alteration at Mt. Leyshon (Plate 4.1). This transition suggests that the potassic alteration replaces the illite - silica alteration, although, it is patchy and commonly overprinted by the late manganosiderite (which partly obscures this relationship).
- (2) Thin section analysis of the three colour zones noted in (1) show an increase in the growth of biotite from the whitish grey zone to the black coloured zone, at the expense of the illite - silica ± albite alteration (Plates 4.3 and 4.4; Figure 4.1).
- (3) Replacement K-feldspar veinlets of the potassic stage overprint and replace this illite - silica alteration (Plate 4.4; Figure 4.1) and cut plagioclase in fragments that was previously altered to albite.

Although some muscovite is present in these samples it is confined to replacement selvages adjacent to fractures (section 4.2.2.3) and these zones cross cut biotite alteration and K-feldspar veinlets.

#### 4.2.2.2 POTASSIC / PROPYLITIC I ALTERATION (STAGE IIIa + b)

Potassic alteration has not been observed outside the NW corner of the Mt. Leyshon breccia complex where it results in a black colouration to basement and main pipe breccia lithologies. Textural evidence already noted in section 4.2.2.1 and documented in Figure 4.1 indicates that potassic alteration developed after illite - silica alteration (stage II) in the Mt. Leyshon complex. The potassic alteration of the main pipe breccia includes silica alteration and takes the following forms:

paragenetic stages		Replacement minerals									
		II			III			IV			V
		illite	quartz	albite	(±cpy, pyr, py) biotite	† Kfeldspar	muscovite1	quartz 2	pyrite	quartz 3	molybdenite
original minerals	rock fragments	—	—	—	—	—	—	—	—	—	—
	breccia matrix	—	—	—?	—	—	—	—	—	—	—
previous replacement minerals	illite 1				—	—	—				
	quartz 1				—	—	—				
	albite										
	biotite					—	—	—	—	—	—
	K-feldspar*						—	—		—	—
	muscovite								—	—	—
	quartz 2								—?	—	—
	pyrite									—?	—
	quartz 3										—?
minor infill component					—?	—	—			—	—

Scale of mineral replacement: major **—** moderate **—** minor **—**

\* Possibility of a second minor Kfeldspar phase prior to stage IV alteration (see section 4.5). † Probably gradational outwards to a propylitic alteration (see section 4.5).

Figure 4.1: Textural evidence for the paragenesis of pre-Mt. Leyshon breccia alteration. The sequence of replacement minerals is listed at the left hand side of the diagram. The replacement minerals are shown in their respective stages (II-V) at the top of the diagram. The replacement of earlier alteration minerals by later minerals is indicated by the horizontal lines (major, moderate, minor and possible minor). Several phases probably have a minor related infill component, indicated at the bottom of the diagram.

- (1) Masses of anhedral biotite flakes (generally < 0.02 mm) which replace dolerite, metasediment fragments and breccia matrix (Plate 4.5).
- (2) Larger subhedral biotite flakes (0.03 mm) which are probably infilling rare cavities within the main pipe breccia.
- (3) Disseminated sulphides of chalcopyrite, pyrrhotite and pyrite.
- (4) Uncommon irregular replacement veinlets of K-feldspar in the main pipe breccia (Plate 4.3) which overprint stage II illite and locally biotite.
- (5) Rare infill K-feldspar veins with euhedral crystals in metasediment.

Elsewhere in the Mt. Leyshon breccia complex a propylitic alteration probably developed during stage III outside the region effected by potassic alteration (but see section 4.5). This alteration resulted in the replacement of breccia matrix by chlorite - silica - pyrite and the growth of epidote - chlorite - quartz - pyrite - albite in dolerite and granite fragments (Plate 4.2). In addition, albite and epidote occur as replacement halos around dolerite fragments.

#### 4.2.2.3 SERICITIC I ALTERATION (MUSCOVITE - PYRITE ± QUARTZ, STAGE IV)

Drill holes to the east of the mine porphyry (eg. MLD 237), reveal narrow zones of muscovite-pyrite +/- quartz replacement overprinting potassic alteration in main pipe breccia. In some cases small seed quartz crystals define a fracture at the centre of the alteration zone. In the region of basement and main pipe breccia between the Mt. Leyshon breccia and the mine porphyry, stage IV alteration is intense and these zones coalesce to form a pervasive sericitic alteration. These zones are developed in the region subsequently effected by stage V quartz - molybdenite veins (see below), although the stage V quartz both replaces and transgresses stage IV alteration (Plate 4.6; Figure 4.1). This alteration (and stage V veins) also occur in outcrop to the N and NE of the mine porphyry, and commonly make interpretation of rock types difficult in these areas.

#### 4.2.2.4 LAMINATED QUARTZ - MOLYBDENITE VEINS (STAGE V)

A persistent and inter-connecting quartz-molybdenite vein system (Plates 3.6 and 4.6) is developed within basement and main pipe breccia units to the east and west of porphyry unit IV. These veins are brecciated by, and therefore predate, the Mt. Leyshon breccia. They represent the last hydrothermal event of episode two. Their characteristics, which are described in section 3.3.3.1, indicate the close relationship between deformation and fluid flow in the breccia complex.

Teale (unpublished report, 1987) and Morrison et al. (1988) suggest that some gold was deposited during the precipitation of quartz-molybdenite-chalcopyrite veins. Gold has not been observed in quartz-molybdenite veins during this study and molybdenite is only consistently associated with laminated quartz. These veins locally show infill zones composed of one or more of the following: quartz, chlorite, sphalerite, chalcopyrite and calcite. Infill zones commonly occupy the central portion of the quartz-molybdenite vein, although they transgress and replace the vein, which indicates that these infill zones were introduced after vein formation. These observations suggest that the gold and chalcopyrite reported in the quartz-molybdenite veins (Teale, unpublished report, 1987; Morrison et al. 1988) was introduced by reactivation during stage XIII and XIV rather than

as part of the quartz-molybdenite vein assemblage.

### 4.2.3 Post-Mt. Leyshon breccia alteration (episode III)

This section of the chapter documents the evidence for dividing the post-Mt. Leyshon breccia alteration into eleven stages (VI - XVI; Table 4.1). Portions of this alteration overprint the Mt. Leyshon breccia and all subsequent units (excluding basalt dykes). The detailed textural evidence for establishing the post-Mt. Leyshon stages is shown in Figure 4.2.

Alteration of Mt. Leyshon breccia is typically confined to breccia matrix, cavities and to a fracture network interconnected with these cavities (Plate 4.7). Replacement rims develop around some of the cavities and wall-rock adjacent to fractures. Igneous units, tuffisite breccia dykes and late breccia dykes are commonly replaced by post-Mt. Leyshon breccia alteration; infill within these units is restricted to small cavities (typically up to 3 mm) and uncommon zones of re-brecciation. Stages XIII-XVI are dominated by cross-cutting infill veins and late cavity infill within the Mt. Leyshon breccia and igneous units.

#### 4.2.3.1 ARGILLIC II ALTERATION (ILLITE - SILICA - ?PYRITE ± ALBITE, STAGE VI)

Both the Mt. Leyshon breccia and tuffisite breccia dykes are generally overprinted and bleached by this alteration stage. Therefore, the character of this alteration stage is critical to the interpretation of the nature of the fluid present during formation of the Mt. Leyshon breccia pipe and tuffisite breccia dykes (Chapter 7).

Because fine tuffisite dykes are primarily composed of igneous material--which the evidence (Chapter 2) suggests was produced during their formation--they provide the clearest evidence for the character and timing of stage VI alteration. In contrast to other tuffisite dykes which are highly altered (Plate 2.13), one tuffisite dyke (in drill hole MLD 236) which intrudes main pipe breccia near the eastern edge of the post-Mt. Leyshon breccia alteration (Figure 4.3), is only weakly altered (Plates 2.14 and 4.8). This tuffisite dyke is altered by an illite - silica - albite assemblage and is largely unaffected by other alteration phases. The textural evidence suggests that during this low temperature alteration, albite replacement of K-feldspar liberated potassium and silica which combined with H<sub>2</sub>O to form illite (as discussed in section 4.2.2.1), and cemented the fine breccia particles. Narrow zones of infill and alteration are associated with minor re-brecciation zones in the tuffisite dyke (Plates 4.8 and 4.9). The re-brecciation zones (which overprint the pervasive stage VI alteration) are infilled by mineral phases which belong to stage VII-XIII (Plate 4.9; see below). In addition, stage XII alteration bleaches the tuffisite dyke and overprints the illite (Plate 4.9; Figure 4.2).

In those portions of the Mt. Leyshon breccia where potassic alteration of its host rock was not totally obliterated by stage IV (sericitic I) alteration, fine grained illite-silica±albite replaces all biotite (stage IIIa) in fragments, and partially bleaches biotite in blocks (Plate 4.7). In these bleached zones interpretation of the mineral paragenesis is complicated by the presence of overprinting later phases. Nevertheless, a transition from biotite alteration to illite - silica ± albite

paragenetic stages		replacement minerals											
		VI <sup>◇</sup>			VII	VIII			IX	X	XI	XII	
		illite2†	quartz 4	albite†	quartz 5	epidote	chlorite	pyrite 2	muscovite2	illite 3	kaolinite	mn-siderite	anatase
original minerals	rock fragments	————	— ? —	———	— — —	———		— — —	— — —				
	breccia matrix	— —	———	— ? —	— ? —								
minerals	quartz 5					———	———	— — —	— — —		— — —		
	epidote						———	— — —					
	chlorite							———	———	— — —		— — —	
	pyrite 2												
	muscovite 2									———	— — —	———	
	pyrite 3‡												
	illite 3										— — —	— — —	
	kaolinite											— — —	
	mn-siderite												— — —
	anatase*†												
infill	sphalerite												
	chalcopyrite‡												
	galena												
	bismuth phases												
	gold												
	calcite												
	magnetite												
	calcite												

Scale of mineral replacement: major ————— moderate ———— minor — — — † Only rarely present as an infill phase.  
‡ Possible minor gold developed here. \* Only rare replacement for phases hereafter. ◇ Possible prograde sericite developed late in this stage.

Figure 4.2: Textural evidence for the paragenesis of the post-Mt. Leyshon breccia alteration. The paragenetic sequence of infill minerals is indicated on the LHS of the diagram (in their respective stages). The replacement component which relates to each infill phase is indicated at the top of the diagram (in its respective stages). The horizontal lines show the textural evidence for replacement of an earlier mineral by a later mineral, in fragments and cavities.

alteration is observed in thin section. A minor proportion of well crystalline white mica is also present in these bleached zones. This white mica (probably muscovite) formed either as a prograde mineral overprinting the illite - silica as the fluid temperature increased, or during a later alteration event. Elsewhere in the Mt. Leyshon breccia, the presence of stage IV (sericitic) alteration in fragments confuses the timing of stage VI alteration.

Linear Mt. Leyshon breccia zones (GR. 4000 5400; Enclosure 1) are crosscut by porphyry units II and IV, all of which predate the hydrothermal alteration in the breccia (Plate 4.10). These breccia zones occur in basement and main pipe breccia outside the area effected by intense pre-Mt. Leyshon breccia alteration (Figure 4.3). They are also only weakly altered by the post-Mt. Leyshon breccia alteration and therefore provide the clearest evidence for the nature and timing of the first alteration in the Mt. Leyshon breccia. The matrix, small feldspar fragments, and igneous fragments in these weakly altered Mt. Leyshon breccia zones are replaced (Figure 4.2), and as a consequence, cemented by the stage VI illite - silica  $\pm$  albite alteration. Stages VIII and XVI infill cavities in these Mt. Leyshon breccia zones and replace the illite - silica altered matrix.

#### 4.2.3.2 QUARTZ INFILL (STAGE VII)

In the Mt. Leyshon and Mt. Hope breccias quartz develops predominantly as cavity infill and replacement of the breccia matrix (Plate 4.11; Figure 4.2), typically causing only limited silicification of the breccia fragment margins. Large euhedral quartz crystals with pyramidal terminations grow outward into the cavities. Minor stage VII quartz infill also occurs in tuffisite breccia dykes (see section 4.2.3.6).

Evidence is presented in section 4.2.3.1 which indicates that stage VI alteration is overprinted by minerals designated as a later stage. The following evidence indicate that quartz alteration is earlier than and overprinted by stage VIII alteration (Figure 4.2):

- (1) Epidote grows off and infills around quartz in cavities in the Mt. Leyshon and Mt. Hope breccias.
- (2) Chlorite rosettes, which infill cavities in the Mt. Leyshon and Mt. hope breccias, have nucleated on and partially replaced stage VII quartz (Plate 4.11).
- (3) Chlorite  $\pm$  pyrite locally replaces alteration quartz in wall rock adjacent to cavities and veins which contain both chlorite and quartz infill (Plate 4.11).

#### 4.2.3.3 PROPYLITIC II ALTERATION (STAGE VIII)

Albite, epidote, chlorite, pyrite and minor arsenopyrite are assigned to stage VIII and possibly also a minor amount of gold. The evidence for the timing of stage VIII alteration is described in section 4.2.3.2 and shown in Figure 4.2. This propylitic assemblage is extensively developed in the breccia complex and occurs in the following forms:

- (1) As a vein and fracture assemblage in portions of the main pipe breccia which have previously been altered to stage II and stage III minerals (but see section 4.5).
- (2) As chlorite - pyrite  $\pm$  epidote infill in the Mt. Leyshon and Mt. Hope breccias and their partially brecciated host rocks (Plate 4.11).

- (3) As epidote  $\pm$  chlorite  $\pm$  pyrite veins in the main pipe breccia, dolerite and granite. Breccia matrix between fragments, small fragments in the breccia (dolerite fragments are generally intensely altered) and narrow rims of larger breccia fragments are also replaced by this association.
- (4) As chlorite - pyrite  $\pm$  epidote  $\pm$  albite replacement of fractured basement units, particularly dolerite dykes.
- (5) As a minor replacement of tuffisite dykes and late breccia dykes.

Within this stage the minerals display differences in their relative time of formation. Albitisation of both plagioclase and small amounts of K-feldspar reflects the onset of alteration in this stage. Subsequently, epidote infills and replaces dolerite fragments in the Mt. Leyshon and Mt. Hope breccias which in turn is partially replaced by chlorite. Large euhedral pyrite forms breccia infill and irregular masses of pyrite replace chlorite and epidote in the cavities and wall rock.

Arsenopyrite occurs in small quantities within cavities in the Mt. Leyshon breccia and porphyry unit IV. Arsenopyrite infills triangular cavities between quartz crystals (stage VII) and replaces chlorite (stage VIII) in the cavity wall rock. In one thin section (sample T1/5 A) arsenopyrite infills part of a cavity and is subsequently overgrown by pyrite (of ?stage VIII). In the same sample, chalcopyrite (stage IX) further infills this cavity, growing around and replacing the earlier deposited arsenopyrite and pyrite. These observations suggest that arsenopyrite was deposited at the end of stage VIII, before the pyrite of this stage.

#### 4.2.3.4 SERICITIC II ALTERATION (MUSCOVITE $\pm$ ?SILICA - ?PYRITE, STAGE IX)

In the Mt. Leyshon and Mt. Hope breccias muscovite replaces both original wall rock minerals at cavity margins and minor amounts of the infill quartz (Figure 4.2; Plates 4.11 and 4.12). In some cavities, infill chlorite is also extensively replaced (Plate 4.12). Pyrite, when developed, occurs as large euhedral infill and minor replacement of muscovite and quartz. In tuffisite breccia dykes stage IX alteration occurs as a pervasive assemblage in the matrix and fragments. Highly crystalline muscovite is particularly common in distributed microcavities both in the groundmass and in feldspar phenocryst fragments of tuffisite dykes (Plate 4.13). The following evidence indicates that stage IX alteration overprints stage VIII alteration:

- (1) Breccia cavities partially infilled by chlorite are further infilled by muscovite. The muscovite partially overgrows and replaces the chlorite, truncating the fine rosette structure of the chlorite (Plate 4.12).
- (2) Muscovite alteration replaces chlorite in wall rock and fragments in the Mt. Leyshon breccia.

Infill pyrite crystals in the Mt. Leyshon breccia rarely contain small inclusions of gold which do not appear to be related to cross-cutting fractures or grain boundaries (Plate 4.17). This gold probably crystallised during stage IX and, if so, predates the larger volume percent of gold (see section 4.2.3.9). Inclusions of pyrrhotite, sphalerite and chalcopyrite also occur within the infill pyrite. Large through-going pyrite - quartz - muscovite veins probably developed by reactivation during stages VII - IX. The veins, which show evidence for fault movement, are commonly barren but locally contain gold. The vein gold (with or without bismuth phases) has only been observed

within and replacing fractured pyrite and, less commonly replacing infill quartz. These observations suggest that the vein gold was introduced during the stage XIV mineralising event by reactivation of the veins rather than at the time of stage VII-IX vein formation.

#### 4.2.3.5 ARGILLIC III ALTERATION (ILLITE - ?SILICA - ?PYRITE, STAGE X)

Crystalline stage IX muscovite is extensively replaced by stage X alteration in breccia cavities and tuffisite dykes. Illite causes recrystallisation of muscovite resulting in irregular muscovite relics in a mass of illite (Plate 4.12). Minor illite infill of breccia cavities is also locally present. Both the stage IX muscovite and this stage X illite could possibly have formed during the same fluid evolution event. However, because muscovite of stage IX commonly occurs in veins and cavities without the stage X assemblage, they have been separated in this paragenesis.

#### 4.2.3.6 KAOLINITE ALTERATION (STAGE XI)

Pervasive kaolinite alteration is inter-grown with illite in tuffisite dykes. Crystalline kaolinite commonly infills cavities together with other minerals within tuffisite dykes but is less common in the Mt. Leyshon breccia. The mineral textures described in this section show classic infill textures (Plate 4.13). Their origin is briefly considered in section 4.5. These cavities are the key to understanding both the timing of kaolinite alteration and the link between the porphyry style and base metal / gold mineralisation in the Mt. Leyshon deposit. Within the cavities a consistent infill sequence is observed (Plate 4.13, Figure 4.2) and is listed below in chronological order:

- (1) Euhedral quartz (stage VII).
- (2) Minor chlorite (stage VIII).
- (3) Coarse muscovite (stage IX).
- (4) Illite (stage X), which locally causes retrograde alteration of muscovite in the cavity, but commonly in the wall rock.
- (5) Crystalline Kaolinite (stage XI) typically infilling the central part of the cavity.
- (6) Manganosiderite (stage XII).

Similar relations are described for cavities within the mine porphyry in section 4.2.4.2. This sequence indicates that some kaolinite formed at the end of the porphyry style hydrothermal system (rather than exclusively as a supergene or weathering clay) and before the manganosiderite, base metal and gold dominant stages.

#### 4.2.3.7 MANGANOSIDERITE - ANATASE ALTERATION (STAGE XII)

Manganosiderite forms a pervasive alteration in portions of the Mt. Leyshon (Plate 4.14) and Mt. Hope breccias (Plate 2.11), tuffisite dykes and fractured basement. In these units manganosiderite generally replaces chlorite (Stage VIII) and muscovite (stage IX) producing pseudomorphs after these mica phases (Plate 4.13; Figure 4.2). Such alteration is particularly well developed in and adjacent to tuffisite dyke breccias. Manganosiderite also occurs as an infill phase within Mt. Hope and Mt. Leyshon breccias.

Anatase forms small aggregates replacing breccia fragments and matrix and occurs rarely in

veinlets. Anatase is commonly inter-grown with or has replaced manganosiderite and is formed during the break down of Ti-bearing minerals (eg.. biotite, titanomagnetite, ilmenite, etc.) by manganosiderite.

The replacement of chlorite (stage VIII), muscovite, illite and kaolinite (stage XI) by manganosiderite (Figure 4.2; Plate 4.13) constrains the timing of this alteration stage.

#### 4.2.3.8 BASE METAL MINERALISATION (STAGE XIII)

Sphalerite, chalcopyrite, galena and minor pyrite are assigned to stage XIII alteration. The base metal content of the Mt. Leyshon ore body is approximately 0.1% copper, 0.2% zinc and 0.05% lead. However, portions of the Mt. Leyshon breccia attain >1 % copper,  $\geq 2$  % zinc and 0.5 % lead over intervals of several metres (I. Hodgkinson, pers. comm.). Stage XIII formed after restricted zones of fault induced re-brecciation within breccia and igneous units and has the following modes of occurrence:

- (1) Sphalerite, chalcopyrite, galena and minor pyrite occur as infill within Mt. Leyshon and Mt. hope breccia cavities, and in discontinuous veins cutting the breccia units (Plate 4.14). Base metal veins also developed along re-activated unit contacts or earlier veins (eg. reactivated quartz - molybdenite veins).
- (2) Base metal sulphides occur as cavity infill, disseminated replacement minerals and narrow replacement veins in strongly altered tuffisite dykes, breccia fragments and basement units.

Teale (unpublished report, 1987) records iron contents for the Mt. Leyshon sphalerite of between 2 - 12 %. Grains of chalcopyrite may contain up to 700 ppm silver and from 0 - 1.7 atomic % Zn in solid solution (Teale). Galena is uncommon in the Mt. Leyshon hydrothermal system. Teale reports a range of galena compositions at Mt. Leyshon from almost pure PbS through to a complex PbS solid solution, which can contain up to 5.5 % bismuth, 2.1 % silver and 1.6 % copper. Base metal sulphides of the Mt. Leyshon system contain a number of inclusions, although these have not been investigated in detail. For example, sphalerite may occur as inclusions in both pyrite and chalcopyrite in addition to cavity infill and replacement forms. Likewise, chalcopyrite occurs as inclusions in sphalerite. Chalcopyrite rarely contains small gold inclusions appear to be unrelated to fractures, suggesting that minor gold was precipitated during stage IX.

Sphalerite, chalcopyrite and galena replace infill quartz, chlorite and manganosiderite within veins and adjacent wall-rock (Figure 4.2). Within cavities and veins, chalcopyrite grains have nucleated on sphalerite grains and in places have encircled and replaced them. Likewise, in a number of cavities the shape of galena grains suggest that they have overgrown and partially replaced chalcopyrite. These observations suggest the crystallisation sequence sphalerite - chalcopyrite - galena. Manganosiderite commonly has a spatial association with the base metal phases of this stage because the two are often found as an alteration product in the same rock. However, the following observations indicate that the manganosiderite alteration developed earlier than the base metals:

- (1) Manganosiderite occurs extensively in fracture networks within fragments and wall rock to

breccias, commonly in a different fracture network to that containing base metals (Plate 4.14).

(2) Base metals locally replace manganosiderite, and base metal veins do not have related manganosiderite alteration selvages.

#### 4.2.3.9 GOLD - BISMUTH MINERALISATION (STAGE XIV)

Bismuth-lead-copper sulphides and gold have been identified optically in this study. Teale (unpublished report, 1987) studied sixty nine sulphide-bearing samples of which twenty nine contained free gold, and in these samples 84 % of the observed gold is associated with various Bi sulphides of the bismuthinite - aitkinite series. Reconnaissance probe work by Teale indicates the presence of bismuthinite, aitkinite, lindstromite, hammarite, and possibly friedrichite and pekoite. In addition, Uemoto et al. (1992) report native bismuth within Mt. Leyshon breccia cavities. Teale also reports electron analyses from Mt. Leyshon with up to 0.67 % copper and 30% Ag, although electron grains commonly contain 0 - 0.2 % copper and 10 - 12 % silver.

Three distinct styles of gold occurrence have been observed during this study:

- (1) Large, irregular grains which are inter-grown with or close to bismuth bearing phases in fractured vein pyrite (Plates 4.15 and 4.16) and locally quartz, or within and adjacent to chalcopyrite.
- (2) Small inclusions in chalcopyrite.
- (3) Rare, small ?inclusions in pyrite (Plate 4.17).

By far the largest volume % of gold grains is observed in style 1. Where gold occurs in association with base metals, both the gold and the bismuth phases commonly occupy the central portion of the vein and are demonstrably later. For example, gold is commonly in contact with or close to bismuth bearing phases and both minerals have textures which suggest they have replaced chalcopyrite and quartz (Plates 4.15 and 4.16). Further justification for separating the bulk of gold and bismuth mineralisation from the base metal stage is provided by drill-hole assay data. Correlation coefficients between gold and each of sphalerite, galena and chalcopyrite are less than 0.3, whereas the coefficient between gold and bismuth is greater than 0.65 for the whole 2 metre assay interval data set (C. Robinson, pers. comm.). The small inclusions in pyrite (Plate 4.17) and chalcopyrite suggest that a small volume percent of gold (type 1 and 2) crystallised during stage IX and XIII (see above). Teale, described gold inclusions in pyrite and similarly considered them to form a minor volume percent of the observed gold. The distribution and controls on gold mineralisation are considered in Chapter 8.

#### 4.2.3.10 MAGNETITE - CALCITE ALTERATION (STAGE XV)

This stage is expressed as minor breccia infill and common irregular veinlets within dolerite (and locally granite or metasediment). Within Mt. Hope breccia, granular magnetite crystals are present as a minor phase and replace epidote, chlorite (stage VIII) and calcite (stage XV) infill. In the fragments adjacent to these cavities, calcite-magnetite veins overprint base metal-dominant veins indicating that the magnetite in the Mt. Hope breccia is younger than the base metal stage. Magnetite has not been observed infilling the Mt. Leyshon breccia, although in dolerite dykes on

Mt. Leyshon it replaces epidote and calcite in veinlets. Magnetite-only infill of re-brecciated porphyry unit IV (in the main igneous centre; GR. 4040 5110) has an unknown paragenesis with respect to other stages of episode III.

#### 4.2.3.11 CALCITE ONLY STAGE (STAGE XVI)

Abundant calcite only veins and breccia veins are common in the breccia complex where they cut all rock units. Calcite also forms breccia infill to Mt. Leyshon and Mt. Hope breccias. Calcite only veins commonly occur within or at the margin of basalt dykes in the breccia complex. The structural features of these and paragenetically earlier veins are described in section 3.3.4.1. The offset of calcite veins across other calcite veins indicates that more than one episode of calcite veining occurred.

### 4.2.4 Alteration and mineralisation within igneous units

All the Mt. Leyshon igneous samples show evidence for post-crystallisation changes to the groundmass and phenocryst phases. This modification takes two forms; textural recrystallisation (commonly of the groundmass) and mineralogical changes due to hydrothermal alteration. These changes are described in this section for whole rock geochemical samples discussed in Chapter 6 (numbers refer to samples in Appendix 2).

#### 4.2.4.1 POST-EMPLACEMENT RECRYSTALLISATION

The Mt. Leyshon igneous rocks have an aphanitic groundmass which is most likely the result of rapid magma chilling (Cox et al., 1979). In thin section, this aphanitic groundmass usually shows a partial to complete recrystallisation. This is particularly true of the felsic units, where the glassy felsic inter-growth has been recrystallised to a micro-graphic texture of quartz and feldspar (Plate 6.2). In contrast, intermediate units which have a coarser grained groundmass, show minor groundmass recrystallisation and the original texture is more commonly preserved (Plates 6.1 and 6.3). Both the felsic and intermediate units, may show a coarser "micropoikilitic" textured groundmass.

A few samples (eg. STD161) display a more extensively recrystallised, micropoikilitic groundmass with patchy spherulite development. Highly recrystallised samples (LDG200, P231) show well developed coarse irregular spherulites that have nucleated on phenocrysts and replaced groundmass minerals. The absence of any textures indicative of high temperature recrystallisation suggests these features are a result of late stage recrystallisation (see section 6.2.2). Furthermore, recrystallisation textures tend to be best developed in samples that have undergone the most intense hydrothermal alteration, suggesting that these two processes are linked.

AGE	ALTERATION TYPE	TEXTURAL CHANGE
YOUNGEST	Clay and hematite	Variable groundmass and phenocryst "dusting" in surface samples.
	Calcite	Vein infill and alteration of groundmass.
	Manganosiderite and anatase	Partial replacement of phenocryst and groundmass feldspar and pseudomorphs after muscovite. Partial to complete anatase replacement of magnetite.
	Kaolinite	Minor replacement of phenocryst feldspar and pervasive alteration of groundmass. Infill of cavities in strongly altered igneous units.
	Pyrite	Minor groundmass replacement in igneous units close to the orebody, especially intermediate units where pyrite is $\leq 1\%$ .
	Muscovite and illite	Scattered replacement of mafic phenocrysts (after chlorite), plagioclase phenocrysts and groundmass minerals.
	Chlorite $\pm$ epidote $\pm$ ?albite	Mostly restricted to the replacement of mafic minerals, although in the intermediate units chlorite occurs as a pervasive replacement phase.
	Quartz <sup>†</sup>	Patchy quartz re-crystallisation of the groundmass and cavity infill in the most altered samples.
OLDEST	Illite $\pm$ albite <sup>†</sup> $\pm$ hematite $\pm$ K-feldspar	Probably overlaps with groundmass re-crystallisation in the more felsic units. Replacement of most phenocryst and groundmass plagioclase and partial to complete replacement of K-feldspar. Actual introduction of K-feldspar probably confined to the EP dyke.

<sup>†</sup> Possible formation of early albite during post emplacement re-crystallisation (see text).  
Base metals  $\pm$  gold are present in the most strongly altered samples.

Table 4.2: Mineralogical and textural changes to the Mt. Leyshon igneous rocks.

#### 4.2.4.2 HYDROTHERMAL ALTERATION

All the samples used for geochemical investigation are hydrothermally altered (Table 4.2). Typically, the alteration minerals in the samples consists of albite - illite - muscovite  $\pm$  carbonate  $\pm$  chlorite  $\pm$  epidote  $\pm$  pyrite. These mineralogical changes pervade the igneous rocks and in the majority of the analysed samples are unrelated to fractures or veins on the microscope scale. This suggests that chemical exchange with fluid filled cavities has been minor. The alteration minerals, however, vary in intensity of development between the different samples. The most strongly altered samples, for example, contain fine veinlets of muscovite and/or abundant chlorite. Additionally, the presence of late infill veins of calcite and calcite spotting of the groundmass in a few samples dilutes the whole rock chemical totals.

The following observations have implications for interpretation of the igneous whole rock chemical data (Chapter 6). Alteration mineral compositions refer to electron microprobe analyses (see Appendix 1) on samples of DG dyke, porphyry unit I and IV. The EP dyke which intrudes the main pipe breccia in drill core at the margin of the ore body displays groundmass replacement and micro-veinlets of clear K-feldspar cut by epidote-chlorite  $\pm$  manganosiderite  $\pm$  sphalerite micro-veinlets. In contrast, no K-feldspar veins have been observed in the other analysed samples, although the turbid groundmass of the felsic phases has a composition of An<sub>0</sub> Ab<sub>5-7</sub> Or<sub>93-95</sub>. This groundmass composition is close to end member K-feldspar, which suggests loss of Na compared to a normal igneous groundmass. It is suggested that these groundmass textures result from local recrystallisation during hydrothermal alteration and element redistribution (section 4.5).

Most of the original plagioclase phenocrysts in the igneous rocks have been replaced by albite (An<sub>5-9</sub> Ab<sub>90-95</sub> Or <sub>$\leq$ 1</sub>) reflecting a considerable loss of calcium from most igneous samples. Alkali feldspar phenocrysts also show replacement by albite, although, they are less susceptible to alteration (Plate 6.4), suggesting that the potassium component of the samples has been less mobile than calcium or sodium. In the more altered samples, however, much of the feldspar phenocrysts and patches within the groundmass are replaced by muscovite. In addition, perthitic K-feldspar phenocrysts occur in porphyry unit IV, which have albite beads (An<sub>8</sub> Ab<sub>92</sub> Or<sub>0</sub>) in an orthoclase host (An<sub>0</sub> Ab<sub>8</sub> Or<sub>92</sub>) in contrast to other K-feldspar phenocrysts which are microperthitic (see section 6.2.1.1).

Chlorite is a minor alteration phase in most of the analysed samples, and is confined to the total replacement of any original amphibole (except for relics in a sample of porphyry unit I) where it is magnesium rich (Appendix 1), and partial to complete alteration of igneous biotite phenocrysts. In addition, minor patches of chlorite occur in the groundmass in some samples. In contrast, DG dykes, for which samples were only available adjacent to the ore body, have been subjected to strong chlorite  $\pm$  pyrite alteration. Here the chlorite is distinctly iron rich (Appendix 1), and in the most intensely altered samples chlorite is inter-grown and replaced by muscovite, which in turn is replaced by manganosiderite.

DG dykes also display irregular elongate "vesicle-shaped" patches of recrystallised quartz. It is

unknown whether these features resulted from gas evacuation from primary igneous vesicles or whether they result from shrinkage during recrystallisation, and infill by hydrothermal minerals. In addition, occasional patches within the groundmass and strongly altered phenocrysts of DG dykes, consist of delicate subhedral crystals of quartz  $\pm$  albite, muscovite, epidote and chlorite, suggesting these minerals formed by infill of cavities within the rock. Infill minerals within these cavities probably formed during hydrothermal alteration because they show the same paragenesis as replacement phases. Cavities also occur in the mine porphyry and host approximately 8% of the gold resource at Mt. Leyshon mine. These cavities consist of obvious zones of re-brecciation and also isolated holes typically after feldspar phenocrysts (Plate 4.18). Partially to completely infilled cavities, display the same infill sequence as that described for tuffisite dykes (section 4.2.3.6; compare Plates 4.13 and 4.18), and confirm that the alteration sequence in the igneous units was broadly similar to that within breccia units.

### 4.3 CLAY ALTERATION IN THE MT. LEYSHON COMPLEX

The presence of three temporally distinct illitic micas and a kaolinite clay have already been described above and related to the hypogene mineral paragenesis. X-ray diffraction and PIMA II infrared spectra of Mt. Leyshon samples generally show a water absorption feature which is characteristic of smectite. Consequently, the minerals referred to as illite in this Chapter are actually illite-smectites. In addition, a number of other supergene and oxide zone clays occur at Mt. Leyshon, although their nature and timing have not been investigated in detail here. Teale (unpublished report, 1987) and Morrison et al. (1988) reported the presence of kaolinite, illite, alunite, natroalunite and jarosite, which they attributed to weathering products in the oxide and supergene zones. However, Scott (1990) has argued that the alunite in the Mt. Leyshon deposit is hydrothermal in origin and related to an acid sulphate epithermal system. The work of Scott (1990) is based on the texture and isotopic characteristics of a few surface samples only, rather than a systematic investigation of the clay minerals present throughout the deposit. In a discussion of this paper, Andrew et al. (1991) point out that Scott (1990) has failed to recognise direct geological and isotopic evidence (Bird et al., 1990) that alunite and jarosite at Mt. Leyshon formed during Plio-Pleistocene weathering. Furthermore, in the present study alunite was not found during XRD work on clay alteration from the hypogene zone at Mt. Leyshon, which supports the conclusions of Andrew et al. (1991).

### 4.4 SPATIAL DISTRIBUTION OF ALTERATION TYPES

The work in this Chapter has concentrated on establishing the detailed paragenesis of alteration and mineralisation rather than their distribution. However, a number of points are made below based on drill core and outcrop observations. Figure 4.3 illustrates the broad map scale distribution of some hydrothermal stages.

Illite - silica alteration (stage II) is strongly developed and only preserved as relict patches in the area subsequently overprinted by the potassic zone, whereas outside the limit of the potassic alteration only a weak illite - silica alteration is developed. The potassic alteration (stage III) has

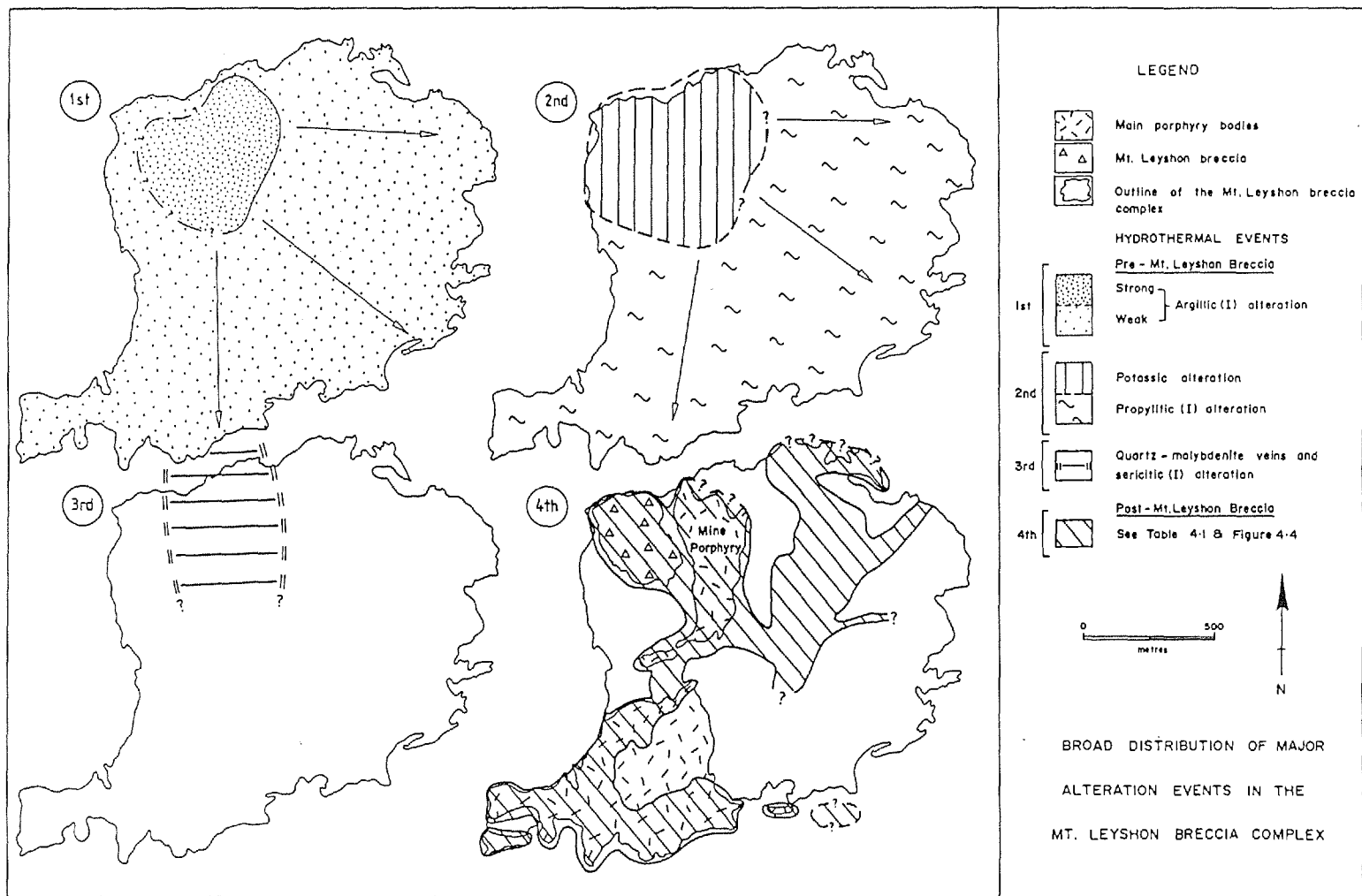


Figure 4.3: Approximate large scale distribution of major alteration events in the Mt. Leyshon breccia complex (oldest-1st to youngest-4th). Distribution is based on mapping and drill core observation. The arrows indicate gradation between alteration types. Note that only weakly altered igneous units, including porphyry unit IV (mine porphyry), occur in the main igneous centre.

only been observed in the NW corner of the breccia complex. Elsewhere, the main pipe breccia is altered to a propylitic assemblage, which is probably gradational with this potassic alteration (see section 4.5).

Laminated quartz - molybdenite veins (stage V) are restricted to a roughly north trending zone in the area subsequently invaded by porphyry unit IV (Figures 310D and 4.3). The veins are developed in basement and main pipe breccia to the east and west of this porphyry body, and have not been observed to the west of the Mt. Leyshon breccia. Muscovite/illite  $\pm$  quartz - pyrite (sericitic I) alteration also occurs throughout this zone. Both these stages result in the loss of the (stage III) biotite alteration in this region, all of which pre-dates the Mt. Leyshon breccia.

Alteration which postdates the Mt. Leyshon breccia (stage VI-X), is largely confined to breccias, porphyry units and their partially brecciated host rocks. In detail there are variations in spatial distribution between stages, and for phases within a given stage. For example, parts of the Mt. Leyshon breccia have well developed zones of a particular mineral, eg.. quartz, pyrite, sphalerite or chalcopryrite. Likewise, chlorite is well developed in the Mt. Leyshon breccia and its partially re-brecciated host rocks but elsewhere is only weakly formed. Presumably, this reflects variations in permeability / fluid-wall rock reactions at each hydrothermal stage. Observations presented in Chapter 3 and this Chapter, suggest that ultimately this permeability variation results from repeated tectonically driven brecciation and hydrothermal sealing. Throughout the breccia complex most of porphyry unit IV, many of the other igneous dykes, and the tuffisite breccia dykes host a pervasive illite/muscovite - pyrite  $\pm$  silica  $\pm$  chlorite  $\pm$  kaolinite replacement (resulting from stages VI - XI alteration). Tuffisite dykes and the more intensely altered igneous units (generally adjacent to the ore body) also develop a pervasive manganosiderite alteration (stage XII). No attempt has been made to spatially quantify these complex variations in detail, and post-Mt. Leyshon breccia alteration is collectively shown on Figure 4.3. Note that an area of porphyry units in the main igneous centre is only weakly altered, and does not show the moderate to intense sericite alteration that occurs in igneous units elsewhere.

The gold and bismuth bearing phases (stage XIV) appear to be confined to cavities and veins within the Mt. Leyshon breccia and igneous units. No gold has been observed in replacement sulphides away from veins or cavities. Zones of base metal and gold mineralisation occur in subeconomic quantities elsewhere within the breccia complex. The spatial distribution of gold is discussed in detail within Chapter 8.

Veins and replacement networks containing epidote-chlorite $\pm$ calcite $\pm$ magnetite occur throughout the breccia complex and are also found vertically over 800 metres, 500 metres SSW of the breccia complex (drill hole MLD 406). The cross-cutting relations within these veins between epidote-chlorite, calcite and magnetite suggest that these veins formed by repeated reactivation. Their wide distribution suggests that (sporadic) large scale hydrothermal fluid flow occurred in an area of at least several square kilometres. In the Mt. Hope breccia, restricted zones of magnetite occur within infilled cavities replacing quartz, epidote, chlorite and calcite. A late breccia dyke beneath Mt.

Hope displays late magnetite replacement veins, and thick magnetite-quartz veins occur in outcrop on the flanks of Mt. Hope. Within the main magmatic centre to the south of the ore zone, magnetite infills crackle-mosaic brecciated porphyry unit IV.

#### 4.5 PROBLEMS WITH INTERPRETATION OF THE MT. LEYSHON HYDROTHERMAL SYSTEM

Certain aspects of the Mt. Leyshon hydrothermal system are only partially resolved. These problems can be summarised as follows and are discussed below:

- (1) A lack of conclusive evidence that the potassic alteration (stage III) in the NW corner of the complex formed synchronously with the propylitic assemblage which is present throughout the remaining main pipe breccia.
- (2) The timing of K-feldspar alteration present in the EP dyke.
- (3) The timing of albite alteration in the igneous units.
- (4) The origin of the intense alteration and cavities which are generally present in the tuffisite breccia dykes and some igneous units.
- (5) The nature of any alteration associated with the gold mineralisation stage.
- (6) The timing of the minor phases magnetite, gypsum and barite.
- (7) The number of pyrite generations formed during the hydrothermal system.

The timing of the propylitic alteration in the main pipe breccia is ambiguous because the boundary between it and the potassic alteration is obscured to the east by the quartz - molybdenite and muscovite - pyrite alteration (stages IV and V), and to the south by the post-Mt. Leyshon breccia alteration (Figure 4.3). Stage VIII veinlets of chlorite - pyrite  $\pm$  epidote  $\pm$  albite occur in several drill holes in the main pipe breccia. The controversy arises because the same assemblage also occurs as a pervasive alteration in the main pipe breccia. Therefore, two possibilities exist concerning the timing of the pervasive propylitic alteration in the main pipe breccia. Firstly, the propylitic alteration is approximately synchronous with the potassic alteration and developed outward from it, away from the NW corner of the complex. Stage VIII veinlets would subsequently overprint the main pipe breccia. Secondly, after the stage II alteration, the main pipe breccia remained mostly unchanged (beyond the limit of the potassic alteration) until the formation of the stage VIII propylitic alteration, which then developed as veinlets and a pervasive alteration. However, the post-Mt. Leyshon breccia alteration is generally restricted to only part of the breccia complex (Figure 4.3). Furthermore, the propylitic alteration in the main pipe breccia is probably overprinted by stage IV and post-Mt. Leyshon breccia alteration (where ED dykes cut the main pipe breccia; Figure 2.1). Together, these observations suggest that the propylitic alteration throughout the main pipe breccia formed during stage III.

As already discussed, K-feldspar alteration of the breccia units is confined to stage III potassic alteration (see section 4.2.2.2). Evidence presented above suggests that the Mt. Leyshon igneous units generally have not been replaced by K-feldspar. In contrast, the groundmass and phenocrysts of the EP dyke have been replaced by K-feldspar (see section 4.2.4.2). However, there is no

associated development of biotite in the EP dyke, whereas potassic alteration of the main pipe breccia develops both K-feldspar and biotite. These observations suggest two possibilities concerning the timing of K-feldspar in the EP dyke. Firstly, the K-feldspar is equivalent in age to that developed in the main pipe breccia (stage III) and the composition of the EP dyke and/or local chemical conditions were not favourable for the development of biotite alteration. Secondly, minor K-feldspar alteration occurred after EP dyke emplacement, but before ED dyke emplacement.

With regard to (3), textural evidence for groundmass and phenocryst recrystallisation is described above for the Mt. Leyshon igneous rocks (see section 4.2.4.1). Such recrystallisation in volcanic rocks commonly involves alkali mobility (Lipman et al., 1969; Sander and Einaudi, 1991) and as a consequence tends to produce K-feldspar or albite alteration. However, these processes are poorly understood in subvolcanic igneous rocks, and it is not known whether they operate on the local scale and are driven by the heat of each igneous intrusion, or if this recrystallisation is a result of a larger hydrothermal system. In addition, because of the small grain size of both the igneous minerals and the subsequent hydrothermal alteration minerals, it is unknown whether the albite alteration in the Mt. Leyshon units formed completely during stage VI and VIII alteration, or if some albite was formed earlier during post-emplacement recrystallisation.

Igneous units (particularly porphyry unit IV and DG dykes) and tuffisite breccia dykes generally show a high degree of alteration throughout the complex. However, the presence of only weakly altered tuffisite dyke and porphyry unit IV has already been noted (sections 4.2.3.1 and 4.4; Figure 4.3). A possible origin of this intense alteration and cavities that are described in these units (sections 4.2.3.6 and 4.2.4.2) is now briefly considered, because these cavities commonly contain gold mineralisation. It is possible that these cavities formed by dissolution of feldspar by late stage magmatic fluids as suggested by Pollard et al. (1989) for tin mineralised cavities in granite from the Zaaipplaats tin mine, S.A. If such an origin could be proved for the cavities (in feldspars) within porphyry unit IV, it would lend support to the possibility of early gold mineralisation precipitated from a magmatic fluid at Mt. Leyshon and/or the presence of a high temperature aqueous fluid phase. The following discussion however, suggests that these cavities are a later feature and are unrelated to a fluid phase that coexisted with the units during emplacement and crystallisation. The porous nature of tuffisite dykes and the mineralogical composition (fine grained feldspar and quartz) of both tuffisite and porphyry dykes partly explains their susceptibility to alteration. Previous workers investigating open space mineral textures in glassy volcanic rocks (Anderson, 1975; Ross and Smith, 1961) have attributed their formation to crystallisation from a vapour phase during early post-emplacement de-vitrification (recrystallisation), in voids thought to have formed from exsolved magmatic gas. The absence of cavities in only weakly altered Mt. Leyshon igneous rocks, however, suggests that their origin in intensely altered rocks is not due to exsolved magmatic gas. In contrast, Lofgren (1971a) observed such infilled cavities in experimentally recrystallised natural rhyolite glass, and suggested the minerals grew from a vapour phase that must have occupied the cavity. He also found that the development of such cavities is consistent with the approximate 10% volume change which accompanies the recrystallisation of

glass. Material science work on synthetic alkali-glasses may help understand the processes of recrystallisation and cavity formation in SiO<sub>2</sub> rich rocks. The following account is based on the discussion of Rogers et al. (1993). Experimental work indicates that alkali oxides (K, Na) in glass disrupt the SiO<sub>2</sub> networks, whereas alkali earth oxides (Ca, Mg) stabilise the networks. During the interaction of glass and an H<sub>2</sub>O fluid phase, the substitution of hydrogen ions for alkali metal ions in the glass results in the formation of microcracks. If alkalis build-up in these cracks a strong alkali solution results which further attacks the glass and forms a pervasive network of cracks. If these processes operate in silica rich igneous rocks (like those at Mt. Leyshon) they would allow fluid access and alteration of the rocks, ultimately forming cavities.

Microfracture may also be important to both the formation of cavities and recrystallisation and alteration of igneous rocks (and tuffisite dykes) in the breccia complex. Observations on the fracture patterns within porphyry unit IV (see Chapter 3) suggest that the rheology of this body favours the formation of a diffuse ellipsoid fracture pattern during shear stress. This micro-fracture pattern appears to anastomose in three-dimensions and would strongly enhance fluid flow and mineral alteration. The presence of stages VII - XIV veins and cavity infill within porphyry and tuffisite dykes indicates that fracturing episodes continued after tuffisite dyke emplacement. Veins in the Mt. Leyshon breccia complex are at least partially structurally controlled and are likely to have been induced by fluctuations in shear stress and fluid pressure (as discussed in Chapter 3). Several workers have discussed the importance of rheology (porosity, elasticity, crystallinity, grainsize, etc.) and shear stress induced microfracture on deformation, brecciation and fluid flow in rocks (Fyfe et al., 1978; Lacy, 1990; Hadizadeh, 1991). This discussion raises the possibility that the cavities in tuffisite breccia dykes and strongly altered igneous units formed as a result of one or both of the following processes:

- (1) Volume change / dissolution during recrystallisation of the glassy groundmass.
- (2) Dissolution of feldspar phenocrysts (igneous units) and phenocryst fragments (tuffisite breccia dykes) during stress induced microfracture.

Once formed, these cavities would provide excellent sites for late gold deposition, which is consistent with the paragenesis of gold in the Mt. Leyshon breccia.

During this study, no alteration phase could be specifically related to the gold mineralisation stage, despite detailed investigation of drill core, slabs and thin sections from ore zones, barren zones and transitional zones. For example, in veins dominated by quartz - chlorite - pyrite alteration, gold and bismuth phases occur both as minor infill and replacement of fractured pyrite and quartz. In other cases, gold occurs in fractured pyrite within veins dominated by manganosiderite - pyrite - chalcopyrite - sphalerite. However, the Mt. Leyshon rocks have such over printing complexity between the different stages, including the formation of more than one phase of illite/muscovite, it is possible that a weak clay alteration formed during the main gold crystallisation event which has been undetected in this study.

Magnetite replaces calcite in breccia cavities in the Mt. Hope breccia. The calcite infills breccia

cavities and grows around base metals indicating that both the calcite and magnetite postdate the base metal dominant stage (XIII). Likewise, evidence is presented in this Chapter that the gold - bismuth dominant stage also postdates the base metals. However, the timing of this calcite - magnetite stage with respect to the gold - bismuth stage is unresolved because both stages have not been observed in the same sample. Elongate euhedral crystals of barite have been identified by microprobe and XRD analysis during this work. Barite occurs as a minor phase in the Mt. Leyshon breccia. The intergrowth of barite with sphalerite in one sample of Mt. Leyshon breccia (supplied by I. Hodkinson) suggests that barite formed during the base metal dominant stage. Gypsum was reported by Teale (unpublished report, 1987) but has not been observed during this study and is of an unknown paragenesis.

#### **4.6 INTEGRATED PARAGENESIS OF IGNEOUS EMPLACEMENT, BRECCIA FORMATION AND HYDROTHERMAL EVOLUTION IN THE MT. LEYSHON BRECCIA COMPLEX**

The facies analysis of breccia and igneous units presented in Chapter 2 suggests breccia generation during igneous emplacement. A paragenesis of brecciation and igneous events in the Mt. Leyshon complex is based on this work (section 2.3; Figure 2.4). This section of the thesis assesses the evidence for establishing the timing of hydrothermal events relative to these rock units. The following observations suggest the integrated paragenesis presented in Figure 4.4:

- (1) The occurrence of stage I quartz veins in fragments of basement units within the main pipe breccia indicates these veins are older than the main pipe breccia.
- (2) Stage II and III alteration overprint the main pipe breccia.
- (3) The timing of porphyry unit I is only partly resolved (see section 2.3). At this point in the research at Mt. Leyshon, the age of porphyry unit I is unknown relative to the EP dyke, ED dykes, and alteration stages III, IV and V. For this reason it has not been included in Figure 4.4. Porphyry unit I, however, was emplaced after the main pipe breccia and prior to the Mt. Leyshon breccia (section 2.3; therefore at some time during episode II, Figure 4.4).
- (4) The timing of EP dyke emplacement is also only partially resolved. It cuts main pipe breccia but crosscutting relations with other igneous units have not been observed. The hydrothermal alteration which effects the EP dyke partly resolves this uncertainty (see section 4.5). If the K-feldspar veinlets which occur in this unit belong to stage III alteration then the EP dyke was emplaced before stage III alteration.
- (5) Stage V quartz - molybdenite veins have been observed cutting ED dykes on two occasions during this study indicating a pre-stage V alteration age of ED dyke emplacement. The ED dykes also show a well developed muscovite - quartz - pyrite alteration interpreted to have formed during stage IV. However, the ED dykes show no evidence for the K-feldspar alteration which effects the EP dyke. Consequently, the ED dykes are designated as post-EP dyke and pre-stage IV alteration.
- (6) Fragments of ED dyke and stage V alteration veins in the Mt. Leyshon breccia indicate the Mt. Leyshon breccia developed after stage V alteration.
- (7) Alteration stages VI - XV overprint and post-date the Mt. Leyshon breccia to fine late dyke sequence (Chapter 2) which indicates that these stages overprint all coeval breccia and igneous

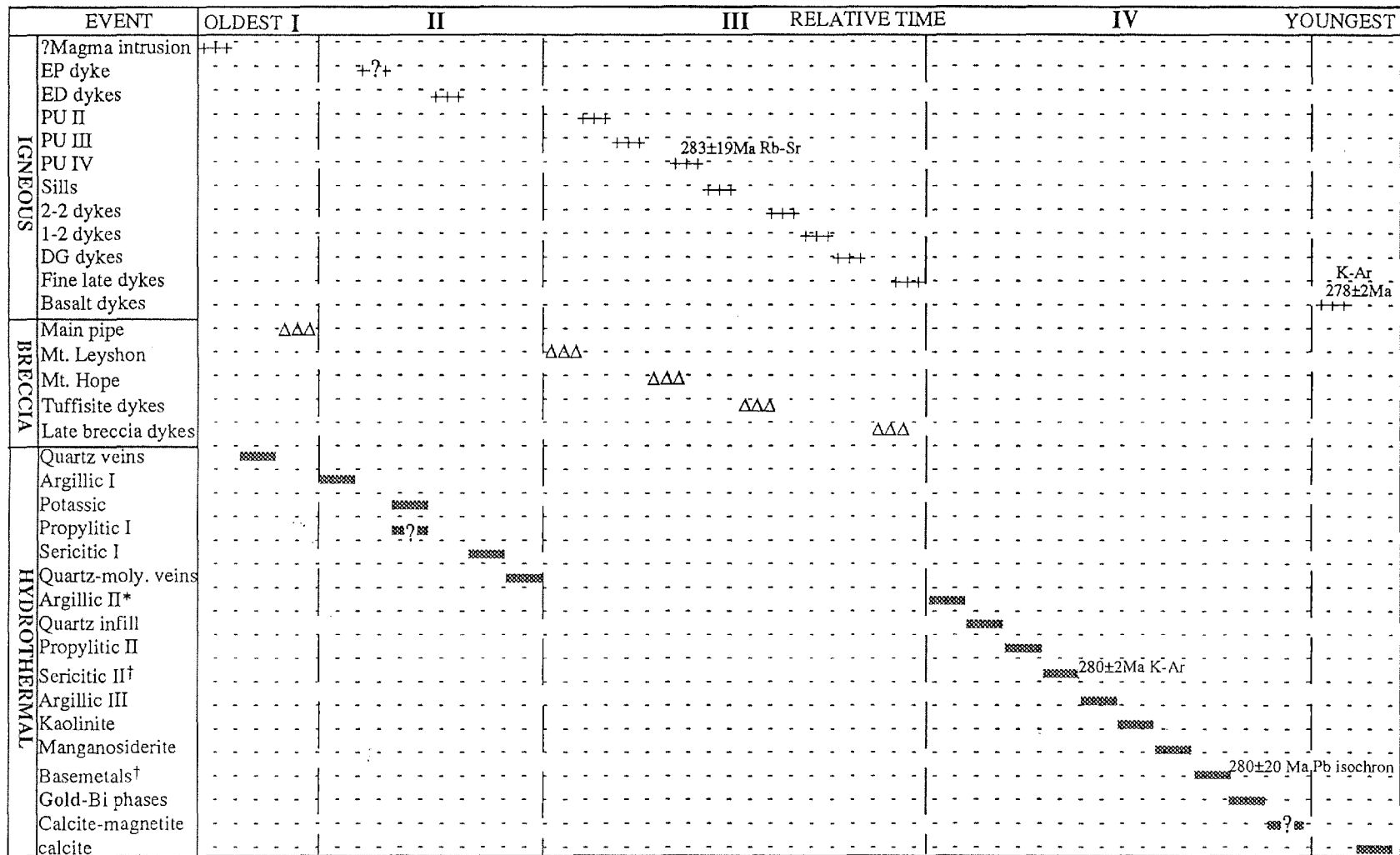
units.

(8) Basalt dykes, which are chemically distinct from other Mt. Leyshon igneous units (see Chapter 6), are unmineralised and only overprinted by calcite veins (stage XII) and clay alteration, in the absence of silica and pyrite, hence their position in Figure 4.4.

Alteration and mineralisation have been investigated collectively and are presented in this form here, although the sulphide component of each stage usually develops after the onset of alteration. For example, disseminated and replacement veinlets of chalcopyrite, pyrite and pyrrhotite overprint biotite and K-feldspar of stage III. Similarly, chlorite alteration (stage VIII) in the Mt. Leyshon breccia is commonly replaced by pyrite alteration of the same stage.

The integrated paragenesis of the Mt. Leyshon breccia complex is divided into four main episodes (Figure 4.4). These episodes are summarised below and have implications for fluid evolution in the Mt. Leyshon magmatic system and breccia mechanisms in the complex (Chapter 7):

- Firstly, the emplacement of a magmatic system (see Chapters 2 and 6) resulted in main pipe breccia formation and the definition of the breccia complex.
- Argillic I (illite - silica - ?pyrite  $\pm$  albite) alteration is the first hydrothermal event to effect the main pipe breccia. The initial development of a low temperature alteration assemblage suggests that a significant time interval separated the formation of the main pipe breccia and the development of subsequent high temperature alteration; hence the separation of these alteration events as episode II. Potassic alteration was the second event in episode II, and was most likely gradational to propylitic alteration throughout the remaining complex. During the latter part of this second episode the emplacement of intermediate and felsic dykes preceded the formation of the sericitic I alteration and quartz - molybdenite vein system.
- Episode three of the breccia complex is characterised by a period of repeated breccia and igneous (intermediate and felsic) emplacement, with only the development of an illite - silica  $\pm$  albite (argillic II) alteration which is present in breccia and igneous units. It is not known whether this alteration in breccia and some igneous units occurred as one event after the episode III sequence (Figure 4.4) was completed, or if separate local illite-silica  $\pm$  albite alteration formed after each successive breccia event.
- Again, this argillic alteration suggests a time break between igneous and breccia emplacement (episode III) and the evolution of the higher temperature mineralising system. Therefore, this alteration and mineralisation of breccia and igneous units is designated as episode IV (Figure 4.4) of the breccia complex evolution. During this period the data suggests that widespread but structurally controlled alteration developed throughout the breccia complex (Figure 4.3) but that no igneous emplacement and only fault and vein style brecciation occurred. Several distinct hydrothermal stages occurred during this final episode (in addition to the argillic II alteration). Minor sericite alteration possibly occurred as a



†Minor gold probably formed at this stage (see text). \*Possible prograde sericite developed late in this stage (see text).

Figure 4.4: Evolution of igneous emplacement (+++), breccia formation (△△△) and hydrothermal alteration (▒▒▒▒) within the Mt. Leyshon breccia complex. Note that: PU=porphyry unit; porphyry unit I is omitted because its timing is ambiguous with respect to EP and ED dykes. Source of four age dates (oldest to youngest): Uemoto et al. (1992), Morrison et al. (1988), Dean and Carr (unpublished, 1988) and this study (in conjunction with Webb, unpublished, 1983).

prograde component to the argillic II alteration. Subsequent stages comprise earlier quartz infill, propylitic II, sericitic II, argillic III and late kaolinite alteration. Minor gold mineralisation probably occurred during the later stages of this porphyry style system. Subsequent alteration and mineralisation record a change in hydrothermal fluid character and resulted in widespread manganosiderite and base metal dominated mineralisation. Again minor gold mineralisation probably occurred during the base metal-dominant mineralising system. The bulk of gold-bismuth mineralisation formed as a very late mineralising event and is concentrated in re-break zones within breccia cavities and existing veins.

Plate 4.1: Main pipe breccia. Transition from illite-silica alteration (stage II; LHS) to biotite-silica-K-feldspar alteration (stage IIIa; RHS). Note the gradation from pale whitish-grey through brownish-grey and then into black. (Polished drill core, sample no. D/237/33.)

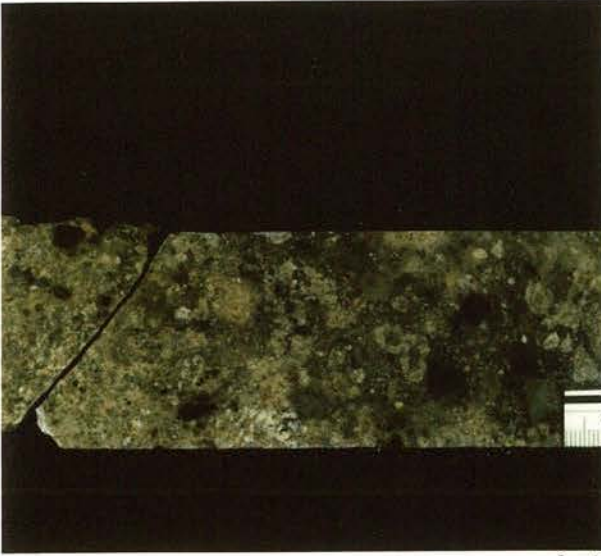
Plate 4.2: Main pipe breccia. Weak illite-silica-albite (stage II) alteration overprinted by epidote-chlorite-pyrite (stage IIIb) alteration. Illite-silica-albite replace breccia matrix and small fragments (A). Epidote-chlorite-pyrite replace dolerite fragment (B) and chlorite-pyrite veinlet (C) replaces fragments and breccia matrix. (Photomicrograph, XPL, photo base = 1.5 mm, sample no. 156/29.)

Plate 4.3: Main pipe breccia, potassic (stage IIIa) alteration overprinting illite-silica-albite (stage II). Illite-silica in an igneous fragment (A) is replaced by biotite (B) and fine networks of Kfeldspar (C). Arrow marks the position of Plate 4.4. (Photomicrograph, XPL, photo base = 4.2 mm, sample no. 237/1.)

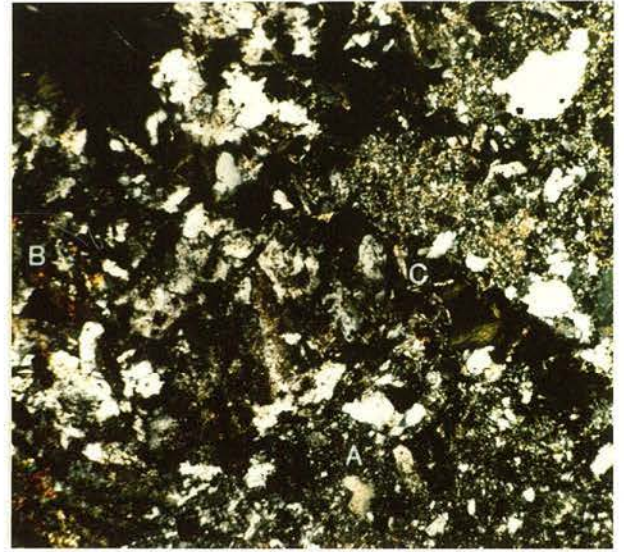
Plate 4.4: Main pipe breccia, close-up of Plate 4.3. Coarsely crystalline illite (A) is replaced by biotite (B) and Kfeldspar (C). Scattered late anatase and manganosiderite also occur. (Photomicrograph, XPL, photo base = 1.6 mm, sample no. 237/1.)

Plate 4.5: Main pipe breccia. Biotite (stage IIIa) alteration of breccia fragments and matrix. Biotite (A) replaces scattered illite-silica-albite (B; stage II) alteration. (Photomicrograph, PPL, photo base = 0.6 mm, sample no. 236/1.)

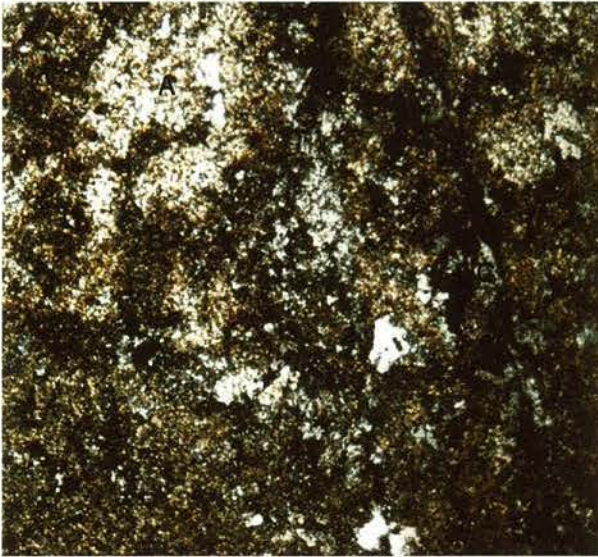
Plate 4.6: Main pipe breccia. Quartz-molybdenite veins (stage V) overprinting muscovite-pyrite (stage IV) alteration. Illite-silica alteration (A) of matrix and fragments is overprinted by muscovite/illite (B), resulting in partial destruction of breccia texture. Narrow quartz-molybdenite vein (C) is oblique to and cross-cuts irregular muscovite / illite boundary. (Thick section; photomicrograph, XPL, photo base = 4 mm, sample no. 237/B.)



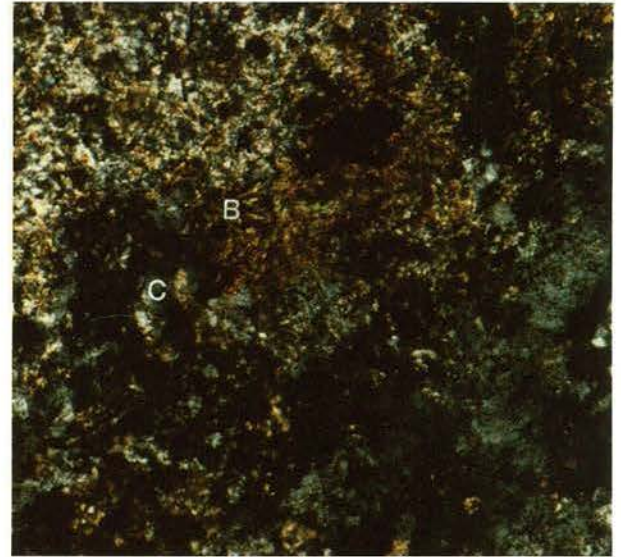
4.1



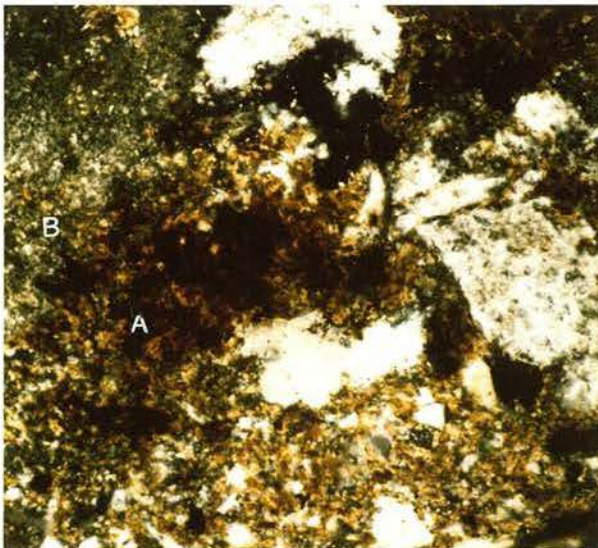
4.2



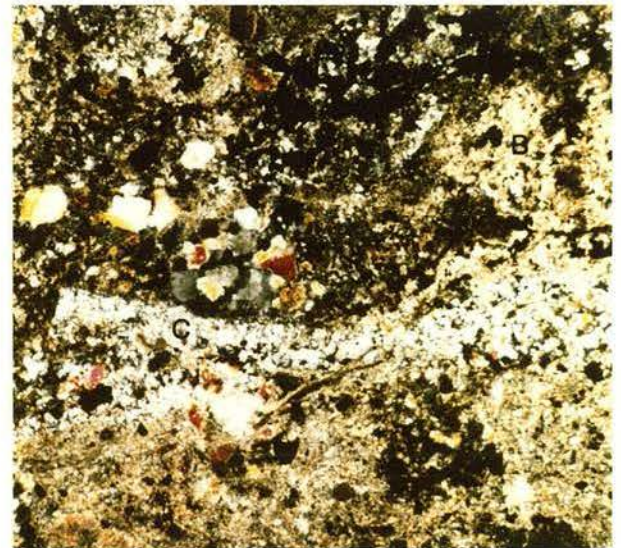
4.3



4.4



4.5



4.6



Plate 4.7: Mt. Leyshon breccia. Contact (at arrow) between fragmental component (RHS) and main pipe breccia block (LHS; see Chapter 5). Note that the fragmental zone consists of main pipe breccia (A) and basement rhyolite (B). Strong comminution of both fragment types is concentrated at the margin with the main pipe breccia block. Argillic II alteration results in the growth of illite-silica-albite (stage VI) in the igneous fragments (B) and forms an alteration margin (C) in the main pipe breccia block (replacing biotite). Stage VII-XII alteration phases subsequently replace the alteration margin of the block, and infill fracture networks (D) crosscutting illite-silica-albite in the comminuted zone. (Polished drill core, sample no. D/168/392.)

Plate 4.8: Fine tuffisite breccia dyke, weakly altered. Dyke consists of coeval igneous particles. The groundmass is pervasively altered to illite-silica (stage VI) and this is crosscut by zones of re-brecciation which host stage VII-XIII infill. Note that the margins of the re-brecciation zones are faintly bleached by stage IX muscovite (A). Arrow marks the position of Plate 4.9 (orange patches on slab are due to polishing resin). (Polished drill core, Sample no. 236/16.)

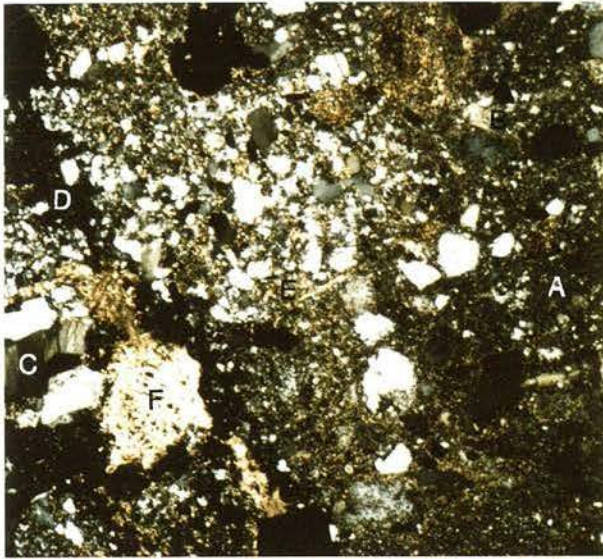
Plate 4.9: Fine tuffisite breccia dyke (shown in Plate 4.8), re-brecciation zone. Note: (1) The illite-silica alteration (A) of the breccia matrix and the albite alteration (B) of Kfeldspar phenocryst fragments. (2) Quartz infill (C; stage VII). (3) Chlorite-pyrite (D) replacement and infill of the re-brecciation zone. (4) Muscovite (E) alteration selvage to the re-brecciation zone. (5) Late calcite (F) replacing muscovite in the re-brecciation zone. (Photomicrograph, XPL, photo base = 4 mm, Sample no. 236/16.)

Plate 4.10: Mt. Leyshon breccia, weakly altered. Breccia fragments include basement rhyolite (A), dolerite (B), metasediment (C) and main pipe breccia (D). Note: (1) Porphyry units II and IV (II, IV) have intruded the breccia. (2) The igneous material has partially infilled the breccia cavities which are in turn infilled by epidote-chlorite-pyrite (arrow; stage VIII) and calcite (stage XVI). Dark colouration in fragments is due to iron oxides. (Polished drill core, 5 cm wide, sample no. 230/12.)

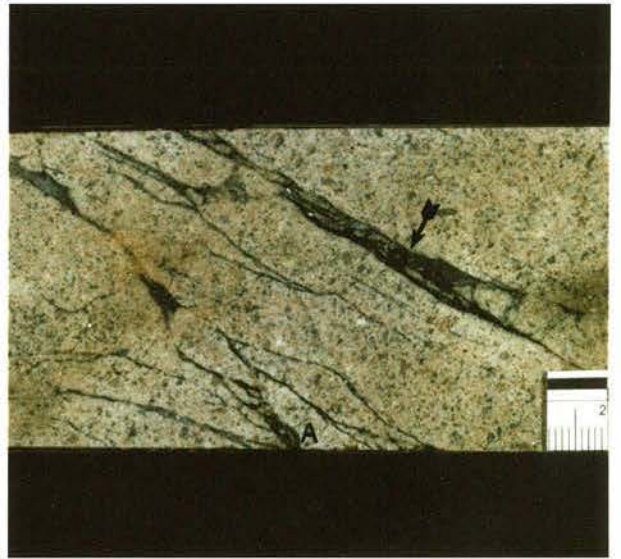
Plate 4.11: Mt. Leyshon breccia. In this sample the breccia cavities are dominantly infilled by stage VII quartz (iQ). Adjacent to this infill, previously altered fragments of main pipe breccia are replaced by quartz (rQ). Chlorite infills the remaining cavity space (A), and replaces both the fragments and infill quartz (note the linear replaced fracture at the top of the plate). Muscovite (B; stage IX) replaces portions of the fragments, replacement chlorite and fractures in infill quartz. (Photomicrograph, XPL, photo base = 1.5 mm, sample no. T1/4B.)



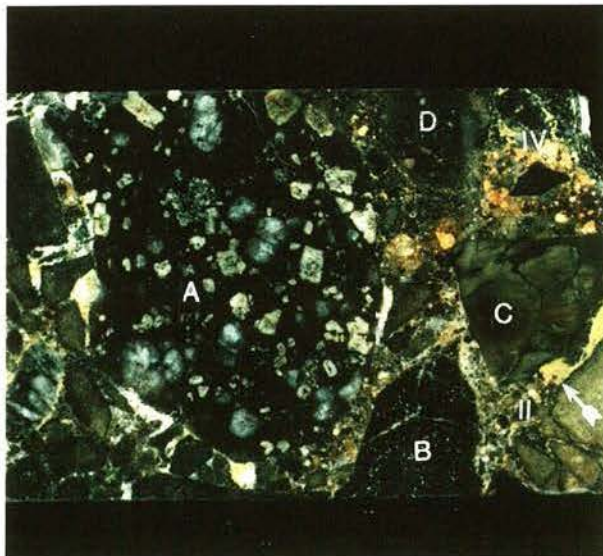
4.7



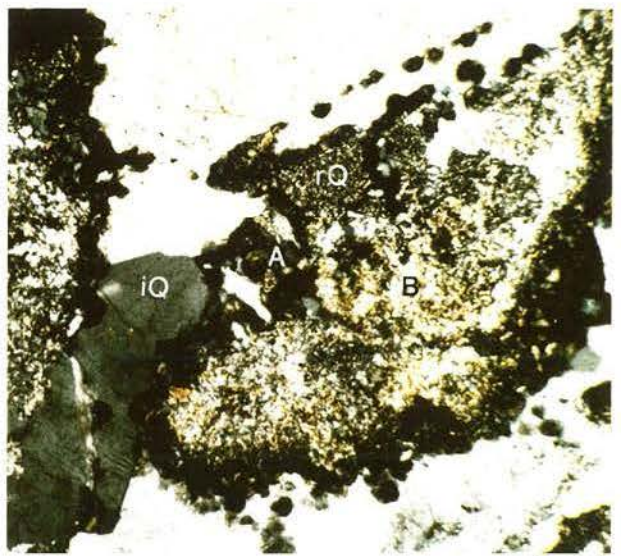
4.9



4.8



4.10



4.11



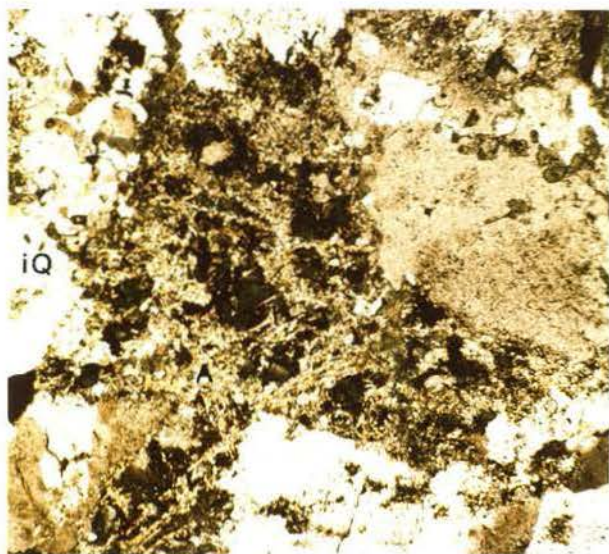
Plate 4.12: Mt. Leyshon breccia. Stage IX muscovite (A) replacing infill and alteration chlorite (dark green). Note that the infill quartz (iQ) is recrystallised suggesting the growth of minor quartz during stage IX. The retrograde alteration of muscovite to illite (stage X) results in a reduction in mica grain size and lower birefringence. (Photomicrograph, XPL, photo base = 1.5 mm, Sample no. T1/2.)

Plate 4.13: Microcavity in tuffisite breccia dyke. Within the cavity, euhedral quartz crystals (Q; stage VII) grow off the host rock (consisting of phenocryst and igneous groundmass fragments). Coarse flakes of highly birefringent muscovite (M; stage IX) have nucleated at the cavity margin and have partially replaced infill quartz. Minor illite (stage IX) has probably replaced the muscovite at the cavity margins. In the cavity, coarse flakes of low birefringent kaolinite (K; stage XI) have nucleated on and partially replaced muscovite, and the terminations of the quartz crystals (now embayed). The remaining portion of the cavity is infilled by fine grained kaolinite. Manganosiderite (S) occurs as scattered mineral replacement throughout the rock, and has replaced most of the muscovite in the cavity, forming pseudomorphs. Manganosiderite postdates all other phases since it transgresses the muscovite / kaolinite boundary in several places (eg. bottom of the plate). (Photomicrograph, XPL, photo base = 0.6 mm, sample no. 183/7.)

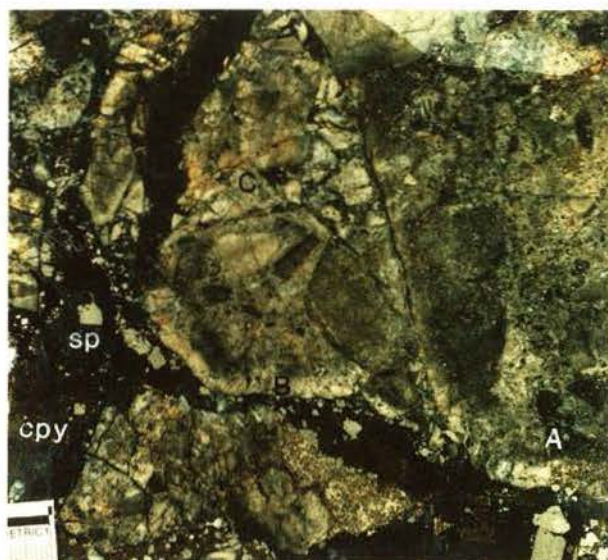
Plate 4.14: Mt. Leyshon breccia (Zone 1, see Chapter 5). Post-Mt. Leyshon breccia stages VI-XI have altered the fragmented main pipe breccia and infilled the minor cavities in the rock. Chlorite-pyrite which has infilled the cavities, replaces dolerite fragments within the main pipe breccia fragment edge (A). A partial white rim (B) that probably includes muscovite (stage IX) overprints the chlorite-pyrite in the dolerite fragment (and elsewhere). Refracturing of the breccia produced a fine fracture network and formed the permeability for manganosiderite alteration (C; orange brown network). Subsequent refracturing occurred during the introduction of base metals; sphalerite (sp) and chalcopyrite (cpy, tarnished to yellow/brown). Note that sphalerite has nucleated on pyrite-chlorite in the vein, which in turn is overgrown by chalcopyrite (islands of sp in cpy; slab no. ST2).

Plate 4.15: Large gold grains in a Mt. Leyshon breccia cavity. Gold (g) occurs at and replaces chalcopyrite (cpy) and quartz boundary. Note the irregular fractures (arrow) in chalcopyrite extending either side of the gold. Largest gold grain is transgressed by a whitish grey mineral which is probably a bismuth bearing phase (B). (Photomicrograph, reflected light, photo base = 0.8 mm, sample no. T1/2A.)

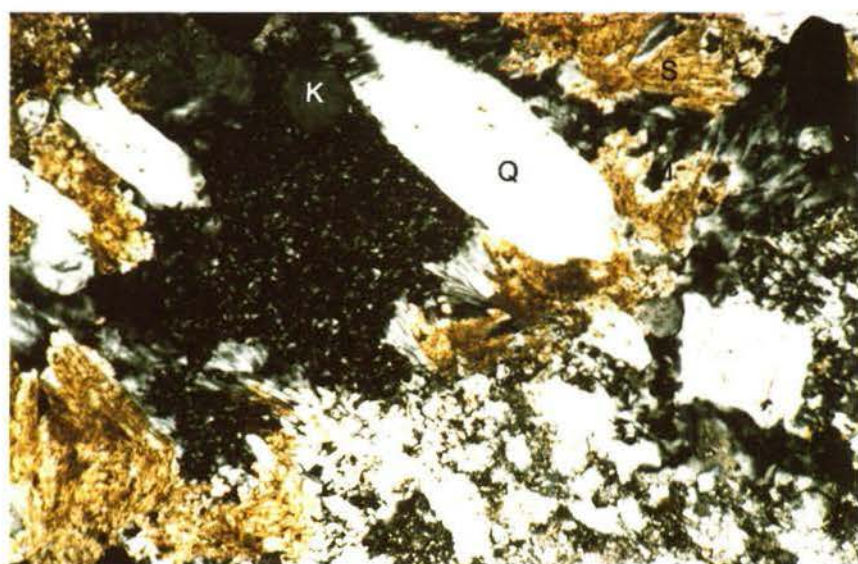
Plate 4.16: Large gold grains in high grade vein (shown in Plate 8.1). Gold (g) occurs at and transgresses chalcopyrite (cpy) - sphalerite (sp) boundary. (Photomicrograph, reflected light, photo base = 0.8 mm, sample no. T/277/GV.)



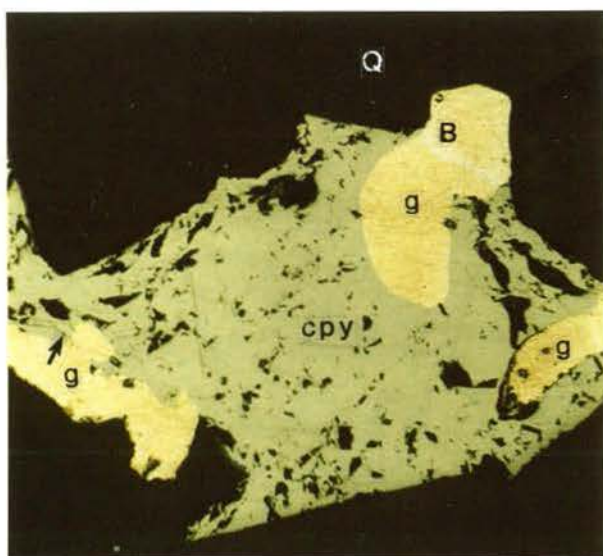
4.12



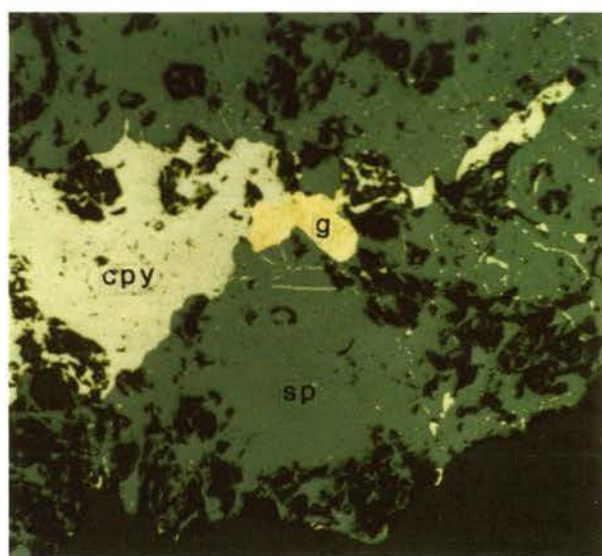
4.14



4.13



4.15



4.16

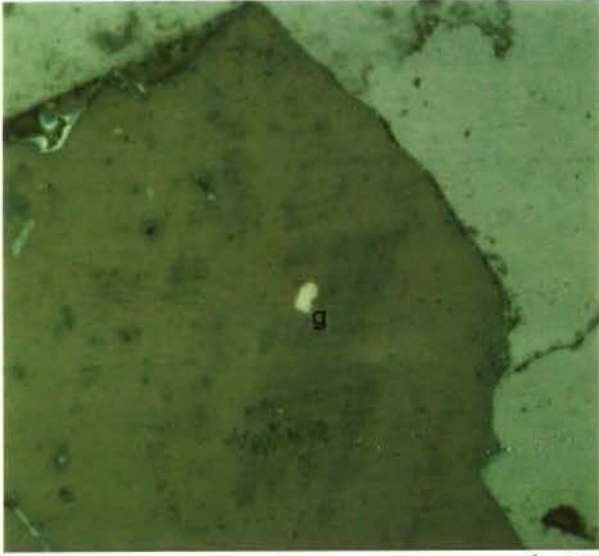


Plate 4.17: Small gold (g) inclusion within pyrite grain in a Mt. Leyshon breccia cavity. Quartz and chlorite are also present in the cavity. (Photomicrograph, reflected light, photo base = 0.4 mm, sample no. T1/2B.)

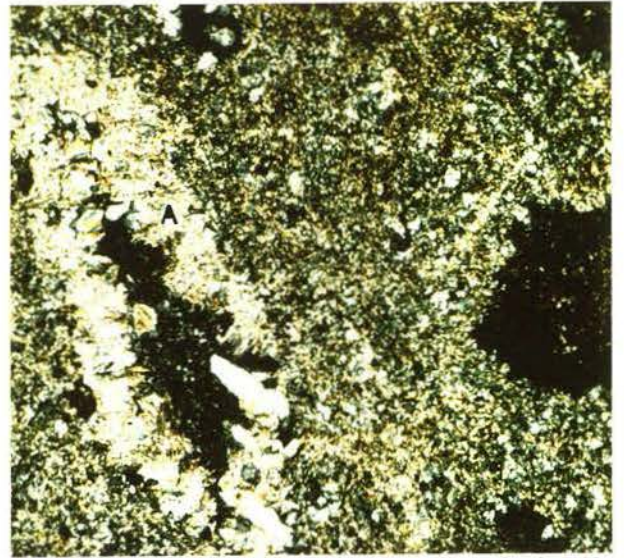
Plate 4.18: Cavities in highly altered porphyry unit IV (mine porphyry). Groundmass is completely altered to illite, quartz, muscovite, pyrite, kaolinite, manganosiderite and anatase. Euhedral quartz crystals extend outwards into the main cavity (LHS). Coarsely crystalline muscovite (A) subsequently infills the cavity and overgrows the quartz. Illite replaces the edge of muscovite flakes in the cavity and within the wall rock. In the other cavity (RHS) only manganosiderite is present. Some infill loss possibly occurred during sample preparation. The absence of other phases in this cavity suggests dissolution of other phases (quartz, muscovite, kaolinite, etc.) prior to manganosiderite crystallisation. (Photomicrograph, XPL, photo base = 1.5 mm, sample 157/16.)

Plate 5.1: Zone 1, Mt. Leyshon breccia. Partially fragmented main pipe breccia. Note: (1) First order fragmentation - the large fragments which have minor separation and that form fragmentation progressions (A). (2) Second order fragmentation - zones of more obvious expansion and small scale fragmentation that contain matrix and splinter textured fragments (B). (MLD 177, 301.70 m.)

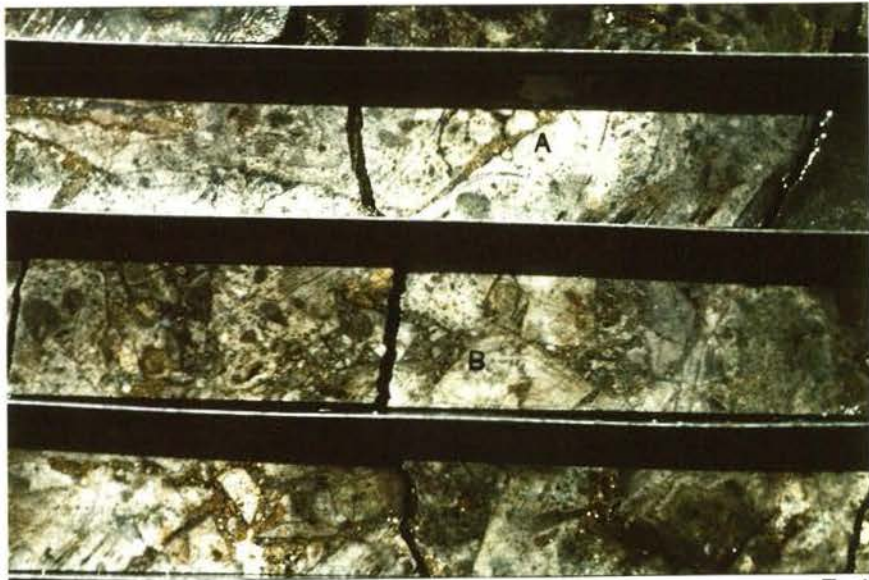
Plate 5.2: Zone 2A, Mt. Leyshon breccia, intact host rock block in breccia. Note the following zones moving down hole (bottom to top): (1) Partially fragmented main pipe breccia (no mixing, few jigsaw fit textures). (2) Large host block (5.5 metres thick; contact at arrow) preserving the following pre-Mt. Leyshon breccia sequence - (a) dolerite dyke, (b) granite rich main pipe breccia, (c) crackle brecciated granite and minor dolerite, note the 20 centimetre zone of dolerite-rubble textured metasediment (S)-dolerite which was *in situ* fragmented during the main pipe breccia event. (3) Partially fragmented main pipe breccia (bottom core run). (MLD 186, 201 m.)



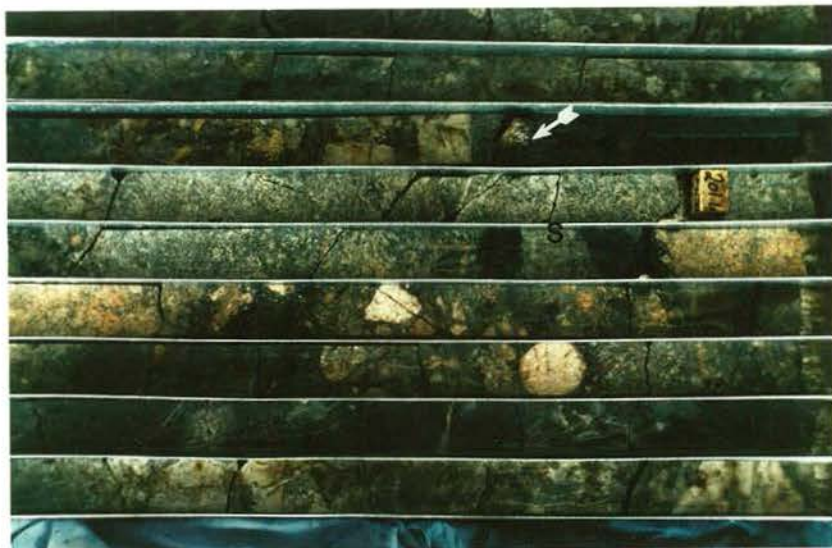
4.17



4.18



5.1



5.2

## Chapter 5

# FACIES ANALYSIS OF THE MT. LEYSHON BRECCIA PIPE

---

### 5.1 INTRODUCTION

Geometrical considerations of the Mt. Leyshon breccia pipe suggest that it closed off approximately 170 metres above the present erosion level (see section 2.4.2). Given the independent evidence concerning the depth of emplacement (Chapter 7), the pipe probably closed (as depicted in Figure 2.6), well beneath the palaeosurface and vented only volatile components. The hydrothermally altered Mt. Leyshon breccia pipe is closely associated with igneous intrusive activity and can be defined as a magmatic-hydrothermal breccia pipe (Sillitoe, 1985).

Many workers have investigated the origin of breccia pipes. Early workers (Wright and Bowes, 1963; Kents, 1964; Bryner, 1968) who investigated pipe-like breccia bodies noted several textural varieties of breccia and attempted a genetic interpretation of breccia formation on the basis of processes assumed to produce these isolated textures. These attempts met with limited success because they were based on general observations of breccia texture, rather than systematic facies analysis of the whole system(s). For example, Kents (1964) classification for breccias in the Andes describes a type of breccia characterised by the presence of numerous faults. However, his interpretation of the mechanism of brecciation was based on speculation about the role of magma and hydrothermal fluids rather than detailed observations of fault distribution and their relationship to fragmentation. One exception is provided by Cloos (1941), who documented the facies characteristics of the Schwabichen tuff pipes with detailed sketches of breccia texture, and the relationship of breccia to host rock. Later workers were less inclined to analyse breccia characteristics and the emphasis of breccia research shifted to an investigation of the hydrothermal alteration and mineralisation associated with breccia pipes (eg. Porter and Ripley, 1985; Norman and Sawkins, 1985); this alteration is generally considered to be closely related to fluids responsible for brecciation (Sillitoe, 1985). Consequently, current models proposed for pipe formation (see Chapter 1) are dominantly based on hypothetical considerations about the relative role of magmatic and hydrothermal processes, rather than detailed facies characteristics. However, in Chapter 4 the bulk of the alteration associated with the Mt. Leyshon complex breccias (and by implication possibly for many other breccia pipes) is shown to be later than the fluid responsible for breccia pipe formation.

At present it is only possible to identify a hyperbyssal breccia pipe by a number of general characteristics and by the absence of facies characteristics associated with near surface diatreme or maar systems. Recently, Baker et al. (1986) provided a practical field guide to the investigation of hydrothermal breccia pipes. They reviewed some of the textures found in breccia pipes in different environments and the possible processes which formed these textures, and proposed a basic facies model for each of the main types of breccia pipe. The facies models (with the exception of near

surface diatreme systems) are based on assumptions about the significance of isolated breccia textures, rather than a systematic analysis of facies characteristics, as a result the models proposed for their formation are speculative. Bradbury (1988) has recently clarified the facies characteristics of phreatic and phreatomagmatic diatreme and hydrothermal breccias, formed in the shallow subvolcanic Olympic Dam breccia complex. There is a need for the definition of facies characteristics commonly found in breccia pipes, particularly those formed at deeper levels in the crust (> 0.75 kilometres).

The present situation in breccia research is akin to that which existed up to the early 1970's for the interpretation of volcanic (extrusive) rocks. Prior to this time, interpretation of volcanic rocks was mostly based on rock mineralogy, geochemistry and general characteristics (Cas and Wright, 1987). Since the early 1970's, facies analysis of volcanic products (where facies models are constructed on the basis of facies characteristics) has led to an accelerated understanding of the dynamic nature of volcanic systems. The foundation stone of facies analysis in volcanology has been the use of graphic logging techniques (cf. Cas and Wright, 1987). The graphic analysis system developed in this Chapter extends the use of graphic analysis in to the subvolcanic environment, and is used to construct a detailed facies model of a magmatic hydrothermal breccia pipe.

This Chapter aims to:

- (1) Design a graphic analysis system for the subvolcanic environment.
- (2) Document the detailed facies characteristics of the Mt. Leyshon breccia pipe.
- (3) Investigate the origin of brecciation in the Mt. Leyshon pipe through an analysis of facies characteristics.
- (4) Produce a facies model of an intrusive breccia pipe as a reference for use in the interpretation of other breccia systems.

The assessment of the control of breccia characteristics on gold grade distribution within the breccia pipe is detailed in Chapter 8.

## 5.2 METHODOLOGY

### 5.2.1 Open cut investigation

The Mt. Leyshon open pit was mapped to assess general breccia characteristics and spatial distribution of textural types. However, the dusty and partially collapsed nature of the bench faces severely restricted data collection. Selected pit walls were washed by using a small fire fighting water pump, although a shortage of water in the pit (40 gallon drums spaced along the faces), and rapid evaporation, once again hampered data collection. Nevertheless, the water sump in the pit floor allowed complete and repeated washing of a portion of the pit face between 370 and 380 RL, which provided valuable information described later in this Chapter. A suite of 35 breccia blocks (around 30 centimetre diameter) was collected during pit mapping, in order to develop a general impression of breccia variation in the Mt. Leyshon breccia pipe. These slabs proved a useful

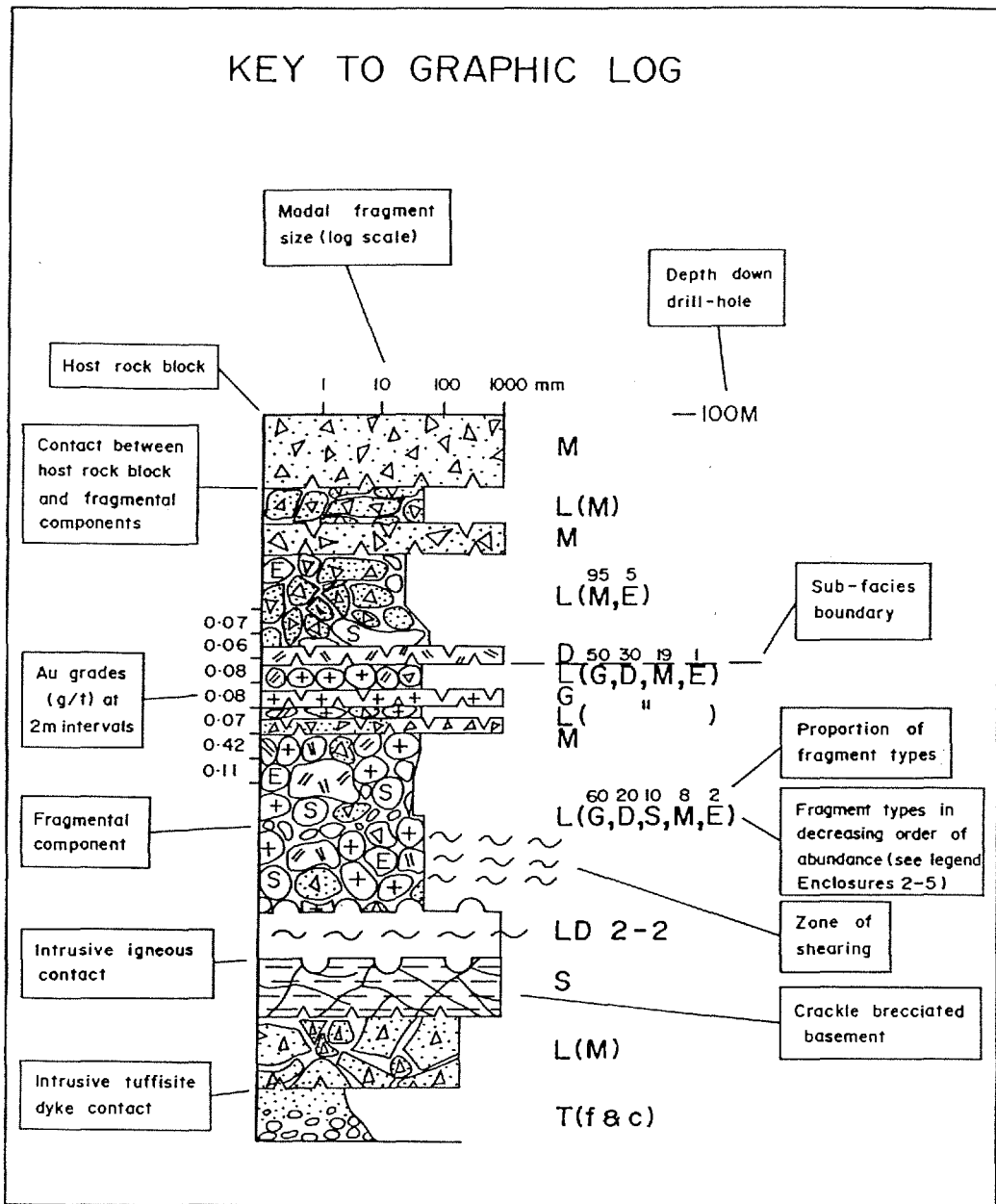


Figure 5.1: Explanation of graphic logging system. Note the blocks of host rock ( $\geq 1$  metre) in the breccia and the fragmental component derived from host rock fragmentation.

framework for mineral paragenesis studies (see Chapter 4), however it was later found during graphic logging in drill core that they gave a simplistic and often misleading view of the variation in breccia texture within the pipe.

### 5.2.2 Graphic analysis system for the subvolcanic environment

A graphic analysis system was developed to undertake a facies analysis of the Mt. Leyshon breccia pipe which represents breccia facies characteristics in one column. The system assesses; fragment angularity and shape, fragment types, relative fragment proportions, fragment to matrix proportion and fragmentation characteristics as explained in Figure 5.1. Additional notes on packing, sorting and detailed fragmentation characteristics were made. Logging was undertaken at a scale of 1:500.

Thirteen drill holes were selected on four east - west sections to provide a wide coverage of the facies variations in the Mt. Leyshon breccia (Figure 5.2). An additional drill hole was graphically logged to provide information on the nature of the northern pipe contact. Together, approximately 4000 metres of drill core was graphically logged for this aspect of the study.

In the analysis of the Mt. Leyshon breccia it was hoped that the early dykes (pre-Mt. Leyshon breccia) would act as a ghost marker unit. These dykes commonly focus brecciation and transport and as a result are poorly preserved in the breccia pipe. Nevertheless, the internal consistency of basement blocks and the preservation of a pre-breccia basement contact provide evidence for relative movement in the breccia pipe (see section 5.5). In other breccia pipe systems where the host rock includes units with a well defined geometry and distinctive character (eg. sedimentary units or thick dykes), graphic analysis should aid a rapid assessment of the offset on such units during brecciation.

During this analysis, basement and the main pipe breccia were used to define the facies architecture of the Mt. Leyshon breccia in a similar way to the use of basement to define the main pipe breccia (section 2.2.1). Recognition of basement and main pipe breccia requires a knowledge of both the facies variations of these two units, and the nature of pre-Mt. Leyshon breccia hydrothermal alteration which affects their appearance and rheology. The post-Mt. Leyshon breccia alteration causes fragment alteration, infills the Mt. Leyshon breccia cavities and affects the fracture network in basement and main pipe breccia. This fracture network results from host rock fracturing prior to and during the Mt. Leyshon breccia event. Consequently the alteration network assists the investigation of host rock fragmentation to produce the Mt. Leyshon breccia. During logging the first step was to isolate these blocks of existing stratigraphy and observe the relationship between these blocks and fragment zones between them. In addition, distributed (vein scale) re-brecciation of the existing breccia pipe occurs at several stages in the post-pipe hydrothermal evolution (Chapter 4).

One draw back of facies analysis in drill core, is the inherent nearly single dimension of the observations, and the 5 centimetre diameter of the drill core. Nevertheless, the down core dimension is large (up to several hundred metres) and the core allows continuous logging of facies

variations in the breccia pipe, which is impossible in the open pit. The pit observations did improve the three dimensional understanding of the relations visible in the drill core.

### 5.3 FACIES CHARACTERISTICS OF THE MT. LEYSHON BRECCIA PIPE

The facies characteristics described below are derived from the detailed graphic / textural analysis presented in Enclosures 2 - 5 and are summarised in Table 5.1.

#### 5.3.1 Fragment size variation

Two distinct fragment size populations occur in the Mt. Leyshon breccia pipe, defining two main components; namely fragments  $\leq 0.20$  metres and blocks  $\geq 1$  metre up to 10 metres (Plates 5.2 and 5.3). Fragments with a size between 0.2 - 0.5 metres are relatively uncommon, and fragments between 0.5 - 1 metre are relatively rare. Blocks of existing lithologies (basement, main pipe breccia and early dyke;  $\geq 1$  metre) retain their pre-Mt. Leyshon breccia designation. These blocks are indicated separately on the graphic log and their size is indicated by the 2 metre assay interval marks on the drill hole. The graphic analysis of the breccia pipe concentrates on the characteristics of the smaller fragment component and their relationship to the larger host rock blocks.

A given zone of Mt. Leyshon breccia is poorly sorted ( $< 0.2$  to 50 centimetres) which complicates rapid assessment of fragment size variations throughout the pipe. For this reason, the fragment size mode was used during the graphic analysis of the breccia. Modal fragment size in the breccia pipe shows surprisingly little variation (Table 5.1). In general, areas of obvious mixing have fragments commonly between 3 - 5 cm or 5 - 10 cm, whereas fragment size is typically 10 - 20 cm in dominantly monolithologic breccia zones (compare 100 m to 250 m, MLD 155, Enclosure 3). The proportion of  $\leq 1$  cm fragments in the breccia increases as the degree of mixing increases, although they generally remain as a minor fragment size subpopulation concentrated in the mixed zones. Fragment size grading in the Mt. Leyshon breccia is uncommon and where developed is erratic and non-continuous. Two forms of grading occur: firstly, weak, uncommon grading in polymict breccia zones dominated by granite and dolerite fragments (eg. 60 m, MLD 177, Enclosure 5); secondly, fragment size grading occurs in rare high matrix zones described in section 5.3.4.

#### 5.3.2 Fragment types and degree of mixing

Fragment types in the Mt. Leyshon breccia consist of all basement units, main pipe breccia and early dyke. In addition, two types of cognate igneous fragment occur in the breccia (their shape and microstructure suggest they were solid at the time of fragmentation). Firstly, a type texturally identical to porphyry unit I and the other type has some textural affinity to porphyry unit IV (though porphyry unit IV intrudes the Mt. Leyshon breccia). The fragment types in the breccia are not evenly distributed nor is the degree of mixing uniform throughout the breccia. Because much of the Mt. Leyshon breccia consists of blocks or zones of partially fragmented existing units (eg. 350 m, MLD 80, Enclosure 4; Plates 5.2 and 5.3), fragment composition ( $< 20$  cm) generally reflects these existing units. As a result, well mixed fragments are generally confined to relatively restricted zones within the breccia pipe and are extremely irregular in their distribution. For

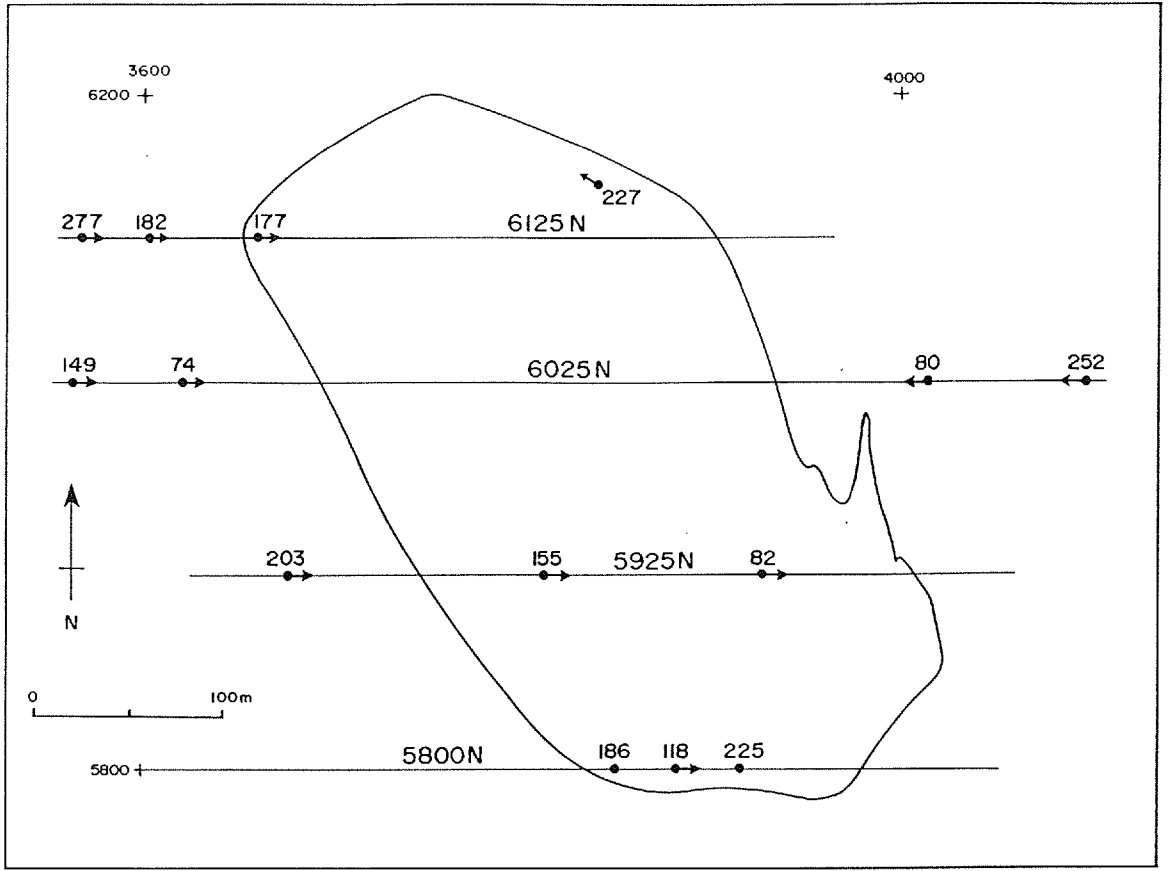


Figure 5.2: Location of drill holes (inclined with arrow, vertical without) used for graphic logging. Outline of Mt. Leyshon breccia at 400 RL also shown.

example, a large proportion of the breccia pipe is composed of partially fragmented main pipe breccia with only minor fragment mixing (few %); the introduced fragments typically consist of early dyke or granite fragments (eg. 225 m, MLD 186, Enclosure 2; Plate 5.4). Early dyke fragments postdate the main pipe breccia and are therefore introduced, however in some cases the provenance of the granite and metasediment fragments is ambiguous (Plate 5.3). At least some of these granite fragments are liberated *in situ* from the main pipe breccia by local fragmentation, whereas others represent introduced fragments derived from new fragmentation of granite. Consequently, in zones of breccia dominated by main pipe breccia fragments the estimation of introduced fragments may be a few percent too high. One region of the breccia pipe is dominated by granite and dolerite fragments (and partially broken blocks) which are relatively well mixed, although the proportion of other fragment types is typically minor (15-30 %; eg. 125 m, MLD 186, Enclosure 2; Plates 5.7 and 5.8). Porphyry unit I fragments are concentrated in minor mixing zones at the southern end of the pipe (see Enclosure 4 and 5), however no pattern in the distribution of other cognate igneous fragments was detected.

### 5.3.3 Fragment shape and matrix proportion

Fragment shape variations are a function primarily of rock composition and to a lesser extent degree of mixing. In polymict breccia zones granite, dolerite, early dyke, and porphyry (cognate igneous) fragments are commonly subrounded, whereas fragments of main pipe breccia, metasediment and basement rhyolite are typically subangular to angular (Plates 5.4 and 5.8). Other than this primary rheological control, little systematic spatial variation in fragment shape occurs within the breccia pipe as a whole. However, because the proportion of subrounded fragments increase in the narrow well sorted zones there is a local correlation between fragment roundness and mixing. Significantly, fragment shape characteristics are different in zones of breccia dominated by main pipe breccia fragments. Here, the number of long aspect ratio (splinter textured) versus equant fragments increases with an increase in fragment expansion and mixing (see 5.3.4). Blocks of existing units (< 1 - 10 m) in the Mt. Leyshon breccia are commonly angular and their shape varies from rectangular (Plate 5.10) to irregular.

Breccia matrix proportion and relative porosity (vughs) within the Mt. Leyshon breccia were initially assessed semi-quantitatively on cut rock slabs (using a transparent grid), and subsequently visually estimated during graphic logging. Assessment of these breccia characteristics is complicated by the infilling of cavities and replacement of matrix, by post-breccia hydrothermal alteration. The proportion of matrix in any given zone of breccia is generally only a few percent or less, and does not show systematic variation with other facies characteristics, such as degree of fragment mixing or fragment roundness (Table 5.1). For example, zones of breccia dominated by granite and dolerite fragments show the highest degree of fragment roundness but little matrix (Plate 5.8). In breccia dominated by main pipe breccia fragments the proportion of matrix is commonly less in the zones of mixed fragments compared to highly expanded monomict zones (Plate 5.4). Importantly, uncommon zones occur in the breccia pipe that contain up to 90% matrix and that are typically only a few centimetres thick (Plates 5.3 and 5.4). These high matrix zones

are locally up to 80 centimetres thick (eg. 66 m, MLD 82, Enclosure 3; Plate 5.12). Despite their erratic distribution high matrix zones are generally confined to regions of the pipe dominated by main pipe breccia fragments and are more common in regions of breccia that show abundant jigsaw fit textures (see section 5.3.4). These high matrix zones are dominated by splinter shaped fragments. A minor fragment component ( $\leq 1$  centimetre) in these zones consist of granite or early dyke which may be elongate splinters, or rounded fragments that are obviously introduced (see section 5.3.4). Abundant cavities (vughs) occur in the Mt. Leyshon breccia pipe, although they are noticeably smaller and less common in zones of breccia dominated by granite and dolerite fragments (general tighter packing). Beyond this, no consistent pattern was observed in vugh distribution nor any systematic relationship of vughs to other breccia characteristics (but see Chapter 8).

### 5.3.4 Fragmentation characteristics

The style and extent of host rock fragmentation within the breccia pipe are the most important characteristics for constraining the processes operating during pipe formation. Two important breccia characteristics are addressed in this section:

- (1) Fragmentation progressions.
- (2) Jigsaw fit textures.

A fragmentation progression is defined as the continuous and traceable disintegration of the host units (Plate 5.13). Fragmentation progressions occur on all scales from local occurrences to the dominant fragmentation characteristic in a particular zone. They are present in all zones in the breccia pipe (but are rare in granite rich zones) and are particularly well developed in breccia dominated by fragments of main pipe breccia. Jigsaw fit textures are defined here as highly expanded host rock which no longer forms a fragmentation progression, although at the local scale the fragments can be obviously fitted back together (Plates 5.6 and 5.12d). Jigsaw fit textures, which are less continuous than fragmentation progressions, occur within fragments, and between fragments and blocks of host rock. At the scale of logging undertaken in this study it is only possible to depict a general impression of these fragmentation characteristics (eg. abundant fragmentation progressions, 390 m, MLD 277, Enclosure 5).

The following description examines the inter-relationship between the two fragmentation characteristics described in this section. Different regions in the breccia pipe show variations in their extent and style of fragmentation. Least brecciated main pipe breccia shows abundant progressions which pass from blocks into zones of equant fragments, with only minor separation (Plates 5.1 and 5.2). In addition, jigsaw fit textures increase at the expense of fragmentation progressions, in breccia dominated by main pipe breccia fragments, as the degree of brecciation and mixing increase. So that, in polymict breccia dominated by main pipe breccia fragments, a complex mass of breccia results with the whole range of fragmentation styles present in a given zone (Plates 5.5 and 5.6). In contrast, these fragmentation characteristics are rarely observed in regions of the granite or dolerite host rock. When fragmentation progressions are present, the

MLB SUBFACIES						
FACIES CHARACTERISTICS	ZONE 1	ZONE 2A	ZONE 2B	ZONE 3	ZONE 4A	ZONE 4B
MODAL FRAGMENT SIZE	Commonly 10 cm, upto 20cm. Narrow zones of ≈ 5 cm.	3 -10 cm 10 - 20 cm.	3 - 5 cm 5 - 10 cm.	3 - 5 cm 5 - 10 cm (frags ≤ 1 cm common in mixed fragment zones).	3 - 5 cm 5 - 10 cm (frags ≤ 1 cm common in mixed fragment zones).	5 - 10 cm 3 - 5 cm.
FRAGMENT TYPES (in decreasing order)†	M only.	M; rare G + E	M; minor G, E, S, D.	S, D, M, G, E, PR.	G, D, S, M, E, PR.	M, PR, S, D, G, E.
SORTING	Poor.	Poor.	Poor.	Poor.	Poor to moderate.	Poor.
MATRIX PROPORTION	Generally none.	Generally < 1% or none. Rare matrix rich zones.	2 - 5 %, rare matrix rich zones (up to 90%).	Commonly 5%, rare matrix rich zones (up to 90%).	Typically < 1% - 2%, uncommonly 5%.	Typically < 1%, rarely upto 5 %; uncommon matrix rich zones.
FRAGMENT ANGULARITY AND SHAPE	Angular. Equant to irregular, minor tabular or splinter shaped.	Angular. Commonly equant (introduced frags subrounded). Tabular shaped frags less common .	Angular (introduced frags subrounded). Commonly tabular and splinter shaped.	Angular to subrounded, commonly angular. Abundant tabular and splinter shaped frags.	Subrounded to subangular, commonly subrounded. Typically equant shaped frags.	Angular to subrounded. Equant to tabular.
DEGREE OF MIXING	None.	Low, few %.	Low, upto 15%, commonly ≤ 10%.	Up to 40% mixing with MPB frags.	High, relatively uniform.	Low to moderate; depends on preexisting strat.
HOST ROCK FRAGMENTATION	Abundant fragm. progs. Limited fragment rotation and jig. fit texts.	Fragm. progs common. Abundant 20 - 50 cm blocks separated by rubble textured zones ± frag. introduction.	20 - 50 cm blocks less common than zone 2a. Fragg. progs common, increase in jig. fit texts and rubble textured zones.	Jig. fit texts more abundant than fragm. progs. Zones of mixed frags are restricted to narrow regions between blocks.	Tightly packed breccia. Fragg. progs and jig. fit texts rare. Uncommon fragment size grading. Minor zones dominated by MPB frags, show poor fragm. and minor mixing.	Very irregular character; many partially broken regions of basement and MPB with narrow well mixed zones.
GENETIC INTERPRETATION	<i>In situ</i> fragmented MPB, slightly expanded.	Weakly expanded MPB. Rare mixing and transport zones.	Moderately expanded MPB. Minor mixing and transport zones.	Highly expanded MPB. Abundant transport and mixing in zones of smaller frags.	Well mixed breccia that reflect the pre-MLB strat. (G, D and minor fingers of MPB). Hence, local frag. mobility dominates.	Variably expanded host rock which reflects the pre-existing strat. (S, D, PR, MPB). Narrow zones of frag. transport.

Abbreviations: MPB-main pipe breccia, MLB-Mt. Leyshon breccia, fragm. progs-fragmentation progressions, jig. fit texts-jigsaw fit textures, strat.-stratigraphy, S-metasediment, G-granite, PR-basement rhyolite, D-dolerite. † Cognate igneous fragments can occur in all zones of mixing.

Table 5.1: Internal facies characteristics of the Mt. Leyshon breccia pipe.

granite and dolerite form a more spherical fracture pattern (section 3.5), which results in greater fragmentation (comminution and poor sorting) than in main pipe breccia; these zones occur between poorly fragmented granite and dolerite blocks. More commonly the granite and dolerite are extensively fragmented which results in a strongly disaggregated poorly sorted "slurry" of fragments (Plates 5.7 and 5.9). Despite this, limited jigsaw fit textures are displayed by individual blocks and fragments in the granite rich polymict breccia. Regions of granite that were silicified by pre-Mt. Leyshon breccia alteration (see Chapter 4) behave in a more brittle manner and develop limited fragmentation progressions and jigsaw fit textures. The minor zones of breccia dominated by metasediment or rhyolite dyke basement show abundant fragmentation progressions and jigsaw fit textures, like the fragmentation of main pipe breccia. But both fragmentation and polymict breccia zones are more erratic than in the main pipe breccia dominated zones (eg. 55 m, MLD 82, Enclosure 3).

Finally, the fragmentation characteristics that occur in the high matrix zones (section 5.3.3) are now described. In these zones, tabular and splinter shaped fragments are common and the fragments typically occur in a highly expanded state, supported by a fine matrix (Plate 5.4). Some of the fragments show jigsaw fit textures (despite being centimetres apart), both with each other and the surrounding larger fragments in the matrix poor breccia. Long aspect ratio fragments may be parallel to each other, or randomly arranged in zones of more obvious fragment mixing. In the high matrix zone noted in section 5.3.3 (66 m, MLD 82, Enclosure 3), the upper portion is dominated by tabular fragments in a highly extended state that are supported by a rock flour matrix (Plates 5.12b, c and d). The high matrix zone grades down hole into typical fragment supported polymict Mt. Leyshon breccia (Plate 5.12a). The orientation of these drill hole examples and the fragments they contain is unknown. However, on the two occasions these high matrix zones have been observed in the open pit, they are nearly flat lying. These zones, one of which is shown in Plates 5.10 and 5.11 (GR. 3880 E 5975 N, 375 RL.), are subparallel to a flat, gradational contact separating breccia dominated by granite and dolerite from breccia dominated by main pipe breccia fragments (similar to the zone around 175 m, MLD 155, Enclosure 3). Likewise, the fragments in these zones are flat lying and parallel to the whole zone with their long axes trending approximately north.

## **5.4 FACIES AND FACIES GEOMETRY OF THE MT. LEYSHON BRECCIA PIPE**

The Mt. Leyshon breccia is divided into six zones (zone 1, 2A, 2B, 3, 4A and 4B), on the basis of the graphic analysis presented in Enclosures 2 - 5, and additional detailed observations on fragmentation characteristics. The collective characteristics of these zones are shown in Table 5.1 and their geometry is indicated in Figures 5.3 and 5.4.

During this study, pipe contacts observed in drill core and at four locations in the open pit (Figure 3.2) are sharp. The western and eastern pipe margins are now bound by strike slip faults (Figure 3.2). The presence of a wide zone of crackle brecciated main pipe breccia outside the eastern pipe

margin, subsequently affected by post pipe alteration and late strike slip faulting, has previously resulted in confusion over where to define the eastern margin.

As discussed in the previous sections certain characteristics show little or erratic variation throughout the breccia pipe. Fragmentation characteristics (progressions or jigsaw fit textures), fragment types and degree of mixing are the most diagnostic criteria for breccia pipe subdivision. These three characteristics are inter-dependent and reflect the configuration of host rock lithologies prior to breccia pipe formation. Fragment types and degree of mixing are quantifiable in the Mt. Leyshon breccia, whereas the complex variation and fine detail of the fragmentation characteristics has required a qualitative approach in this study. Firstly, the basis for the subdivision is discussed and then the geometry of the breccia pipe and each sub-zone is highlighted.

All zones discriminated in the breccia pipe are gradational although the transition between zone 1 and other zones is the most abrupt. Dominant fragment type in the Mt. Leyshon breccia most obviously divides the breccia into two types, zones dominated by main pipe breccia fragments (zones 1, 2A, 2B and 3), and zones generally dominated by basement fragments (metasediment, granite, rhyolite and dolerite dyke; zones 4A and 4B). Further subdivision of the breccia pipe is based on the additional characteristics of rock fragmentation and degree of mixing (Figure 5.5, Table 5.1). A simplified impression of the dominant breccia characteristics of each major zone is shown in Figure 5.6. The definitive characteristics of each breccia pipe zone are noted below:

- Zone 1 is composed exclusively of main pipe breccia fragments (no mixing), dominated by fragmentation progressions, and has little to no matrix (Plate 5.1; eg. 600 m, MLD 252, Enclosure 4).
- Zone 2 is distinguished from 1 by the presence of up to 10-15% mixed fragments, a small matrix component, increased fragmentation of the main pipe breccia host, a higher proportion of jigsaw fit textures, and the presence of high matrix zones. Zone 2 is further divided into two sub-zones on the basis of degree of fragment mixing and fragmentation, although the division between the sub-zones is to some extent arbitrary. Zone 2A shows only very limited fragment mixing (few %; Plate 5.2; eg. 450 m, MLD 80, Enclosure 4), whereas zone 2B has up to 10% mixing (locally 15%) and an increased proportion of jigsaw fit textures (Plates 5.3 and 5.4, eg. 395 m MLD 80, Enclosure 4).
- Zone 3 is also dominated by main pipe breccia fragments but is differentiated from zones 1 and 2 by the presence of relatively abundant mixing with other fragment types, less persistent fragmentation progressions, an increase in jigsaw fit textures and tabular shaped fragments (Plates 5.5 and 5.6; eg. 200 m, MLD 80, Enclosure 4). The proportion of fragments  $\leq 1$  cm in diameter is greater in zone 3 than in zones 1 and 2, though they are still present in narrow zones of increased mixing within the breccia. Furthermore, matrix proportion is probably slightly greater throughout zone 3, than through zones 1 and 2.
- Zone 4A is differentiated from zones 1, 2, and 3 by being dominantly composed of granite and dolerite fragments, generally having a higher degree of fragment roundness and packing (though

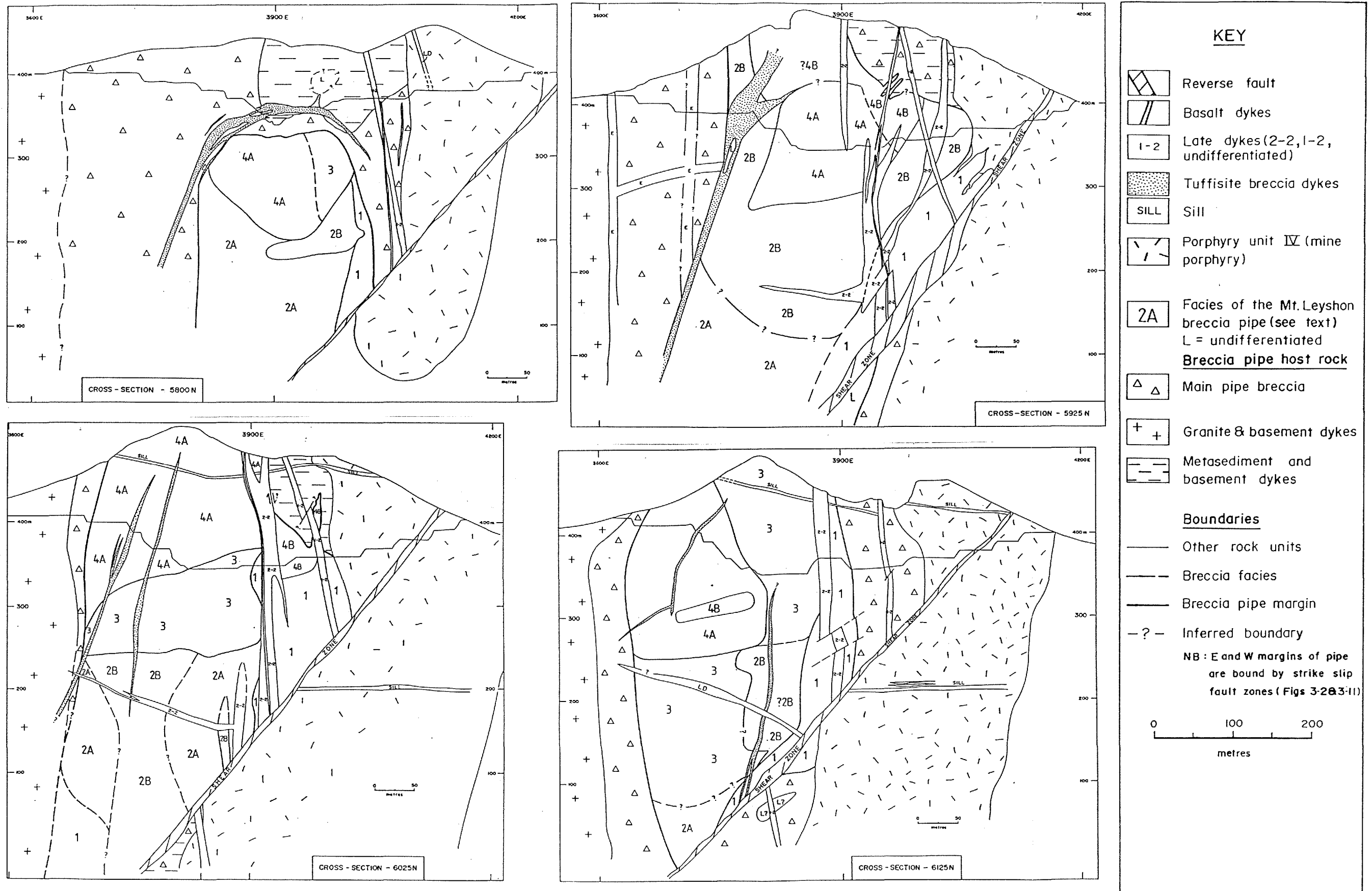


Figure 5.3: Cross-sections through the Mt. Leyshon breccia pipe. Sections show the facies variations within the breccia pipe based on graphic logging. The framework geology is modified from the mine drill-hole data base. Note that the breccia pipe is offset by a late reverse fault. Stepped horizontal line is the pit outline.

matrix proportion is still low) and showing very few fragmentation progressions or jigsaw fit textures (except on the local fragment scale; Plates 5.7 and 5.8; eg. 100 m, MLD 186, Enclosure 2).

- Zone 4B forms only a minor proportion of the breccia pipe investigated here and is differentiated from zones 1, 2, 3 and 4A by being dominantly composed of partially fragmented basement rhyolite, main pipe breccia, metasediment and dolerite (eg. 90 m, MLD 82, Enclosure 3). Fragmentation progressions and jigsaw fit textures are common and the breccia is particularly blocky; mixing zones are restricted to narrow regions between the larger blocks. High matrix zones occur, in contrast to zone 4A. In addition, a component of zone 4A and 4B is dominated by main pipe breccia blocks (and fragments) which have the facies characteristics of zones 1, 2 or 3 (eg. 200 m, MLD 177, Enclosure 5). This component is typically only poorly fragmented and may be dominated by the same fragments which make up partially brecciated basement also in these zones. Therefore, these zones of partially brecciated main pipe breccia probably represent tongues that were intruded into the basement, both components being brecciated during the Mt. Leyshon breccia event.

The breccia pipe forms an irregular rhombohedron with a near vertical northern margin but the pipe plunges steeply to the south at approximately 60°; the central portions of the breccia pipe also have a steep westward dip (Figure 5.3). The central portion of the pipe (300 RL) has the widest cross-section and at lower levels (100 and 200 RL) the pipe also narrows downwards and takes on a slot-like form despite the effect of the late reverse fault (Figure 5.4). As noted in Chapter 2 (and discussed further in Chapter 7), the breccia pipe probably also closed upwards. The presence of a small pipe of Mt. Leyshon breccia on Mt. Hope and dyke-like regions to the south west (see Chapter 2), suggests that the pipe bifurcated at depth.

The three dimensional geometry of a portion of the breccia pipe (from 480 to 100 RL) is shown in Figure 5.7, and the approximate geometry of the internal facies within the pipe is represented in Figure 5.8. The defined sub-zones within the breccia pipe in part reflect the pre-pipe configuration of host rock types before pipe formation (Figures 5.4 and 5.9). Zone 1 is generally confined to the eastern and southern margin of the pipe but occurs on the western margin of the pipe below approximately 110 RL on section 6025N (Figure 5.3). At the levels investigated by graphic logging (430 - 0 RL), the southern half and lower levels of the pipe are dominantly composed of zone 2. Here, zone 2B narrows at the expense of 2A until at 100 RL, 2A dominates. Hence, zone 2B generally occurs adjacent to zones 3 and 4, whereas 2A dominates when zones 3 and 4 are absent. In the northern half and upper levels of the pipe zones 3 and 4 dominate. Zone 3 forms an irregular, steeply dipping region in the northern portion of the pipe. In addition, a small "lens" of zone 3 occurs on the 300 RL at the southern end of the breccia pipe. Zone 4A forms a gently dipping region in the pipe which does not extend below 195 RL. Part of the lower surface of this region was mapped in the pit (GR. 3785 5960, 385 RL) and here the contact has an approximate dip and strike of 135° / 29°W. Facies analysis for this study extends from 5800 N to 6125 N. At the north of the breccia pipe the distribution of breccia zones and the pipe contact are constrained by

pit mapping and a graphic log of MLD 227 (not included in this Chapter; see Figure 5.2 for location). The geometry of the southern breccia pipe contact was constrained by mine drill hole sections at 25 metre spacing. However, at the 100 and 200 RL the shape of breccia facies at the southern pipe margin is inferred by projection from the north and the presence of weakly brecciated main pipe breccia (mine drill hole data).

### **5.5 INTERPRETATION OF BRECCIA FACIES CHARACTERISTICS AND FACIES DISTRIBUTION IN THE MT. LEYSHON PIPE**

The graphic logging observations presented in this Chapter allow a qualitative classification of breccia pipe zones based on the relative proportion of fragmentation progressions, jigsaw fit textures and mixed fragment zones (Figure 5.5). Together with the proportion and types of fragments, these characteristics define three main interactive processes in the formation of the breccia pipe as discussed below:

- (1) Host rock fragmentation.
- (2) Host rock expansion.
- (3) Fragment transport / mobility.

Three types of host rock fragmentation are recognised in this study:

- (1) Fragmentation resulting in equant to irregular fragments that form a monomict breccia. This is merely *in situ* fragmented host rock because this type of fragmentation is dominated by fragmentation progressions with little fragment expansion (or rotation).
- (2) Fragmentation of particularly main pipe breccia which results in elongate tabular to splinter shaped fragments in erratic expanded zones.
- (3) The local break up of fragments and blocks, both within and marginal to mixed fragment zones. The resulting fragments may be either equant, irregular or tabular; presumably the initial host rock fragmentation styles (and associated micro-fracturing) controlled the time dependent disintegration of fragments in mixed zones.

The degree of host rock expansion in the breccia pipe is likewise extremely irregular. However, expansion is concentrated in regions between host rock blocks (not dominated by fragmentation progressions), particularly in zone 3. Jigsaw fit textures and zones of mixed fragments replace fragmentation progressions as brecciation of the host rock increases. Consequently, these textural changes are a measure of host rock expansion at any given point in the breccia pipe. On the scale of the whole pipe this textural evolution is crudely shown by zones 1 through to 3. High matrix zones that typically have expanded jigsaw fit textures, are common in poorly fragmented main pipe breccia and consequently indicate local host rock expansion during breccia pipe formation. In extreme cases these high matrix zones are up to 80 centimetres thick, are flat lying and the tabular fragments they contain define a gently dipping layering. Furthermore, because some of these fragments display a highly telescoped jigsaw fit texture, together these features suggest zones of vertical extension. In addition, horizontal extension of the host rock at the scale of the breccia pipe is suggested by both the overall geometry of the breccia pipe (Figure 5.7) and the association of

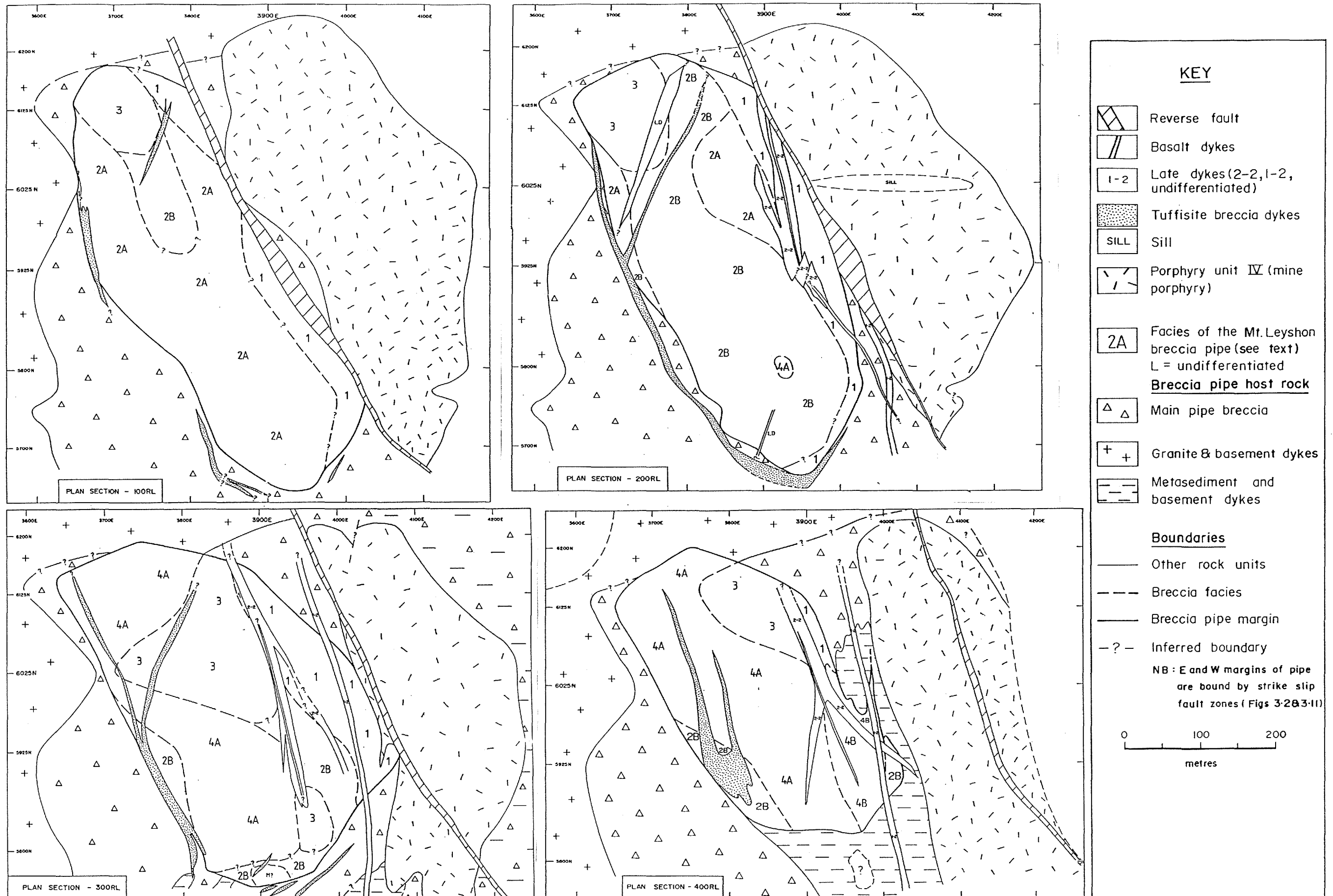


Figure 5.4: Plans through the Mt. Leyshon breccia pipe compiled from the graphic logged cross-section shown in Figure 5.3. The framework geology is modified from the mine drill-hole data base.

zone 2B with the widest portion of the pipe (at lower, narrower portions of the pipe zone 2B is replaced by zone 2A; Figure 5.8).

A mixed fragment breccia (bimict to polymict) indicates that fragment transport and/or mobility has occurred. Fragment mobility is used here in the sense of local relative movement between fragments. Fragment transport refers to actual removal from the sight of fragmentation. The distinction between fragment transport and mobility is sometimes problematic. Nevertheless, local fragment mobility dominates over fragment transport in the pipe because the pipe largely consists of host rock that has a high degree of connectivity. Transport zones commonly occur as narrow, irregular and discontinuous zones between partially fragmented host rock. Narrow regions of monomict breccia which lack fragmentation progressions or jigsaw fit textures are also probably transport zones. However, zones of merely partially fragmented host rock (particularly main pipe breccia) may be mistaken as a well mixed breccia composed of completely liberated fragments. This confusion arises because the post-Mt. Leyshon breccia alteration typically blurs the fragmentation characteristics, although can be avoided by carefully looking for fragmentation progressions or jigsaw fit textures in these zones.

Documentation of facies characteristics in this Chapter indicate that the transported breccia component **does not** represent the central part of the Mt. Leyshon breccia pipe as has been suggested for other breccia pipe models (Sillitoe, 1985; Baker et al., 1986). Rather, the transported zones form in the regions of maximum expansion (extension) and form a diffuse chaotic network during break-up of the existing stratigraphy. However, because of the lack of reliable marker horizons the relative motion of the transported/mobile fragment component is only partially resolved. The following observations relate to the degree and direction of fragment movement in the breccia pipe:

- (1) As already noted the high degree of connectivity of fragment and block components in large parts of the breccia pipe (zones 1, 2A and 2B account for  $\geq 60$  volume % of the pipe) suggests that fragment transport was minor in these regions.
- (2) The general preservation of the gross host rock stratigraphy, despite brecciation, suggests only local mobility of much of the host rock in the pipe. Several other workers have reported the preservation of a ghost stratigraphy in breccia pipes (eg. Sillitoe, 1985; Baker and Andrew, 1991).
- (3) The existence of narrow, well mixed polymict breccia zones that are relatively well sorted suggests that significant transport of fragments did occur locally.
- (4) The existence of a flat lying region dominated by granite and dolerite fragments (zone 4A) implies that a horizontal cell formed during breccia pipe formation. Because fragment exchange with this zone was limited, local fragment mobility probably dominated over fragment transport in this zone. If this is true it also implies a low vertical stress to enable fragmentation and horizontal mobility during pipe formation
- (5) The cognate igneous fragments which locally occur in the pipe may be present in all regions of polymict breccia. Blocks of this igneous material (which could have provided the source for these fragments) do not occur in the breccia pipe over 600 m of drill holes, and the fragments do not

show evidence for chilling or plastic deformation, which suggests that these igneous fragments were derived from the break-up of an existing igneous unit at depth. This implies limited, upward fragment transport over at least 600 metres in the pipe. However, the possibility that these cognate igneous fragments were derived from small intrusive fingers of igneous rock injected into the host rock before pipe formation, cannot be discounted. Such intrusive networks have been described for igneous units adjacent to the main magmatic centre.

(6) Local lateral fragment transport is implied by the presence of gently dipping flow fabric in the high matrix zones.

The Mt. Leyshon breccia is generally poorly sorted and shows little systematic variation in modal fragment size, indicating hydraulic sorting of fragments was generally not an important process in breccia formation. Hydraulic sorting was, however, locally important as indicated by the increase in fragment sorting in:

- (1) The zone of breccia dominated by granite and dolerite fragments (zone 4A) where uncommon fragment size grading occurs.
- (2) Narrow regions of well mixed fragments which separate poorly fragmented host rock.
- (3) The presence of fragment size grading in some of the matrix rich zones (see below).

Despite the limited fragment size sorting there is a decrease in mean fragment size as the degree of fragmentation, expansion and transport increases. This evidence for restricted fragment transport and limited hydraulic sorting suggests that a fluid phase accompanied brecciation. The role of a fluid phase in brecciation within the Mt. Leyshon complex is considered in Chapter 7.

Breccia pipe workers (eg. Sillitoe, 1985 and Baker et al., 1986) generally consider that fragment roundness, and the proportion of matrix present in a given zone of breccia, is related to the amount of fragment transport and hence abrasion ("milling") in that zone. However, because rheology dictates the style and extent of initial rock fragmentation (angular versus subrounded, and discrete fracture versus grain scale disaggregation, as discussed in section 3.5), the gross configuration of host rock lithology has an important control on fragment shape characteristics. Degree of transport / agitation effects fragment roundness through the period of abrasion subjected to the fragments as does rock composition. Likewise, the following additional observations suggest that the proportion of matrix present in a given zone of breccia is dominantly related to the degree of host expansion, rather than degree of fragment transport:

- (1) Zones 2A and 2B (dominated by partially fragmented main pipe breccia) uncommonly have 2 - 20 centimetre zones which are up to 100% matrix (Plate 5.4). This matrix and small fragments in these zones sometimes show an alignment (?flow fabric) which suggests that the material was introduced.
- (2) Where high matrix zones are well developed they commonly contain highly telescoped fragment trains indicating only limited movement of at least these fragments (Plate 5.12). In contrast, the matrix and smallest fragments between the larger fragments may show a fabric, suggesting that the matrix moved rapidly in to support the larger fragments. Where cavity margins

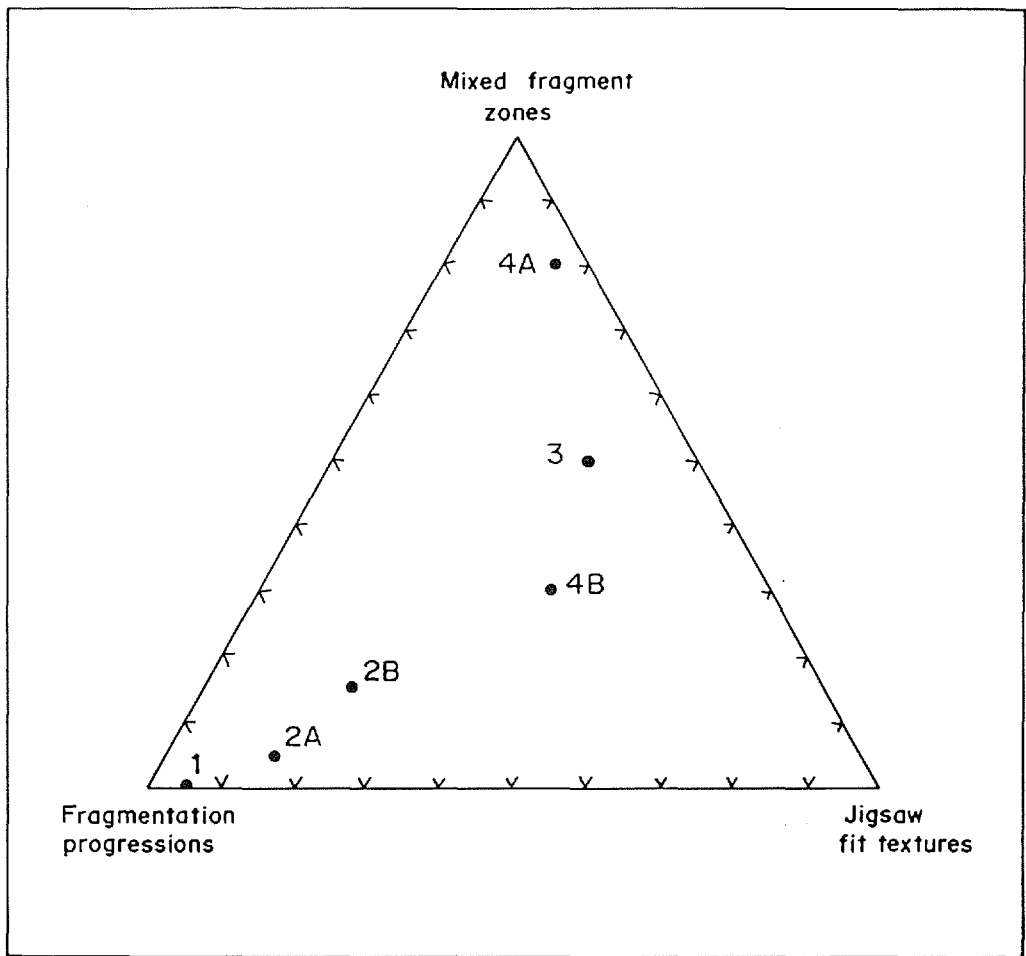


Figure 5.5: Subdivision of the Mt. Leyshon breccia pipe based of the relative proportions of three facies

Figure 5.6: Gross, simplified breccia facies of the Mt. Leyshon breccia pipe. Fragments are main pipe breccia unless labelled as follows: +-granite, =-dolerite, S-metasediment, E-early dyke, P-cognate igneous fragments, and  $\Delta$ -main pipe breccia in zone 4A.

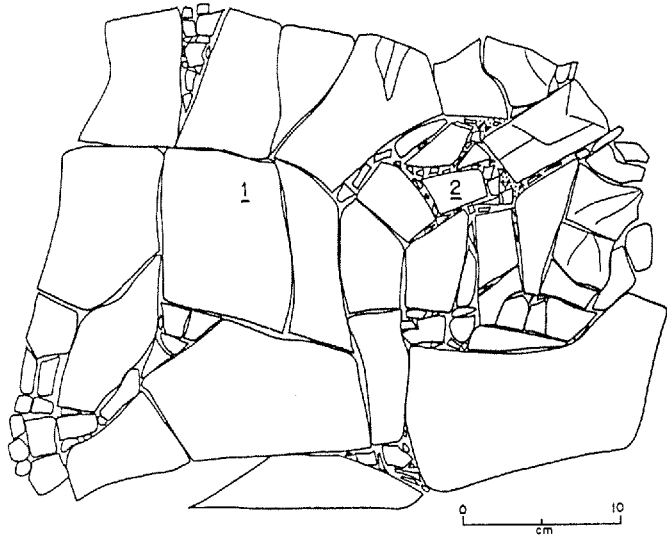
(A) Zone 1- dominated by main pipe breccia fragmentation. Note this drawing refers to the breccia characteristics between large main pipe breccia blocks. Fragmentation progressions (1) are abundant and there is no fragment introduction, little to no fragment rotation or transport, and little to no matrix. Minor zones of second order fragmentation (2) occur erratically in this zone.

(B) Zone 2 (2A and 2B combined) - dominated by fragmentation and expansion of main pipe breccia. Note: fragmentation progressions (1) are more common than jigsaw fit textures (2), the narrow zones of fragment mixing and transport (3), and the high matrix zones with splinter textured fragments (4).

(C) Zone 3 - dominated by expansion and mixing of main pipe breccia. Note: local jigsaw fit textures (1) are more abundant than fragmentation progressions, there is a higher proportion of fragment mixing than in zones 1 or 2, and the narrow zones of well mixed and sorted fragments (2).

(D) Zone 4A - dominated by mixed granite and dolerite fragments. Note: the breccia is well packed and has relatively uniform matrix distribution, fragments show a higher degree of rounding than other zones, jigsaw fit textures are uncommon, fragmentation progressions and high matrix zones are typically absent.

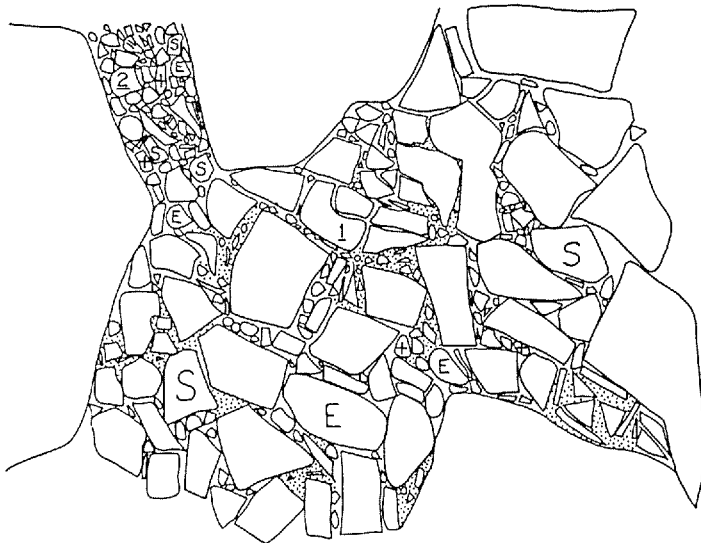
(A) Zone 1



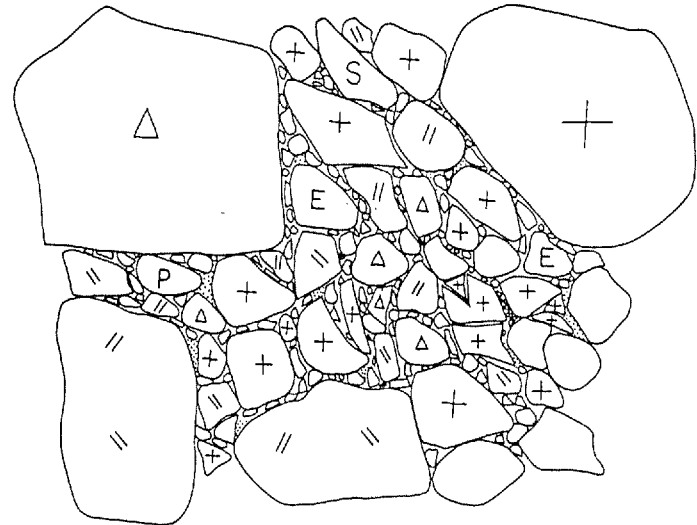
(B) Zone 2 (2A + 2B combined)



(C) Zone 3



(D) Zone 4A



are visible, in some weakly altered areas of the breccia, they are commonly coated with matrix and small fragment splinters are embedded in the matrix. This suggests that during host rock fragmentation and expansion, matrix was sucked into the cavity margins and adhered to the walls.

(3) These matrix rich zones, absent from well mixed breccia, are dominated by dolerite and granite fragments (zone 4A). Together with a significantly lower cavity volume in zone 4A, these facies characteristics suggest that fragmentation of the host granite and dolerite was dominantly due to disaggregation, rather than expansion. Furthermore, the tight packing of zone 4A and its general low matrix proportion, suggests that if a larger volume of matrix was ever present it was transported elsewhere in the breccia pipe. Many fragments would have undergone only local mobility. These observations are consistent with fragmentation in zone 4A being compressional/dilational but purely dilational in other zones.

Therefore, in conclusion to the above discussion, increased fragment mixing (polymict nature), loss of fragmentation progressions, few to no jigsaw fit textures, and an increase in the proportion of  $\leq 1$  centimetre fragments indicate transport zones rather than fragment shape or matrix proportion alone.

Zone 1 is dominated by characteristics which indicate *in situ* fragmentation of main pipe breccia, limited expansion and little fragment movement (Figures 5.5 and 5.6A). Two types of fragmentation occur in these zones. First order fragmentation of host rock commonly produces equant to irregular fragments, whereas second order fragmentation produces more splinter shaped break-up of larger fragments. Such second order fragmentation is concentrated in the minor expanded zones between larger blocks and fragments (Plate 5.1). Evidence presented in Chapter 3 also suggests that extensive host rock fragmentation occurred before breccia pipe formation. The following additional facies evidence supports this assertion, and suggests that zone 1 dominantly reflects a period of fault induced host rock fragmentation:

(1) Zone 1 is confined to the eastern side of the pipe and below 110 RL on the western side (Figure 5.3). This suggests that zone 1 was initially more widespread but has been destroyed in other areas of the pipe by further fragmentation, expansion and transport. The second order fragmentation noted above possibly represents the outer effect of this distributed brecciation

(2) The larger modal fragment size of zone 1, as compared with other zones, suggests that an additional process contributed to host rock fragmentation elsewhere in the breccia pipe.

Zone 2 is dominated by facies characteristics which indicate both host rock fragmentation and expansion (Figures 5.5 and 5.6B). Numerous blocks of main pipe breccia are connected by fragmentation progressions. Other zones show jigsaw fit textures, and hence signify greater expansion. Locally high matrix zones with expanded splinter shaped fragments occur which indicate considerable expansion. Limited regions between these areas of high connectivity comprise transported fragments. Zone 2B shows less host rock connectivity and more abundant mixing than 2A, and is therefore a more highly fragmented and expanded zone of the pipe.

Zone 3 is dominated by facies characteristics which indicate host rock expansion and fragment mobility / transport (Figures 5.5 and 5.6C). Most of the host rock in this zone has become disconnected. However, highly expanded regions of main pipe breccia which maintain a degree of connectivity are locally present. These regions preserve evidence for host rock expansion in zone 3. When viewed as part of a continuum, zones 2A, 2B and 3 trace the dynamic evolution of the breccia pipe in the main pipe breccia lithology. Already fragmented host rock (zone 1) is further fragmented and expanded. Transport of fragments occurs in the zones of maximum expansion. Host rock expansion and fragment transport are complexly distributed in the pipe (zones 2A and 2B) but are concentrated in the northern portion of the pipe as an irregular steeply dipping zone (zone 3 approximately 150 by 150 metres in diameter; Figure 5.8).

Despite being well mixed, granite and dolerite fragments in zone 4A generally account for >70% of the breccia, and the matrix proportion is low. Fragmentation progressions and jigsaw fit textures are rare, hence evidence for expansion is rare (Figures 5.5 and 5.6D). However, granite or dolerite blocks in zone 4A locally pass into a zone of rubble textured monomict breccia of the same composition preserving fragmentation of the host rock. Some of the remaining  $\leq 30\%$  of fragments in this zone were derived from "fingers" of main pipe breccia that had intruded the granite before Mt. Leyshon breccia pipe formation. Despite the obvious fragment mobility, the degree of fragment introduction and by implication transport external to zone 4A, is low. The whole zone is flat lying and has gradational but abrupt contacts with other zones. The zones of partially fragmented main pipe breccia with a high connectivity and their relationship to granite blocks, suggest that the granite region existed prior to the formation of the main pipe breccia. A zone of 4B breccia (ie. dominated by basement other than granite) occurs above the granite rich region in the pipe on section 5925 N (Enclosure 3), suggesting the granite did not extend upwards. If this is true, two possible explanations may account for the geometry of zone 4A, as follows:

- (1) The pre-complex configuration of the original granite / metasediment contact had a flat lying protrusion into the metasediment.
- (2) A granite slab was intercalated with metasediment slabs by (?thrust) faults prior to formation of the breccia complex, and the main pipe breccia subsequently removed the metasediment beneath the granite slab.

Zone 4B shows abundant textural variation which dominantly reflects the rheological difference between the three non-granite basement units and fingers of main pipe breccia intruding this basement zone. The facies characteristics of this zone suggest that fragment mobility dominated over transport in a similar way to that proposed for zone 4A. The rheological differences between units in zone 4B probably encouraged the development of restricted zones of increased expansion and fragment transport.

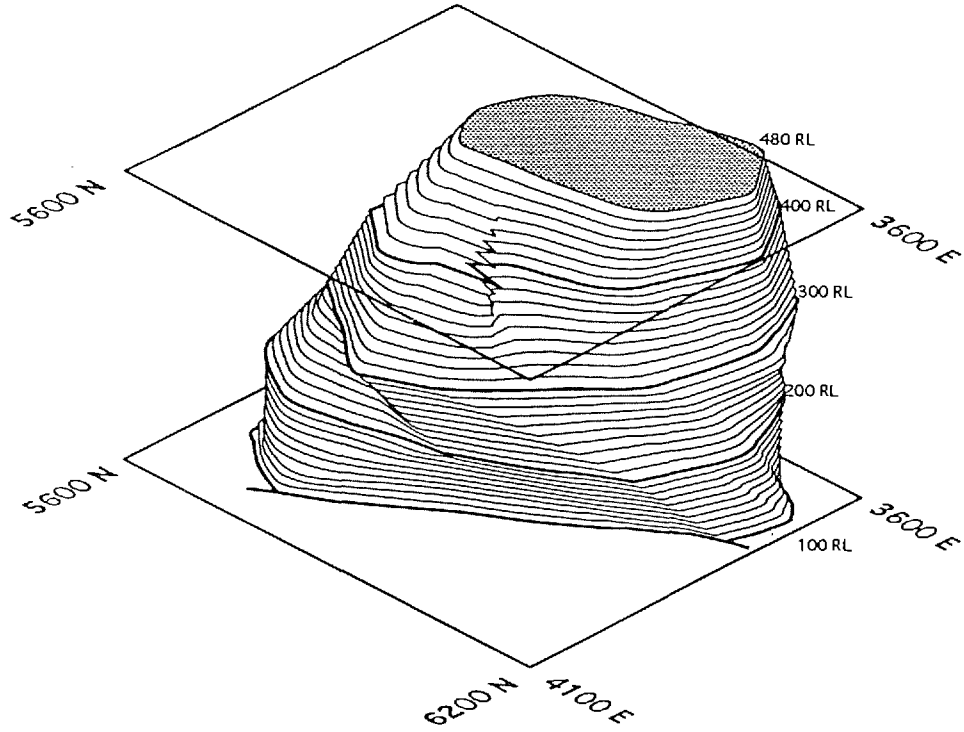


Figure 5.7: Part of the Mt. Leyshon breccia pipe (480 to 100 RL), isometric view looking towards the south west. Note: (1) the pipe narrows upwards and downwards, (2) that the central portion of the breccia pipe is widest at the 300 RL. (Computer construction in collaboration with N. Tate).

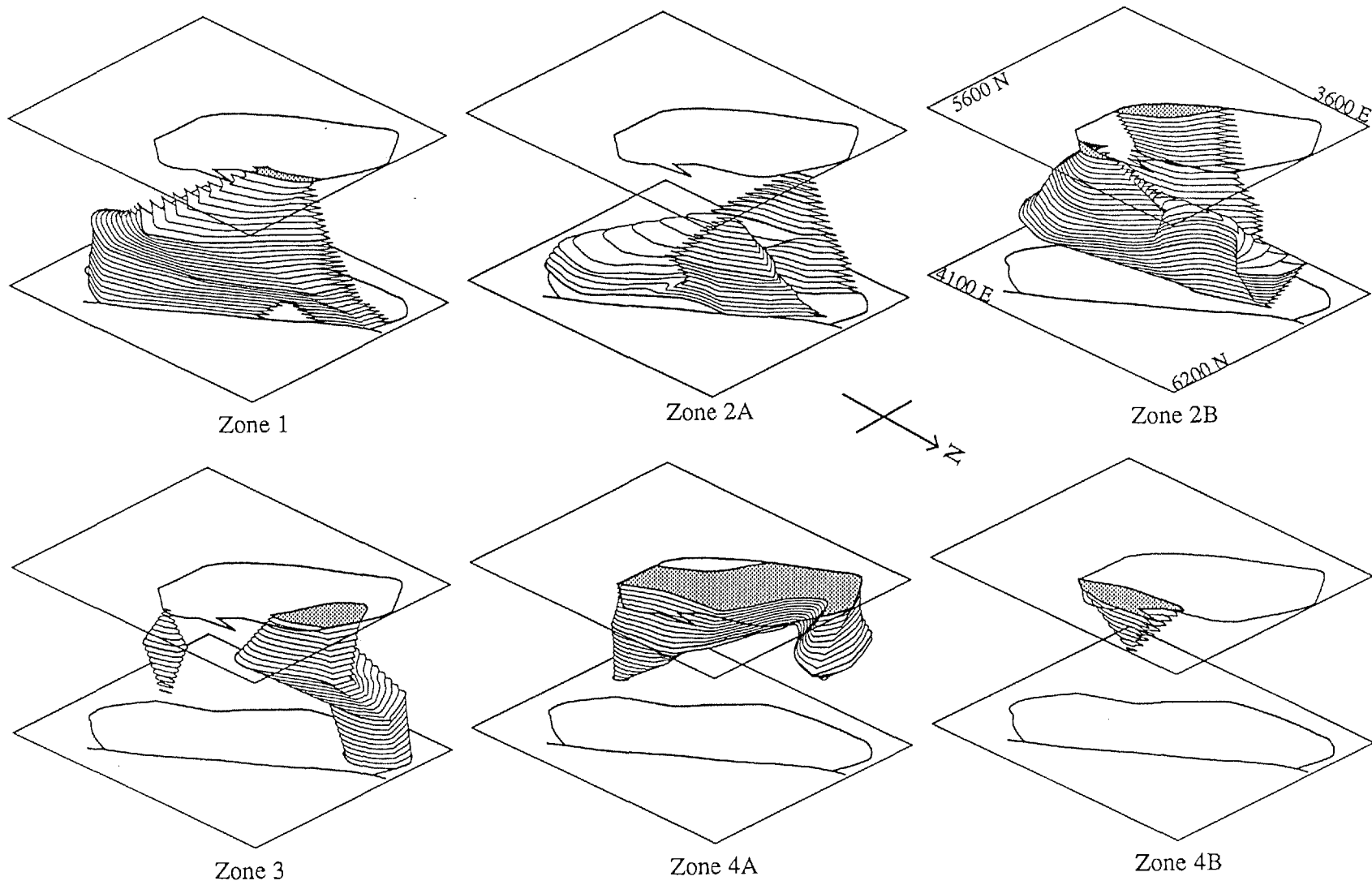


Figure 5.8: Approximate geometry of the Mt. Leyshon breccia pipe facies (400 to 100 RL), isometric view looking towards the south west. Diagram is based on plans and sections compiled from graphic logging. (Computer construction in collaboration with N. Tate.)

## 5.6 FACIES MODEL FOR THE MT. LEYSHON BRECCIA PIPE

The facies analysis undertaken in this Chapter suggests the following facies model for the Mt. Leyshon breccia pipe (Figure 5.9; Table 5.1):

- Fragment size variations in the breccia pipe define two main components; host rock blocks and smaller fragments. Host rock outside the breccia pipe and as blocks within the pipe provide the frame of reference to investigate host rock fragmentation and pipe formation.
- The breccia pipe is divided into six zones based on variations in fragmentation characteristics (fragmentation progressions and jigsaw fit textures) mixed fragment zones and fragment types.
- These facies variations are interpreted to reflect variations in intensity of host rock fragmentation, host rock expansion, rock type (rheology), and degree of fragment transport / mobility.
- Facies characteristics such as zones of mixed fragments that have increased sorting and reduced fragment size indicate fragment transport. Together with the presence of local fragment size grading and probable flow fabrics, these characteristics suggest the presence of a fluid phase during brecciation (Figure 5.9B).
- Much of the pipe consists of partially fragmented host rock (Figure 5.9B); variation in fragment types defines a pre-pipe host rock stratigraphy (Figure 5.9A). Zones of fragment transport are restricted to narrow discontinuous zones throughout the breccia pipe and a steeply dipping irregular zone at the northern end of the pipe (Figure 5.9B).
- The proportion of matrix in the breccia pipe is generally low and does not relate to the proportion of mixed fragments or fragment roundness. The facies characteristics suggest that high matrix zones occur in the zones of concentrated extension within the breccia pipe. Locally, these high matrix zones are well developed and imply marked host rock extension (horizontal and vertical) during pipe formation (Figure 5.9B). Likewise, the geometry of the whole pipe suggests extension of the host rock during breccia pipe formation (Figures 5.7 and 5.9B).
- Structural evidence (Chapter 3) suggests extensive pre- to syn-breccia pipe host rock fragmentation (Figure 5.9A). The facies characteristics and geometry of zone 1 suggest it formed during a period of fault induced host rock fragmentation. The minor irregular zones of more expanded breccia in zone 1 (second order fragmentation) possibly result from the dynamic fragmentation associated with breccia pipe formation.
- The distribution of zone 1 and the presence of only partially disconnected host rock throughout a large portion of the pipe (zone 2, Figure 5.9B) suggests that zone 1 was also initially present throughout a large portion of the pipe.

- The complex textural variations in zones 2 and 3 reflect the dynamic evolution of the breccia pipe (Figure 5.9B). In these zones jigsaw fit textures and mixed fragment zones dominate over fragmentation progressions as the degree of fragmentation, expansion and mixing increase.
- Zone 3 which is the most highly expanded and mixed portion of the host rock, is concentrated in the northern portion of the pipe and does not reflect the geometry of the whole pipe. This suggests that the processes which conferred to produce the whole breccia pipe were different to those that resulted in the formation of zone 3.
- Portions of the breccia pipe which are dominated by basement lithologies (zones 4A and 4B) have different characteristics to the bulk of the pipe (zones 1, 2 or 3). This variation in characteristics is dominantly due to rheological differences which dictate the style of host rock fragmentation in a given portion of the breccia pipe. The facies characteristics of zone 4A suggest that it generally results from host rock disaggregation (? extensional shear) and local mobility, rather than distributed extension as for other zones.

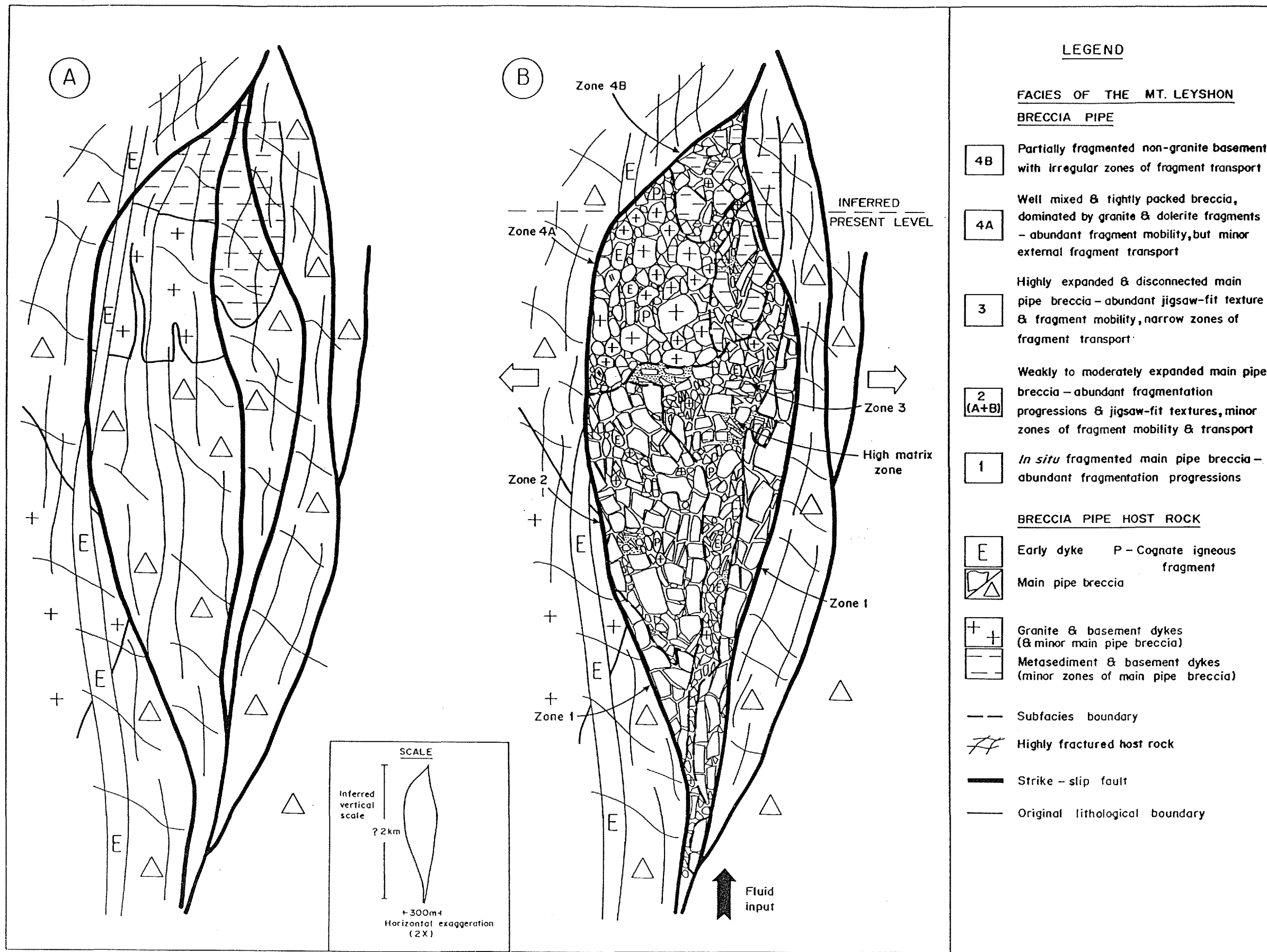


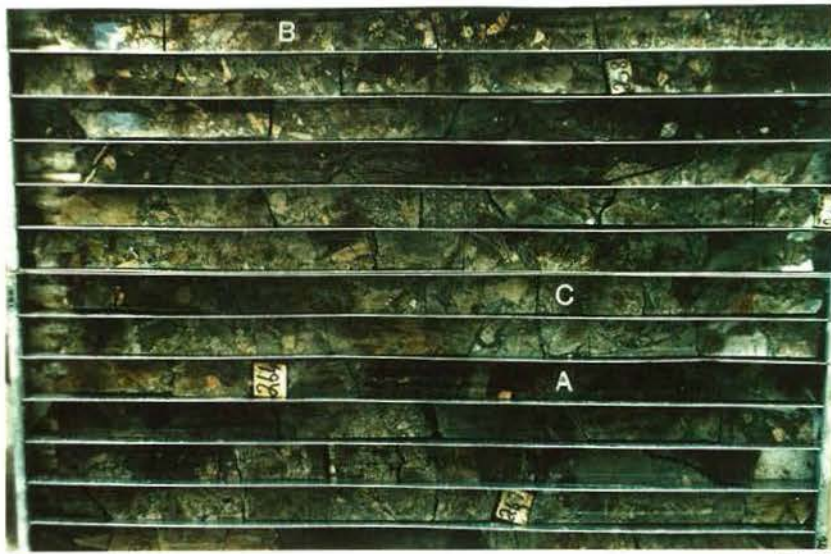
Figure 5.9: Facies model for the Mt. Leyshon breccia pipe depicted as a cross-section. (A) Pre-pipe host rock configuration. Note: (1) Brittle infrastructure and inferred strike slip fault architecture. (2) The regions of metasediment and granite within the main pipe breccia. (B) Mt. Leyshon breccia pipe. Note: (1) The crude preservation of the host rock configuration after pipe formation. (2) The effect of host rock type on breccia characteristics.



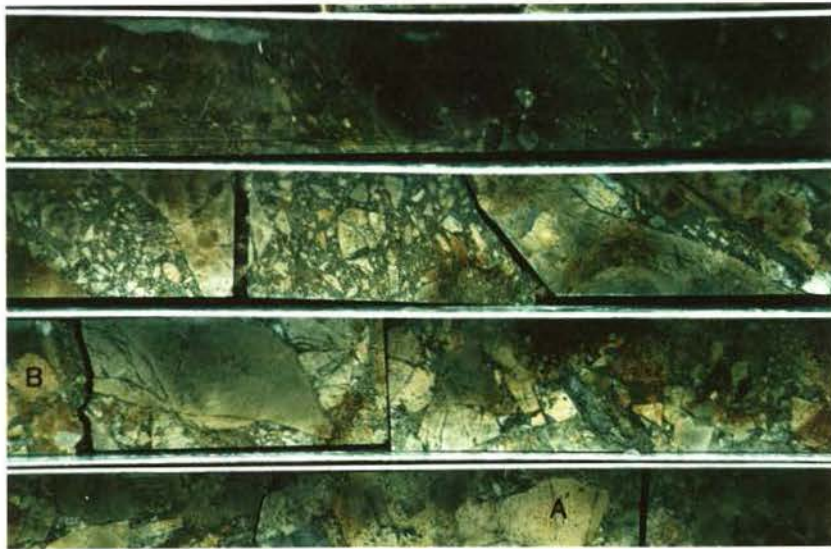
Plate 5.3: Zone 2B, Mt. Leyshon breccia. Note: (1) Blocks of main pipe breccia host rock (dark coloured, eg. A). (2) Partially fragmented main pipe breccia (B). (3) Poorly mixed regions dominated by main pipe breccia fragments but with minor early dyke and granite fragments (C). (4) High matrix zones which are shown in Plate 5.4 (centre of photo). (5) This breccia zone is more highly expanded than zones 1 or 2A. (MLD 203, 263 m.)

Plate 5.4: Zone 2B, Mt. Leyshon breccia (close-up of Plate 5.3). Note: (1) Expanded high matrix regions (centre) with splinter shaped and tabular fragments, supported by breccia matrix. The region at the LHS is more linear and the tabular detached fragments jigsaw fit together. (2) Polymict breccia (top), dominated by main pipe breccia with minor early dyke (A) and granite (B). (3) Fragmentation progressions in main pipe breccia (bottom). (MLD 203, 263 m.)

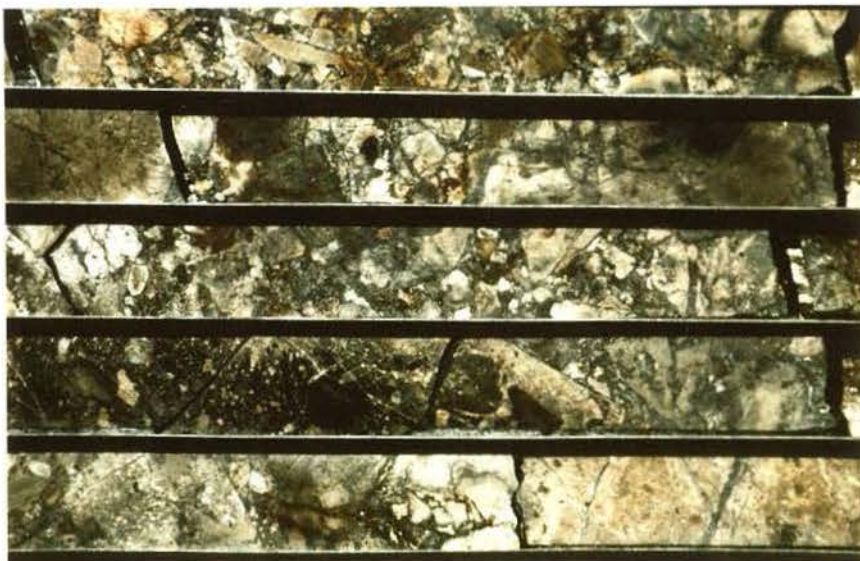
Plate 5.5: Zone 3, Mt. Leyshon breccia. Note: (1) The textural variability in this zone. (2) Partially fragmented main pipe breccia with quartz-molybdenite veins (bottom core run). (3) Intact block of main pipe breccia (black colouration). (4) well mixed breccia regions (centre and top core runs) mostly main pipe breccia and a few percent metasediment fragments. (MLD 80, 191.60 m.)



5.3



5.4



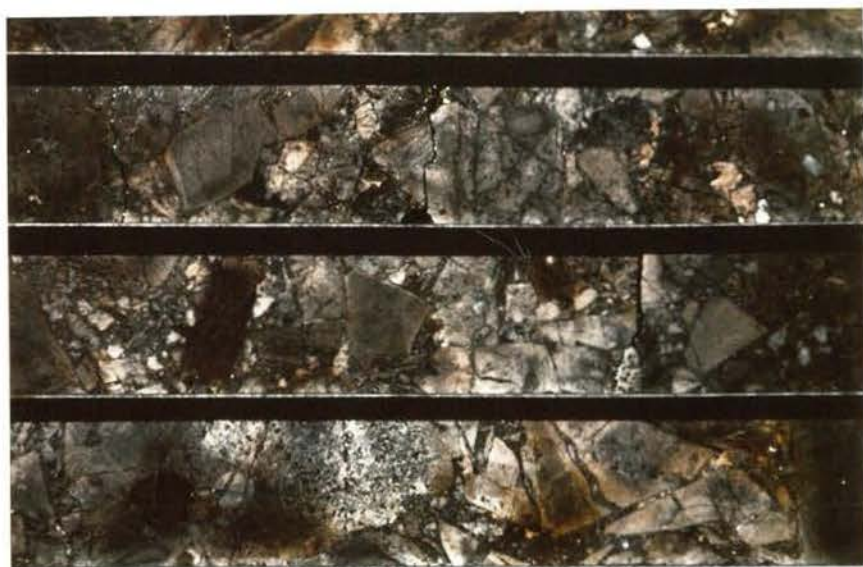
5.5



Plate 5.6: Zone 3, Mt. Leyshon breccia. Abundant jigsaw fit texture (eg. bottom) are present in a chaotic mass of partially fragmented main pipe breccia with limited fragment introduction. (MLD 80, 208.80 m.)

Plate 5.7: Zone 4A, Mt. Leyshon breccia. Well packed polymict breccia dominated by granite and dolerite fragments. Note the approximately 2 m thick intact main pipe breccia block (A) and zone of increased sorting and fragment size reduction (B). (MLD 155, 105.50 m.)

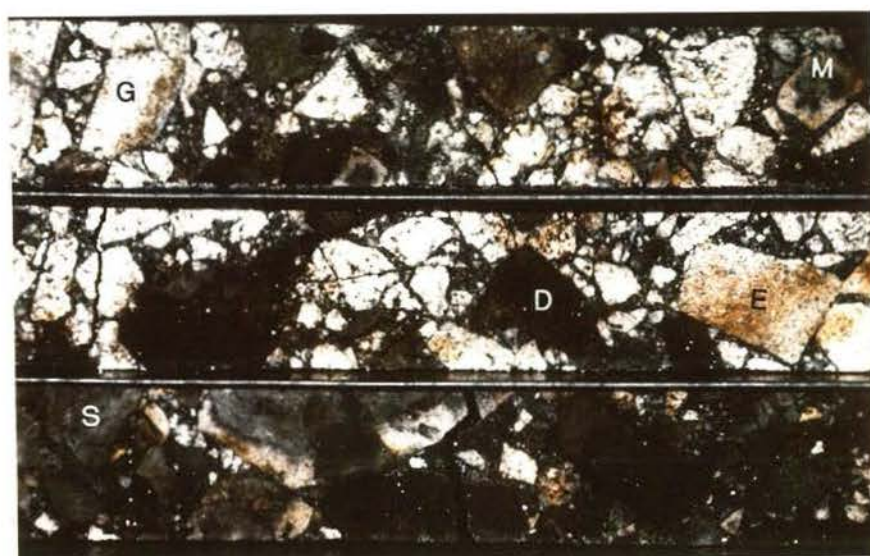
Plate 5.8: Zone 4A, Mt. Leyshon breccia. Breccia is dominated by granite and dolerite fragments, but also including metasediment (S), early dyke (E) and main pipe breccia (M) fragments. Note general absence of fragmentation progressions or jigsaw fit textures. Local intra-fragment break up results in limited jigsaw fit textures visible at Plate centre. (MLD 155, 99 m.)



5.6



5.7



5.8



Plate 5.9: Zone 4A, Mt. Leyshon breccia. Small scale dilational zone in dolerite dyke block. Mobilised "slurry" of disaggregated granite has been injected into this zone from block of granite (extreme RHS). Note: (1) The fine network of granite injected into the *in situ* fragmented dolerite. (2) That further post-breccia extension in this zone (at arrow) has resulted in open space infill of quartz and sphalerite. (MLD 149, 189 m; lines near top of core are due to water reflection.)

Plate 5.10: Contact between zone 4A and zone 3, Mt. Leyshon breccia. Upper zone 4A is dominantly composed of granite and dolerite fragments (A). Lower zone is transitional into zone 3 which consists of polymict breccia, including granite and dolerite fragments, and main pipe breccia blocks (dark colouration) Arrow marks the position of a gently dipping, discontinuous high matrix zone shown in Plate 5.11. Also note the large granite block in zone 4A (RHS) and the iron stained joint face (LHS) which highlights the granite rich nature of the upper zone. The face shown is approximately 7 metres high. (open pit, 375 RL, GR. 3880 5975.)

Plate 5.11: High matrix zone in transitional region between zones 4A and 3 (close-up of Plate 5.10), Mt. Leyshon breccia. Note the strong alignment of fragments and the expanded blocks of main pipe breccia (A; black colour). The arrows mark the contact between the high matrix zone and a main pipe breccia block.



5.9



5.10

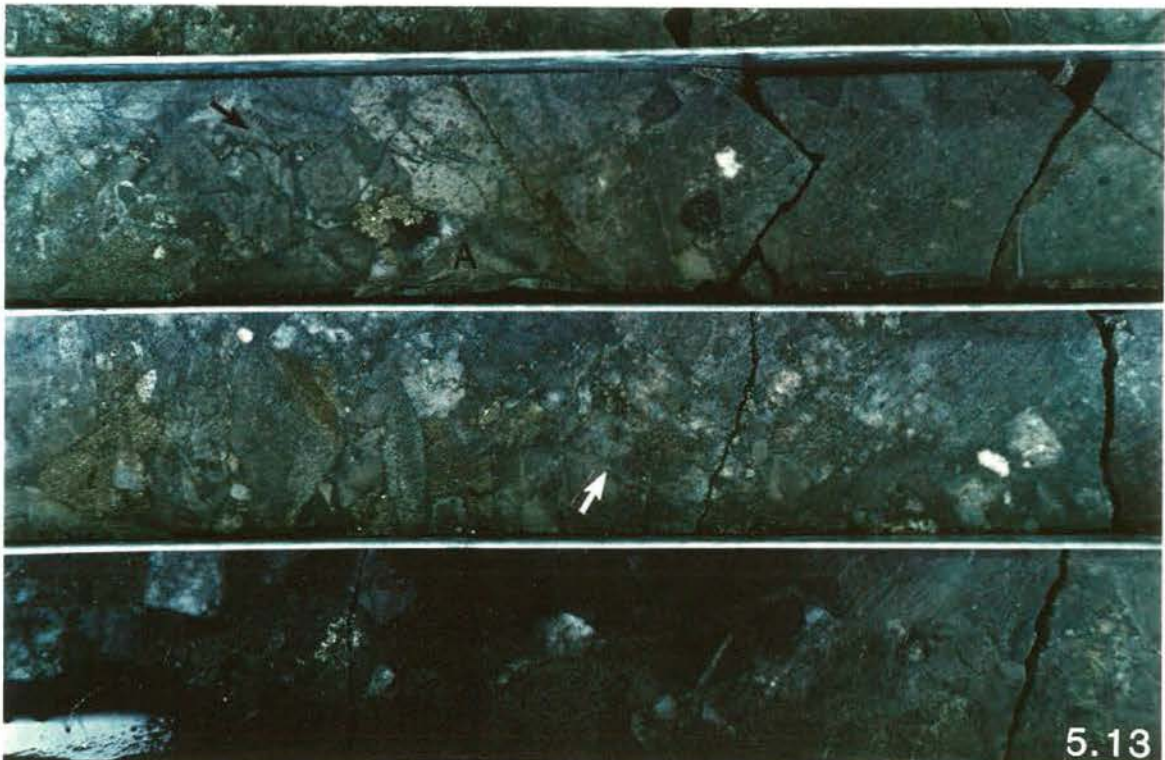
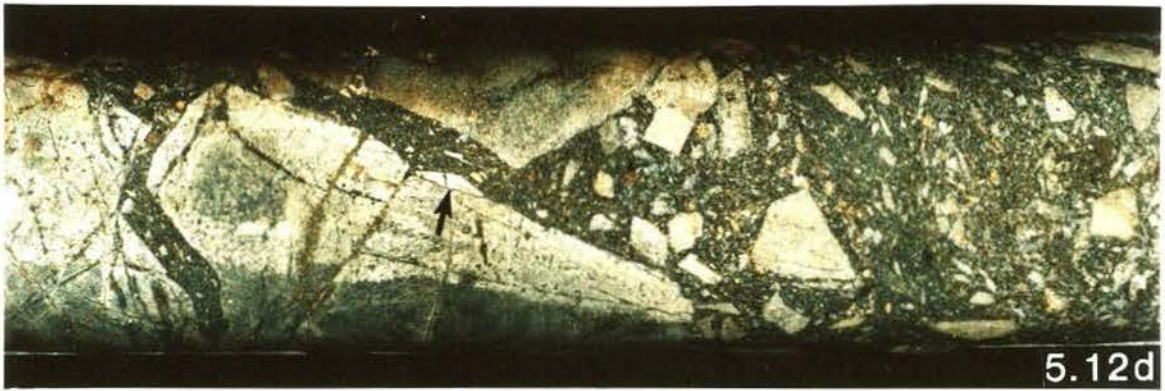
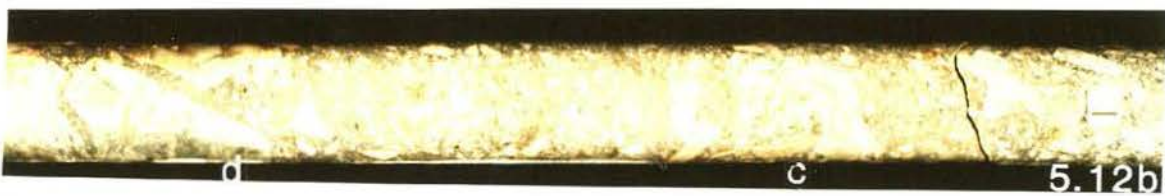


5.11



Plate 5.12: Well developed high matrix zone in drill core, Mt. Leyshon breccia. Lower case letters indicate the location of detail photos. (a) Whole zone passing gradationally from fragment supported well packed breccia (RHS) to high matrix zone with tabular fragments (LHS). (b) Back of core showing the high matrix zone in (a). Most fragments shown are main pipe breccia, which can be seen detaching from a larger block on the LHS. Note: (1) that the small splinter shaped fragments and matrix define a weak flow fabric, and (2) that the largest fragments have a geometry which suggests that they once fitted together and have since been highly expanded. (c) Detail of (b) centre, to show the cusped fragments with a near geometric fit. (d) Detail of (b) LHS, showing detaching main pipe breccia fragments, supported in a flow aligned fine matrix and small tabular fragments. Note that the expanded fragments show a close but not perfect geometric fit which suggests that some rock has been removed during the expansion process. Detachment of the splinter at the arrow would achieve this reduced fit. (MLD 82, 66 m.)

Plate 5.13: Fragmentation progressions in Mt. Leyshon breccia, Zone 2B. Note, (1) the main pipe breccia host rock with a black colour due to pre-Mt. Leyshon breccia biotite alteration, (2) the development of fragmentation progressions (at the arrows) that result in Mt. Leyshon breccia formation, and result in loss of the black colouration during post-breccia alteration, (3) the complete loss of biotite alteration from the main pipe breccia host at the RHS of the Plate, (4) the fragmentation progressions in the middle and upper core runs, which at a casual glance appear as a mixed fragment breccia, because of the compositional heterogeneity of the main pipe breccia, and (5) the breccia cavity (A), that formed during host rock expansion and has subsequently been infilled by quartz, chlorite-pyrite and then sphalerite. (MLD 277, 250 m.)



## Chapter 6

# PETROGRAPHIC AND GEOCHEMICAL CHARACTERISTICS OF THE MT. LEYSHON IGNEOUS ROCKS

---

### 6.1 INTRODUCTION

Extensive work has been undertaken on the petrogenesis of the basalt-andesite-dacite-rhyolite magmatic sequence developed in many unmineralised volcanic terrains and shallow level intrusive complexes. Although, there is considerable debate concerning the relative roles of partial melting, crystal-liquid fractionation of parental basalt, andesite or both, or magma mixing (Eichelberger, 1975).

In recent years, mounting evidence has indicated that mixing and assimilation are ubiquitous, and that few igneous rock suites are likely to reflect strictly closed system fractionation of single magma batches (e.g. O'Hara and Mathews, 1981; Hildreth et al, 1986). For example, the role of magma mixing in the formation of calc-alkaline rocks is particularly implied by the studies of magmatic mafic enclaves (e.g. Vernon, 1983; Bacon, 1986; Koyaguchi, 1986; Sparks and Marshall, 1986) and evidence from xenocrysts and dis-equilibrium phenocryst assemblages (Thompson et al., 1986; Rottura, et al., 1991; Zorpi et al., 1991). Considerable evidence exists for the generation of granitoid magmas by partial melting of the lower to middle crust due to basalt injection (Pitcher, 1987; Huppert and Sparks, 1988; Trial and Spera, 1990), with the resulting granitoids inheriting both a mantle and crustal derived component (Rottura et al., 1991). Nevertheless, the role of fractional crystallisation remains central in producing many of the observed chemical variations in rock series (Hildreth et al., 1986). A recent isotope and trace element study of a basalt to rhyolite sequence by Musselwhite et al. (1989) suggests that the generation of magmas with a SiO<sub>2</sub> content of greater than 60% is dominated by crystal fractionation with minimal assimilation of upper crustal rocks.

Few detailed studies have been made on the petrogenesis of igneous suites associated with porphyry copper ± gold deposits. In addition, no published studies of igneous petrogenesis associated with porphyry style mineralisation hosted in large scale intrusive breccia complexes are known to the author. Investigation of igneous petrogenesis in both of these styles of deposit is hampered by the hydrothermal alteration, which generally accompanies the mineralisation in these deposits, and post-emplacement recrystallisation. In some cases these processes strongly modify igneous rocks (e.g. Cas and Wright, 1987), thereby obscuring their original mineralogical and chemical characteristics, and consequently their petrogenesis.

In a study of intrusive igneous rocks associated with porphyry copper deposits from the Papua New Guinea-Solomon Islands region, Mason and McDonald (1978) recognised three igneous suites, principally on the basis of whole rock potassium content, a low K, normal K and high K calc-alkaline suite. These suites are partly correlated with tectonic setting, although the whole

range of igneous compositions occurs in a continental margin and island arc setting (Mason and McDonald, 1978). The compositional variability of the Papua New Guinea-Solomon Islands igneous suites is consistent (though not exclusively) with their derivation by variable partial melting and segregation of mafic crystalline material. Recently, Richards et al. (1990) developed a petrogenetic model for the Porgera intrusive complex which contains a series of small mafic, alkali stocks and is associated with a large epithermal gold deposit. They suggest that deep partial melting is responsible for the Porgera magmas which developed by limited fractional crystallisation (alkali basalt and gabbro through to mugearite) during rapid emplacement and cooling. Likewise, the alkaline lavas (alkali basalts to trachy-andesites) of Lihir Island which also hosts a large gold deposit are considered to be cogenetic and related by fractional crystallisation (Kennedy et al., 1990).

The petrology and chemistry of the igneous rocks in the Ray porphyry copper district (Arizona) were investigated by Cornwall (1982). In this area, hydrothermal alteration has been well focussed, into the host rocks surrounding the igneous centres allowing an investigation of their petrogenesis. At least 12 different intrusive rocks spanning a 10 Ma period and with compositions ranging through quartz diorite-granodiorite-quartz monzonite and rarely granite, show a strong correlation between a large number of major and trace elements, which suggests a comagmatic origin for the igneous units of the Ray district (Cornwall, 1982). However, Cornwall (1982) did not distinguish between common source partial melting and upper crustal batholithic differentiation as an origin for the Ray igneous rocks.

A number of recent papers, have dealt with the composition of igneous rocks associated with Cu-Au porphyry systems. For example, igneous rocks associated with porphyry copper deposits within cratons typically show alkali-calcic to calc-alkaline tendencies (Titley, 1990). Furthermore, the composition of rock suites associated with mineralisation in arc terrains tend to be more tholeiitic and show an alkaline character (Titley, 1990). Gold rich porphyry copper deposits of the circum-Pacific rim show similar compositional tendency (Sillitoe, 1990). However, beyond these broad generalisations, attempts to define the composition of magma types most closely associated with Au rich porphyry systems are conflicting (compare Sillitoe, 1990 and Jones and Thompson, 1991). In fact, as Jones and Thompson (1991) indicate there is a complete overlap in igneous composition between these petrologic associations with respect to Cu / Au ratios.

In Chapter 2, facies relations of the Mt. Leyshon igneous rocks are examined and the evidence for breccia generation during igneous emplacement is discussed. In this Chapter, petrographic and whole rock chemical data for the Mt. Leyshon igneous rocks are examined and used to assess igneous petrogenesis during magma / breccia interaction.

The aims of this Chapter are to:

- (1) Investigate the petrology of the Mt. Leyshon igneous rocks.
- (2) Undertake a preliminary geochemical study of the igneous rocks within the Mt. Leyshon breccia complex.

IGNEOUS UNIT	HANDSPECIMEN DESCRIPTION	XENOLITHS AND ENCLAVES	PHENOCRYST TYPES	PENOCRYST AND GROUNDMASS TEXTURES	NOTES
Unit I (Interm.)	Dark grey to black. Fine grained. Sparsely porphyritic, aphanitic groundmass.	<b>Xen.s</b> -All basement units. <b>Enc.s</b> -Trachytic, granophyric and seriate textured types.	<b>Total ph.s</b> ~2% <b>Plg.</b> ~- zoned -andesine to oligoclase <b>Amp. (R)</b> ~-	Generally isolated ph.s. upto 3mm in size, also in groups. Ph.s usually euhedral. Very fine grained, weakly trachytic textured gm. Many plg. microl.s in glass with abundant fine sub-hedral opq. minerals.	<b>Splinter textured</b> qtz. and alk. fld. <b>xenocrysts</b> occur in narrow xen. and enc. bearing zones. Alk. fld. have plg. reaction rims. Qtz ph.s and some plg. have 2 and 3 phase (high salinity) fluid inclusions
EP dyke (Interm.)	Pale pink to pale greenish grey. Moderately porph.	None observed.	<b>Total ph.s</b> ~10% <b>Fld. Plg&gt;alk</b> ~7% <b>?Amp. (S)</b> ~3% <b>Qtz.</b> ~<1%	Glmporph. fld.s (mostly plg.) in a seriate gm. of plg. microliths	Phenocryst and groundmass feldspar now mostly replaced by alk. fld.
Early dykes (Felsic)	Pale pink to greenish white (depending on degree of alteration), moderately porphyritic dyke.	None observed.	<b>Total ph.s</b> ~15% <b>Fld. alk&gt;plg</b> ~10% <b>Bio. (S)</b> ~4% <b>Qtz.</b> ~1% <b>Apatite, abund.</b>	Isolated and glmporph. ph.s. Quartz generally sub-hed. to rounded, rarely embayed. Some evidence of sub-grain development. Very fine grained micrographic gm. of qtz. and fld.	
Unit II (Felsic)	Has the appearance of a breccia. Contains > 70% angular to rounded fragments in a primary igneous matrix.	<b>Xen.s</b> - All basement units. <b>Enc.s</b> - Several texturally distinct igneous fragments, intermediate and felsic types.	<b>Total ph.s</b> - < 10% <b>Qtz.</b> ~- <b>Fld.</b> ~- <b>Bio.</b> ~-	Ph.s are generally < 0.8 mm (upto 2 mm), often broken and angular and show a strong flow alignment. Very fine grained micrographic gm.	In some samples narrow <b>clastic textured zones</b> occur, preserved within "swirls" in the igneous gm.
Unit III (Felsic)	Pale olive to pale orange, sparsely porph. unit with an aph. gm.	<b>Enc.</b> - (1) Small ?alk. fld. porphyritic type. Gm. is fine interlocking, sub-radial fld. laths and opaques. (2) Very small ophitic textured enc. with sub-radial plg., ?bio. and opaques set in qtz?.	<b>Total ph.s</b> ~2% <b>Fld. alk&gt;plg</b> ~- <b>Amp.(S)</b> ~- <b>Bio.(R)</b> ~- <b>Qtz. rare.</b>	Weakly glmporph. fld.s upto 1mm in size. Microph. qtz. granules upto 0.2 mm in size compose ~20% of the gm. Fine grained fld. laths and small opaques make up the remainder. Fine grained gm. shows weak trachytic texture and banding (grain size variation).	No zircon or apatite observed. One sample has a coarser g.m. with larger and more abund. qtz. granules and alk. fld. ph.s., suggesting it is more felsic than the other PP III samples.
Unit IV (Felsic)	Dark orange to whitish green unit (depending on the degree of alteration) with a crowded porph. texture and an aph. gm.	<b>Xen.</b> - All basement types. <b>Enc.</b> - Blocks and partially invaded zones of phase II.	<b>Total ph.s</b> ~35% <b>Qtz.</b> ~14% <b>Alk. fld.</b> ~15% <b>Plg.</b> ~6% (Oligoclase to albite) <b>Bio.</b> ~<1% <b>??Amp. (S)</b> ~- <b>??Pyr. (S)</b> ~-	Glmporph. alk. fld.s occur upto 4mm in size, optically enclosing plg. ph.s upto 0.4 mm in size. Most qtz ph.s are partially embayed. Many have sharp, splinter textures. Fine grained gm. with relic patches of intergranular qtz and fld. microl.s.	Two samples (FP230 and FF230) have a similar ratio of qtz. to fld. but only 20% total ph.s. with an incr. in mafic mins. (~2%) and a finer grained gm.
Sill (Interm.)	Porphyritic with an aphanitic gm., pale green in colour (due to alteration).	None seen.	<b>Total ph.s</b> ~5% <b>Fld.all plg.?</b> ~3% <b>Amp.</b> ~2% <b>Qtz.</b> ~<1% <b>??Pyr.(S)</b> ~-	Amp. clots (upto 5mm) have conc. of plg. microl. as an overgrowth text. Glmporph. plg. Qtz. ph.s are strongly embayed. Fine grained, flow aligned gm. of plg.+ amp. laths, set in qtz.	Upto 1% pyrite and abundant carbonate alteration.

Table 6.1: Petrography of the Mt. Leyshon igneous rocks (abbreviations on the second page).

IGNEOUS UNIT	HANDSPECIMEN DESCRIPTION	XENOLITHS AND ENCLAVES	PHENOCRYST TYPES	PENOCRYST AND GROUNDMASS TEXTURES	NOTES
2-2 dykes (Felsic)	Pale orange brown to pale orange grey dyke. Moderately porphyritic with an aphanitic. grm.	Enc.- Rare microgranitoid enclaves (<0.5 %; see below). Xen.- Medium grained fragments, now completely pseudo. by chlorite. Shape of pseudo. crystals suggests pyr. and olivine morphology.??	Total ph.s ~25% Fld.alk>plag ~17% Bio.(R) ~6% Qtz. ~2% Apat. abund. ~	Qtz. ph.s are often strongly and complexly embayed, otherwise rounded. Fld.s are glmporph. Grm. is very fine grained micrographic qtz and ?alk. fld.	
1-2 dykes (Felsic)	Dark orange brown to pale orange, fld. crowded dyke.	Enc.- Microgranitoid enclaves, becoming crowded in these south of Mt. Hope.	Total ph.s ~20-30% Fld.alk.>plg. ~15-22% ?Amp.(S) ~3-5% Bio.(S) ~1% Qtz. <1-1% Apat.abund. ~ ?Pyr.(S) -	Seriate to porphyritic texture. Glmporph. fld., bio. and ?amp. Amp. clots act as nuclei for plg. which forms overgrowths and partially replaces it. Fine grained grm. composed of amp., plg. and qtz. granules set in granophytic patches of qtz. and alk. fld.	Narrow dykes farthest from the main magmatic centre contain fewer phenocrysts than the thick central dyke body.
Micro-granitoid enclaves (Interm.)	Medium grained, sparsely porphyritic, pale pinkish brown in colour.	None seen.	Total ph.s ~? Approx. modal %: Plg.-50%, alk.fld.-30%, mafics-10% (amp.>bio.), qtz.-10%	Glmporph. of ??alk. fld. (upto 3.5mm, now sericite and carbonate). Amp. clots sub-ophitic to grm. plg. Bio. either clustered with amp. or isolated. Grm. of variolitic plg., alk. fld., and mafics set in an interstitial intergrowth of qtz. and alk.fld.	Texturally similar to 1/2 dykes which host these enclaves.
DG dykes (Interm.)	Dark green unit (due to chloritic alteration). Porphyritic with a turbid to aphanitic grm.	?Enc.-Coarser grained, basic enclaves.	Total ph.s ~6% fld. all plg.? ~4% Amp.(+bio.?) ~2% Qtz. <1%	Generally isolated ph.s. Rare strongly embayed qtz. ph.s. Fine grained grm., similar in texture to porphyry phase I.	Always moderately to highly altered. Rare alter. ph. whose shape suggests bio. Most mafic pseudo.s have a shape suggesting amph.
Sparse late dykes (Felsic)	Pale orange sparsely porphyritic dykes.	Xen.- Fine grained equigranular, and fld. rich basement rhyolite types.	Total ph.s ~15% Fld.alk.>plg. >10% Bio. <4% Qtz. <1%	Isolated and glmporph. crystals upto 2mm in size. Abund. bio. laths, mostly within grm. but occasionally overgrowing fld. Very fine grm. of micrographic qtz. and fld.	
Basalt dykes	Dark olive green sparsely porphyritic dyke.	None seen.	Total ph.s ~2% ?Olivine(S) ~2% Approx. modal %: ?olivine-2%, plg.-53%, hornb.-40% and Fe-oxide-5%.	Acicular crystals of hornb.(generally 0.6mm in length) show trachytic and spherulite textures. Plg. is interstitial to ?olivine and hornb. crystals. In plg. rich areas (either around ?olivine or independ.), plg. shows variolitic and spherulitic textures.	Post mineralisation and associated alteration. Ph.s pseudomorphed by chl. then carb. Most likely olivine but possibly orthopyroxene.

Notes: The igneous units are listed from oldest to youngest and include a petrographic description of the large microgranitoid enclaves found in 1-2 dykes and rarely 2-2 dykes. All igneous units contain accessory apatite, zircon and opaque minerals unless specified. All rocks have been effected by post-crystallisation changes (see text).  
Abbreviations: R-relic observed, S- inferred from shape of pseudomorph, plg.- plagioclase, alk.- alkali, fld.- feldspar, qtz.- quartz, amph.- amphibole, biot.- biotite, pyr.- pyroxene, opq.- opaque minerals, apat.- apatite, ph.- phenocryst, microl.- microlith, grm.- groundmass, glmporph.- glomeroporphyritic, xen.- xenolith, enc.- enclave, incr.- increase, decr.- decrease, euh.- euhedral, anh.- anhedral, abund.- abundant, alt.- alteration, pseudo.- pseudomorph, frag.- fragment.

Table 6.1: Petrography of the Mt. Leyshon igneous rocks (abbreviations on the second page).

- (3) Classify the Mt. Leyshon igneous rocks.
- (4) Compare the Mt. Leyshon and regional igneous units to identify the important igneous characteristics associated with large scale breccia formation in the Mt. Leyshon breccia complex.
- (5) Develop a petrogenetic model for the Mt. Leyshon and regional igneous units.

The work in this Chapter involved the following investigations of the Mt. Leyshon igneous rocks: (a) a petrographic study of thin sections ( $n = 40$ ), (b) the preparation of whole rock chemical data (36 new XRF analyses), and (c) electron micro-probe analyses of phenocryst and alteration minerals. Whole rock chemical analyses for the regional igneous units were provided by the Department of Resource Industries and the Bureau of Mineral Resources (I. Rienks, written communication).

## 6.2 THE MT. LEYSHON IGNEOUS ROCKS

### 6.2.1 Petrography of the Mt. Leyshon igneous rocks

The post-crystallisation changes to the Mt. Leyshon igneous units outlined in Chapter 4, strongly restrict petrographic observations on the original mineralogy of the igneous rocks. This is particularly true for both the composition and types of feldspar and mafic minerals present. Consequently, detailed modal counts of the phenocryst minerals present have not been made. Nevertheless, in all but the most intensely effected rocks the alteration is generally only weakly texturally destructive, allowing some observations to be made on original igneous petrography (Table 6.1). An approximate phenocryst mode for each Mt. Leyshon igneous unit has been estimated where possible, based on mineral counts for a number of different thin sections, carried out with the aid of standard grain estimation charts.

Many of the Mt. Leyshon igneous units contain small xenolithic fragments, although their small size and generally advanced state of alteration has prevented an investigation of their characteristics. Fragments found in the igneous units have been divided into 'accidental' types referred to here as xenoliths (basement and main pipe breccia), and those termed enclaves (after Vernon, 1983) whose igneous texture suggests that they are genetically related to the evolving magmatic system under investigation here (Chapter 2). The composition of relic igneous minerals and replacement mineral phases quoted in the text have been investigated by electron micro-probe (see Appendix 1).

#### 6.2.1.1 GENERAL PETROGRAPHIC FEATURES

The intrusive igneous rocks of the Mt. Leyshon breccia complex have a porphyritic texture with an aphanitic groundmass (Plate 2.16 and 2.20). Excluding the basalt dykes, which are thought to be unrelated to other units (see below), the Mt. Leyshon igneous units can be divided into two groups on the basis of their igneous petrography; an intermediate and a felsic group. The intermediate group is characterised by a fine grained flow aligned to trachytic textured groundmass (Plates 6.1 and 6.3) and a phenocryst assemblage of plagioclase, amphibole, minor quartz (?xenocrystic)  $\pm$  ?biotite  $\pm$  ??pyroxene. In contrast, felsic phases, other than porphyry unit III and 1-2 dykes (see

below), generally have a fine grained micrographic to micro-poikilitic textured groundmass (Plate 6.2) and are characterised by a phenocryst assemblage of alkali feldspar, plagioclase, biotite and quartz (Table 6.1). Quartz phenocrysts in DG dykes, the EP dyke and the "sill" are generally large and strongly embayed, whereas those in the felsic phases which are generally rounded to moderately embayed.

Accessory mineral phases in the Mt. Leyshon units consist of apatite, zircon and opaque minerals. In the Mt. Leyshon igneous rocks, apatite and zircon micro-phenocrysts often occur within or at the margins of biotite and less commonly amphibole phenocrysts. Apatite and zircon microphenocrysts are less common or absent in intermediate units. Opaque phases commonly occur in the intermediate unit groundmasses but are a minor component of felsic units and typically show partial to complete replacement / oxidation. Nevertheless, opaque minerals are well preserved in one sample each, of porphyry unit I and microgranitoid enclaves. Thin section investigation (grey, 3 distinct cleavage orientations, no bireflectance / pleochroism, no anisotropy) and semi-quantative microprobe analysis indicates the presence of magnetite in these samples. However, some opaque minerals in these samples showed textures suggesting the presence of exsolution lamellae (distinct birereflectance / pleochroism, moderate anisotropy) in the magnetite. No chemical difference was detected in a microprobe analysis of these regions, and they remain unexplained.

Data concerning specific igneous units and which have bearing on igneous petrogenesis are listed below:

#### Porphyry unit I

The bulk of porphyry unit I contains phenocrysts of biotite, amphibole, and plagioclase (oscillatory and normally zoned,  $An_{39-18} Ab_{59-77} Or_{2-5}$ ). Narrow zones occur within porphyry unit I containing phenocrysts, accidental xenoliths and several types of enclaves. The maximum size and distribution of these zones is unknown (zones up to 30 cm thick have been observed). In contrast, the fragment bearing zones contain quartz and alkali feldspar ( $An_{\leq 1} Ab_{37} Or_{63}$ ) crystals which are often "splinter" like suggesting they have been broken. Unbroken quartz faces are euhedral and clear suggesting that these crystals represent igneous quartz phenocrysts. K-feldspar crystals are partially embayed and show reaction rims of plagioclase ( $An_{16-18} Ab_{82-61} Or_{2-12}$ ) with inclusions (Plate 6.3).

#### Porphyry unit II

Porphyry unit II has a very fine grained igneous groundmass, unusually small phenocrysts (generally < 2mm in diameter) and generally > 70% fragments (see Chapter 2). Clastic textured zones are rarely preserved between the fragments within "swirls" in the dominantly igneous groundmass.

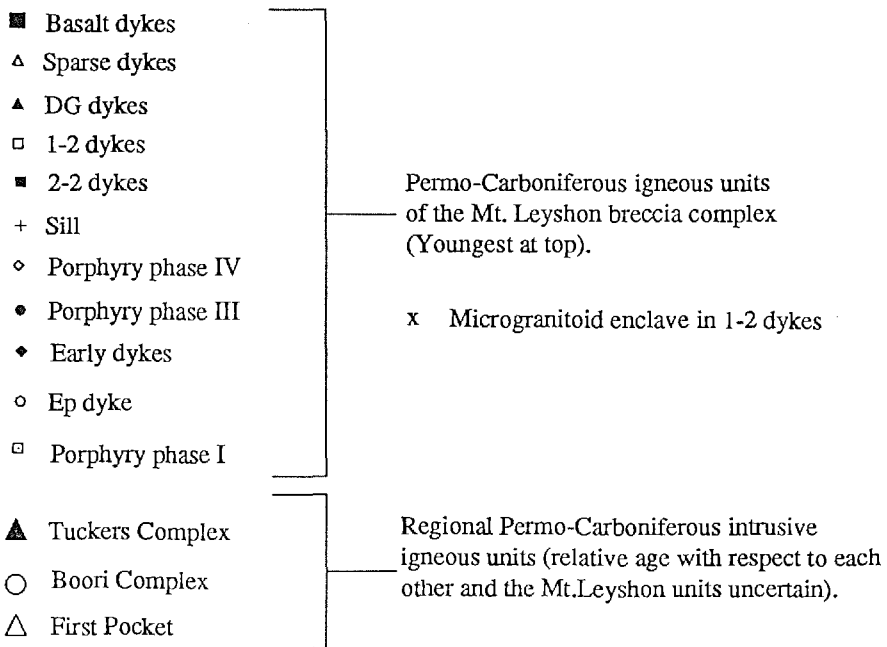
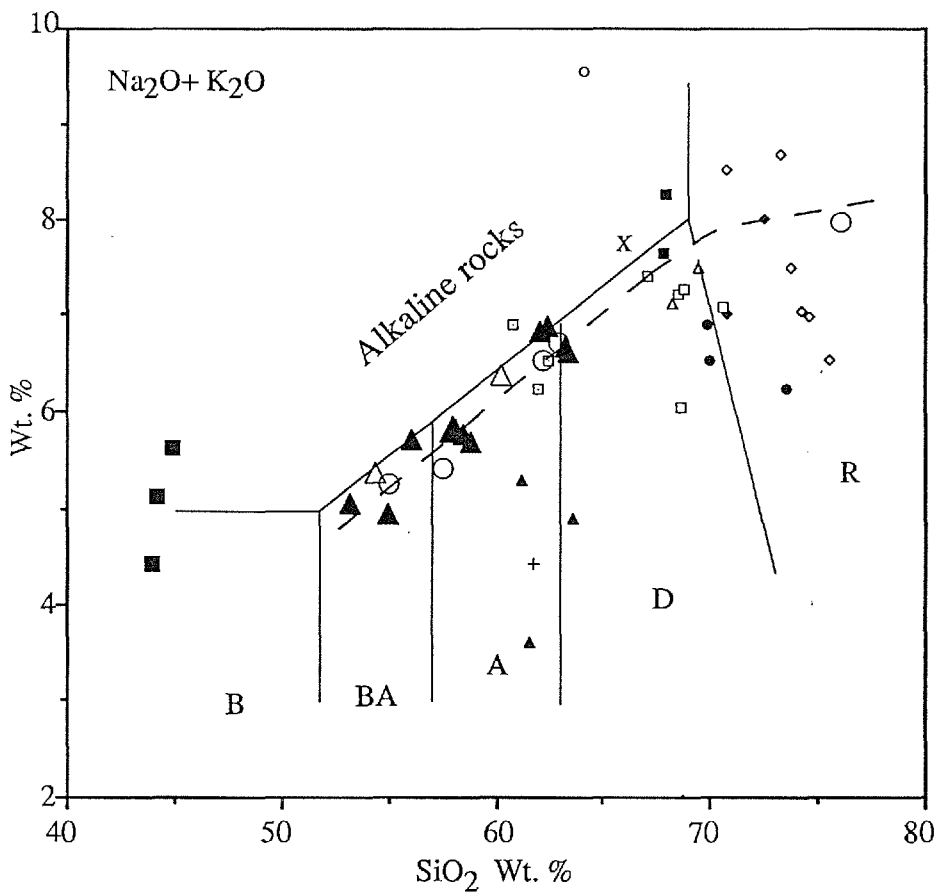


Figure 6.1: Total alkali vs silica diagram for the Mt. Leyshon and regional Permo-Carboniferous igneous rocks (regional data from D.R.I. and B.M.R.). Note the scatter of the Mt. Leyshon samples which is due to alteration, whereas the regional igneous units show a linear trend. The solid lines represent the calc-alkaline, basalt (B)-basaltic andesite (BA)-andesite (A)-dacite (D)-rhyolite (R) classification after Le Bas et al. (1986). The dashed line is the inferred evolution line of the Permo-Carboniferous sequence prior to alteration of the Mt. Leyshon igneous rocks.

### Porphyry unit III

The groundmass of porphyry unit III is composed of 20% microphenocryst quartz granules (~ 0.2 mm in size), in contrast to most other felsic igneous units which have a fine grained micrographic texture. The geochemical sample from the main body of porphyry unit III, has a groundmass texture which is coarser and has larger and more abundant quartz granules and K-feldspar phenocrysts than the other two geochemical samples which were collected from a smaller dyke like zone of porphyry unit III.

### Porphyry unit IV

Plagioclase phenocrysts are now mostly altered to albite (see Chapter 4) but contains relict oligoclase with a composition  $An_{23} Ab_{73} Or_4$ . Likewise K-feldspar megacrysts which have a composition of  $An_1 Ab_{28} Or_{71}$ , are altered to albite, although approximately 50% of the original K-feldspar megacrysts remain in the least altered samples (Plate 6.4).

Porphyry unit IV is characterised by the presence of numerous 'splinter' textured, angular quartz phenocrysts (Plate 6.4), which are generally absent from other igneous units. Diffuse edges to some of the quartz margins suggests that some of this phenocryst angularity is due to magmatic resorption. However, the quartz typically has sharp edges which implies the phenocrysts have been broken. Furthermore, these angular phenocrysts generally have a uniform distribution, although gradational zones containing only 20%, rather than 35% total phenocrysts have been observed in the Mt. Leyshon open pit. Additionally, one 10 cm thick zone in a drill hole within porphyry unit IV on Mt. Hope, contains approximately 50% quartz phenocrysts.

Two drill core samples (FP230 and F230; Appendix 2) collected for the whole rock geochemistry, came from a dyke through a zone consisting of several cross-cutting igneous and breccia units (GR 4050 5400; Figure 2.3b, Enclosure 1). This dyke-like body has a similar texture to the bulk of porphyry unit IV (Table 6.1), although the dyke has fewer phenocrysts and a higher proportion of mafic minerals.

### 1-2 dykes

The 1-2 dykes have a seriate to porphyritic texture and contain chlorite pseudomorphs probably after hornblende phenocrysts, and granophyric intergrowths of alkali feldspar and quartz (Table 6.1; Plates 6.5). In contrast, other felsic units probably do not contain hornblende and have a fine grained groundmass (Plate 6.2). Narrow 1-2 dykes distal to the main magmatic centre have fewer phenocrysts than the thicker 1-2 dyke body within the main magmatic centre (Figure 2.3a, Enclosure 1). In addition, the 1-2 dykes (and less commonly 2-2 dykes) contain microgranitoid enclaves texturally similar to 1-2 dykes (Table 6.1), although the enclaves are more basic, have fewer phenocrysts and are medium grained. Furthermore, the enclaves contain abundant fine needles of apatite (Plate 6.6) and have both chilled and unchilled margins which are smooth or irregular.

### Basalt dykes

Basalt dykes have a radiate and spherulitic textured groundmass composed of amphibole and plagioclase crystals, with abundant opaque minerals (Plate 6.7). The basalt dykes contain large phenocrysts (now pseudomorphed by chlorite and carbonate) whose shape suggests they are olivine or possibly pyroxene (Table 6.1).

#### 6.2.1.2 PARAGENESIS OF THE PHENOCRYST MINERALS

The interpretation of mineral paragenesis in igneous rocks is problematic for a number of reasons which include the crystallisation of a mineral phase due to the local depletion of elements forming early minerals in the magma (Cornwall, 1982). Despite these problems, the following general comments are made on phenocryst paragenesis in the Mt. Leyshon igneous rocks.

The Mt. Leyshon intermediate units rarely contain chlorite pseudomorphs which have a shape that suggests they were originally pyroxene. Plagioclase is an early mineral phase and most mafic mineral pseudomorphs and phenocryst relics (Appendix 1) are probably after amphibole. Biotite relicts are generally absent in intermediate units. Apatite and zircon crystals in intermediate units are rarely found intergrown with amphibole phenocrysts but they generally form microphenocrysts with groundmass plagioclase, K-feldspar and opaque minerals. The features of the large quartz phenocrysts in the intermediate units suggest that they did not crystallise as an early mineral phase and their origin is discussed in section 6.7.1.

In the felsic units, plagioclase is poikilitically enclosed by K-feldspar phenocrysts indicating early plagioclase crystallisation and also occurs as free crystals. Biotite commonly occurs as isolated phenocrysts but is rarely poikilitically enclosed by large K-feldspar phenocrysts or overgrown by quartz. Zircon and apatite micro-phenocrysts rarely occur as clusters in or at the margins of biotite phenocrysts but generally form isolated grains together with opaque minerals in the groundmass of felsic units.

These observations suggest that amphibole and plagioclase crystallised early in intermediate units. Quartz and K-feldspar crystallised early in felsic units relative to the opaque minerals. Zircon and apatite formed at early and later stages of crystallisation relative to the mafic minerals.

### 6.2.2 Chemical effects of the post-crystallisation changes

The post-crystallisation modification of the Mt. Leyshon igneous rocks (Chapter 4), suggests that the whole rock geochemistry of these units has been effected. In this section the chemical effects of these post-crystallisation changes are assessed to determine which elements have remained immobile during alteration and recrystallisation.

The whole rock geochemistry of shallow level intrusive and extrusive rocks are effected by some or all of the following post-crystallisation processes (Ewart, 1971; Turner, 1982; Cas and Wright 1987):

(1) Early recrystallisation (termed devitrification in extrusive igneous rocks).

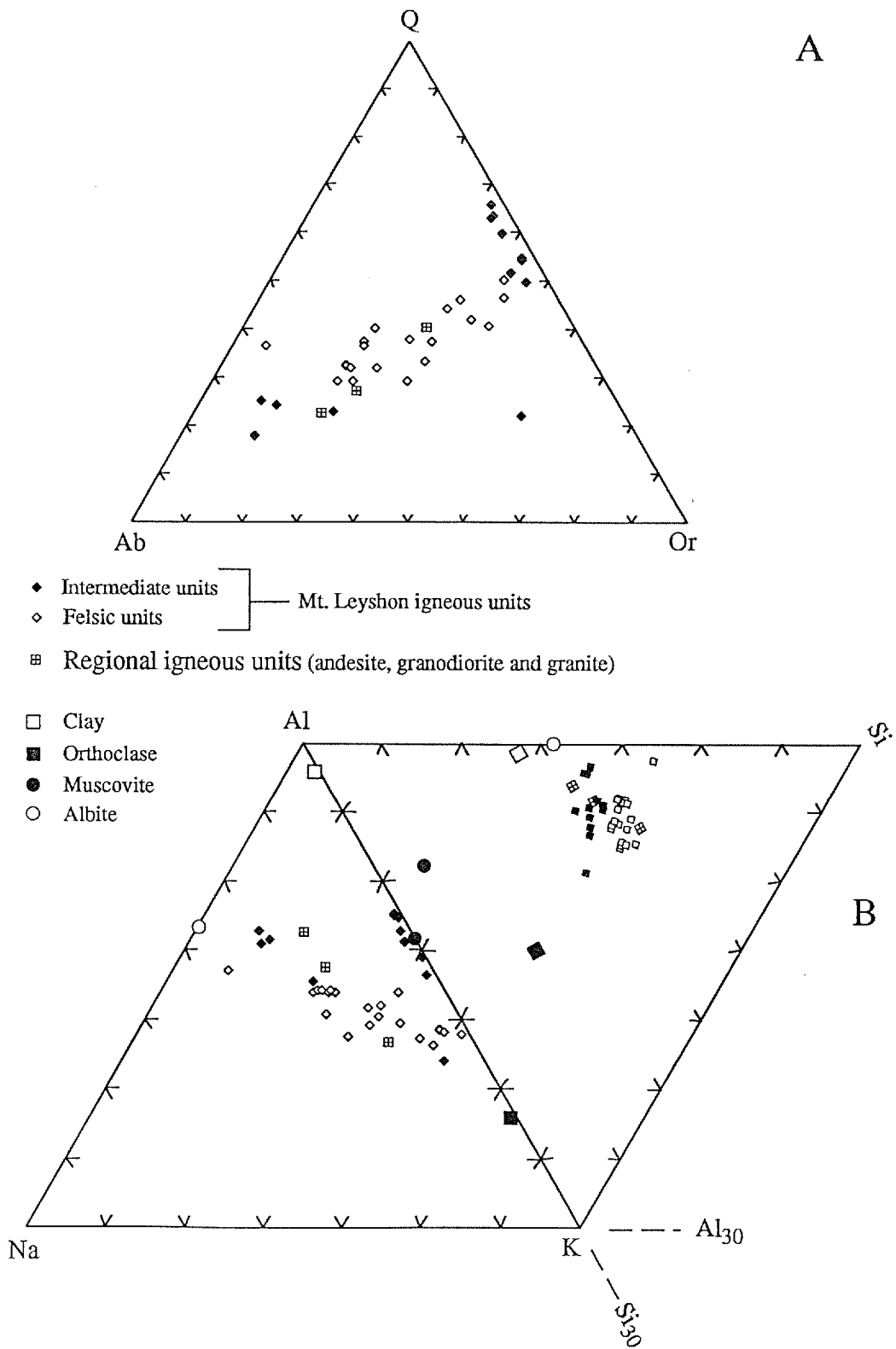


Figure 6.2: Alteration effects on the chemistry of the Mt. Leyshon igneous rocks.

(A) Q-Ab-Or ternary plot of the CIPW norm data (Appendix 3).

(B) Atomic % Al-Na-K and Si-Al-K triplots (Appendix 4).

Three unaltered regional samples highlight the chemical changes effecting the Mt. Leyshon units. Note that in (B): both the Al and Si ranges are from 30 - 100 atomic %, Na and K ranges are from 0 - 100 atomic %; Mineral points represent microprobe analyses of alteration minerals in the Mt. Leyshon igneous rocks (see Appendix 1). In (A) all ranges are from 0 - 100 %.

- (2) Hydration.
- (3) Vapour-phase crystallisation.
- (4) Late-stage recrystallisation (devitrification).
- (5) Hydrothermal alteration.

Other workers investigating the effect of recrystallisation and hydration on igneous whole rock chemistry have concentrated on lavas, glassy pyroclastic rocks or their analogues rather than intrusive igneous rocks (e.g. Noble, 1967; Lipman et al., 1969; Lofgren, 1970; Scot, 1971 and Ewart, 1971). This work may not be directly applicable to chemical changes occurring in igneous rocks in the subvolcanic environment because of the difference in parameters such as pressure, cooling rate and element solubility. Nevertheless, observations on the chemical effects associated with the post-crystallisation processes outlined above probably have general application to subvolcanic intrusive rocks which have undergone similar recrystallisation.

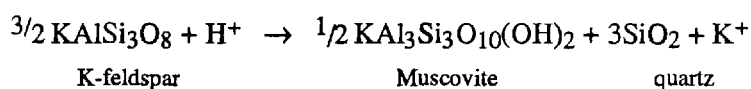
In the Mt. Leyshon igneous rocks evidence for post-crystallisation processes is generally present as a change from a glassy to a micrographic or micropoikilitic textured groundmass, overprinted by hydrothermal minerals (see Chapter 4). Furthermore, the intensity of this recrystallisation in the Mt. Leyshon igneous units is proportional to the degree of hydrothermal alteration, suggesting that it is a late feature which developed immediately before / accompanied the hydrothermal alteration. These minor textural changes to the Mt. Leyshon igneous rocks are in contrast to more extreme cases of late stage recrystallisation in other areas (resulting in large scale spherulite development; e.g. Ernst and Hall, 1975).

Experimental work with rhyolite glass (Marshall, 1961; Lofgren, 1970; Lofgren, 1971a) and textural studies of natural lavas (eg. Ewart, 1971) suggests that micrographic or micropoikilitic textures, similar to those in the Mt. Leyshon units (section 4.2.4.1), result from very slow and intermediate recrystallisation rates respectively. The whole rock chemical effects due to recrystallisation / hydration are dependent on the rate of these processes (controlled by temperature, pressure and fluid composition; Lofgren, 1970; Turner, 1982). Chemical changes during recrystallisation and hydration of rhyolite glass and silicic volcanics involve alkali exchange, oxidation of iron, halogen loss and increase in  $H_2O^+$  (Lipman, 1965; Simons, 1962 and Lofgren, 1971b). Several igneous samples (eg. P231, LDG200; Appendix 2) have been omitted from the geochemical study in this Chapter because they are strongly recrystallised, and as a consequence are likely to have undergone significant chemical changes. Only minor chemical changes involving alkali mobility, halogen loss and the oxidation of iron are expected to have resulted from the recrystallisation and hydration of the remaining Mt. Leyshon igneous rocks.

Extensive chemical changes commonly effect igneous rocks during hydrothermal alteration (e.g. Barrett and MacLean, 1991). The combined effects of the late recrystallisation and hydrothermal alteration on the alkali content of the Mt. Leyshon igneous rocks can be seen in Figure 6.1. The Mt. Leyshon samples show a strong scatter, whereas the regional igneous units, which are also plotted on this graph, maintain a tight curve. Because Clarke (1971) describes fresh mafic minerals

in the regional igneous rocks and other major element variation plots show a strong correlation (section 6.4.1) this suggests that the scatter is due to alteration. If this is true, the regional igneous units plotted on Figure 6.1 highlight the effect of post-crystallisation processes on the Mt. Leyshon igneous rocks. According to this total alkalis plot, most Mt. Leyshon igneous samples have undergone a decrease in total alkalis which indicates Na and K mobility, consistent with the described post-crystallisation (Chapter 4).

The effects of the post-crystallisation processes on the whole rock data have been further investigated by the generation of CIPW norm data and atomic % data for the Mt. Leyshon samples (Appendices 3 and 4 respectively). A normative plot of Ab-Or-Q for the Mt. Leyshon units is shown in Figure 6.2A, on which the position of normative andesite, granodiorite and granite of the regional suite are also plotted. The atomic % proportions of Al, Si, Na and K of the Mt. Leyshon igneous samples together with alteration minerals from these samples are shown in Figure 6.2B. The Mt. Leyshon samples form a linear trend on Figure 6.2A which is similar to the trend of the regional samples, although a number of felsic and most of the intermediate samples are displaced towards the Q-Or tie line. The displaced intermediate samples also show an increase in normative quartz and atomic % Al but not atomic % Si (Figure 6.2A and 6.2B). Three other intermediate samples and one felsic sample plotted on Figure 6.2A and 6.2B indicate albite introduction during alteration. These observations are in agreement with the textural evidence for the replacement of K-feldspar by albite and illite, and the further breakdown of feldspar to produce muscovite in the Mt. Leyshon igneous rocks (see Chapter 4) by a reaction such as (Burt and Rose, 1979):

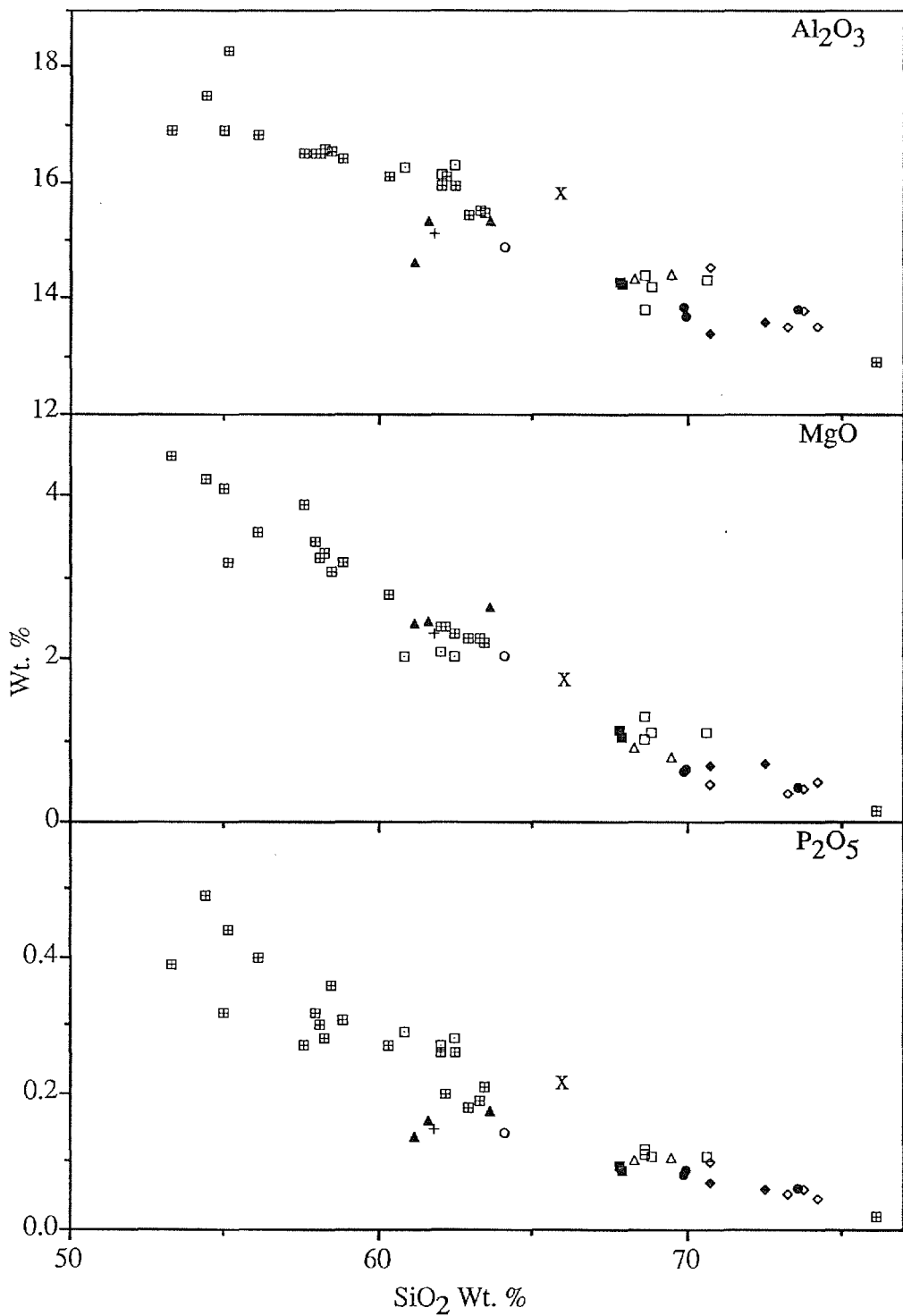


The most strongly altered Mt. Leyshon samples show an increase in normative quartz (Figure 6.2A) consistent with the observed sericite and chlorite formation, although SiO<sub>2</sub> appears to be generally immobile in the moderately altered samples (Figure 6.2B). Sample number EP166 is distinctive on Figure 6.2A (bottom right data point) and indicates a whole rock increase in normative orthoclase, consistent with textural evidence for K-feldspar alteration in this sample (Chapter 4), suggesting that K-feldspar was not a significant alteration phase in other samples. With the exception of the Mt. Leyshon samples already mentioned, the remaining samples indicate minor hydrothermal effects which are not distinct on Figure 6.2.

The trends shown by the Mt. Leyshon igneous units on these ternary plots (Figure 6.2) are consistent with their petrography, both of which suggest the following sequence of events:

- (1) An initial andesite to rhyolite igneous sequence.
- (2) Albitisation of plagioclase and K-feldspar resulting in minor potassium (Or) loss (and major calcium loss, see Figure 6.3b).
- (3) Potassium increase associated with the sericite alteration.

The following Mt. Leyshon igneous samples (based on Figure 6.2 and petrographic examination) are considered to be the most altered and indicate significant SiO<sub>2</sub> mobility, in contrast to the



- |  |                      |  |
|--|----------------------|--|
| △ Sparse dykes   | ◇ Porphyry phase IV  | Mt. Leyshon igneous units (oldest bottom right). |
| ▲ DG dykes   | ● Porphyry phase III |  |
| □ 1-2 dykes  | ◆ Early dykes        |  |
| ■ 2-2 dykes  | ○ Ep dyke            |  |
| + Sill   | ▣ Porphyry phase I   |  |
| x Microgranitoid enclave in 1-2 dykes                                |                      |  |
| ⊞ Regional igneous units (Tuckers, Boori and First Pocket complexes) |                      |  |

Figure 6.3a: Selected major element variation diagrams comparing the Mt. Leyshon and regional igneous units.

moderately altered samples, and are therefore excluded from the assessment of igneous petrogenesis in this Chapter: LD200, LD219, LDG200, DG173, P231 and TP201 (Appendix 2).

Harker diagrams of silica against elements other than Na, K, Ca (see Figure 6.3) show tightly constrained data trends. Furthermore, the trends on the Harker diagrams are not those generally shown by alteration effects on a series of igneous rocks (which would pass through the origin at a high angle to the observed trends; MacLean, 1990), suggesting the other elements have been largely immobile during the hydrothermal alteration described above. DG dykes, however, show high values of  $\text{Fe}_2\text{O}_3$  and MgO on plots against  $\text{SiO}_2$  (Figure 6.3a), although other samples on these plots maintain a tight curve. This increase in  $\text{Fe}_2\text{O}_3$  and MgO for the DG dykes is consistent with the textural evidence which shows strong chlorite and sericite alteration of these dykes (see Chapter 4), and the work of Barrett and MacLean (1991) which indicates whole rock introduction of FeO and MgO during such alteration. The manganosiderite alteration in the DG dykes also causes a marked elevation in their MnO value (Appendix 2) in contrast to other units whose MnO values are strongly correlated with  $\text{SiO}_2$ . Finally, because a sulphate mineral (gypsum  $\pm$  barytes) is present in some samples, which is not detected by XRF analysis, their geochemical total is upto 1% low.

In conclusion, with the exception of Na, K, Ca and by chemical association Sr and Rb (together with  $\text{Fe}_2\text{O}_3$ , MgO and MnO for the DG dykes only) which appear to have been mobile during the post-crystallisation changes noted above, the remaining geochemical data discussed in the following section probably reflects primary magmatic processes.

### 6.3 THE REGIONAL IGNEOUS UNITS

Permo-Carboniferous igneous rocks of North Queensland can be divided into two groups: (1) an older Carboniferous group with Rb-Sr age dates of 311 Ma (Webb, unpublished report, 1988), and (2) a younger earliest Permian group with K-Ar biotite ages of 280 Ma (Webb, 1969). Dating of the Mt. Leyshon igneous rocks suggest that they were emplaced at around 280 Ma (section 3.6.2). Consequently, the Mt. Leyshon igneous units may be comagmatic with the second group of Permo-Carboniferous igneous units, which are referred to hereafter as the regional igneous units. This possibility is tested in section 6.4.

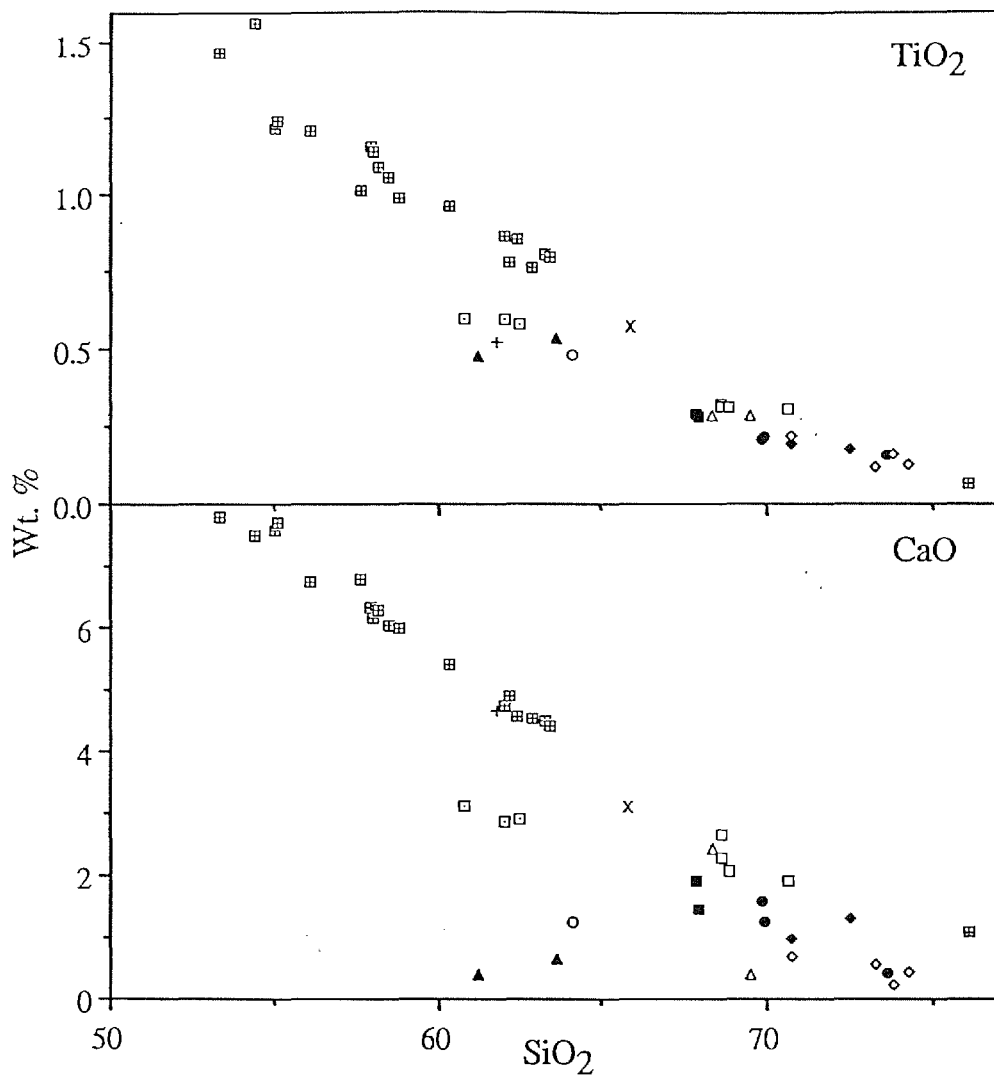
#### 6.3.1 Field and petrographic relationships of the regional igneous units

Regional igneous units considered to have a similar age to those at Mt. Leyshon occur in three complexes, namely Tuckers, Boori and First Pocket Hut (Clarke, 1971; I. Rienks, pers. comm.; Figure 1.1). The igneous units of these complexes are mostly composed of diorite and granodiorite with minor adamellite (monzogranite), tonalite and granite (Clarke, 1971; see Appendix 5). In addition, Clarke (1971) reports gabbro, diorite and mangerite (monzodiorite) at the northern end of the Tuckers complex, which have both sharp and gradational contacts with a granodiorite-tonalite unit.

Regional igneous units are usually fine to medium grained with an equigranular texture, although some are porphyritic (Rienks, pers. comm.), and they commonly contain plagioclase (generally andesine), K-feldspar, quartz, hornblende, biotite  $\pm$  clinopyroxene and between 1-3 % magnetite (6.5% in the gabbro; Clarke, 1971). Apatite and zircon are rare in the Tuckers and Boori igneous complexes (in contrast to the Mt. Leyshon units), although they occur as accessory phases in three units within these complexes (Clarke, 1971), which suggests only minor apatite and zircon fractionation during crystallisation of the regional igneous units.

Adamellite (monzogranite) portions of units which are dominantly granodiorite from the Tuckers and Boori complexes are reported by Clarke (1971) as having interstitial micrographic intergrowths of quartz and alkali feldspar; these are similar to those reported in the 1-2 dykes and their microgranitoid enclaves at Mt. Leyshon. Clarke (1971) further reports vertical variations in modal mineralogy in the Tuckers complex. For example, the proportion of clinopyroxene decreases upwards and is replaced by hornblende, which suggests progressive differentiation of the intrusion from the base upwards (Clarke, 1971).

One granodiorite-tonalite unit of the Tuckers igneous complex and a small isolated stock (Rochford stock) both mapped by Clarke (1971) as one unit, contain abundant fine grained xenoliths (Clarke, 1971). The xenoliths are described by Clarke (1971) as being generally ovoid with an average diameter of 10 centimetres, and the one dioritic xenolith sample sectioned by him has a flow lineated porphyritic texture and contains K-feldspar poikiloblasts. Furthermore, these xenoliths tend to occur in clusters and are rarely densely packed. The features of these xenoliths in the Tuckers igneous complex are similar to the xenoliths described for the Mt. Leyshon igneous rocks.



- |   |  |   |                    |  |
|---|--|---|--------------------|--|
| △ | Sparse dykes   | ◇ | Porphyry phase IV  | Mt. Leyshon igneous units (oldest bottom right). |
| ▲ | DG dykes   | ● | Porphyry phase III |  |
| □ | 1-2 dykes  | ◆ | Early dykes        |  |
| ■ | 2-2 dykes  | ○ | Ep dyke            |  |
| + | Sill   | ▣ | Porphyry phase I   |  |
| x | Microgranitoid enclave in 1-2 dyke                                 |   |                    |  |
| ⊞ | Regional igneous units (Tuckers, Boori and First Pocket complexes) |   |                    |  |

Figure 6.3b: Selected major element variation diagrams comparing the Mt. Leyshon and regional igneous units.

Field relationships of the regional igneous units, such as the shearing and fracturing of the country rock adjacent to the intrusions, and the subsequent shearing of the intrusion margins (Clarke, 1971), suggest emplacement during active fault movement, in a similar manner to that proposed for the Mt. Leyshon igneous rocks (see Chapter 3). Moreover, a number of small breccia bodies are reported by Clarke (1971) at the margins of the first igneous unit (leucogranite) emplaced into the Boori complex and at the western end of the Tuckers range. Thus, the regional igneous rocks have several similar field and petrographic features to the Mt. Leyshon igneous units.

## 6.4 CHEMICAL ANALYSES

In this section of the Chapter, whole rock chemical analyses of the Mt. Leyshon igneous rocks are presented and compared to the regional igneous units. One analysis of the micro-granitoid enclaves commonly found in the 1-2 dykes is also plotted. Basalt dykes have been omitted from the chemical plots (other than on Figure 6.7) in this section for reasons discussed below, which imply that they are not co-magmatic with other Mt. Leyshon igneous units. The methodology and sample collection approach employed in this study are outlined in Appendix 6.

### 6.4.1 Major elements

Harker variation plots for the Mt. Leyshon and regional igneous units (Figure 6.3a and 6.3b) for  $\text{TiO}_2$ ,  $\text{Al}_2\text{O}_3$ ,  $\text{Fe}_2\text{O}_3$ ,  $\text{MgO}$  and  $\text{P}_2\text{O}_5$  show regular linear or curved trends from the intermediate through to the felsic units. A minor compositional gap exists, however, between the more basic and more felsic units. This compositional gap defines two groups corresponding to the petrographic sub-division made in section 6.2.1. These are, an intermediate group with a  $\text{SiO}_2$  content of 60-64 wt.% and a felsic group with a  $\text{SiO}_2$  content of 68-74 wt.%. The microgranitoid enclave analysis is notable in having a whole rock  $\text{SiO}_2$  content between the felsic and intermediate groups.

Porphyry unit I plots off the data trends for  $\text{Al}_2\text{O}_3$ ,  $\text{P}_2\text{O}_5$ , and  $\text{MnO}$  (see Appendix 2), which suggests that this unit is chemically different to other Mt. Leyshon units. The data scatter on the plots of  $\text{Na}_2\text{O}$ ,  $\text{K}_2\text{O}$  (Figure 6.1) and  $\text{CaO}$  (Figure 6.3b; as well as the  $\text{Fe}_2\text{O}_3$  values for DG dykes) as a result of recrystallisation and hydrothermal alteration, have already been discussed (section 6.2.2). The large compositional difference between one highly evolved unit of the Boori complex ( $\text{SiO}_2 = 76$  wt. %) and the other regional igneous units is also noteworthy.

### 6.4.2 Trace elements

The strong positive correlation between Nb and  $\text{SiO}_2$  for igneous samples from regional centres and the Mt. Leyshon complex, indicates a systematic enrichment in Nb with increasing  $\text{SiO}_2$  during Permo-Carboniferous magmatic evolution (Figure 6.6). Plots of  $\text{SiO}_2$  versus Y and Zr (Figure 6.4) for the Mt. Leyshon and regional igneous units form two separate groups, each with distinct trends, although the Zr versus  $\text{SiO}_2$  variation trend diverge from a common origin. In addition, the Mt. Leyshon suite shows an inflection in the Zr versus  $\text{SiO}_2$  variation trend ( $\text{SiO}_2 = 67$  wt. %; in contrast to the regional samples). Porphyry unit I has higher Y values than other igneous units of a similar  $\text{SiO}_2$  content, but is not distinctly different on Nb or Zr plots.

On first inspection, a plot of Zr against SiO<sub>2</sub> appears to show scattered data points, however, the samples generally maintains tight groups with respect to Zr content for individual units. These similar Zr values for each unit suggest this Zr pattern is not a function of alteration, rather that it reflects a primary igneous process. The order of emplacement (section 2.3) reveals a repeated pattern involving fluctuation between units with relatively high Zr and units with low Zr (eg. EP dyke followed by early dykes, sill followed by 2-2 dykes, etc.). Four samples (two porphyry unit IV samples and both sparse dyke samples) have a higher Zr/SiO<sub>2</sub> ratio than the other Mt. Leyshon samples, which suggests the involvement of a different process during the evolution of these particular rocks.

### 6.5 CLASSIFICATION OF THE MT. LEYSHON IGNEOUS ROCKS

Igneous rock classification is commonly based on the volume % (modal) quantity of quartz, feldspar (and/or feldspathoid) ± mafic minerals (Streckeisen, 1979), or is based on whole rock values of total alkalis versus silica content (Le Bas et al., 1986). However, for the reasons already noted, both of these classifications are generally unworkable in altered rocks like those within the Mt. Leyshon breccia complex. Nevertheless, for the moderately altered Mt. Leyshon igneous units, which show only minor MgO and Fe<sub>2</sub>O<sub>3</sub> mobility (Figure 6.3a), the SiO<sub>2</sub> content of the rocks should be close to the original (MacLean, 1990; Barrett and MacLean, 1991). As discussed previously (section 6.2.2), the assumption can be made that the alkali element values for the regional units would also have correlated well with those for the Mt. Leyshon igneous samples prior to their alteration.

Thus, it is possible to classify the Mt. Leyshon igneous suite meaningfully through a combination of:

- (1) A total alkalis versus silica diagram (Figure 6.1).
- (2) A K<sub>2</sub>O versus SiO<sub>2</sub> plot (Figure 6.7), both constrained by regional data trends.
- (3) The approximate modal values for the phenocryst felsic minerals (Table 6.1), when these are determinable.

On this basis, the Mt. Leyshon igneous rocks (excluding the basalt dykes) range in composition from andesite to rhyolite as shown in Table 6.2.

Basalt dykes have whole rock geochemistry and CIPW norm data (see Figures 6.1 and 6.7; Appendices 2 and 4) which indicate an alkaline character, in contrast to other Mt. Leyshon igneous units which have a high K calc-alkaline character (Figure 6.7). Chemical, field and petrographic relationships of the basalt dykes, suggest that they are unrelated to other Mt. Leyshon igneous units, and are therefore not considered further in this Chapter.

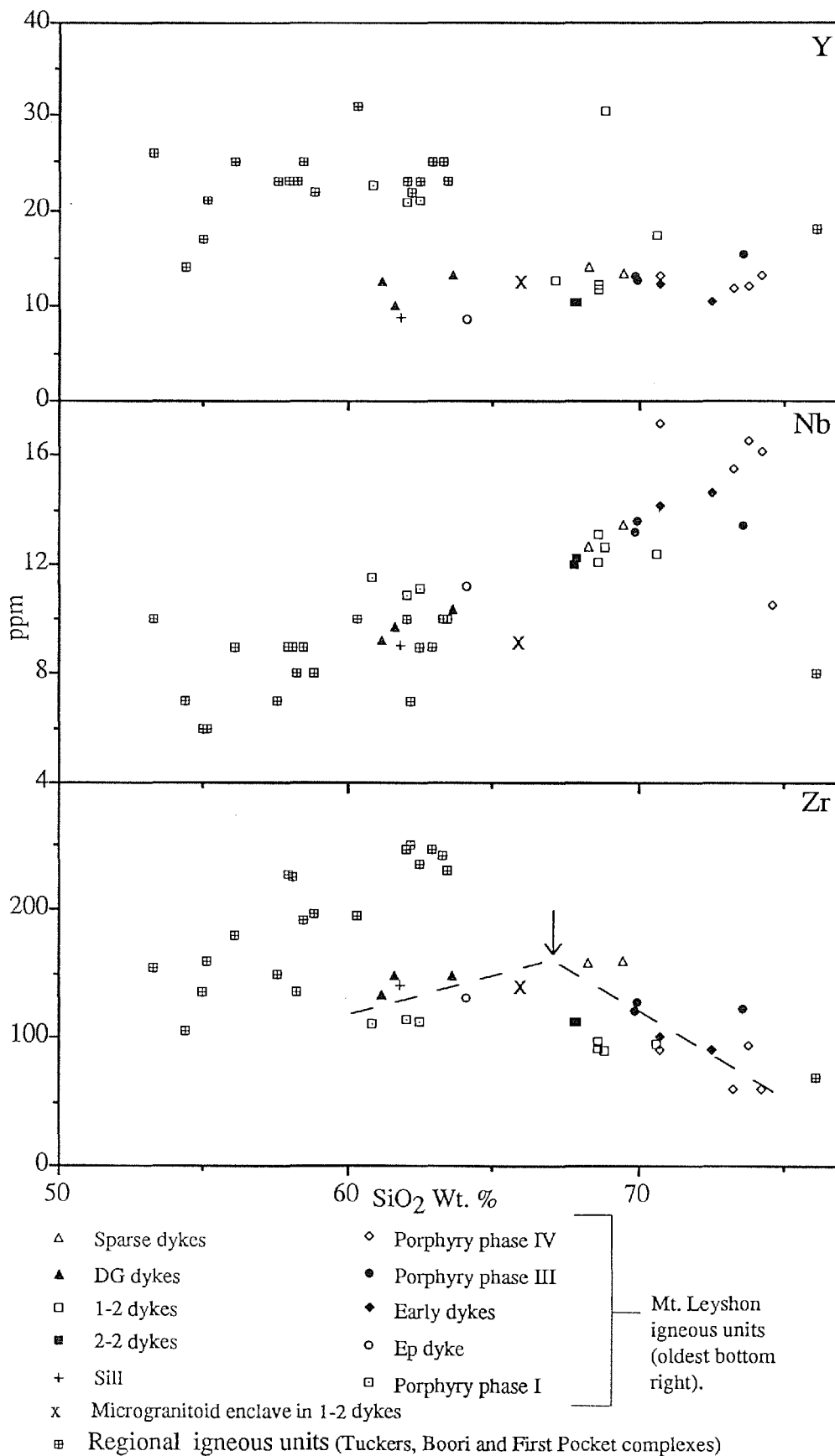


Figure 6.4: Zr, Nb and Y characteristics of the Mt. Leyshon and regional igneous units. A strongly altered porphyry unit IV sample is included on the Nb versus SiO<sub>2</sub> plot of this diagram (see discussion in section 6.6.2). Note that: (1) the Zr data for the Mt. Leyshon igneous units shows an inflection point at approximately 67 Wt. % SiO<sub>2</sub> (arrow) and (2) that the leucogranite of the Boori complex is distinct.

IGNEOUS UNIT	COMPOSITION
porphyry unit I	andesite
EP dyke sill DG dyke	quartz andesite
microgranitoid enclaves (in 1-2 dykes)	quartz latite
sparse late dykes 2-2 dykes 1-2 dykes porphyry unit III	rhyodacite
porphyry unit IV early dykes	rhyolite

Table 6.2: Classification of the Mt. Leyshon igneous rocks.

## 6.6 A COMPARISON OF THE MT. LEYSHON AND REGIONAL IGNEOUS ROCKS

Igneous rocks of both the Mt. Leyshon breccia complex and the regional Permo-Carboniferous centres show evidence for undercooling (more rapid crystallisation of a portion of the magma). This is more extreme in the Mt. Leyshon igneous units, however, which are porphyritic with an aphanitic groundmass, suggesting rapid crystallisation. In contrast the regional units are generally medium grained with an equigranular texture, which suggests a longer period of crystallisation. Furthermore, at Mt. Leyshon, multiple intrusive episodes form dyke like bodies with limited evidence for *in situ* differentiation, which implies emplacement in a structurally active zone. In contrast, the regional igneous centres are formed by fewer, larger bodies with an elongate outline and evidence for *in situ* differentiation (Clarke, 1971), implying igneous emplacement in a less structurally active zone.

With the exception of one sample (leucogranite of the Boori complex 76 wt.% SiO<sub>2</sub>), the Mt. Leyshon igneous rocks (60 - 74 wt.% SiO<sub>2</sub>) are more evolved than the regional units (53 - 63 wt.% SiO<sub>2</sub>). The Mt. Leyshon igneous rocks, therefore, sit within the compositional gap between the highly evolved Boori complex unit and the remaining regional units (Figure 6.3). Both suites of igneous rocks have a similar mineral assemblage (sections 6.2.1 and 6.3.1) but pyroxene, if present, is rare in the Mt. Leyshon units. However, distinct differences exist between the chemical variation of the Mt. Leyshon and regional igneous units (section 6.4). These differences are:

- (1) The Mt. Leyshon igneous units are generally more evolved than the regional suite and have differentiated to a higher SiO<sub>2</sub> content.

- (2) The continual enrichment of Zr in the melt during differentiation of the regional igneous units, in contrast to the Mt. Leyshon units which show initial Zr enrichment, then depletion in the melt during differentiation (Figure 6.4).
- (3) The low Y values of the Mt. Leyshon igneous suite compared to the regional suite (Figure 6.4).

In regard to this last point, both the Mt. Leyshon complex and the regional Permo-Carboniferous centres have a broadly calc-alkaline character according to the classification of Miyashiro (1974; Figure 6.5;  $\text{FeO}^*$  = total iron as FeO). In the interpretation of this data it is assumed that by plotting only the least altered Mt. Leyshon samples, the effect of alteration on total iron content will be minimal, and the graph trends therefore reflect the approximate magmatic FeO variation.

Compared to the regional suite the Mt. Leyshon suite is characterised by:

- (1) A low total iron content.
- (2) greater increase in the  $\text{FeO}^*/\text{MgO}$  ratio with increasing  $\text{SiO}_2$  (Figure 6.5a).
- (3) less pronounced  $\text{FeO}^*$  decrease with increasing  $\text{FeO}^*/\text{MgO}$  ratio (gentler slope in Figure 6.5b).

Additionally, the plots in Figure 6.5 suggest once more that porphyry unit I of the Mt. Leyshon complex is more closely related to the regional suite, while the leucogranite of the Boori complex may have a closer affinity to units from the Mt. Leyshon complex.

In fresh volcanic rocks, Winchester and Floyd (1977), and in altered volcanic rocks, Floyd and Winchester (1978), have used the Nb/Y ratio as a measure of the alkalinity of a magma series. For all except the most siliceous rocks (rocks with a  $\text{SiO}_2$  content of >73wt. %) a Nb/Y ratio of 0.67 appears to divide generally sub-alkaline magma suites from those that are alkaline (Winchester and Floyd, 1977). Their work allows further comparison of the Mt. Leyshon and regional igneous units. A graph of the Nb/Y ratio plotted against  $\text{SiO}_2$  for the Mt. Leyshon (excluding the most altered samples) and regional igneous units is shown in Figure 6.6. A tendency towards alkaline character is suggested for the Mt. Leyshon igneous samples by a Nb/Y ratio of > 1 for many samples (Figure 6.6), which is consistent with the presence of biotite as an abundant phenocryst phase in felsic units. However, the regional igneous units are clearly sub-alkaline on this diagram; note this also includes the leucogranite ( $\text{SiO}_2 = 76 \text{ Wt.}\%$ ) of the Boori complex.

The Mt. Leyshon breccia complex is not strictly a porphyry copper system, but since porphyry units are present, the definition of porphyry copper deposits are often economically based and Mt. Leyshon locally contains significant copper (Chapter 4), a comparison is made here. Compared with other igneous rocks associated with porphyry related mineral deposits, the regional and Mt. Leyshon igneous rocks together correlate with the high K calc-alkaline suite of Mason and McDonald (1978; Figure 6.7), consistent with their tectonic setting in the Australian continental block. In this regard, the Mt. Leyshon and regional suites may be grouped with igneous rocks associated with porphyry copper systems of Papua New Guinea such as OK Tedi, Yuat North, Panguna and Limbo River. Compared to igneous rocks in the calc-alkaline Mt. Shamrock-Ophir complex (SE Queensland; Au-Ag-As; Williams, 1991) the Mt. Leyshon igneous rocks are more

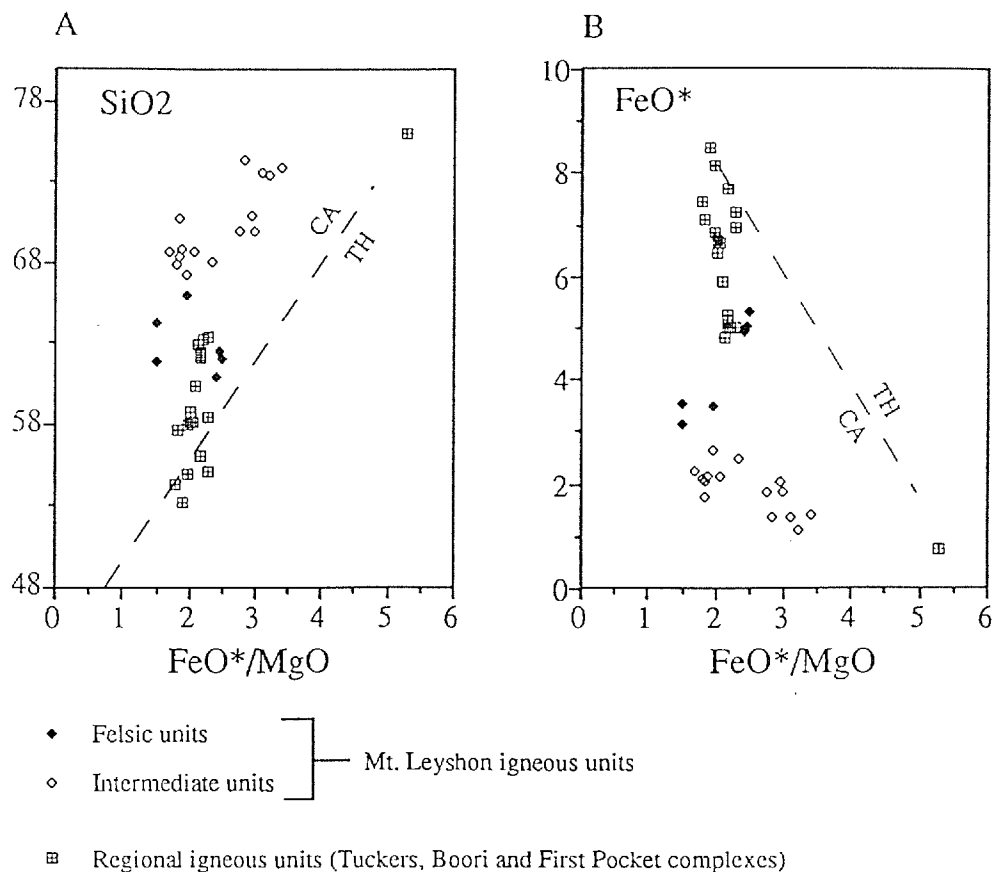


Figure 6.5: Comparison of SiO<sub>2</sub>, FeO\* and FeO\*/MgO characteristics of the Mt. Leyshon and regional igneous units. The dashed line is the calc-alkaline (CA) / tholeiitic (TH) definition of Miyashiro (1974).

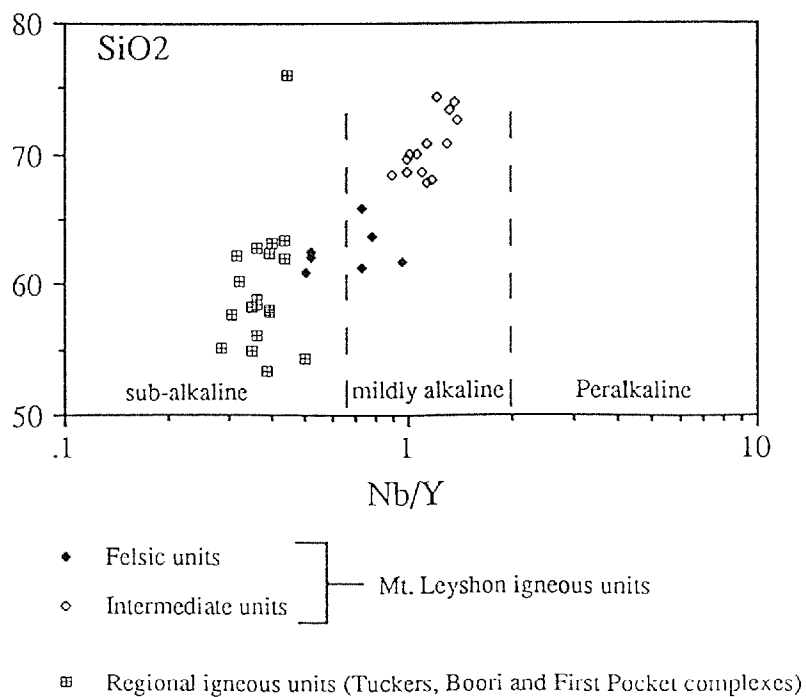


Figure 6.6: SiO<sub>2</sub> versus Nb/Y diagram examining the evolution of the Mt. Leyshon and regional igneous suites. The dashed lines are the subalkaline, mildly alkaline and peralkaline magma suites after Winchester and Floyd (1977).

alkaline (higher Nb / Y ratios) but show similar Zr / TiO<sub>2</sub> ratios, for a given SiO<sub>2</sub> content (P. Williams, written communication). No published data for the geochemistry of igneous units in other porphyry style breccia complexes such as the Kidston gold mine (NE Queensland) is known to the author.

## 6.7 PETROGENESIS OF THE PERMO-CARBONIFEROUS IGNEOUS ROCKS

### 6.6.1 Petrogenesis of the Mt. Leyshon igneous rocks

In this section, geologic and chemical evidence is discussed for the late stages of magmatic evolution associated with breccia formation in the the Mt. Leyshon complex. Processes effecting the magma during its passage through the crust from the source region to high level emplacement beneath the complex are not considered here.

#### 6.7.1.1 EVIDENCE FOR FRACTIONAL CRYSTALLISATION WITHIN A ZONED MAGMA SYSTEM

The post-crystallisation changes to the Mt. Leyshon igneous rocks have prevented a full examination of phenocryst chemistry and textures, and an assessment of the compatability of phenocrysts with their igneous groundmass. Nevertheless, the composition of phenocrysts in porphyry unit I (andesite) and phenocryst relics in porphyry unit IV (rhyolite) are consistent with an origin due to fractional crystallisation, rather than having been introduced from another magma during mixing. The general paucity of features that would indicate magma mixing in the Mt. Leyshon igneous units, such as abundant enclaves and streaks of incompletely mixed magma, and phenocryst dis-equilibrium textures, further suggests that fractional crystallisation was the dominant process controlling igneous evolution of the petrological characteristics of the suite.

The progressive depletion in Al<sub>2</sub>O<sub>3</sub>, Fe<sub>2</sub>O<sub>3</sub>, MgO and probably CaO, and increase in Nb from andesite to rhyolite in the Mt. Leyshon igneous rocks is consistent with the crystal fractionation of the observed phenocryst phases from a more basic parental magma (SiO<sub>2</sub> < 60 wt. %). The inflection in the Zr versus SiO<sub>2</sub> variation diagram (section 6.4.2, Figure 6.4), suggests a change in compatibility of this elements during differentiation. Given zircon is rare to absent in Mt. Leyshon intermediate igneous units, this inflection is probably due to the onset of zircon crystallisation. Other workers (Allegre et al., 1977; Mann, 1983) have reported similar inflections during the evolution of igneous suites which they also suggest are due to a change in the crystallising assemblage.

In addition to the evidence for crystal fractionation the following observations suggest the possibility that the Mt. Leyshon magma chamber was compositionally zoned, and further that these layers had internal compositional variation:

(1) Samples collected from narrow dyke like portions of porphyry unit III and IV are more basic than the bulk of these units. The dykes have the same paragenesis as, and are texturally similar to, the bulk of porphyry unit III and IV, which suggests they represent less fractionated portions of

these units. Furthermore, the nature and distribution of quartz phenocrysts within porphyry unit IV implies limited mechanical and gravitational sorting of crystals during internal convection of the porphyry unit IV magma.

(2) Porphyry unit III and IV are generally uniform in texture and mineralogy, although porphyry unit IV mingled with and plastically deformed porphyry unit III margins during emplacement (section 2.4.2). These features suggest that porphyry unit III and IV were simultaneously molten and possibly coexisted in a magma chamber prior to their intrusion. Mathematical modelling of eruptions from magma chambers suggests that upwardly converging streamlines of magma can tap separate horizons in a pre-eruptive chamber (Blake, 1981). Such a process may explain the compositional difference of simultaneously intruded magma in the Mt. Leyshon breccia complex.

#### 6.7.1.2 EVIDENCE FOR MAGMA RECHARGE AND MINOR MAGMA CONTAMINATION

The paragenesis of igneous emplacement described in Chapter 2 provides indirect evidence for repeated recharge of more basic magma into the Mt. Leyshon magma system. Specifically, the periodic emplacement of intermediate dykes into the complex, prior to paired events of brecciation and felsic dyke emplacement. The compositional gap in  $\text{SiO}_2$  contents of intermediate and felsic units together with the oscillation in Zr contents of the igneous units provides further evidence for the supply of several magma batches of a similar composition to the Mt. Leyshon magma chamber.

Despite the evidence for fractional crystallisation described above, a number of observations suggest minor magma mingling (the formation of inclusion bearing magma) between more basic and more felsic magma beneath the Mt. Leyshon breccia complex. For example, porphyry unit I contains rare narrow fragment bearing zones with broken quartz and K-feldspar crystals. The combined features of these broken crystals (such as the presence of oligoclase reaction rims on the K-feldspar phenocrysts) suggests that these crystals are xenocrysts inherited from a more felsic magma during limited magma mingling.

The Mt. Leyshon felsic igneous units are associated with brecciation events and contain quartz phenocrysts which are probably rounded by resorption during pressure decrease (as suggested theoretically by Whitney, 1989). Intermediate igneous units ( $\text{SiO}_2$  content of 61-63 wt. %) of the Mt. Leyshon complex should not crystallise quartz as an early phenocryst phase, but commonly contain (< 1%) randomly distributed, large and complexly embayed quartz phenocrysts. This implies that the quartz phenocrysts in the intermediate units were derived by contamination with more felsic magma (prior to or during emplacement) and phenocryst embayment in these units resulted from resorption because the quartz was out of equilibrium with the melt.

The occurrence of magmatic enclaves within the Mt. Leyshon igneous units further suggests minor magma mingling prior to igneous emplacement. Enclaves with similar features to those described within the Mt. Leyshon igneous units have been interpreted to form by mechanisms including (Huppert et al., 1982; Vernon, 1983; Bacon, 1986):

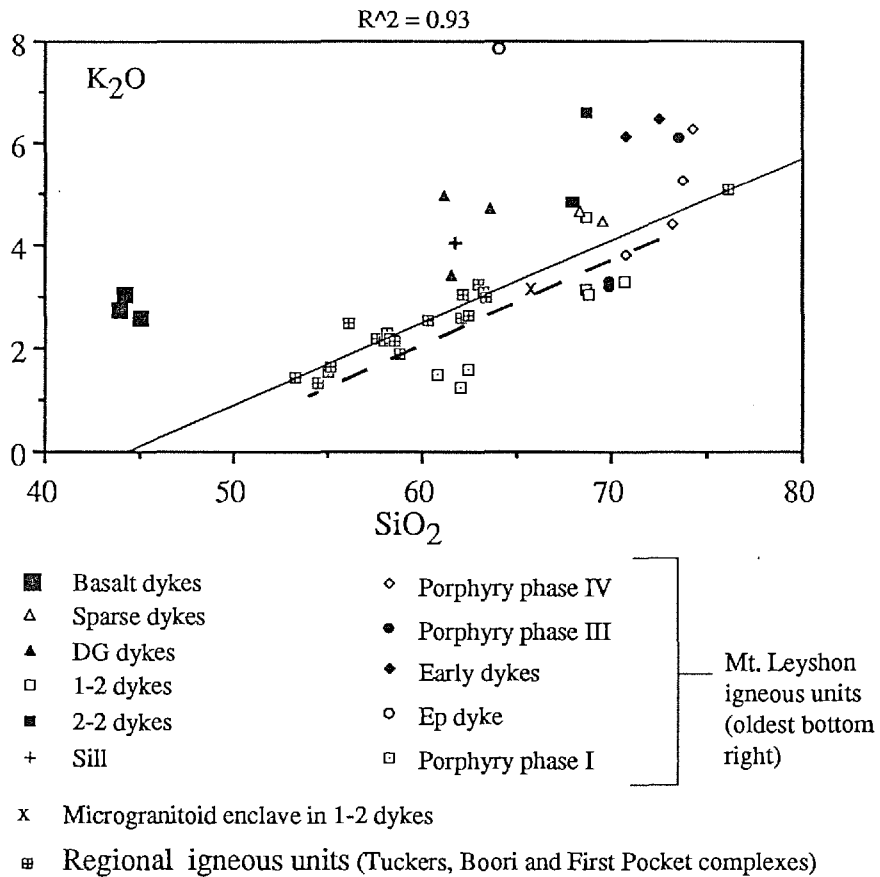


**Figure 6.7:**  $K_2O$  versus  $SiO_2$  variation for the Mt. Leyshon and regional igneous units.

Note the scatter of the Mt. Leyshon data points due to alteration, compared with the unaltered regional samples. Solid line is a calculated linear regression line for the regional data,  $R^2 =$  the correlation coefficient for this linear regression fit. Dashed line separates the high-K and normal-K igneous suites of Mason and McDonald (1978).

- (1) Magma mingling during underplating of a more basic magma beneath a silicic magma.
- (2) Injection of a more mafic dyke of magma into a silicic magma.
- (3) Mechanical disruption, during convective overturning, of a hybrid mixed layer formed by mixing between the felsic and mafic layers.

The combined petrographic and chemical features of the Mt. Leyshon microgranitoid enclaves (sections 6.2.1.1 and 6.4) suggest that they formed through small scale magma mingling between a felsic and more mafic magma, prior to or during intrusion. For example, the enclaves found in a number of the felsic units are texturally similar to the intermediate igneous units. In addition, the analysed sample of the enclaves commonly found in the 1-2 dykes has a major and trace element chemistry which suggests the enclaves are related to the Mt. Leyshon igneous suite. Features of the 1-2 dyke enclaves such as rare chilled margins and abundant apatite needles are commonly interpreted to result from magma quenching during mingling (Vernon, 1983; Bacon, 1986).

If the enclaves in the Mt. Leyshon igneous rocks formed by these processes, volatile transfer between intermediate and felsic magma is an expected consequence of mingling.

### 6.7.2 Petrogenesis of the regional igneous rocks

The combined features of the regional igneous units such as their similar mineralogy and style of emplacement, together with their co-linear major and trace element variation (Figures 6.3 and 6.4) suggest that the regional igneous units are comagmatic. Clarke's (1971) description of gradational compositional layering and vertical differentiation between units of the Tuckers complex suggests that fractional crystallisation was the dominant process controlling the petrological evolution of regional igneous units. That minor magma mingling occurred in the Tuckers complex is suggested by the presence of dioritic enclaves in one unit of this complex, in a similar manner to that argued for the Mt. Leyshon enclaves.

The similarity in mineralogy, major element and Nb variation of the Permo-Carboniferous igneous rocks, and the SiO<sub>2</sub> range of the Mt. Leyshon units with respect to the regional units, implies a genetic link during their evolution. However, Goellnicht et al. (1991) have shown that granitoid suites typically show linear trends and limited chemical variability, so that variation diagrams should be used with caution when interpreting genetic relationships between granitoid suites. The following evidence, therefore, casts doubt on a co-magmatic origin for the two suites (Mt. Leyshon and regional igneous units):

- (1) The difference in the behaviour of Zr and Y in the two suites.
- (2) The low total FeO content of the Mt. Leyshon igneous units and the variation of FeO during differentiation of the two suites.
- (3) The marked difference in the Nb/Y ratio of the two igneous suites.

Nevertheless, the first igneous unit intruded into each of the Mt. Leyshon and Boori complexes (porphyry unit I and the leucogranite) have consistently different geochemistry to the other units from their respective suites. Porphyry unit I has many characteristics of the regional suite, though

its TiO<sub>2</sub> and Zr behaviour is different. The leucogranite of the Boori complex shows chemical affinity to the Mt. Leyshon suite which raises the possibility that it is comagmatic with the Mt. Leyshon suite. However, the low value of Nb for the leucogranite compared to the Mt. Leyshon samples is not consistent with this interpretation. Assuming this low Nb value is not an analytical error, and in the absence of any reported alteration (Clarke, 1971) it is most likely due to the tendency for Nb to be depleted during protracted fractional crystallisation (Taylor, 1965), or the mobility of Nb as fluoride complexes in late stage magmatic fluids (Cerny et al., 1985). Indeed, one porphyry unit IV sample (P231, Appendix 2) from the Mt. Leyshon complex also shows a marked decrease in Nb (Figure 6.4). This sample shows the strongest post-emplacement recrystallisation and alkali mobility of any of the Mt. Leyshon samples and suggests that Nb may be mobile during strong alkali exchange.

### 6.7.3 Towards a trace element model for the Mt. Leyshon igneous rocks

The observations made above on igneous petrology and geochemistry of the Mt. Leyshon igneous rocks, are consistent with the dominant process of evolution due to fractional crystallisation. As noted above however, evidence for minor magma mixing is present. An assessment of the role of source terrains and crustal assimilation (for the Mt. Leyshon igneous rocks) versus magma mixing during the passage of magma through the crust, is clearly complex and requires the derivation of isotopic or trace element models beyond the scope of this study. Nevertheless, Nb, Zr, Y and TiO<sub>2</sub> have been shown to be immobile during moderate hydrothermal alteration (Winchester and Floyd, 1977; Floyd and Winchester, 1978; this study). Using these elements it may therefore be possible to further investigate the dominant process controlling the Mt. Leyshon igneous evolution.

#### 6.7.3.1 RATIONALE

For volcanic suites, Allegre et al. (1977) have described an extended application of the Rayleigh distillation law to trace element behaviour in fractional crystallisation studies. This application was modified and extended to plutonic rocks by Cocherie (1986). These workers have used this trace element behaviour on a log-log plot to determine which of several processes (partial melting, mixing or fractional crystallisation) is dominant in producing the observed chemical variation in a rock suite.

The evolution of the concentration of two elements in a magma (C<sub>1</sub> and C<sub>2</sub>) which have very different crystal/liquid partition coefficients (D<sub>1</sub> and D<sub>2</sub>) is shown in Figure 6.8, according to the corresponding models proposed by the workers cited beneath the diagram. For example, a curve which shows a strong decrease in the value of a compatible element (high D; e.g. Cr, Co, Ni) with a corresponding small variation in the value of the incompatible element (low D; e.g. U, Th or Ta), reflects a crystallisation process (curve A in Figure 6.8; Cocherie, 1986).

If D<sub>1</sub> and D<sub>2</sub> are constant throughout the igneous process, a plot of Log C<sub>1</sub> versus Log C<sub>2</sub> gives a straight line whose slope is  $a$  (Cocherie, 1986).

$$a = D_1 - 1 / D_2 - 1$$

If we have an independent estimate of  $D_2$  then we can calculate  $D_1$  from the slope of the Log - Log plot. The  $D$  value so calculated can be compared to published mineral/liquid partition coefficients to further assess the validity of the model.

Allegre et al. (1977) include the requirements that only aphyric rocks should be sampled, sampling should include the entire rock sequence, and a large number of different trace elements should be used in the model. The chemically analysed Mt. Leyshon igneous samples include the full range of the intrusive episodes identified, and generally contain less than 15% phenocrysts. The samples should therefore represent an approximation to the evolving liquid compositions. However, porphyry unit IV of the Mt. Leyshon complex, contains 35% phenocrysts and may not represent an approximate liquid composition. Only a small number of trace elements have been considered in this study which precludes the development of a full trace element model. The aim here, however, is to make a qualitative assessment of the dominant process controlling igneous evolution in the Mt. Leyshon complex. The trace elements which have generally remained immobile during hydrothermal alteration (Zr, Nb, Y, and  $TiO_2$ ) should therefore allow a preliminary examination of this problem.

The choice of elements with a high and low  $D$  value for the Permo-Carboniferous igneous rocks has been made for the following reasons:

- (1) The low variability and almost constant value of Y in the igneous rocks with increasing  $SiO_2$  content suggest Y would not be a suitable element in the trace element model.
- (2) Published values of mineral/liquid partition coefficients suggest that the  $D$  value for  $TiO_2$  is very high (around 100; Allegre et al., 1977) when ilmenite is involved in the differentiation process. Data for the Mt. Leyshon igneous units discussed in this Chapter, is consistent with the fractional crystallisation of Fe-Ti oxides. Therefore,  $TiO_2$  has been chosen to represent a high  $D$  element for the Mt. Leyshon suite.
- (3) Mann (1983), indicates that Nb behaves as a low  $D$  element in the calc-alkaline Santorini volcano (Greece; basalt-andesite-dacite-rhyodacite), and derived a distribution coefficient for Nb  $\approx$  0.26. The continuous enrichment in Nb with increasing  $SiO_2$  for all Mt. Leyshon samples (Figure 6.4), also indicates that Nb is strongly partitioned into the melt during igneous evolution, behaving as a low  $D$  element.
- (4) Zirconium is commonly strongly partitioned into the melt phase during early to intermediate stages of magmatic evolution which results in Zr behaving as a low  $D$  element (Allegre et al., 1977). Observations discussed above however, suggest a change in the behaviour of Zr resulting in Zr fractionation in the Mt. Leyshon felsic samples (Figure 6.4). This suggests that Zr behaves as a high  $D$  element in the Mt. Leyshon felsic magma.

### 6.7.3.2 THE TRACE ELEMENT MODEL

A plot of  $\text{TiO}_2$  versus Nb for the Mt. Leyshon igneous rocks which represents a comparison of a high and low D element, respectively, is shown in Figure 6.9. The Mt. Leyshon samples display a good correlation ( $R^2 = 0.77$ ) and the shape of this curve (compare Figure 6.9 to Figure 6.8) suggests that the major process governing the petrological evolution of the Mt. Leyshon suite is a fractional crystallisation model according to the Rayleigh law. The minor scatter on this diagram, shown by some samples of porphyry unit IV, may be due to analytical error or because the samples do not represent liquid compositions. A similar comparison was made between Zr and Nb for the felsic igneous units, however the data are poorly correlated ( $R^2 = 0.41$ ), probably reflecting the large analytical error of Zr, and do not allow a comparison.

Using the distribution coefficient for Nb derived by Mann (1983;  $D_2 = 0.26$ ), an approximate bulk partition coefficient for Ti in the magma is 303 (derived from the slope of the line on Figures 6.9). For reasons discussed above (section 6.7.3.1) and the analytical precision of Nb ( $\pm 2.4$  ppm, at  $3\sigma$ ), this value is only qualitative and provides an order of magnitude number for comparison to other systems. This partition coefficient is three times the values for Ti quoted by Allegre et al. (1977), although their results are derived from an investigation of basic to intermediate igneous suites, rather than intermediate to felsic suites like the Mt. Leyshon units. Further work is required to test the validity of the trace element model and the Ti partition coefficient derived for the Mt. Leyshon suite in this study.

## 6.8 SUMMARY

A petrogenetic model is proposed for the evolution of the Mt. Leyshon igneous units which suggests fractional crystallisation of the observed phenocryst phases. However, the indicated periodic input of more basic magma into the Mt. Leyshon magma chamber, induced minor magma mingling that possibly resulted in a compositionally zoned magma chamber, from which periodic igneous emplacement and volatile loss into the Mt. Leyshon breccia complex occurred. Likewise, the data suggests that the compositional variation of the regional igneous units results from fractional crystallisation. The data indicates that both the Mt. Leyshon and regional igneous suites are broadly calc-alkaline, although significant chemical differences between the two suites are apparent, which suggests that the Mt. Leyshon and regional igneous suites generally evolved as separate magma systems.

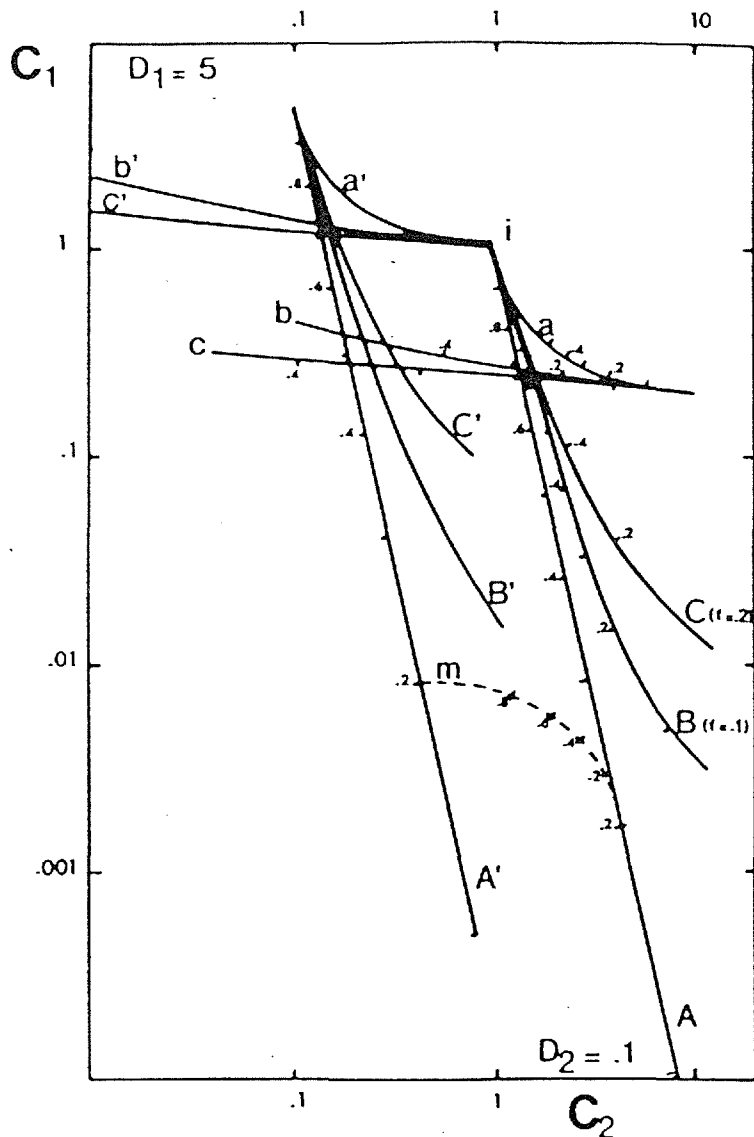
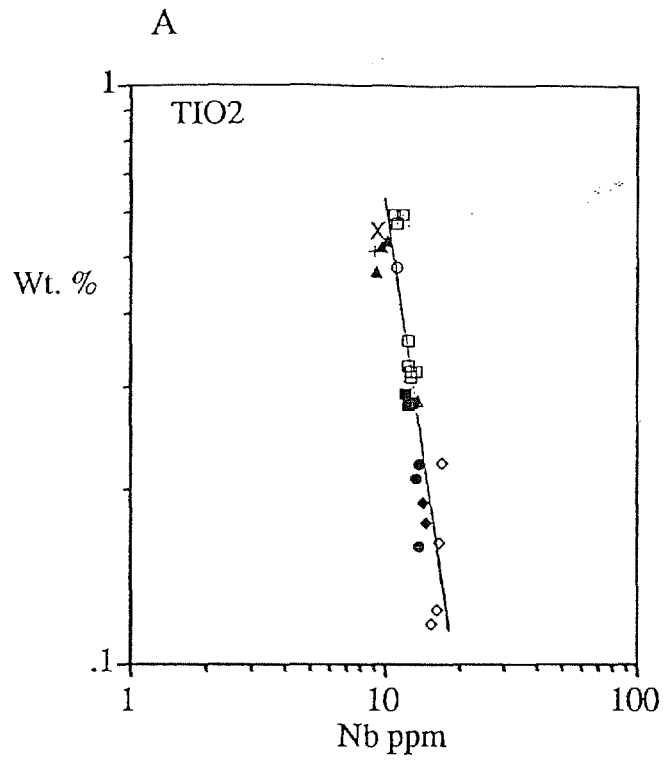


Figure 6.8: Evolution of the concentrations  $C_1$  and  $C_2$  for two elements 1 and 2 having bulk distribution coefficients  $D_1$  and  $D_2$  respectively equal to 5 and 0.1. The numbers plotted along the curves indicate the values of the parameter  $F$  (weight proportion of the melt).

*Crystallisation processes:* i-the initial liquid; A-fractional crystallisation, evolution of the liquid (Neumann et al., 1954); A'-straight line evolution of the corresponding solid phases; a-crystallisation with total equilibrium between solids and melt, evolution of the liquid (Arth, 1976); a'-corresponding solid phases; B and C-incremental equilibrium crystallisation (McCarthy and Hastay, 1976); B' and C'- corresponding solid phases; m-mixing curve of crystals formed and residual melt for a fractional crystallisation process.

*Fusion processes:* l-the initial solid material; a-batch partial melting (Shaw, 1970); a'-corresponding residual solid; c-fractional fusion with continual removing of the melt formed (Shaw, 1970); c'-corresponding residual solid; b-aggregate melting or fractional fusion with extraction of the mixed melts (Shaw, 1970; Langmuir et al., 1977); b'-corresponding residual solid.



- |   |   |  |
|---|---|--|
| <ul style="list-style-type: none"> <li>△ Sparse dykes</li> <li>▲ DG dykes</li> <li>□ 1/2 dykes</li> <li>■ 2/2 dykes</li> <li>+ Sill</li> <li>x Microgranitoid enclave in 1-2 dykes</li> </ul> | <ul style="list-style-type: none"> <li>◇ Porphyry phase IV</li> <li>● Porphyry phase III</li> <li>◆ Early dykes</li> <li>○ Ep dyke</li> <li>◻ Porphyry phase I</li> </ul> | <div style="border-left: 1px solid black; border-right: 1px solid black; border-bottom: 1px solid black; width: 100px; height: 100px; display: flex; align-items: center; justify-content: center;"> <div style="text-align: right; padding-right: 5px;">Mt. Leyshon<br/>igneous units<br/>(oldest bottom<br/>right).</div> </div> |
|---|---|--|

Figure 6.9:  $TiO_2$  versus Nb trace element model for the Mt. Leyshon igneous rocks.



Plate 6.1: Intermediate igneous unit (porphyry unit I) consisting of plagioclase (faint oscillatory zoning) and magnetite phenocrysts in a weakly flow aligned groundmass (amphibole phenocrysts not shown). Arrow indicates xenocryst shown in plate 6.3. (Photomicrograph, XPL, base of photo = 5 mm; Sample no. S2.)

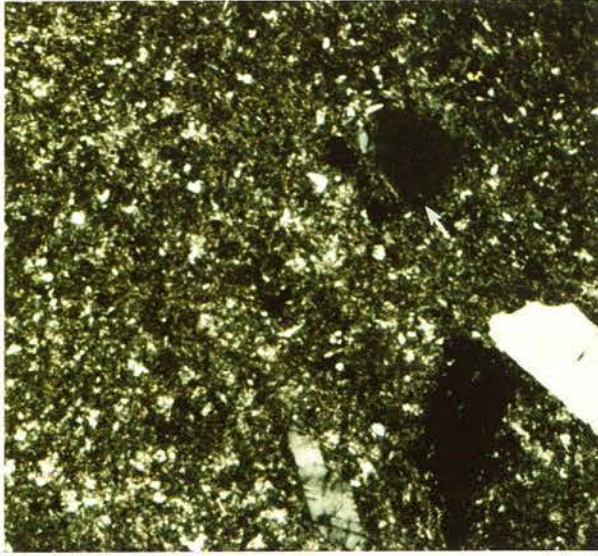
Plate 6.2: Felsic igneous unit (2-2 dyke), consisting of strongly embayed quartz (A), large altered K-feldspar (B) and biotite (C) phenocrysts in a fine grained micrographic groundmass. (Photomicrograph, XPL, base of photo = 5 mm; Sample no. 22/254.)

Plate 6.3: Broken K-feldspar xenocryst in enclave bearing zone of porphyry unit I (detail of Plate 6.1). Note the irregular boundary and the melt reaction rim (A) of the K-feldspar crystal against the flow aligned porphyry unit I groundmass. (Photomicrograph, XPL, base of photo = 1.5 mm; Sample no. S2.)

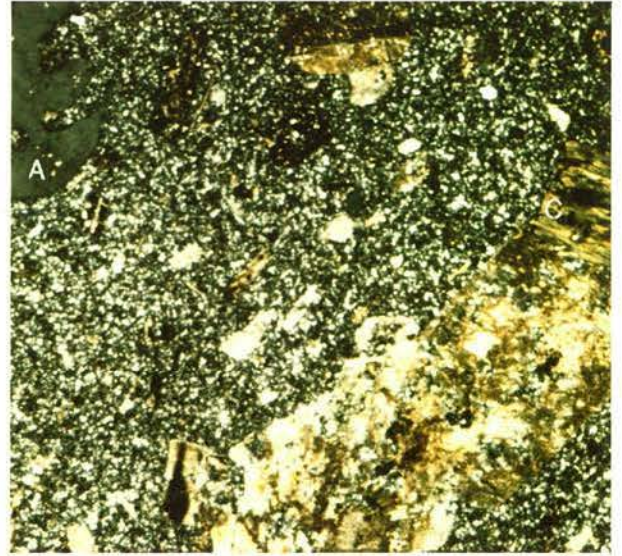
Plate 6.4: Felsic igneous unit (Porphyry unit IV). Large Kfeldspar phenocrysts are partially replaced by albite at their rim (A). Note that one of the quartz phenocrysts (Q) is splinter textured and angular. (Photomicrograph, XPL, base of photo = 4 mm; Sample no. S14.)

Plate 6.5: Felsic igneous unit (1-2 dyke). Note chlorite pseudomorph probably after amphibole (A) and granophyric intergrowth in quartz and alkali feldspar (B). (Photomicrograph, XPL, base of photo = 1.5 mm; Sample no. T/230/9.)

Plate 6.6: Microgranitoid enclave (in 1-2 dyke). Note the granophyric patches (A) and acicular apatite needles (B). (Photomicrograph, XPL, base of photo = 0.6 mm; Sample no. I4X.)



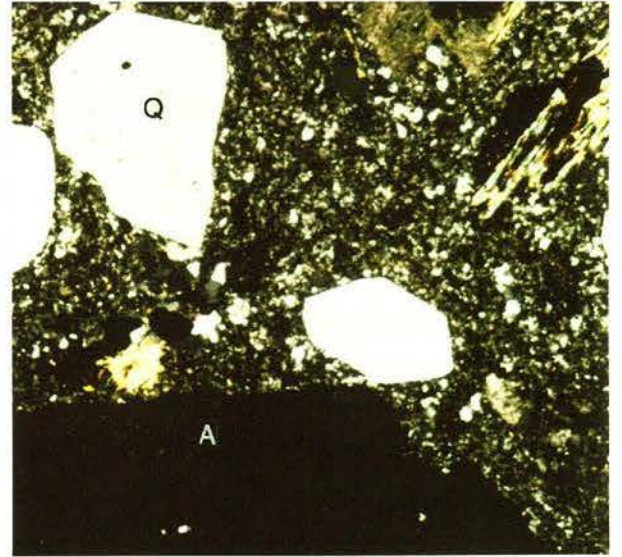
6.1



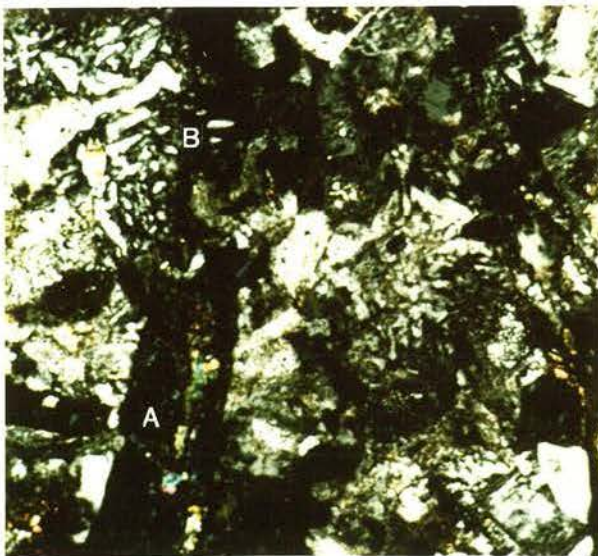
6.2



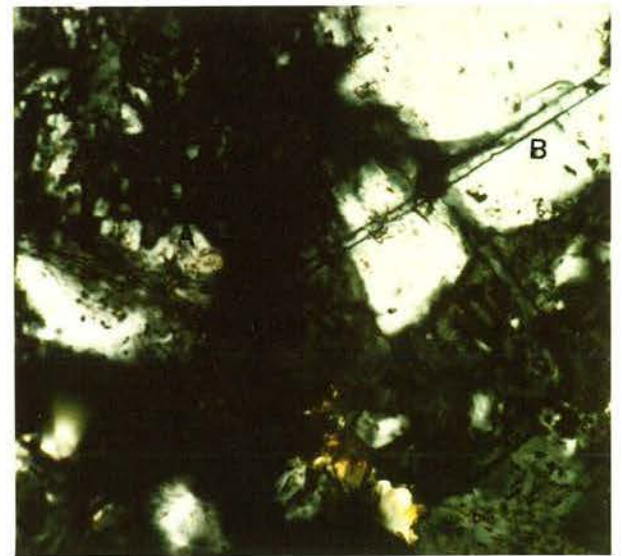
6.3



6.4



6.5



6.6

## Chapter 7

# BRECCIA MECHANISMS AND MAGMATIC PROCESSES WITHIN THE MT. LEYSHON BRECCIA COMPLEX

---

### 7.1 INTRODUCTION

Current models for magmatic hydrothermal breccia pipes largely focus on the role of the magmatic system in breccia formation (Sillitoe, 1985; Burnham, 1985; Baker et al., 1986; Laznika, 1988). These models essentially view the magma system as closed to material transfer. All fracturing, brecciation and hydrothermal alteration are considered to have resulted from, and formed broadly synchronously with, the late stages of magma evolution.

These models take little account of the overall structural setting of the breccia pipe or recent work on the mechanics of faulting (e.g. Segall and Pollard, 1980; Sibson, 1986, 1992), fluid and magma flow in the crust (Shaw, 1980; Sibson, 1989b). Many breccia pipes clearly in areas that were tectonically active at the time of their generation (e.g. Leadville breccia bodies, Colorado; Hazlitt and Thompson, 1990; Ortiz breccia pipe, New Mexico; Wright, 1983), though few current models take account of processes that are thought to occur in actively deforming crust.

This Chapter integrates the geological evidence for brecciation processes within the Mt. Leyshon complex, and provides a framework for constraining current theoretical models and guiding future experimental work. The intention here is to propose a dynamic model for breccia mechanisms based on the work in this thesis and the evidence of recent work on upper crustal processes. It does not, however, attempt to answer certain specific questions on the brecciation process such as the composition, pressure and temperature of the fluid phase during breccia formation.

The discussion of processes in this Chapter is divided into three main sections, *structural*, *fluid phase* and *magmatic*. However, as highlighted in the final section, these processes are complex and variably coupled during different stages of the brecciation cycle. The orders of magnitude variation in rate of processes results in a further conceptual difficulty associated with brecciation mechanisms.

This Chapter therefore aims to:

- (1) Synthesise the essential elements of the brecciation process in the complex.
- (2) Suggest possible breccia mechanisms responsible for these processes, in the light of what is presently known of the physical basis for brittle deformation, fluid flow and magmatic processes in the upper crust.
- (3) Derive a dynamic model for breccia mechanisms in the Mt. Leyshon complex.

## 7.2 REGIONAL CRUSTAL SETTING AND EVIDENCE FOR DEPTH OF EMPLACEMENT

The Charters Towers block forms a region of continental crust that was probably in a back-arc setting during the Late Palaeozoic to Mesozoic (Johnson and Henderson, 1991). This region has a prolonged history of structural activity involving reactivation of existing structures (Chapter 3). In and around the complex, dyke injection, brecciation and hydrothermal fluid flow overlapped with strike slip faulting (Chapter 3).

Modern wrench systems are dominated by earthquake faulting which occurs primarily through frictional reactivation of existing faults (Sibson, 1986 and 1989a; Thatcher and Hill, 1991). The zone of seismic faulting is defined by background microseismicity and appears to represent the region of unstable frictional faulting, whose base is defined by the onset of greenschist facies metamorphic conditions (temperatures around 250-300° C). In actively deforming crust the seismogenic zone generally extends to depths of 10-15 kilometres, but may shallow to as little as 4 kilometres in regions of geothermal activity, such as the Salton Sea (Sibson, 1989b). The following factors indicate that the region around the Mt. Leyshon Breccia complex was an area of high heat flow and high temperature fluid flow:

- (1) The occurrence of high temperature hydrothermal alteration (Chapter 4; 500-200° C, Morrison et al., 1988; Uemoto et al., 1992) within the complex, extending at least 500 metres from the complex margin (section 4.4). Similar high temperature hydrothermal systems occur in many porphyry style systems (e.g. the porphyry copper system at Tintic, Utah; Norman et al., 1991).
- (2) The abundant coeval igneous activity (Chapters 2 and 6), implying the existence of a well established magma system, which would have increased the crustal heat flow in the region.

In these environments, earthquake activity and fluid migration in the upper half of deforming continental crust are commonly linked, both with the fluid acting as a possible triggering mechanism for seismic faulting, and through post-seismic fluid discharge (Nur and Brooker, 1972; Sibson, 1985, 1989b). This has important implications for magma and fluid flow into the breccia complex and as a consequence brecciation and mineralisation. It is inferred (Chapter 3) that transfer zones have played an important role in magma transport in and around the Charters Towers block. At least in the Mt. Leyshon Corridor (transfer zone), both the Mt. Leyshon and the Seventy Mile Mt.-Mathews Pinnacle complexes are located at the intersection of major suborthogonal strike slip fault systems (defined here as cross-over zones). These regions will give rise to structural irregularities where diffraction of fault slip links between the different fault systems, and during earthquake faulting may produce sites of dilation. Because the strike slip faults forming these corridors are 4 - >100 kilometres long, and as discussed the seismogenic zone is likely to be shallow in these areas of high heat flow, these regions potentially extend to the base of the seismogenic zone. Therefore, as a consequence of their fault architecture these cross-over zones provide enhanced zones of permeability for magma and fluid flow in the crust.

The depth of the present erosion level is poorly constrained (section 2.4.2) and hence the confining pressure relating to the observations made in this thesis. Nevertheless, the change in the nature of

the structural and hydrothermal evolution during the development of the complex suggests significant uplift and erosion (Chapter 3). Because breccia pipes commonly have vertical dimensions several times greater than their maximum horizontal dimensions (Sillitoe, 1985) and the Mt. Leyshon breccia complex is approximately 2 kilometres in diameter, it is possible that the complex originally had a vertical dimension greater than six kilometres. Likewise, the Mt. Leyshon breccia pipe has a maximum horizontal dimension of > 550 metres, and both geometric considerations and drilling strongly suggest a vertical extent approaching 1 kilometre. A vertical extent of 1.5 - 2 kilometres is therefore possible.

The absence of both volcanic (pyroclastic) facies and any direct evidence for a juvenile magma component in the main pipe breccia, suggests a deeper crustal level than inferred for diatreme formation (section 2.4.2). The lack of features indicative of mineral precipitation during boiling in the complex is also significant. The presence of a quartz-molybdenite vein system, suggests a depth of  $\geq$  two kilometres because vapour saturation and subsequent release, which is critically tied to this style of mineralisation (Carten et al., 1988), generally occurs at or greater than these depths (Burnham, 1979).

The presence of cohesive fault rocks which cut the main pipe breccia (Chapter 3) probably also implies a depth of > 2 kilometres during initial stages of the complex because faulting at higher levels in the crust (like that subsequently formed in the complex) form non-cohesive fault rocks (Sibson, 1989). The theoretical calculations of Burnham and Ohmoto (1980) suggest complexes dominated by porphyritic textured igneous rocks (like Mt. Leyshon), should crystallise at  $\leq$  4 kilometres. Hence a tentative estimate represented by the present erosion level is 2-3 kilometres beneath the palaeosurface at the time of complex formation.

### **7.3 THE ROLE OF STRUCTURE IN BRECCIA COMPLEX FORMATION**

The role of the regional wrench system in brittle reactivation of basement structures and controlling the location of the complex has been discussed in Chapter 3. In this section the possibility that the actual brecciation process is related to the wrench system is considered.

#### **7.3.1 The role of structure in brecciation**

The rheological contrast across the granite/metasediment contact and the inhomogeneity of the metasediment accentuated the development of the brittle fault infrastructure, and as a consequence fault irregularity within the fault offset contact. Basement fragmentation characteristics (sections 2.2.1 and 2.4.1) and fault and fracture meshes (section 3.3.2.2) suggest that extensive (first order) fault induced brittle deformation of basement occurred early in the complex evolution. This deformation was most likely produced as a consequence of the brecciation mechanism, because it is only weakly developed outside the margin of the complex. Erratic, second order fragmentation (attributed to explosively driven hydrofracture; section 7.4.3), was superimposed on this initial distributed deformation. Considerable expansion of the host rock was associated with both styles of deformation and the absence of hydrothermal infill minerals between their formation, suggests they overlapped with catastrophic brecciation.

To understand the likely origin of the brittle fault infrastructure in the complex and the evolution to fault and fracture meshes, it is important to consider recent work on the mechanics of brittle deformation in the upper crust. Detailed field studies (e.g. Segall and Pollard, 1983) of brittle fault zones, suggest they commonly develop by the progressive incorporation of newly formed and pre-existing shear and extensional fault segments (Sibson, 1986). With repeated stress cycling, one or more through-going principal slip surfaces develops which accommodates most subsequent shearing. As already noted, earthquake faulting is the dominant process of fault slip in the brittle upper crust. Because earthquake behaviour is fairly regular with particular faults or segments of major fault zones often rupturing at fairly regular intervals, this demands the existence of strong structural control on the initiation and termination of earthquake ruptures (Sibson, 1989b). Propagating earthquake ruptures are commonly perturbed by fault irregularities (Sibson, 1986). Two basic varieties of simple fault irregularity are recognised:

- (1) Fault jogs.
- (2) Isolated fault bends.

These irregularities may be further classified into *dilational* or *antidilational*, depending on whether areal increase or reduction tends to occur during incremental slip transfer, accompanying rupture propagation across the irregularity. In contrast to what is expected from quasi-static analysis (Segall and Pollard, 1980), extensive work on recent strike slip faults indicates that large dilational irregularities (across strike widths in excess of one kilometre) act as preferential sites for rupture termination (Sibson, 1985, 1986). Sibson (1985) has suggested that the arrest of propagating ruptures at dilational jogs and bends, and time-dependent slip transfer are both due to the difficulty in opening a linking extensional mesh within fluid saturated crust, in times comparable to earthquake slip durations of a few seconds. This recent work does not consider the consequence of fault irregularity resulting from the intersection of two strike slip fault systems, as is proposed for the Mt. Leyshon complex (Chapter 3). Given the two kilometre width of the breccia complex and the internal fault complexity resulting from the linking of the two systems, it is likely that the brittle fault infrastructure of the complex would also act as a serious impediment to rupture propagation.

Hill (1977) and Sibson (1985, 1986, 1989b) suggest that slip transfer between en-echelon segments of dilational jogs is accomplished by the opening of linking subvertical extension and shear fractures, inside the step-over region. In contrast, slip transfer between en-echelon segments at antidilational jogs produce a broad swathe of subsidiary faulting, extending outside the step-over into regions where mean stress has been reduced (Sibson, 1986). Brittle fault and fracture meshes are restricted to the area of the Mt. Leyshon complex within the cross-over zone of the two fault systems, and are at least partly extensional in nature. Sibson (1986) describes three mechanisms of brecciation in fault zones:

- (1) Attrition brecciation developed by frictional wear and grain cataclasis during both seismic and aseismic slip on principle slip surfaces.
- (2) Distributed crush brecciation at antidilational jogs or other fault obstructions, distributed

cataclasis crushing during rupture termination and after shocks.

(3) Implosion brecciation hydraulic implosion of wall rocks into cavities, as a consequence of the sudden fluid pressure differentials generated in dilational jogs during rupture arrest.

As noted by Sibson (1986), crustal heterogeneity and the finite lifetime of a fault infrastructure in a particular configuration, may lead to the intermingling of breccias derived from all three processes. The structural history of the breccia complex also suggests such an intermingling. For example, the overprinting of distributed crush brecciation outside the eastern margin of the Mt. Leyshon pipe by attrition brecciation (Plate 3.12) However, we are concerned with proposing a mechanism for the distributed extension of the basement early in the history of the breccia complex. The internal structure of the distributed deformation forming the complex (Figure 3.10C), though only partly resolved, is consistent with the following structural model:

(1) Propagation of a (?sinistral) earthquake rupture in the Mt. Leyshon corridor under an inferred crudely N-S maximum compression direction for the regional stress field.

(2) Termination of the propagating rupture at the cross-over zone as a consequence of from fault irregularity.

(3) Sinistral movement on NE trending faults and dextral movement on SE trending faults resulting in brittle fault and fracture meshes, and extension between the segments of the two fault systems (Figure 3.10C).

(4) Extensional reactivation (hydrofracture) of N-trending basement faults during catastrophic gas release and main pipe breccia formation (Figure 3.10C; section 7.4.3).

Hydrothermal fluid flow lithified the main pipe breccia and was most intense in the NW corner of the breccia complex. This fluid resulted in the formation of a mechanically strong, isotropic region, as discussed below (section 7.4). Considerable host rock fragmentation and extension also occurred during Mt. Leyshon breccia pipe formation (Chapter 5), though this was concentrated in the NW corner of the complex. First order host rock fragmentation (*in situ* fragmented host rock) is dominant in zone 1 of the Mt. Leyshon breccia pipe but occurs in isolated zones throughout the pipe. Similar intense and rather equant fragmentation, is present in the periphery to the pipe margins and is overprinted by post breccia strike slip faulting. Several workers (e.g. So and Sheldon, 1983, Baker et al., 1986; Colley et al., 1991) have also noted a zone of faulting, slickensides, and/or fracturing peripheral to breccia pipe margins. These workers attribute such features to hydraulic fracturing of the wall rocks prior to breccia pipe formation or subsidence of unsupported wall rock into the pipe following magma withdrawal. However, the following evidence (Chapters 3 and 5) suggests that these mechanisms are inappropriate for first order fragmentation in the Mt. Leyshon breccia pipe, and instead this fragmentation is dominantly tectonically derived:

(1) Evidence for large scale subsidence in the breccia pipe is absent because the host rock configuration is preserved and the breccia pipe appears to close downwards.

(2) The presence of inter-breccia shear zones indicates late tectonic deformation preceded pipe formation. These shear zones have deformed main pipe breccia after its hydrothermal alteration

("lithification").

- (3) Some of the distributed host rock deformation in blocks within the breccia pipe pre-dates catastrophic brecciation.
- (4) Zone 1 of the breccia pipe forms a partial, truncated zone in the pipe suggesting it was once present throughout the pipe but has been modified by further brecciation.

The shape of the breccia pipe (expanded central portion and westward dip) is not easily reconciled with an origin due to upward directed gas release. In pipes where this demonstrably occurs (diatremes) they typically have an upward flaring cone shape (section 2.4.2). In contrast, the Mt. Leyshon breccia pipe, and hyperbyssal pipes elsewhere (Kents, 1964; Sillitoe, 1985) probably closed upwards and downwards, precluding an origin due to collapse following magma withdrawal in these pipes. Hence, the geometry of the pipe and host rock fragmentation characteristics are better explained by active tectonic extension accompanying pipe formation. Furthermore, it is not clear if sufficient extension of the host rock to make room for the brecciation process could occur during explosive gas release alone. Tectonic extension is most easily explained as resulting from movement on one or both of the strike slip faults which now approximately bound the Mt. Leyshon breccia pipe. The presence of marginal fracture zones which contain subhorizontal slickensides in the San Pedro de Cachiyuyo breccia pipes (Chile; Sillitoe and Sawkins, 1971) suggests that tectonic extension likely plays an important role in breccia pipe formation elsewhere.

Coalescence of faults, and decreasing structural complexity through time are an expected consequence of incremental strike slip faulting (Wesnousky, 1988). However, the mapped faults are fundamentally controlled by brittle reactivation of ductile basement faults and have remained active in their present configuration for a considerable period of time, despite probable slip reversals. The "inter-breccia shear" zones suggest these faults were established in a similar pattern to their present configuration and active before Mt. Leyshon pipe formation. The present fault architecture at the pipe (Figure 3.10E), is consistent with a dilational fault bend (see above) created where a SSE trending and SE trending fault meet. This fault bend (small scale dilational irregularity) would perturb seismic ruptures propagating through this fault and open a linked shear and extension mesh as discussed above for rupture termination.

The available evidence (section 3.6.2) suggests that during Mt. Leyshon breccia time, local aberration in the regional stress conditions resulted in broadly E-W compression (Figure 3.10 D and E). The following structural model is based on this assumption and the evidence for pre- to syn-breccia pipe host rock extension (section 5.5):

- (1) Renewal of the brittle fault infrastructure in the region of the breccia pipe resulting in quartz-molybdenite veins, inter-breccia shear zones and oblique slip normal faults (Figure 3.10D). The geometric configuration of these structures and the incremental nature of the veins, suggests they formed in a shared stress field, possibly related to stress cycling, as already discussed.
- (2) Release of stress accumulation in the Mt. Dean corridor by propagation of a sinistral seismic

rupture from the Mt. Dean corridor through SSE trending strike slip faults which traverse the breccia complex (Figure 3.1). Perturbation of the seismic rupture at a dilational fault bend, opening E-trending extension fractures and dislocating the granite/ main pipe breccia contact (Figure 3.10E).

(3) Considerable horizontal extension of the host rock formed a rhombohedral zone bounded by strike slip faults. This strain was concentrated in the central portion of the pipe.

(4) The presence of both expanded host rock and deformed fragments within the fragmental component of the breccia pipe is consistent with extensional shear failure of host rock during pipe formation.

(5) Elsewhere in the pipe, cavities in high dilation breccia zones are coated with matrix and small splinter shaped fragments possibly implying rapid introduction of the matrix during implosion.

Structure played a minor role in the formation of later breccia units, and instead their facies characteristics reflect the role of a fluid phase (section 7.4) and an obvious connection to the magmatic system (section 7.5). Nevertheless, the occurrence of crack-seal like veins in basement blocks in the Mt. Hope breccia indicates host rock extension occurred previously at this site. The elliptical geometry of the Mt. Hope breccia which coincides with the site of an existing strike slip fault zone implies tectonic extension of the host rock occurred on this fault during brecciation. Gently dipping tuffisite breccia dykes locally pinch-out into narrow gouge fault zones, with little associated distributed deformation. Steeply dipping tuffisite dykes are parallel to the trend of faults in the host rock (Figure 5.3). These observations suggest tuffisite dykes may have been emplaced by reactivation of an existing fault or were triggered by fault movement, although tectonically driven extension was probably not an important mechanism. Likewise, late breccia dykes are parallel to faults in the host rock but almost devoid of distributed deformation, suggesting a similar mechanism of formation to tuffisite breccia dykes. The possible role of fluid pressure in triggering this failure is discussed below (section 7.4.2).

As noted previously (section 3.1), there is evidence from other breccia pipe systems that active, structurally induced extension was an important part of the brecciation mechanism. Bryant (1968), described the close association between fault zones and intrusive breccia pipes in the Warren mining district (Arizona). He states that the breccia: "pipes and irregular masses generally are in areas of intense shattering produced by fault intersections or drag folding of brittle rocks. Pipe-like breccias also fill the opening created by movement along curved faults" (i.e. dilational fault bends; Sibson, 1989b). The observations of Cloos (1941) on the mechanism of formation of the Schwabischen tuff slots (elongate pipes; Chapter 2) also suggests strong structural control on pipe formation. The presence of a clearly defined sedimentary layering, allowed him to make detailed observations of the rock fragmentation mechanism during tuff slot formation. The following observations of Cloos (1941) indicate the importance of fault control on initial fragmentation and host rock extension during tuff slots formation:

(1) Large blocks which occur in the slots, though "tuffified", preserve their internal stratigraphy and are rotated to a steep dip. Untuffified blocks near the margin of the slots contain many faults,

and are folded and flexured which results in extensive fragmentation of the host stratigraphy. However, equivalent stratigraphic layers outside the slot contact zone do not show this deformation which indicates that the structures formed during slot development.

(2) The relationship between the major fault at the margin of the tuff slot and the linking small scale antithetic faults suggests oblique slip extension during slot formation.

(3) Tuff dykes at the margin of the slots fill faults and fractures in the host rock. Because one set of tuff dykes is offset by a fault which is filled by a second tuff dyke, fault movement overlapped with tuff dyke injection.

In the Balbriggan Inlier (eastern Ireland), Murphy (1984) suggests fluidised breccias, emplaced in a brittle/ductile environment, are localised by syn-breccia extensional sites in the overall D<sub>2</sub> stress field. At high crustal levels, in the absence of associated magmatic processes, dilational jogs are characterised by features which suggest incremental extensional opening (crustiform fissure veins) or by high dilation breccias (hydrothermally cemented wall rock fragments; Mckinstry, 1948; Sibson, 1987). Larger active dilational jogs are inferred to consist of a mesh of linked extensional fractures and subsidiary shears (Hill, 1977; Sibson, 1989a), which are commonly mineralised, though the large driving faults are generally barren of hydrothermal mineralisation. Mitcham (1974) suggested breccia pipes result from rock burst into dilational sites on fault planes. The mechanism proposed here differs from that of Mitcham (1974) because, though tectonic extension is important for host rock deformation and extension in the breccia complex, facies characteristics of the breccia units demand the involvement of a magmatic fluid phase during brecciation (see section 7.5).

### 7.3.2 Igneous emplacement

At the regional scale there is little doubt that the wrench system (Mt. Leyshon corridor) and associated transtension localised magmatic activity at the intersection between the two regional scale corridors. Indeed, several workers in other areas (Glazner, 1991; Hutton and Reavy, 1992; Petford and Atherton, 1992; Tikoff and Teyssier, 1992) have recently argued that batholith emplacement at transpressional continental margins, at mid to upper crustal levels, is controlled by both extensional and transcurrent shear on strike slip faults. Meyers and Foland (1991) have also recently described magmatic-tectonic interaction during early Rio Grande rift extension (Questa, New Mexico). At upper crustal levels, they infer overlying brittle normal faults rooted in a zone of ductility provided by the magma chamber.

In outcrop of the Mt. Leyshon breccia complex there is little direct evidence to suggest that igneous emplacement was controlled by active faulting. Observations of dyke contacts in the pit and drill core sections suggest that minor vertical and horizontal offset is associate with the intrusion of some dykes. Despite the general absence of marker units to assess the style of fracturing associated with dyke emplacement, most dykes appear to have been intruded by extensional fracture. The reactivation of pre-existing structures by dykes and the coincidence of the dominant dyke trends in the complex with those of dominant structures (Chapter 3) indicates

reactivation during dyke emplacement. The orientation of porphyry units II and III are consistent with the inferred local stress conditions (E-W compression) and emplacement during extensional shear fracture on conjugate fault sets. Other porphyry bodies and dykes are multi-directional, suggesting that high magma pressure controlled the orientation of these bodies (section 7.4.2). Nevertheless, mineral alignment fabrics, which are locally found in outcrop at a high angle to flow banding and the strike of dykes and porphyry bodies are possibly due to emplacement related deformation (see Petford and Atherton, 1992).

The fracture mechanics of magma transport in the crust was reviewed by Shaw (1980). He considered that the process of magma ascent in the crust involves incremental episodes of magma injection that follow fracture pathways controlled by the stress state in the rock, and the locally acting magma fluid pressure. Magma is considered by Shaw (1980) to act as a distributed fluid phase and can control the stress state through the principle of effective stresses in a similar way to pore fluid pressure (by reducing the level of normal stress on existing planes and encouraging extensional shear failure). That this process was occurring in the crust during the formation of the Mt. Leyshon breccia is suggested by the occurrence of fine networks of porphyry unit III and IV magma laterally and above the main igneous bodies (Chapter 2). In addition, the cognate igneous fragments present in breccia units of the complex may possibly be derived by break up and transport of such fine igneous networks during brecciation. Post-breccia igneous networks occur within the Mt. Leyshon and Mt. Hope breccias.

#### 7.4 THE ROLE OF A FLUID PHASE IN BRECCIATION

The facies characteristics of the Mt. Leyshon breccia units (Chapters 2 and 5) strongly suggest the involvement of a fluid phase in the brecciation mechanism. Breccia units show signs of having formed by forceful injection of a high pressure fluid phase into the host rock (rather than low pressure open system discharge to the surface). Extreme attrition of host rock and hydrodynamic sorting of fragments in main pipe breccia and tuffisite breccia dykes indicates fluid release was prolonged during the formation of these units.

The role of volatiles and magmatic evolution in the formation of the Mt. Leyshon breccia complex was clearly protracted. A discussion on the later stages of fluid / magma evolution associated with the Mt. Leyshon complex must be able to account for the observed sequence of igneous emplacement, breccia generation and hydrothermal activity. Detailed mapping, core logging, polished slab and thin section studies have defined four episodes of breccia complex evolution (Chapter 4). This evolution which includes twelve igneous emplacement events, five major brecciation and at least sixteen hydrothermal events are summarised in Figure 4.4. A complete analysis of the implications of this data to fluid evolution in the breccia complex constitutes a separate study, involving extensive fluid inclusion and geochemical investigation.

Some preliminary work on the nature of the hydrothermal fluid was undertaken by Morrison et al. (1988) who developed a basic mineral paragenesis and discriminated three stages of hydrothermal evolution. His isotope data are based on this basic paragenesis and do not relate to the fluid

responsible for brecciation (see below), which is the main concern of this section, and are discussed later (Chapter 8). In the first part, the evidence for the likely character of the fluid accompanying brecciation is assessed. In the second part, evidence for the role of non-explosive hydrofracture in the complex is examined. Finally, the fragmentation characteristics of the breccia units are related to possible physical processes during rapid fluid release.

#### **7.4.1 Source and nature of the fluid phase**

The facies characteristics of later breccia units strongly suggest involvement of a magmatic fluid phase in the brecciation process. The source of the fluid accompanying main pipe breccia formation is unknown, though it follows from the inferences made above (section 7.2) that the fluid release possibly occurred at a depth of several kilometres beneath the present level of exposure. It is possible the source of high pressure fluid driving breccia intrusion was from a large non-magmatic source (e.g. mantle degassing). However, the presence of intermediate and felsic (?cognate) xenoliths in the main pipe breccia implies the existence of a well established magma system coextensive with breccia formation. For these reasons the source of the fluid phase accompanying main pipe breccia formation is also assumed to be from a magmatic system.

Critical evidence for the nature of the fluid phase accompanying brecciation is provided by detailed documentation of the hydrothermal alteration paragenesis in the complex (Chapter 4). This evidence indicates that the first hydrothermal event in at least four of the five brecciation events was an alteration including the following mineral phases illite/smectite-silica-albite. In the main pipe breccia this alteration replaced breccia matrix, and where intense, replaced fragments. Prograde alteration (episode II; Figure 4.4) overprints this low temperature assemblage. Likewise, zones of relatively fresh Mt. Leyshon breccia, tuffisite breccia dykes and late breccia dykes provide indirect evidence for the nature of subsequent magmatic vapour release (episode III). The matrix in these units is again replaced by an illite/smectite-silica-albite assemblage, and prograde alteration (episode IV; Figure 4.4) overprints this initial alteration.

Considerable recent work has shown that illite/smectite clays are very useful indicators of metamorphic grade (cf. Eberl, 1993). This work is based on tertiary and younger shales, sandstones and volcanics, and suggests in these rocks a temperature of approximately 200°C for the illite/smectite to illite transition and approximately 275°C for illite to muscovite. Hedenquist and Reid (1984) also suggest a similar temperature for illite/smectite clays formed as a hydrothermal product. These data suggest the early argillic alteration in the breccia units resulted from a fluid phase of approximately 200°C. Because the fluid was most likely of magmatic origin, and cooled adiabatically by expansion, it is likely to have been significantly hotter than 200°C, the simple interpretation is that during brecciation the fluid phase did not produce any discernible alteration (see section 7.4.2 for the origin of argillic alteration).

This conclusion is contrary to the common belief that much of the alteration associated with breccia pipes is a consequence of the breccia mechanism; exsolution of a high salinity aqueous fluid phase (second boiling) in the magma (e.g. Burnham and Ohmoto, 1980; Sillitoe, 1985;

Whitney, 1989). However, as discussed later (section 7.5.2), it is consistent with the extensive work of Giggenbach (1992), who concludes that magmatic vapours are rich in volatile phases such as HCl and CO<sub>2</sub> and that at temperatures above 600°C the fluid will be inert with respect to rock alteration. Therefore, these observations suggest that the magmatic system underwent several periods of extensive degassing, and also that this degassing was an important precursor to hydrothermal fluid evolution.

#### 7.4.2 Non-explosive processes resulting from high fluid and magma pressure

The following geological phenomena indicate the existence of high fluid pressures during the formation of the breccia complex:

- (1) Stage I quartz veins (steep).
- (2) Laminated quartz molybdenite veins (steep).
- (3) Igneous sill injection.
- (4) Vertical and gently dipping tuffisite breccia dykes.
- (5) Late veins (vertical and gently dipping) and irregular rebrecciation zones.
- (6) Reactivation of severely misorientated strike slip faults.

Both the regional and local stress conditions were important controls on the Mt. Leyshon breccia complex because they directly control the style of brittle failure of the host rock. As already discussed, the structural setting of the breccia complex is dominated by strike slip faults. At the inferred depth of the breccia complex, the rock mass is likely to be fluid saturated, with a uniform internal fluid pressure ( $P_f$ ). The fluid pressure acts to counteract any normal stress, but has no effect on the level of shear stress. Thus, the *effective* normal stresses are given by  $\sigma_n' = \sigma_n - P_f$  (Sibson, 1989a). The mechanical response of the rock mass is then governed by the *effective* principle stresses [ $\sigma_1' = (\sigma_1 - P_f) > \sigma_2' = (\sigma_2 - P_f) > \sigma_3' = (\sigma_3 - P_f)$ ]. The fluid pressure at a depth ( $z$ ) in the crust with an average density ( $\rho$ ) is related to the overburden pressure (vertical stress,  $\sigma_v$ ) by means of a pore fluid factor ( $\lambda_v = P_f / \sigma_v = P_f / \rho g z$ ) and the effective overburden pressure may then be written (Sibson, 1989a):

$$\sigma_v' = (\sigma_v - P_f) = \rho g z (1 - \lambda_v)$$

A state of hydrostatic fluid pressure prevails when  $\lambda_v \sim 0.4$ . However, fluid pressure in areas of actively deforming crust (at  $> 2$  kilometres) are commonly supra-hydrostatic (Yerkes et al., 1990) and can approach lithostatic values with  $\lambda_v \rightarrow 1$ , in which case  $\sigma_v' \rightarrow 0$  (ie. the effective vertical stress approaches a tensile state). That fluid pressures periodically exceeded lithostatic load in the breccia complex is indicated by the presence of flat lying extensional veins of a number of stages in the paragenesis. In a similar way, and already eluded to above (section 7.3.2), the magma pressure can control the effective stress state in the crust. The injection of igneous sills around Mt. Leyshon indicates that magma pressure exceeded lithostatic load at this time.

The structural and mechanical significance of the stage I quartz veins is poorly resolved, as a consequence of their disruption and partial destruction during the main pipe breccia. Likewise, the nature of the quartz molybdenite veins is only partly resolved (Chapter 3). However, both have

textures suggesting they formed by incremental episodes of extension and the quartz-molybdenite veins appear to have formed under the influence of the local stress field. Hydraulic (extension) fractures form in intact rock perpendicular to  $\sigma_3$  when  $P_f = \sigma_3 + T_0$ , provided that the differential stress ( $\sigma_1 - \sigma_3$ )  $< 4T_0$  is, where  $T_0$  is the tensile strength of the rock (Etheridge, 1983). It is probable that the crack-seal-like veins (Ramsay and Huber, 1987) in the Mt. Leyshon breccia complex formed in response to cyclic fluid pressure fluctuations. These types of veins are increasingly suggested in some cases to be related to the earthquake stress cycle (Sibson, 1981; Mawer and Williams, 1985; Sibson, 1989b). Furthermore, high fluid pressure levels are a plausible triggering mechanism for earthquake ruptures (Sibson, 1992). The formation of these veins in the complex, as a pre-cursor to large scale brecciation, is consistent with the suggestion that earthquake ruptures are responsible for some of the distributed deformation and host rock extension, associated with main pipe, Mt. Leyshon and Mt. Hope breccias (section 7.3.1).

Reactivation of faults which are orientated at  $> \sim 54^\circ$  to  $\sigma_1$ , like those in the Mt. Leyshon complex (section 3.6.2), maintain that the effective least compressive stress should become tensile ( $P_f > \sigma_3$ ), to keep the differential stress level below that which would cause shear failure of the surrounding intact rock (Sibson, 1989a). Severely misorientated strike slip faults are typical in areas of actively deforming crust (Thatcher and Hill, 1991). The stability of these planes is determined by the standard Coulomb relationship (Sibson, 1989b):

$$\tau = C + \mu_s (\sigma_n - P)$$

where,  $\tau$  and  $\sigma_n$  are the shear and normal stress on the plane,  $P$  is the rock fluid pressure,  $C$  is the cohesion across the plane and  $\mu_s$  is its coefficient of friction. Because regional strike slip faults intersecting the complex are commonly formed by reactivation of ductile basement faults, the reactivation of severely misorientated strike slip faults and veins in the vicinity of the complex, strongly suggests the operation of a high fluid pressure mechanism.

The fluid pressure imbalance and suctional forces apposing slip transfer, resulting from rapid extensional rupture across large scale dilational fault irregularities (section 7.3.1), forms the basis of the increasingly accepted "suction-pump mechanism" (Sibson, 1985). During, and following after shock activity, the lowered fluid pressure within the jog is restored by inward fluid percolation from the surrounding rock. Shear failure of these planes can occur by increasing  $\tau$  or  $P_f$  and Nur and Brooker (1972) provide an explanation for the pattern of aftershock activity due to fluid redistribution. Sibson (1989a) argues that the fluid pressure imbalance leads to time-dependent shear failure as fluid pressure is progressively restored in the regions of reduced mean stress. The cyclic nature of earthquake activity, therefore leads to cyclic variations in fluid pressure and as a consequence repeated mineralisation within dilational segments on strike slip faults. This mechanism is possibly responsible for the initial low temperature alteration event overprinting the breccias (suggesting an influx of low temperature fluid; section 7.4.1), given the likely mechanism by which strike slip fault induced host rock extension occurred in the complex (section 7.3).

The prograde sequence of hydrothermal alteration identified in the breccia units would be due to increased mixing of this diffusing pore fluid with magmatic vapour. It is possible low pressure magmatic vapour discharge became partially coupled with aftershock activity and pore fluid infiltration. In the main pipe breccia, such a mechanism may have caused lithification of fragments and matrix, and restored the mechanical strength to the crust. In the Mt. Leyshon breccia, the repeated sequence of extensional and shear-fibre veins (Chapter 3 and 4) which controlled episode IV mineralisation (Figure 4.4) is consistent with such cyclic variations in fluid pressure during after shocks. Indeed, McKibben and Elders (1985) suggest that in the Salton Sea geothermal system, periodic seismic fracturing allowed fluid flow and precipitation of mineralisation. Dynamic modelling of fluid flow during deformation has recently begun (Ord and Oliver, 1992) and should provide interesting implications for mineralisation in actively deforming crust.

Because there is considerable evidence for the role of a gas phase in brecciation within the Mt. Leyshon complex, transient high gas pressures would also effect the local stress state. It is argued (section 7.5) that magmatic systems which display evidence for open system behaviour are potentially capable of transferring volatiles through the crust. Such volatile transfer may become decoupled from the magma source region and give rise to high gas pressures at upper crustal levels in combination with volatile exsolution from the magma. The presence of gently dipping tuffisite dykes, which have facies characteristics suggesting a close association with a gas phase, indicate transient supra-lithostatic gas pressures. The presence of this gas phase also would reduce the density of the magma column and assist dyke injection (Carrigan et al., 1992).

The previous discussion emphasised the critical role of pore fluid, magma and gas pressure through effective stress, on the style and mechanics of brittle deformation. It is proposed here that, where magmatic activity occurs in areas of actively deforming crust, such as at Salton Sea and the Mt. Leyshon breccia complex, the state of stress is likely to be dependent on the coupled effects of tectonic stress, and pore fluid, magma and volatile pressure. Clearly, these processes are independent and will control the style of brittle deformation during a given brecciation event. Hence a wide variety of breccias are possible, without the need to resort to different mechanisms in each case. Thus, in the following section, the style of brecciation, is related to the dominant mode of hydrofracture. The episodes of strike slip faulting and associated extensional failure in the region around the breccia complex would provide the means for communication between the different parts of the magma / magmatic gas / crustal fluid systems.

### **7.4.3 Explosively driven hydrofracture and time dependent gas discharge**

Facies analysis in the Mt. Leyshon breccia complex (Chapters 2 and 5) recognises three texturally and geometrically distinct fragmentation styles. These are best defined in the Mt. Leyshon breccia, where facies characteristics and the geometry of the pipe zones suggest:

- (1) Initial (1st order) host rock fragmentation and extension throughout the pipe area.
- (2) Subsequent erratic (2nd order) host rock fragmentation and expansion.

(3) Further (3rd order) fragmentation, attrition and mixing resulting from fragment mobility/transport.

The probable origin of first order fragmentation resulting from strike slip faulting and tectonically driven extension is discussed above (section 7.3.1). The possible origin of second and third order fragmentation is considered in this section. Second order host rock fragmentation typically develops irregular distributed zones of expansion and fragmentation. Tabular and splinter shaped fragments are common in these zones. In the Mt. Leyshon breccia, highly telescoped tabular shaped fragments in a flow aligned matrix define regions of localised host rock expansion coeval with brecciation, in the presence of a fluid phase/matrix. Erratic high expansion zones in basement linked to main pipe breccia zones also have a similar form (though tabular shaped fragments are less common, probably due to rheological considerations). Sillitoe and Sawkins (1971) describe vertical and horizontal tabular shaped fragments, very similar to those in the Mt. Leyshon breccia pipe, from several Chilean breccia pipes. They interpret their origin as resulting from toppling and down settling of detached fragments following host rock collapse in the pipe. However, the highly expanded nature of fragments in the Chilean and Mt. Leyshon breccia pipes, with abundant jigsaw fit textures and a high matrix proportion (compare figure 5 of Sillitoe and Sawkins, 1971, with Plates 5.11 and 5.12), suggests a more explosive origin, contemporaneous with host rock extension.

Tabular and splinter shaped fragments in breccia pipes have also been inferred to result from processes such as decompressive shock, hydraulic implosion, and hydraulic fracturing followed by collapse (cf. Phillips, 1972; Baker et al., 1986; Laznika, 1988). However, the author has found little work demonstrating the physical basis for these interpretations of fragmentation process in breccia pipes. Observations from underground excavations in deep mines indicates that tabular fragmentation in cavities results from wall rock failure under conditions of high differential stress (Hoek and Brown, 1980). When the excavation is unstable, tabular shaped rock fragments spall off the perimeter during rock burst. Similar shaped rock fragments described in the Mt. Leyshon breccia pipe are associated with the development of free space (distributed extension), and possibly formed by this process. According to Hoek and Brown (1980), rock burst conditions are possible in an excavation in very good quality quartzite when:

$$P_z / \sigma_c > 0.5$$

where,  $P_z$  is the vertical applied stress, and  $\sigma_c$  is the tensile strength of intact rock. It is also assumed that the tensile strength of the rock is isotropic. Assuming that the Mt. Leyshon breccia pipe formed at a depth of 2-3 kilometres, this approximates to a 54 - 80 MPa vertical stress ( $P_z$ ; as measured in underground tests). Point load testing of main pipe breccia (unpublished report, Sullivan, 1992) suggests a tensile strength of approximately 130 MPa ( $\sigma_c$ ). According to these values,  $P_z / \sigma_c = 0.4 - 0.6$  during host rock extension in the pipe. Given that the host rock to the pipe was probably not intact nor isotropic, due to the action of inter-breccia shear zones (Chapter 3), rock burst conditions are a likely consequence of extension and local space development

during breccia pipe formation, as proposed by Mitcham (1974).

Sibson (1986), has suggested the sudden fluid pressure differentials generated in dilational jogs during rupture arrest (Sibson, 1985), and consequent hydraulic implosion, is the more common mechanism for producing high dilational breccias. High dilational breccias at the southern end of the Mt. Leyshon breccia pipe, possibly resulting from this mechanism have already been noted (section 7.3.1). However, neither of these mechanisms alone accounts for the presence of a flow aligned matrix supporting the tabular fragments or the local mixing with transported fragments. Furthermore, the presence of gently dipping highly expanded tabular fragment bearing zones in the Mt. Leyshon breccia pipes (and probably also in the Chilean pipes) indicates vertical extension of the host rock, and that fluid pressures exceeded lithostatic load during pipe formation. Based on fluid inclusion data, Norman and Sawkins (1985) also suggested that the fluid pressures were well above lithostatic, during the early mineralisation stage in the Tribag breccia pipes (Ontario). Thus, it is proposed that the formation of tabular and splinter shaped fragments in breccia pipes results from explosive release of magmatic vapour into the space produced by distributed tectonic extension. The inferred gently dipping contact between main pipe breccia and granite (section 5.5), provided one locus for vertical extension resulting from a fluid pressure greater than lithostatic. Further liberation of splinter shaped fragments in these inflated regions may have occurred by hydraulic implosion (or free surface spall) during explosive hydrofracture. The theoretical considerations of Burnham (1979, 1985) demonstrate the tremendous energy released from magmatic systems undergoing decompression. However, the important difference between his model and the one suggested here is that failure of the magmatic system, and as a consequence vapour decompression, results from tectonic extension, rather than second boiling.

There is a textural gradation between erratic, expanded high-matrix zones and polymict breccia zones. Third order fragmentation involves local break-up of previously liberated fragments and attrition of fragments during transport, and further liberation of fragments as material is injected into host rock. These processes are largely the result of the mechanical action of a high pressure fluid phase. The degree to which third order fragmentation and associated hydrodynamic features (grading, layering, sorting, etc) are developed in a breccia unit is likely to be strongly time dependent. Thus, fluid dynamic considerations coupled with time dependent vapour discharge are likely controls on many of the variations in third order fragmentation characteristics of breccia units (pipes or dykes).

Explosively driven hydrofracture refers to gas driven fracture propagation in rock, and has a variety of geotechnical applications (e.g. rock blasting, hydrofracture of petroleum wells and underground nuclear testing). The limiting factors on this style of hydrofracture may help to explain the mechanism of breccia formation in the Mt. Leyshon complex and elsewhere. Nilson et al. (1991) illustrate the processes involved in explosively driven hydrofractures, through numerical modelling of underground (low yield) nuclear explosions detonated in a pre-mined spherical cavity. The following account of this phenomena is based on their work. The model of Nilson et al.

(1991) combines for the first time stress wave dynamics with fluid mechanics and includes many features thought to be important in controlling the speed and extent of explosively driven hydrofractures (e.g. heat and seepage losses from the fluid to the rock, dynamic rock motion, single or multiple discrete fractures, etc.).

There are obviously several differences between explosively driven hydrofracture during a nuclear explosion and that which possibly occurs in breccia pipe formation. For example, the pre-mined cavity is probably under lower confining stress and an external fluid source is inferred for explosive hydrofracture in the Mt. Leyshon complex. In the nuclear case, the explosive release of very high temperature gas (10 000° K) results in further cavity growth during extensive vapourisation and expansion of the host rock. Nevertheless, the gas phase cools extremely rapidly to below the vapourisation temperature, due to the addition of mass, and thereafter would behave in a similar way to hydrofracture inferred in breccia pipes. The facies model of brecciation in the complex suggests explosive gas release into a region of either distributed or localised extension. Therefore, general implications of their hydrofracture model may also be applicable to breccia mechanisms.

There are two primary mechanisms which constrain the growth of gas-driven fractures in rock:

- (1) Stress wave dynamics are important controls on the stress field, the expansion of the cavity and the cavity pressure. These solid dynamic considerations also control the small scale near field fracturing associated with explosive release.
- (2) The long-range extension of the most prominent fractures is critically dependent upon gas dynamic considerations (e.g. turbulent friction, heat and fluid loss to fracture walls) because the penetration of cavity gases into fractures can cause a tenfold to hundredfold increase in their length. The ultimate extent of the long range fractures is generally controlled by the depletion of the cavity which, in turn, depends upon the rate of these heat and seepage losses, in addition to the number of fractures and their respective volumes and surface areas.

The model results suggest that as the degree of expansion increases fluid dynamic constraints on hydrofracture become dominant over solid dynamic (stress induced) constraints. Consequently hydrofracture evolves from a stress limited to depletion limited system, favouring long range propagation of fractures. In addition, as the loading rate decreases the stress wave dynamics will become less important and the overall rate of the process will be controlled by fluid dynamic considerations. The circular fracture patterns reported from some breccia pipes (e.g. in the Shoshone Range, Nevada; Gates, 1959) may be due to shock wave rebound stresses at the pipe margin, following explosive vapour release.

These results imply that explosive hydrofracture is possible in breccia pipe formation if during dynamic host rock extension (structural and shock wave induced) the cavity pressure is greater than the minimum compressive stress at a given point in the pipe. In addition, explosive hydrofracture will be least effective in breccia pipe formation when a network of distributed fractures (allowing considerable seepage) forms part of the brecciation mechanism. In contrast,

when only few fractures are present, explosive hydrofracture will lead to long range extension dependent on depletion of the cavity. Host rock rheology will also effect the formation of both near field fractures and long range fracture extension during brecciation.

It was also found that as the size of the pre-mined cavity is increased (up to a critical size) less of the explosive energy is expended in rock melting, vapourisation and deformation, leaving a greater fraction of energy within the cavity gas. Obviously, at the likely gas temperatures involved in the complex (800-500°C) melting or vapourisation of the host rock will not be involved. However, as host rock extension increases, and as a consequence the void space in which brecciation can occur, more of the available energy in the gas is available for hydrofracture. Two aspects of their numerical modelling process highlight the possible effect of hydrofracture in breccia pipes. Firstly, there can be any number of preselected fractures to which fluid pressure is applied or alternatively fractures can be made to open wherever the local fluid pressure exceeds the minimum confining stress. In this later case, hydrofracture sometimes results in swarms of cracks and inflated regions of fluid intrusion. If explosive hydrofracture does contribute to breccia unit formation then existing strongly deformed regions of host rock (e.g. metasediment in the breccia complex) will become further fractured and inflated during extension and vapour release. Second order fragmentation in the breccia complex possibly formed by this mechanism. In contrast, when significant distributed deformation does not form part of the brecciation process (e.g. tuffisite breccia dykes) hydrofracture would favour explosively driven discrete long range fractures. In this case, third order fragmentation (prolonged transport and attrition) would dominate, such a situation is observed for tuffisite breccia dykes.

As the size of the cavity increases the fracturing regime changes in a qualitative manner as the explosion becomes progressively decoupled. Three different regimes of fracture constraint can be distinguished:

- (1) *Stress limited cracking* where the hoop stresses around the cavity are always sufficient to terminate crack growth.
- (2) *Speed limited cracking* where a window of time exists when the confining stresses are too weak to contain the cavity pressure, and explosively driven hydrofracture results. Within this time period the crack speed is controlled by solid dynamic and fluid dynamic constraints; if the crack runs slow enough and the (stress wave induced) rebound occurs soon enough, it may still be possible to slam the crack shut.
- (3) *Depletion limited cracking* where hydrofracture takes place because the surrounding rebound stresses are either too weak or too late to stop the crack propagating out of the near field. In this case the ultimate extent of the fracture is controlled by the decay of cavity pressure which results from gas flow into the fracture and losses of heat and mass to the fracture walls.

These model results suggest that the role of the fluid phase in breccia formation will be partly dependent on the style of hydrofracture and the decoupling of the fluid phase from host rock extension. The characteristics of the Mt. Leyshon breccia can be interpreted as resulting from a

tendency towards stress limited hydrofracture, whereas tuffisite breccia dykes have characteristics consistent with a depletion limited system. The characteristics of the main pipe breccia are consistent with initial stress limited hydrofracture, but as host rock extension or rate of vapour release increased, fluid dynamic constraints would dominate, favouring depletion limited vapour discharge, and prolonged fragment transport/mobility and attrition.

## 7.5 THE ROLE OF THE MAGMATIC SYSTEM IN BRECCIATION

Facies analysis of the igneous units (Chapter 2) and igneous unit geochemistry (Chapter 6) provide evidence for the role of the magmatic system in brecciation. Possible physical processes in the magmatic system and the nature of volatile evolution in the magma are now discussed with reference to brecciation.

### 7.5.1 Geologic constraints on physical processes in the magmatic system

As noted previously, little geologic evidence can be derived for the nature of the magmatic system contributing to main pipe breccia development. If a batholith did provide the fluid phase accompanying the main pipe breccia, it was probably at a depth of several kilometres below the present level of exposure. However, the presence of intermediate and felsic cognate igneous fragments in the breccia is consistent with the later style of igneous evolution, and implies the early presence of magmatic cycles. A large negative magnetic anomaly offset to the SW of the complex possibly represents an intrusive body genetically related to the post-main pipe breccia units. Geophysical modelling of this anomaly suggests several possible depths to the top of the body and drilling beyond the shallowest level (800 metres) did not locate an igneous body.

The field relations of the Mt. Leyshon igneous units indicate a complex sequence of intrusion, beginning (at the present level) during potassic alteration of the main pipe breccia. Initial igneous emplacement (porphyry unit I and EP dyke) occurred after lithification of the main pipe breccia but before the brittle infrastructure of the crust had become firmly re-established. This period was probably dominated by aseismic events and would have encouraged magma stability (no magma recharge) and relatively closed system behaviour, both of which favour a high degree of fractional crystallisation (ED dyke emplacement). Geologic, petrographic and geochemical evidence (Chapters 2 and 6) for the subsequent sequence of igneous intrusion, and enclaves in felsic units, suggests the following repeated cycle:

- (1) Recharge of more basic magma into the felsic magma system.
- (2) Fractionation to felsic magma compositions.
- (3) Intrusive breccia generation during vapour release.

The intrusion of intermediate units (EP dyke, porphyry unit I, sills, and DG dykes) at a number of stages in the igneous sequence indicates repeated recharge of more basic magma to the system. This is also implied by the intermediate enclaves in a number of felsic units (porphyry units II and III; 1-2, 2-2 and "fine" late dykes) which probably represent magma addition to the system not forming dykes at the level of exposure. The presence of magmatic inclusions (more basic than their host), demonstrably part of the evolving system in which they occur, has been interpreted by

many workers as indicating the process of magma mingling (as discussed in section 6.7.1.2).

During magma mingling, the turbulent transfer of heat from the basic lower layer to the felsic upper layer leads to crystallisation, volatile exsolution (providing vapour pressure  $\geq$  confining pressure) and a reduction of the bulk density in the lower layer (Turner et al., 1983). The transfer of volatiles (including CO<sub>2</sub> and H<sub>2</sub>O) to the felsic magma occurs and depending on the bulk density contrast, magma mixing (homogenisation) or mingling (formation of enclaves, xenocrysts, etc.) takes place (Turner et al., 1983; Vernon, 1983; Bacon, 1986). In the case of a sub-surface magma chamber, magma mixing or mingling and ex-solution of gas would lead to violent eruption. At the deeper levels in the upper crust, magma mingling in the Mt. Leyshon breccia complex provides indirect evidence for volatile transfer to felsic magma chambers, which would strongly enhance breccia formation. These, later igneous events represent a complex, dynamic period of magmatic evolution where the emplacement of igneous bodies both overlapped with and resulted in breccia generation. This interactive period occurred during structurally induced host rock extension. It is likely that the coincidence of widespread intrusion and breccia formation reflects the large scale destabilisation of the magma system during transtension.

No igneous body can be directly related to formation of the Mt. Leyshon breccia because vapour release possibly occurred up to two kilometres below the present level of exposure. The presence of cognate igneous fragments in the breccia possibly result from fragmentation of small scale failed intrusions during early stages of tectonically driven host rock extension. The degree of fragment transport and attrition in the Mt. Leyshon breccia, resulting from the action of a fluid phase, is significantly less than for other breccia units. The possible reasons for this are examined in section 7.6, but one possibility of significance to physical magmatic process, is considered now. Porphyry unit II also preserves evidence of small scale failed intrusions as cognate xenoliths, and it is possible that the emplacement of porphyry unit II is contemporaneous with the formation of the Mt. Leyshon breccia. If this is true, then as host rock extension proceeded during earthquake rupture perturbation (section 7.3), failure of the host rocks above the main igneous centre, would result in switching of explosive vapour release to this area.

This scenario, provides a plausible explanation for both the formation of the fragmental component of porphyry unit II, as a consequence of the redirected vapour discharge, and the limited action of a fluid in the Mt. Leyshon breccia pipe. Whatever the case, the characteristics of porphyry unit II suggest it intruded the fragmental component rapidly and turbulently, causing further fragmentation and rounding during emplacement (Chapter 2). Other workers have described similar breccias, formed in a broadly similar tectonic environment during magma intrusion of the coastal batholith of Peru. Myers (1975) describes the formation of "Baranda" sheets, which are linear zones of fragment crowded porphyry, and attributed their formation to a combination of tectonic cataclasis, magmatic stoping and mechanical rounding in the gas rich magma. Elsewhere, in the same batholith, Bussell and McCourt (1977) describe intrusive breccias formed during tectonic extension, as a result of vapour release from intruding magma.

Where exposure has allowed detailed mapping of the magmatic system associated with breccia pipe formation (Carter, 1969; Bussell and McCourt, 1977; this study), fluidly intermixed and chilled magma is spatially and temporarily associated with intrusive brecciation, igneous breccias and a larger body of more crystallised magma. Because they are not associated with wall rock chilled zones, a possible explanation for these characteristics is that these zones are chilled as a result of the dramatic cooling effect of expanding gas as it escapes from the magma system to form breccias. The general absence of magma vesiculation textures in both the Mt. Leyshon igneous units and probable quenched magma particles comprising the fine tuffisite dykes, may result from a high confining pressure.

These observations suggest brecciation in the complex resulted from vapour release, prior to and during igneous emplacement. Present models for breccia formation, recognise the need to create a void for the breccia process, and include proposals that the void formed by magma withdrawal (Perry, 1961), doming of roof rocks during magmatic fluid exsolution (Burnham, 1985; Sillitoe, 1985) or the evacuation of a vapour bubble (Norton and Cathles, 1973; Sillitoe, 1985). These models are inappropriate for breccia formation in the Mt. Leyshon complex because evidence for large scale collapse is absent. Instead, void space probably occurred by distributed extension for three breccia units and brecciation overlapped with magma intrusion not withdrawal. Furthermore, the facies characteristics of the Mt. Leyshon igneous units and elsewhere suggest that current models for late stages of magmatic evolution (e.g. Norton and Cathles, 1973; Burnham, 1985; Whitney, 1989), envisaging cylindrical shaped igneous intrusions largely behaving as closed systems, and solidifying by annular shells of magma, require modification to reflect the more realistic geological situation.

## **7.5.2 volatiles in the magmatic system**

In this section of the Chapter, available geological evidence and the results of experimental and analytical work on silicic magma systems are considered briefly to help constrain the physical magmatic processes accompanying igneous emplacement and brecciation in the Mt. Leyshon complex.

### **7.5.2.1 EXPERIMENTAL STUDIES OF SILICIC MAGMA SYSTEMS**

Holloway (1976) noted the common occurrence of CO<sub>2</sub> in likely source materials of granitic magma. He suggested that granitic magmas may be accompanied by a CO<sub>2</sub>-H<sub>2</sub>O fluid phase during their ascent in the crust, and demonstrated experimentally that the evolutionary course of a magma can be greatly altered through the presence of a finite quantity of CO<sub>2</sub>. Few estimates for CO<sub>2</sub> solubility in synthetic granitic magmas have been made, though Swanson (1979) quotes values in the range 0.5-0.9 wt. % CO<sub>2</sub> (the amount depending on pressure, temperature, magma composition and water content). Basic less polymerised melts dissolve more CO<sub>2</sub> than acidic melts (Mysen et al., 1976). In granitic melts CO<sub>2</sub> is strongly partitioned into the volatile phase and lowers the activity of water,  $a_{\text{H}_2\text{O}}$  (Holloway, 1976). This buffering of  $a_{\text{H}_2\text{O}}$  is much more effective for high values of CO<sub>2</sub>, and Holloway (1976) demonstrated that the presence of CO<sub>2</sub> can

have a large effect on the behaviour of H<sub>2</sub>O in magmatic systems.

Swanson (1979), however, investigated the effect of CO<sub>2</sub> on phase equilibria and crystal growth rate in a synthetic granite system. He found that granitic magmas that contained CO<sub>2</sub> rich fluids and crystallised at pressures greater than 3 Kb should contain primary calcite if they behaved as a closed system. Since most granitic rocks do not contain primary calcite he concluded that the vapour in equilibrium with granitic magmas at the level of emplacement is H<sub>2</sub>O rich (CO<sub>2</sub> poor). Subsequent workers (e.g. Burnham and Ohmoto, 1980; Candella and Holland, 1986) have developed crystallisation and vapour evolution models which assume that magmatic fluids are H<sub>2</sub>O rich and that crystallising granitic bodies behave as closed systems.

As discussed previously (Chapter 6) however, few if any magmatic systems likely behave as closed systems, particularly when intermediate or basic magma compositions are involved in the differentiation process. There is also a lack of data on the behaviour of CO<sub>2</sub> in realistic granitic compositions (as opposed to haplogranite or albitic melt analogues) which additionally contain Fe, Mg, Al, P and variable quantities of Cl and F. Little data are also available on the effect on bulk CO<sub>2</sub> in melts which results from fluid-melt immiscibility or the presence of CO<sub>3</sub><sup>2-</sup> (Mysen et al., 1976) and HCO<sub>3</sub><sup>-</sup> molecules dissolved in the melt. In addition, the dynamic and punctuated crystallisation history proposed for the Mt. Leyshon magmatic system (with magma and volatile re-charge) suggests the use of closed system models such as those proposed by Burnham (1985) will be misleading when attempting to understand the processes resulting in vapour evolution in some porphyry style systems. However, such models may be more applicable to the genesis of porphyry molybdenum deposits, which are more highly differentiated and indicate progressive inward migration of repeated events involving crystallisation, resurgent boiling, fracturing and volatile loss in the apical regions of small stocks (Carten et al., 1988).

The preceding discussion highlights the problems with applying simplified crystallisation models to natural magma systems. Nevertheless, these models allow a qualitative assessment of the effect of water on the degree and rate of crystallisation in granitic systems, through the use of phase diagrams. Using this approach, Whitney (1989) showed experimentally the strong dependence of water content on degree of crystallisation within a synthetic granite in the vapour undersaturated region, at a given pressure (e.g. 5 and 2 wt.% H<sub>2</sub>O at approximately 20% compared to 70% crystallisation, respectively). Crystallisation in the water vapour saturated region (for a given set of conditions), will lead to shorter temperature ranges of crystallisation and finer grain size.

No analytical estimate has been made of the water content in the Mt. Leyshon magmatic system in this study. Several estimates have been made of water content in natural granitic magmas. For example, Naney (1983) studied the experimental stability of amphibole and biotite, as a function of P, T, and a limited range of bulk composition. He concluded that a minimum initial water content of 4 wt. % was required to crystallise amphibole in intermediate rocks at 2 Kb pressure. Maaloe and Wyllie (1975) concluded that the initial water content of most granitic rocks is <1.5 % on the basis of experimental work and the usual position of biotite in the crystallisation sequence

of many granitic rocks. Whitney et al. (1988) investigated the magmatic evolution of the Carpenter Ridge Tuff (Colorado), which has a similar phenocryst assemblage (including plagioclase, sanadine and biotite but no quartz) and bulk composition to the Mt. Leyshon felsic units. They suggest that the magma resided at depths of 1-2 Kb, contained 3-5% H<sub>2</sub>O and was close to saturation. According to their data, the presence of quartz in the liquidus phase of the Mt. Leyshon felsic igneous units suggests a lower H<sub>2</sub>O content than for the Carpenter Tuff.

This discussion suggests that the intermediate units of the Mt. Leyshon complex (which crystallise amphibole ± biotite phenocrysts) had an initial water content of around 4-5 wt. %, falling to approximately 2 wt. % for the felsic igneous units (which crystallise biotite only). However, the 1/2 dykes which appear to have "mingled" with more basic magma, resulting in enclave formation and amphibole as a phenocryst phase, are likely to have absorbed water (and other volatiles) into the melt prior to intrusion, although significantly they are not associated with a breccia forming event.

Based on a probable initial water content of 2 wt. % for the Mt. Leyshon felsic igneous units, their observed crystallinity (2-35 % phenocrysts) and a pressure of 2-1 kb (assuming a magma system at 5-3 kilometres depth), the data of Whitney et al. (1988) and Whitney (1989) suggests that the felsic units were undersaturated with respect to water. Therefore, a vapour phase dominated by H<sub>2</sub>O was probably not present during the partial magma crystallisation and emplacement (although this does not preclude a vapour phase of another composition, e.g. CO<sub>2</sub> ± H<sub>2</sub>O, see below). The occurrence of K-feldspar phenocrysts as an early crystallising phase in the felsic units is in agreement with these observations. Furthermore, the common occurrence of rounded (resorbed) quartz phenocrysts in the Mt. Leyshon felsic units is consistent with isothermal decompression in the water vapour undersaturated region (Whitney, 1989). Intermediate units of the Mt. Leyshon breccia complex are also poorly crystalline (2-10 modal % phenocrysts) and therefore are also likely to have been water undersaturated at the time of their emplacement. Banks (1976) and Cornwall (1982) point out that several petrographic and geochemical features of the intrusive rocks associated with the Ray Porphyry copper deposit (Arizona) suggest that they too did not saturate early in their crystallisation nor evolve much water.

Consequently, the igneous rocks of the Mt. Leyshon complex whose groundmasses are aphanitic probably developed these textures as a result of rapid isothermal crystallisation during "pressure" quenching in a water vapour undersaturated condition. This discussion implies that during brecciation, the second boiling reaction did not occur in the Mt. Leyshon magmatic system. Hence, alternative vapour sources not involving second boiling are considered in the subsequent section.

### 7.5.2.2 PRESENT MODELS FOR VOLATILE EVOLUTION IN PORPHYRY STYLE SYSTEMS

Recent work on magmatic evolution has centred on tin (e.g. Taylor, 1980), and molybdenum bearing systems (e.g. White, 1981), where extensive field, petrographic and geochemical investigations, most notably by Carten et al. (e.g. 1988) at the Henderson molybdenum deposit (Colorado) have resulted in the modelling of processes leading to ore formation in such systems. Furthermore, there is now a good agreement between the predicted magmatic, chemical and fluid evolution of these models and the actual observed sequence of intrusion, fracturing, fluid release and mineralisation. Existing models leading to porphyry molybdenum mineralisation suggest the following sequence of events (Carten et al. 1988):

- (1) emplacement of a small (< 0.5 kilometre diameter) compositionally zoned magma body, which is enriched at its apex in Mo, H<sub>2</sub>O, S and incompatible trace elements.
- (2) Volatile saturation at the apex leads to the evolution of an aqueous fluid, resurgent boiling and simultaneous fracturing of the host rock, releasing the volatiles. Pressure quenching of a layer of magma adjacent to the apex and uni-directional solidification textures result.
- (3) Inward crystallisation over narrow fronts (as narrow as 5 mm) and progressive enrichment of the remaining magma in the apex continues, as does resurgent boiling and fracturing of the host rock. Fluid filled fractures deposit molybdenum-silica veins ± potassic alteration.
- (4) Ore mineralising processes cease once the lowest zone of universal solidification textures form (presumably when the volatile budget is depleted). The change to more normal crystallisation may have resulted in volatiles becoming trapped in small pockets rather than becoming concentrated along broad fronts in the apex.
- (5) Further molybdenum mineralisation requires the emplacement of new magma batches.

Isotopic, fluid inclusion and alteration data for porphyry copper systems may be interpreted as resulting from either strong interaction of circulating groundwater with porphyry intrusions (Norton and Knight, 1977; Cathles, 1981), or to interaction of low density magmatic vapour with surrounding groundwater systems (Henley and McNabb, 1978; Giggenbach, 1987). However, most models proposed for magma and fluid evolution (e.g. Burnham and Ohmoto, 1980; Candella and Holland, 1986; Dilles, 1987; Whitney, 1989; Webster and Holloway, 1990) leading to brecciation, hydrothermal alteration and mineralisation involve variations on the generation of a water vapour saturated magma (second boiling), initially evolving an aqueous vapour phase. Elements including metals are partitioned into this aqueous phase, leading to hydrothermal alteration and mineralisation upon fluid release. These models are based on the extensive research noted above which is constrained by detailed field, petrographic and chemical data on tin and molybdenum mineralising systems.

Such models are commonly used to infer magmatic and hydrothermal processes leading to fluid evolution, breccia generation and mineralisation in porphyry copper deposits. However, these models require some refinement to explain many features of porphyry copper deposits. The work that has been done (e.g. Gustafson and Hunt, 1975; Titley, 1982; Cornwall, 1982; Giggenbach,

1992; this study) does not indicate successive inward crystallisation of a vapour saturated magma and mineralisation synchronous with aqueous fluid evolution. This study suggests hydrothermal evolution occurs after a considerable period of aqueous vapour undersaturated igneous emplacement, and by implication magma degassing. In addition, most existing models developed from porphyry molybdenum systems assume highly differentiated granite compositions (e.g. haplogranite) and that the initial vapour exsolved from the melt (leading to brecciation and mineralisation) during crystallisation is an aqueous fluid with negligible CO<sub>2</sub>, SO<sub>2</sub>, etc. However, as discussed above, these models do not take account of the likely open system behaviour of porphyry style magma systems, involving the emplacement of more basic magma (e.g. quartz diorite, monzonite or granodiorite) which as argued here would allow significant melt and volatile (CO<sub>2</sub>, H<sub>2</sub>O, H<sub>2</sub>, SO<sub>2</sub>, etc.) re-charge. The history of fluid evolution in gold ( $\pm$  basemetal) rich porphyry systems like Kidston, Red Dome and Mt. Leyshon is even less well known, though some work (Baker and Andrews, 1991; Heinrich et al., 1992) implies a low density magmatic vapour phase may be important in copper and by analogy gold transport.

The suggested evolution of the Mt. Leyshon complex (Chapter 4) also differs from the models discussed, and suggests that the magmatic system underwent several periods of extensive degassing, and that this degassing was an important precursor to hydrothermal evolution. Potassic and propylitic alteration overprinting the argillic alteration in the main pipe breccia supports this assertion. Subsequent events, prior to quartz-molybdenum veining, are consistent with magmatic re-charge (evidence: intermediate EP dyke and possibly porphyry phase I emplacement) and volatile transfer, extensive fractionation (evidence: felsic ED dykes) with only minor volatile loss (evidence: sericite I alteration). Quartz molybdenum veins formed in association with magmatic vapour release, though structural control is implied by their incremental growth and preferred orientation (Chapter 3, section 7.3.1).

The paragenesis of subsequent events (Figure 4.4), further suggests four periods of inert vapour degassing produced four progressively smaller brecciation events. These brecciation events preceded the evolution of the second major hydrothermal system (episode IV, Figure 4.4). The absence of coeval igneous emplacement during and after episode IV hydrothermal alteration, together with the interactive nature of igneous intrusion and brecciation, suggests that this later hydrothermal system formed from the extensively de-gassed magma during a period of no magma recharge. The wrench system, however, remained active during this period of no igneous intrusion (as evidenced by the formation of strike slip faults and shear fibre veins; Chapter 3). The implications of active faulting and fluid flow for mineralisation and alteration in the Mt. Leyshon breccia complex are noted in Chapter 8.

Several other workers have noted the weak to non-existent development of hydrothermal alteration associated with intrusive breccias elsewhere (Gates, 1959; Bryant, 1968; Carter, 1969; Myers, 1975; Bussell and McCourt, 1977), suggesting that although not widely recognised, a high temperature "inert" volatile phase is an essential component to breccia mechanisms. A corollary to

STRUCTURAL PROCESSES	FLUID PHASE PROCESSES	MAGMATIC PROCESSES
<b>CYCLE I</b>		
Earlier earthquake stress cycles develop brittle infrastructure within regional wrench system.		Emplacement of batholith at depth.
	Stage I quartz veins indicate high fluid pressure possibly triggering seismic rupture.	
<b>Main pipe breccia formation</b>		
Propagation of seismic rupture, accompanied by violent ground motion.		Rupture propagation may result in magma recharge to batholith.
Termination of propagating rupture at the large scale fault irregularity resulting from intersection of two wrench systems; opens linking fault and fracture meshes throughout the seismogenic crust (first order fragmentation). Mean stress is lowered inside the complex but increased outside.		Incipient extension may initially encourage small scale igneous intrusion at depth (hence cognate xenoliths in MPB), but as extensional opening continues, magma system becomes destabilised, leading to catastrophic failure of magma system.
	Explosively driven hydrofracture produces extensive (second order) fragmentation and host rock expansion. As expansion increases, hydrofracture system evolves from stress limited to depletion limited case, favouring long range extension of near field fracturing.	Rapid decompression of the magma system (first boiling) resulting in explosively driven hydrofracture. Second boiling of the magma system may occur during time dependent vapour discharge.
Reactivation of N-trending basement faults resulting from high vapour pressure during MPB emplacement. Vapour discharge temporarily counteracts induced suction effect resulting from fluid pressure differential between opening fractures and host rock. This may allow rapid opening of linked extension mesh and elastic strain dissipation.	Time dependent vapour discharge resulting in prolonged fragment transport, attrition, mixing and high degree of sorting. Lack of high temperature alteration, suggests the initial vapour discharge involved inert components.	
<b>CYCLE II</b>		
After-shocks (time dependent shear failure) in rhombohedral zone of complex as fluid pressure levels are progressively restored (in accordance with the coulomb criterion).	Redistribution of fluid around seismic rupture termination by diffusion from regions of increased mean stress to regions of lowered mean stress (area of complex). Argillic I alteration results from pore water collapse mixed with magmatic vapour that was highly cooled during expansion.	
	Magmatic degassing in conjunction with fluid redistribution, results in prograde hydrothermal alteration of MPB (potassic and propylitic I), loss of permeability and restoration of full mechanical strength to the crust.	Intermediate EP dyke and PU I indicate magma recharge (implying volatile transfer) and emplacement at higher crustal levels, possibly during after-shock sequence. Low pressure magmatic degassing.

Table 7.1: Inferred breccia mechanisms for the Mt. Leyshon complex. Cycles I-IV refer to main episodes of complex evolution denoted in Table 4.3 and shown in Figure 7.1.

<b>CYCLE III</b>		
Increase in shear stress during inter-seismic period results in renewal of brittle fault infra-structure. Evolution of inter-breccia structures by stress cycling.		Extreme magma fractionation and ED dyke emplacement during inter-seismic period.
Incremental opening of quartz-molybdenite veins and their orientation with respect to fault sets implies they are related to earthquake stress cycling.	Quartz-molybdenite veins crystallise from hydrothermal fluid dominated by magmatic vapour. Veins imply high fluid pressure, possibly triggering seismic rupture.	Magma degassing during sericitic I and quartz-molybdenite vein formation.
<b>III a-Mt. Leyshon breccia</b>		
Propagation of seismic rupture, accompanied by violent ground motion.		Intermediate cognate xenoliths in PU II imply magma recharge (and volatile transfer) possibly as a consequence of seismic rupture.
Perturbation of seismic rupture at inferred releasing bend, resulting in rapid slip transfer and incipient opening of extensional fault mesh (first order fragmentation). High dilation zones in MLB pipe may result from high fluid pressure differentials.		Distributed magma intrusion (rapidly cooled) resulting from incipient extension. Further opening would destabilise the magmatic system resulting in catastrophic failure (and cognate xenoliths in MLB).
High vapour pressure results in distributed high expansion zones and local vertical host rock extension. This is consistent with rebound stress restricting hydrofractures to the near field.	Explosively driven hydrofracture within rhombohedral shaped zone of incipient extension, resulting in (second order) host rock fragmentation and extension. Hydrofracture (and vapour discharge) is concentrated in steeply dipping northern pipe zone suggesting brecciation is controlled by stress limited cracking.	Rapid decompression of the magma system resulting in explosively driven hydrofracture.
	Time dependent vapour discharge, resulting in fragment mobility and limited fragment transport in zones of maximum extension. Compared to other breccia units vapour discharge was short lived or energy was dissipated rapidly (see text for possible causes).	
<b>IIIb-Fragmental component of porphyry unit II</b>		
Distributed host rock fragmentation as a result of main Mt. Leyshon breccia forming rupture or associated aftershocks.	Relative importance of depletion limited hydrofracture, time dependent vapour discharge and mechanical attrition in the magma to breccia formation is unknown. Facies relationships and absence of high temperature alteration suggest post-MLB units are closely spaced in time.	Magmatic system becomes unstable possibly resulting from distributed extension above magma chamber (see text for discussion). First boiling during breccia formation, rapidly followed by digestion of the fragmental component by PU II. Local magmatic stoping, but magma was rapidly chilled as it intruded the existing breccia.

Table 7.1: Inferred breccia mechanisms for the Mt. Leyshon complex. Cycles I-IV refer to main episodes of complex evolution denoted in Table 4.3 and shown in Figure 7.1.

<b>IIIb-Mt. Hope breccia</b>		
Crack-seal like veins in host rock to MHB suggest high fluid pressures preceeded breccia formation. Field relations imply extensional shear of host rock during formation (see text for a discussion of fragmentation mechanism).	Explosively driven hydrofracture dominated by depletion limited cracking. Moderate time dependent vapour discharge resulting in fragment transport and mixing.	Intermediate enclaves in PU III imply magma recharge as part of this breccia forming cycle. Field relations imply MHB formed during PU IV emplacement and vapour decompression.
<b>IIIc-Tuffisite breccia dykes</b>		
	Intrusion of sills indicates high magma fluid pressure.	Intrusion of intermediate sills and enclave formation in felsic dykes suggests magma and volatile recharge to system.
Lack of distributed host rock fragmentation associated with TBDs suggests structural processes of minor importance to breccia mechanism. Though their injection along faults suggests they formed either during the final seismic period of dominantly aseismic shearing or during static hydrofracture resulting from high magma or fluid pressure.	Depletion limited hydrofracture leads to long range extension of a limited number of existing fractures/faults.	First boiling and possibly inter-system vapour transfer.
High fluid pressure results in vertical host rock extension during fine FTD injection. Coarse and medium variants may result more from attrition and replacement of host rock during fluid hydrofracture and streaming, rather than extension.	Time dependent vapour discharge focused into long range hydrofractures results in extreme fragmentation, mobility and transport. Fluid phase system possibly evolves from fixed bed discharge to true fluidisation, once sufficient porous network of CTD has developed.	Once connectivity of expanded hydrofractures is sufficient, magma disaggregation and injection into hydrofractures during vapour discharge. The absence of vesiculation during magma chilling and disaggregation, may result from a high confining pressure.
<b>IIId-Late breccia dykes</b>		
		DG dyke emplacement suggests recharge of more basic magma into system, implying volatile exsolution and transfer.
Passive hydrofracture resulting from magma pressure or seismic rupture.	Depletion limited explosively driven hydrofracture of a single fracture during dyke emplacement. Time dependent vapour discharge along structure.	Magma disintegration and quenching results from vapour discharge from leading edge of dyke during intrusion.
<b>CYCLE IV</b>		
After-shocks in western half of the breccia complex as fluid pressure levels inside the complex are restored. Deformation is discrete in homogenous lithologies but forms diffuse microfractures in porphyry bodies and enechelon veins in breccia units. Repeated sequence of veins that form initially in extension but high fluid pressure allows shear failure.	Fluid diffusion into the breccia complex as a result of pressure differential between host rocks and western half of complex. Initial pore water collapse forms argillic II alteration of units. Subsequent prograde and retrograde alteration sequence (Figure 4.4) forms during cyclic fluid pressure fluctuations. Hydrothermal alteration reflects the relative proportion of magmatic vapour in the fluid.	Low pressure magma degassing, possibly coupled to aftershocks.

Note: MPB=main pipe breccia, PU I-PU IV=porphyry unit I-IV; MLB=Mt. Leyshon breccia; MHB=Mt. Hope breccia; TBD=tuffisite breccia dyke, FTD+CTD=fine + coarse variants.  
Table 7.1: Inferred breccia mechanisms for the Mt. Leyshon complex. Cycles I-IV refer to main episodes of complex evolution denoted in Table 4.3 and shown in Figure 7.1.

this is that because breccia pipes are ubiquitous in porphyry style deposits, degassing may represent a vital link between igneous emplacement and subsequent magmatic evolution resulting in hydrothermal alteration and mineralisation. Support for this hypothesis indirectly comes from Giggenbach (1992), who suggests two modes of magma degassing are possible:

- (1) High temperature degassing at temperatures of  $> 1000^{\circ}\text{C}$  which he suggests is only associated with freely degassing of liquid magma.
- (2) At deeper levels in the crust, solidified magma will form a barrier to direct release of magmatic volatiles. In this case degassing of volatiles occurs only from pore spaces in the solidified magma once brittle fracture is possible ( $<400^{\circ}\text{C}$ ), at which point they will escape into invading ground water.

However, a third mode of degassing is suggested by the work in this thesis. Geologic (section 7.5.1) and paragenetic (section 7.4.1) evidence suggests early high temperature degassing driven by distributed tectonic extension. In this mode, later degassing from solidified magma (and still molten pockets) into invading groundwater is consistent with the observed paragenetic sequence of hydrothermal alteration.

In addition to geologic, mineralogic, textural and paragenetic evidence already discussed, several observations are made in this section on the likely important to the brecciation process of volatile species other than  $\text{H}_2\text{O}$  ( $\text{CO}_2$ ,  $\text{HCl}$ ,  $\text{SO}_2$ ,  $\text{H}_2$ , etc) in magmatic systems, particularly those in which open system exchange is indicated. Investigation of volcanic emissions (Gerlach, 1986, 1991; Giggenbach et al., 1990) indicates that they are dominated by  $\text{CO}_2$  (which is clearly of magmatic origin) but also include  $\text{HCl}$ ,  $\text{SO}_2$  and  $\text{HF}$ . These studies also indicate that extensive  $\text{CO}_2$  degassing occurs from active volcanos of the mid-oceanic ridge system, convergent plate (continental margin and island arc) and intra-plate (continental volcano and oceanic hot spot). This is also true of volcanic emissions where there is little possibility for a crustal contribution of  $\text{CO}_2$ . In addition, published  $\text{CO}_2$  emission rates for sub-aerial volcanos (7 values; Gerlach, 1991) suggest that  $\text{CO}_2$  emission rates during eruptive periods are 1 to 2 orders of magnitude higher than during quiescent periods. Furthermore, the monitoring of volcanic degassing on the Kilauea (Gerlach, 1986) and Navado del Ruiz volcanos (Giggenbach et al., 1990) suggest early loss of "volatile"  $\text{CO}_2$  leading to high relative sulfur and chlorine contents in vapours produced from already gas depleted magmas.

Hydrogen and oxygen isotope data indicate extensive degassing of  $\text{H}_2\text{O}$  from an obsidian dome rhyolite melt (Taylor, 1991) and carbon isotope data indicates  $\text{CO}_2$  degassing from a tholeiitic basalt melt (Gerlach and Taylor, 1990). The effect on the fluid phase coexisting with a felsic magma which becomes underplated or contaminated by mafic magma has not been examined.  $\text{CO}_2$  in mafic magmas will usually exsolve but not escape from the melt until final residence in a summit reservoir (Gerlach and Taylor, 1990). However if such a magma was undercooled by contact with a felsic magma,  $\text{CO}_2$  transfer would be likely, and as a consequence, brecciation would be enhanced upon decompression. A degassing model (Taylor, 1991) for the Obsidian

Dome rhyolite (California) involves both first boiling (i.e. depressurisation driven degassing) which evolves from a closed to an open system, and second boiling (i.e. crystallisation driven degassing). Thus, although it is argued that second boiling is not an important mechanism for driving initiation brecciation, once decompression occurs, second boiling may provide additional vapour for time dependent vapour discharge where this is prolonged.

The ubiquitous occurrence of carbonate as an alteration mineral phase up to high temperatures, even in regions where a crustal source for the CO<sub>2</sub> is precluded (e.g. in large scale granitic terrains), suggests that some of the carbonate is originally derived from a magmatic fluid source or that CO<sub>2</sub> rich fluids commonly coexist with magmas. The common occurrence of CO<sub>2</sub> in fluid inclusions from granitic quartz (Roedder, 1972) may be due to a high CO<sub>2</sub> content in the volatile phase released during crystallisation of felsic magma.

These observations suggest that magma degassing and the role of CO<sub>2</sub> in this process are central to the formation of both large scale brecciation and, through extended periods of magma recharge and degassing, high chlorine and sulphur saline brines. Such brines have been implicated by several workers in the formation of porphyry copper mineralisation (e.g. Candela and Holland, 1986; Dilles, 1987) and porphyry gold mineralisation (Baker and Andrews, 1991). Because the initial fluid evolved from a crystallising magma is assumed by these workers to be an aqueous fluid, the role of CO<sub>2</sub> and other gas phases is usually considered to be minor. Whether it is necessary for these brines to interact with a meteoric component to form gold mineralisation is presently unclear. However, repeated crustal fluid pulses are an expected consequence of the structural setting (Chapter 3) of the Mt. Leyshon breccia complex (section 7.3).

## 7.6 DISCUSSION OF BRECCIATION MECHANISMS

Previous sections in this Chapter have examined the possible role of structural, fluid phase and magmatic processes in controlling the three fundamental brecciation mechanisms identified in the complex:

- (1) Host rock fragmentation.
- (2) Host rock expansion.
- (3) Host rock transport/mobilisation.

Though discussed separately, the evidence suggests that the geological processes are complexly interdependent. A number of breccia forming cycles have also been identified in this study (Table 7.1). They comprise the following suggested processes, which control breccia mechanisms:

- (1) Crustal stress/fluid pressure cycling.
- (2) Vapour exsolution in the magmatic system as a consequence of fractional crystallisation combined with periodic magma recharge.
- (3) Brittle faulting by seismic rupture.
- (4) Perturbation/arrest of seismic rupture.
- (5) Rapid opening of linked extensional fault and fracture mesh.
- (6) First boiling (rapid vapour decompression) of the magmatic system.

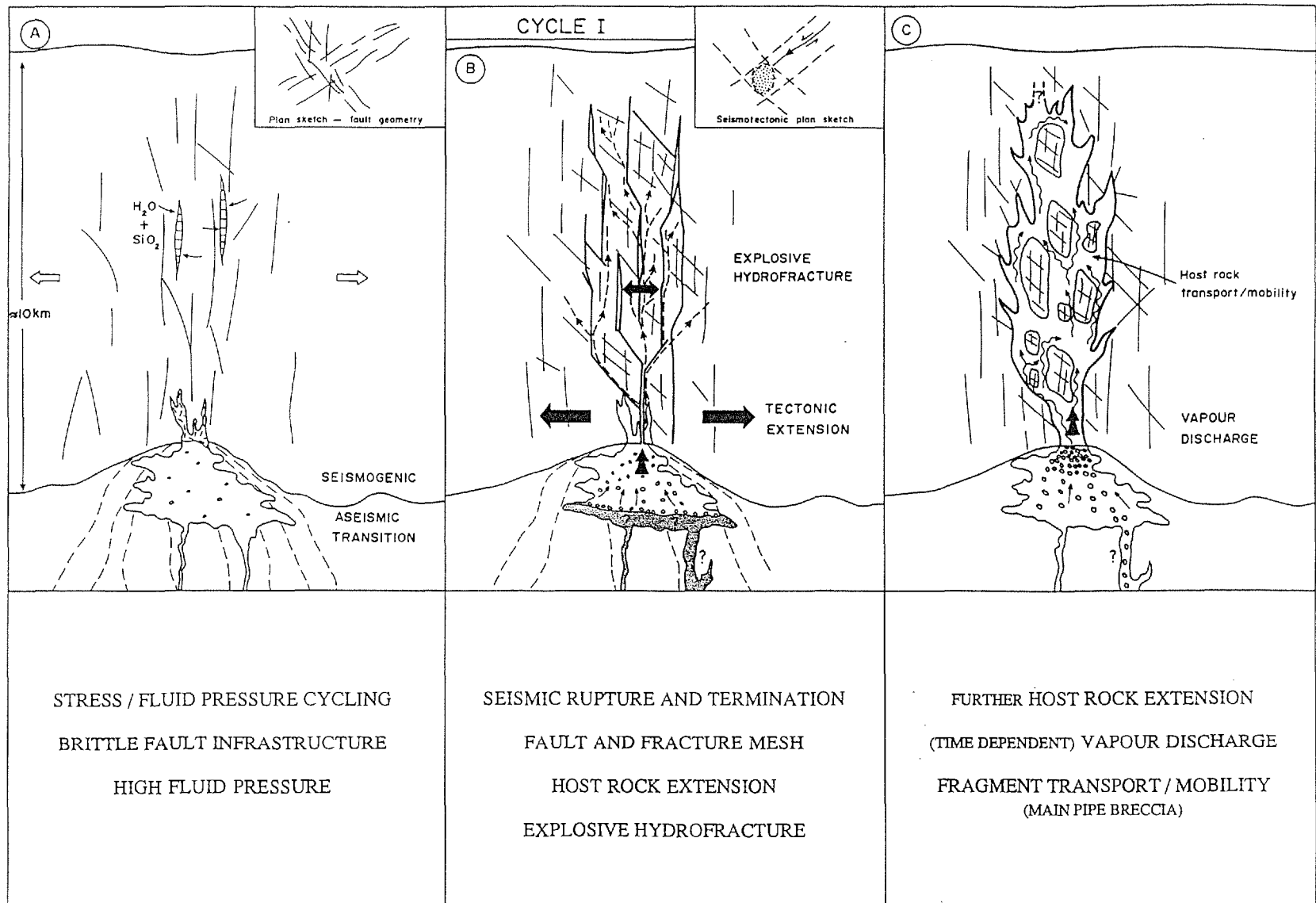


Figure 7.1: Dynamic model geological model for the Mt. Leyshon breccia complex, Cycle I (A, B and C).

- (7) Explosively driven hydrofracture.
- (8) Time dependent vapour discharge.

These processes are interdependent and operate synchronously or stepwise and, as a consequence the final breccia characteristics will reflect their complex interaction. For example, the formation of a brittle infrastructure and subsequent host rock extension is probably related to tectonic stress cycling. Magma emplacement is possibly coupled to this stress cycle through incremental accumulation, and in turn will influence the stress state. Likewise, distributed host rock extension as a possible consequence of seismic rupture arrest, may link with vapour decompression in the magma, resulting in explosively driven hydrofracture within the void space. However, as a consequence of the geological rate at which these processes operate they become variably decoupled. As an example, consider the slow accumulation of shear stress in the crust over tens to thousands of years. At a critical point, the stress conditions and brittle infrastructure of the crust result in seismic faulting. Earthquake motion and fault propagation last for 1-10 seconds, arrest/perturbation and opening of an extension mesh is likely accomplished over the space of hours to weeks or longer. At some point during this extension, breaching of the magmatic system would result in explosively driven hydrofracture over tenths of a second.

A third aspect of the link between process and variability of breccia character is the time dependent nature of these processes. For example, compared to other breccia units, vapour discharge was short lived or energy was dissipated rapidly during Mt. Leyshon breccia formation, as a possible result of:

- (1) Stress limited hydrofracture absorbing a high proportion of energy and causing gas condensation.
- (2) Low vapour generation in the magma or little capacity for inter-system vapour transfer.
- (3) Early sealing of magmatic system by quenching.
- (4) Failure of host rocks (and destabilisation of magmatic system) and consequently switching of vapour discharge to south, to produce fragmental component of porphyry unit II.

The important conclusion of this discussion is fundamental variation in the rate and extent of the same combination of structural, fluid phase and magmatic processes, can produce a wide variety of breccia types without the need to resort to largely different mechanisms or levels in the crust.

## 7.7 A DYNAMIC MODEL FOR BRECCIA COMPLEX FORMATION

In summary (Figure 7.1, Table 7.1), analysis and discussion presented in this Chapter suggest the following geological cycles:

### CYCLE I - main pipe breccia

- Stress/fluid pressure cycling within the regional wrench system (Figure 7.1A), results in:
  - (1) Brittle fault infrastructure (see insert) and extensional (stage I) quartz veins.
  - (2) Incremental magma accumulation near the base of the seismogenic zone.
  - (3) High fluid pressure, possibly triggering earthquake rupture.
- Termination of propagating earthquake rupture at fault irregularity (Figure 7.1B), results in:
  - (1) Opening of linking fault and fracture mesh throughout the seismogenic zone.
  - (2) Host rock extension, possibly triggering magma recharge and vapour exsolution.
  - (3) Catastrophic failure of magma system and explosively driven hydrofracture.
- First boiling (rapid vapour decompression) in the magmatic system (Figure 7.1C), results in:
  - (1) Time dependent vapour discharge.
  - (2) Further host rock extension and possibly inter-system vapour transfer.
  - (3) Main pipe breccia formation, during prolonged fragment transport, attrition and mixing.

### CYCLE II - episode II alteration

- Time dependent shear failure in the breccia complex (region of lowered mean stress) as fluid pressure levels are restored (Figure 7.1D), results in:
  - (1) After shock activity in the complex (stippled area in inset to B).
  - (2) Pore fluid diffusion into the breccia complex.
  - (3) Liberation of trapped magmatic vapour.
  - (4) Argillic alteration of the main pipe breccia.
  - (5) Partial restoration of the mechanical strength to the crust.
- Partially renewal of brittle infrastructure during aftershocks as a consequence of the mechanical strength increase (Figure 7.1E), result in:
  - (1) Magma intrusion to a higher crust level and intermediate (EP) dyke emplacement.
  - (2) Increased magmatic vapour discharge producing prograde (potassic and propylitic I) hydrothermal alteration.
  - (3) Reduction in permeability and complete restoration of mechanical stress to crust, encouraging prolonged magma fractionation.

### CYCLE III - interactive magma/breccia sequence

- Stress/fluid pressure cycling (Figure 7.1F), results in:
  - (1) Renewal of brittle fault infrastructure (see insert).
  - (2) Oblique slip normal faults and inter-breccia shear zones.
  - (3) Felsic (ED) dyke emplacement.

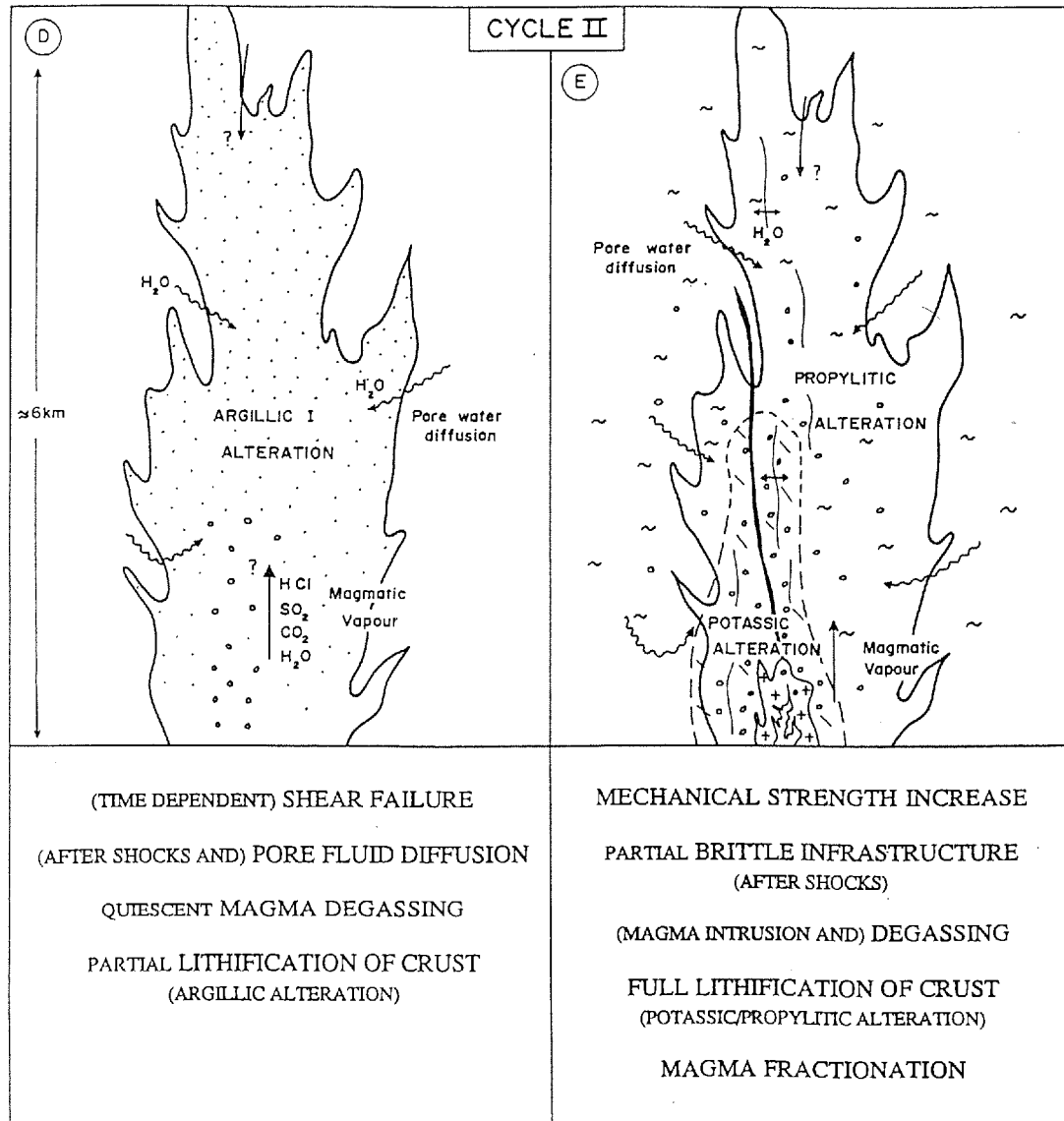


Figure 7.1: Continued, Cycle II (D and E).

- (4) Incremental growth of quartz-molybdenite veins, possibly resulting from coupling of magmatic vapour discharge with pore fluid pressure cycling.
- (5) High fluid pressure possibly triggers seismic rupture.

#### SUB-CYCLE IIIa - Mt. Leyshon breccia formation.

• Perturbation of seismic rupture at releasing bend (Figure 7.1G; see insert), results in:

- (1) Opening of a linked fault and fracture mesh.
- (2) Host rock extension, possibly triggering magma recharge and vapour exsolution.
- (3) Catastrophic failure of magma system and explosively driven hydrofracture.

• Rapid vapour decompression (first boiling) in the magmatic system (Figure 7.1Ha), results in:

- (1) Limited time dependent vapour discharge.
- (2) Distributed host rock expansion and local vertical extension.
- (3) Limited fragment transport, attrition and mixing within zones of maximum extension in the Mt. Leyshon pipe.

#### SUB-CYCLE IIIb - fragmental component of porphyry unit II and Mt. Hope breccia.

• Destabilisation of the magma system (Figure 7.1Hb), resulting in:

- (1) Extensive hydrofracture and time dependent vapour discharge forming the fragmental component of porphyry unit II.
- (2) Rapid digestion of this fragmental component by felsic magma (porphyry unit II) intrusion.
- (3) Further widespread felsic magma intrusion (porphyry units III and IV), and vapour discharge forming the Mt. Hope breccia.

#### SUB-CYCLE IIIc - tuffisite breccia dyke formation.

• More basic magma recharge to the system (Figure 7.1Hc), resulting in:

- (1) Igneous sill intrusion and enclave formation.
- (2) Vapour exsolution and transfer from the more basic to felsic magma.
- (3) Reactivation of existing fault structures as a consequence of high vapour pressure and depletion limited hydrofracture propagation.
- (4) Prolonged time dependent vapour discharge, evolving from a fixed bed to a fluidised system as host rock extension proceeds.
- (5) Fine tuffisite dykes are intruded when gas pressure exceeds lithostatic load, allowing escape of rapidly chilling magma into extended host rock system.
- (6) Widespread felsic (1-2 and 2-2) dyke intrusion.

#### SUB-CYCLE IIIId - late breccia dykes.

Further small scale magma recharge (not figured), results in:

- (1) Intermediate (DG) dyke intrusion.
- (2) Vapour exsolution and transfer from the more basic to felsic magma.
- (3) Reactivation of existing fault structures as a consequence of high vapour pressure and depletion limited hydrofracture propagation.

(4) Intrusion of felsic (fine late) dykes driving late breccia dykes during vapour discharge.

**CYCLE IV - episode IV alteration and mineralisation.**

• Time dependent shear failure in the Mt. Leyshon breccia pipe area, as fluid pressure levels are restored (Figure 7.1I), results in:

- (1) Pore water diffusion and argillic II alteration (lithification) of matrix and fragments in breccias and igneous units.
- (2) After shock activity in the breccia pipe region (stippled area in inset to Figure 7.1G).
- (3) Fluid pressure cycling leads to intermittent fracturing and pore water diffusion, coupled with liberation of trapped magmatic vapour, and as a consequence hydrothermal alteration, base metal and gold mineralisation (episode IV).

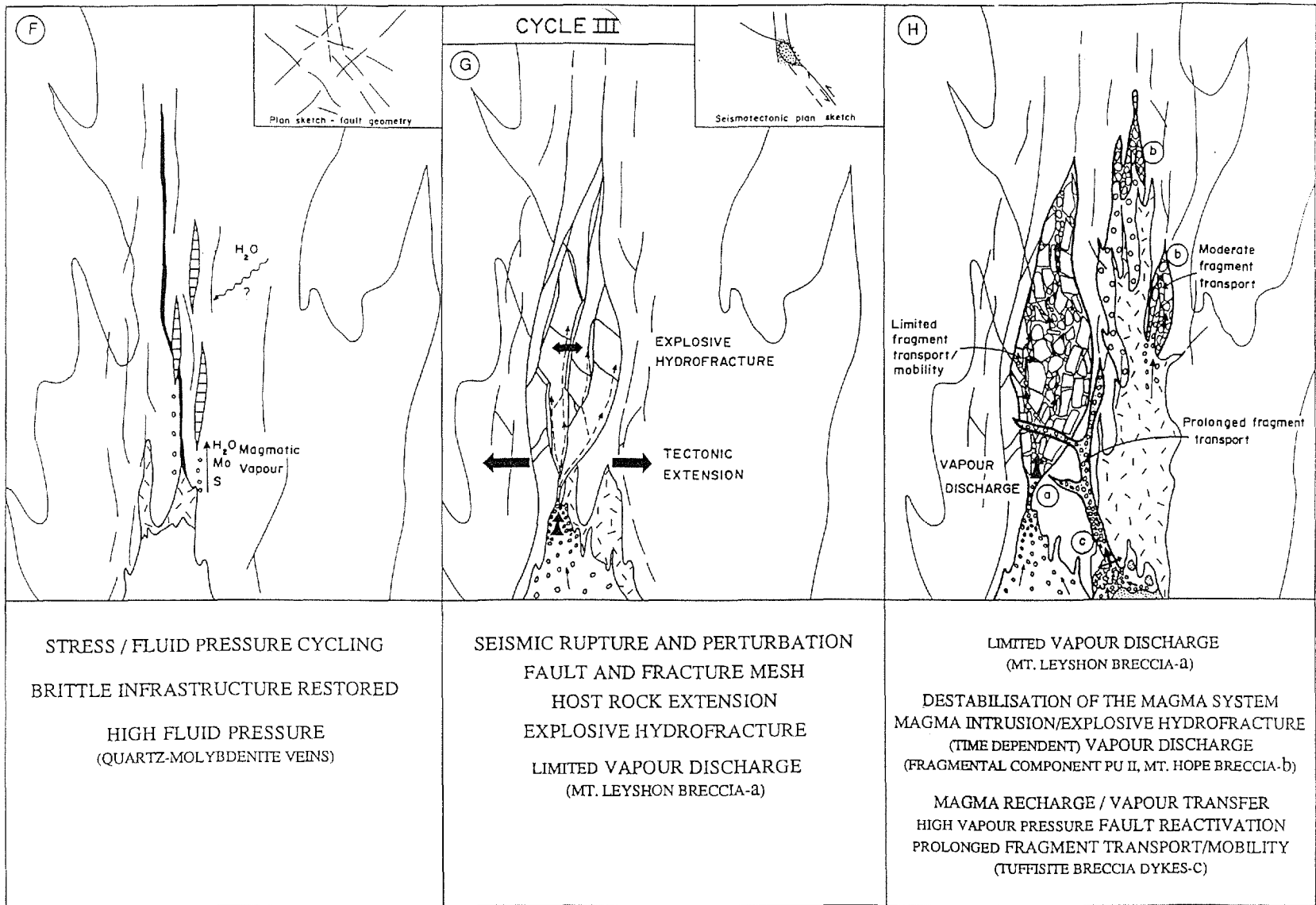


Figure 7.1: Continued, Cycle III (F, G and H).

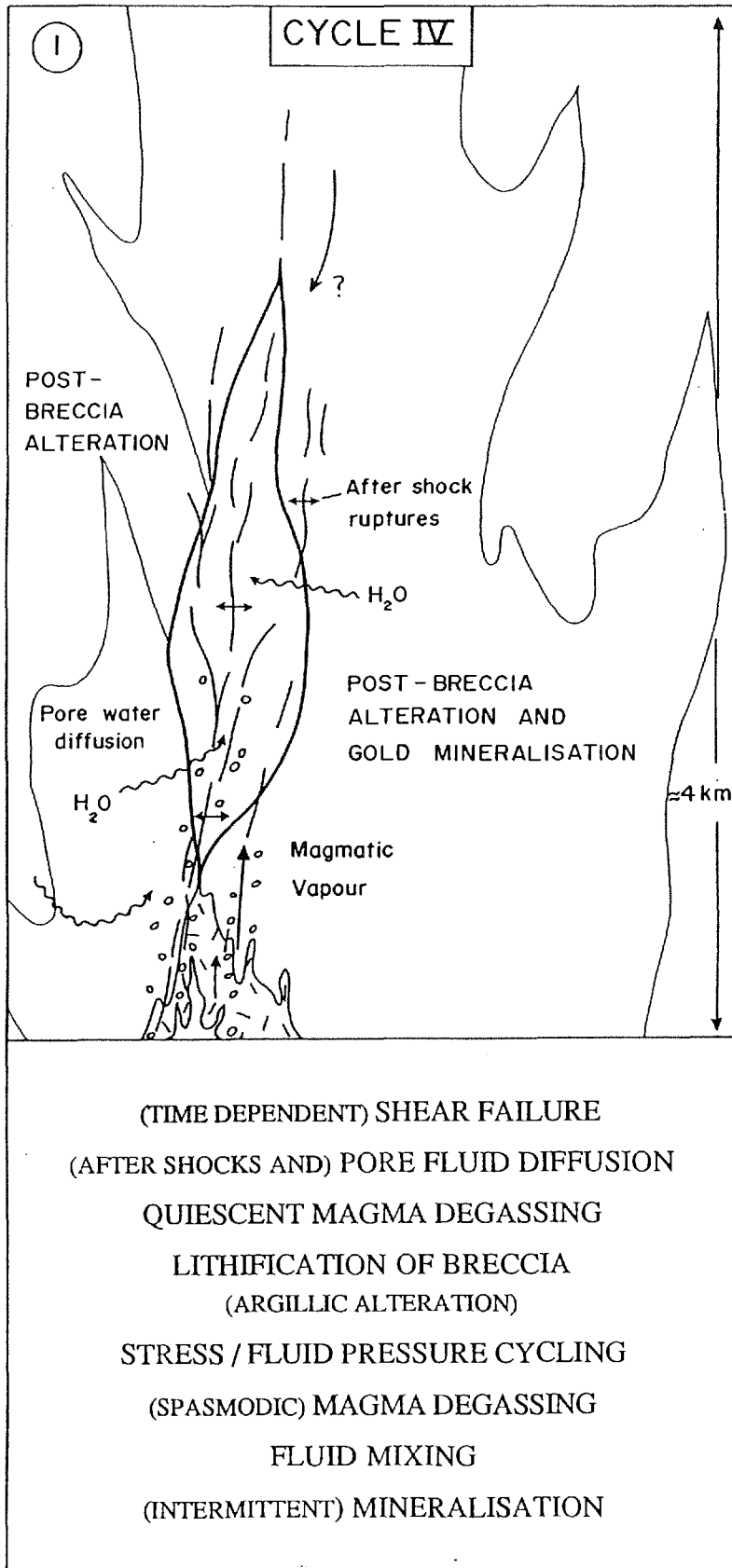


Figure 7.1: Continued, Cycle IV (I).

## Chapter 8

# GOLD DISTRIBUTION AND CONTROLS IN THE MT. LEYSHON BRECCIA COMPLEX

---

### 8.1 INTRODUCTION

Emphasis in this study is on determining the origin of the geological framework which hosts the ore body. Nevertheless, several aspects of this study provide information concerning physical controls on gold mineralisation. To assess the relevance of the work noted in this Chapter, it is helpful to first appreciate that large scale hydrothermal fluid flow in the crust is controlled by the following interdependent factors (Heinrich et al., 1989):

- 1) Source(s) of energy which drives the system.
- 2) Source(s) of the fluid phase.
- 3) Development and distribution of permeable structures which control the flow of fluid between source and discharge regimes.
- 4) The chemistry of the fluid phase and extent of fluid-rock interaction.

Gold mineralisation in breccia pipes has recently been the subject of increasing research. For example, at the Kidston breccia pipe (Queensland; Baker and Andrew, 1991) gold is hosted in late stage vein and cavity mineralisation cutting the breccia. On the basis of isotopic data, Baker and Andrew (1991) imply that gold is genetically related to rhyolite intrusions via condensation of magmatic vapour in the breccia pipe. In the Golden Sunlight breccia pipe (Montana; Porter and Ripley, 1985), gold and gold tellurides occur as disseminations in breccia cavities and in high grade veins. Mineralisation is interpreted to have formed from an isotopically exchanged magmatic fluid that was drastically cooled. Sillitoe (1985) briefly describes the distribution of gold and other ore minerals in breccia pipes. He notes they are commonly associated with the part of the breccia pipe adjoining marginal sheeted zones. Alternatively, gold may be restricted to pipe interiors, as at Ortiz (New Mexico) where the star shaped ore body coincides with the portion of breccia carrying the least matrix (Sillitoe, 1985).

Relatively little work on gold mineralisation in breccia pipes has focused on the detailed distribution of gold, its structural control, or its detailed paragenesis in relation to previous evolution. It is these aspects that are considered here, and integrated with implications from the dynamic geological model (Chapter 7), to propose a model for gold mineralisation in the breccia complex.

Detailed investigation of geologic, structural and paragenetic data, together with a compilation of gold resource model plans for the Mt. Leyshon deposit provides the following information:

- 1) A three dimensional model of the gold ore body.
- 2) The timing of gold mineralisation (Chapter 4).

- (3) The distribution of gold mineralisation both with respect to physical sites of precipitation and geological facies.
- (4) The structural controls on gold mineralisation (Chapter 3).
- (5) A hypothetical model for gold mineralisation to focus further research based on the integrated dynamic geological model derived in this thesis.

## 8.2 DISTRIBUTION OF GOLD MINERALISATION

The bulk of gold mineralisation occurs within the Mt. Leyshon breccia, though significant ore reserves also occur within porphyry unit IV (the mine porphyry) and anomalously high gold values occur sporadically throughout the breccia complex. The distribution of gold in the host rocks, and the nature of host rock porosity and permeability are described in this section. These observations provide information on gold trap sites within the breccia complex.

A preliminary assessment of the gold distribution within Mt. Leyshon breccia and tuffisite breccia dykes was undertaken during this work. Early during the study, thirty Mt. Leyshon breccia blocks (used for paragenesis study, Chapter 4) were cut, and half of each block was assayed for gold. From this suite twelve variably mineralised (0.1-1.4 g/t Au) slabs were polished. Slabs were systematically assessed to investigate gold grade versus breccia characteristics; vugh porosity and matrix proportion (employing a millimetre overlay grid), fragment types and size, and alteration types. With the exception of vugh porosity (Plate 5.13), which shows a weak correlation with gold grade ( $R^2 = 0.65$ ), no other breccia characteristic showed a systematic variation with gold distribution. As part of the graphic logging exercise, eight drill holes (MLD 82, 149, 177, 182, 225, 252 and 277) in the Mt. Leyshon breccia were also assessed qualitatively for a correlation between breccia porosity and gold grade. To ensure impartial judgement of porosity, drill holes were logged without prior knowledge of the gold grades. In seven of the drill holes, there is an increase in breccia porosity with the presence of gold grades  $> 1\text{g/t}$ , again suggesting a broad correlation between primary porosity and gold grade.

Gold distribution and the nature of the porosity in the Mt. Leyshon deposit were further investigated by petrographic study and gold assay on selected drill hole and open pit samples. Mine drill core gold assay data (2 metre intervals) were used to guide the collection of breccia cavity and vein samples for thin section paragenesis studies (Chapter 4). Pit samples of veins were collected through ore zones (on the 380 and 370 RL), and vein and wall rock portions of the same samples assayed separately for gold. The following gold assay values for vein and wall rock were recorded:

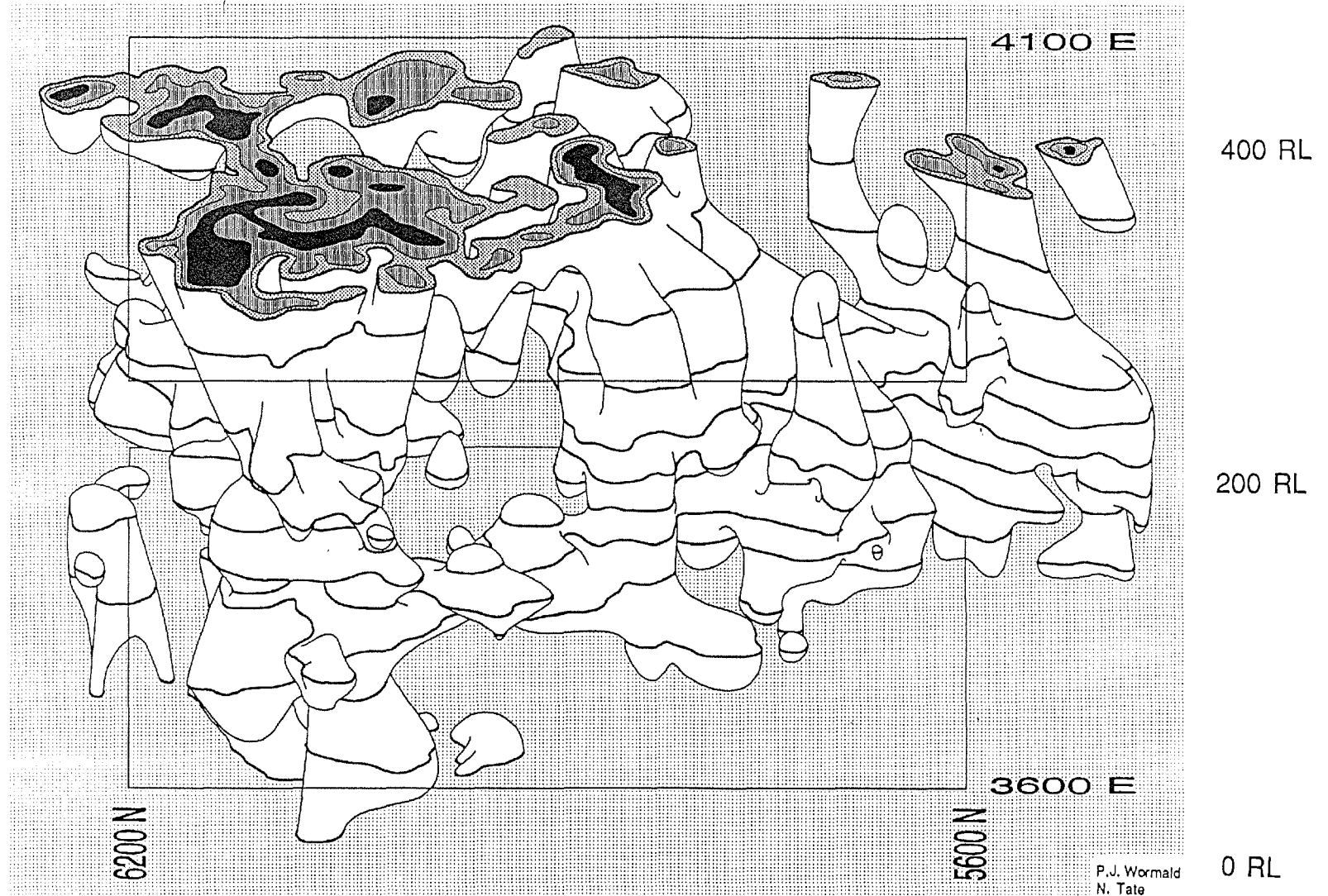


Figure 8.1: Orthographic projection of the Mt. Leyshon ore body (0 - 400 RL), looking due east. Compiled from the mine bulk block model data, contours are approximately 0.96, 1.44, > 2.4 g/t gold. Dark lines indicate the form surface contours (0.96 g/t gold) from which the model was compiled. (In collaboration with N. Tate.)

Sample no.	Rock type	Wall rock (g/t Au)	Vein sample (g/t Au)	Dominant ore mineralogy
S14*	Tuffisite dyke	1.8	9.4	py
S17*	Tuffisite dyke	3.4	101.0	py-cpy
S18*	Tuffisite dyke	1.2	2.2	sph
SP2	Mt. Leyshon breccia	1.6	9.4	py-sph-cpy
SP3	Mt. Leyshon breccia	2.1	22.3	py-sph-cpy-ga

\*In collaboration with I. Taylor.

These data indicate that much of the gold within some portions of the ore body is in high grade veins cutting the rock units (Plate 8.1). However, in the Mt. Leyshon breccia discrete planar veins are relatively uncommon and instead gold (and base metal) mineralisation occupies irregular zones of distributed rebrecciation cutting cavities and fragments (sections 3.3.4.1, 3.5 and 4.2.3.9; Plate 4.14). The consistent cross-cutting paragenesis of these rebrecciation zones suggests periodic refracturing of the breccia provided permeability and secondary porosity for successive stages of mineralising fluid (Chapter 4; section 7.4.2).

The distribution of gold mineralisation in fine tuffisite breccia dykes was also examined with scanning electron microscope images of freshly broken surfaces. These images reveal the large primary porosity of tuffisite dykes (Plate 8.2). Secondary electron emission images (where the intensity of a material in the image is proportional to its atomic number) were used to locate gold particles (Plate 8.2). In three samples investigated, gold (together with micron- to ten's of micron-sized galena and bismuth-copper-lead sulphosalts) occurs as free particles fixed to the surface of pyrite grains. Knipe et al. (1992) have recently suggested gold particles (and other precious metals) precipitated from hydrothermal solutions are formed by a process of adsorption to pyrite (and other sulphide) surfaces. The location of gold in the Mt. Leyshon samples supports their work. In the samples investigated, the Mt. Leyshon gold commonly overgrows illitic clay crystals also bound to the pyrite surfaces (Plate 8.3) suggesting illite may play a role in trapping gold in the rock.

With regard to this last point, XRD and petrographic analysis of tuffisite dyke blocks (slab no. SLA37T and S15) low in gold content (0.18 and 0.09 g/t, respectively) indicate a high kaolinite content in these samples. Likewise, a drill core sample (sample no. 157/16) of highly clay altered mine porphyry has two distinct textural regions; (1) a region where the porphyritic texture is preserved, and (2) a porous region where the porphyritic texture is largely destroyed. Thin section and Pima spectral analysis (see section 4.3) of this sample indicate that the porphyritic textured zone is rich in kaolinite (Plate 4.18). In the porous zone, this kaolinite (and other mineral phases) are much less prominent in the feldspar phenocryst pseudomorphs. Instead the rock pores have a partial filling of manganosiderite  $\pm$  base metals (Plate 4.18). These observations suggest partial rock dissolution of tuffisite dykes and mine porphyry resulted in enhanced (tertiary) porosity and permeability, encouraging both the permeation of base metal and gold bearing fluid into the rock,

and their precipitation in cavities. Dissolution porosity probably also encouraged gold precipitation at pyrite-base metal-gangue surfaces. This possibility of effective porosity control on gold transport and deposition in the Mt. Leyshon rocks is further supported by the (SEM) observation that the freshest tuffisite dyke (sample no. 236/16; section 4.2.3.1), also carries abundant minute free gold particles. Illite/smectite is the dominant clay in this sample and porosity is very high. In addition to the three types of porosity discussed above, other possibly important controls on gold distribution are:

- (1) Type of clay mineral in the rock.
- (2) Proportion of expandable layers (smectite) in the clay.

### 8.3 GEOMETRY OF GOLD BEARING ZONES AND RELATIONSHIP TO FACIES DISTRIBUTION

In this section, the geometry of the gold bearing zones discussed in the previous section is constructed and related to the geological framework established in Chapter 5. This work has implications for structural controls on gold mineralisation (section 8.4).

A three dimensional model (Figure 8.1) of the Mt. Leyshon ore body was compiled during this study (in collaboration with N. Tate) to investigate the spatial control on ore deposition. Plan sections from the mine bulk block model (generated on Data Mine by T. Orr) were taken at 50 m spacing between 0 - 400 RL (25 m slices between 150-250 RL to depict flat lying ore zones). The plans comprise gold grades in each ten by ten metre block at a particular RL and are approximately 20 % greater than the final resource model (0.7 g/t cut-off). Therefore, hand drawn contours traced around the blocks to construct the three dimensional models correspond to approximate grades of 0.96-1.44, 1.44-2.4 and >2.4 g/t gold. These grade contoured slices were scanned into a Macintosh computer, stacked at the appropriate vertical spacing and a form surface developed from the 0.96 g/t contour. The model is an orthographic projection viewed from 30° to the horizontal, looking due east. A second three dimensional model was developed to show the internal grade distribution at the 100, 200, 300 and 400 RLs (Figure 8.2). This model is viewed from the same direction but has had perspective added by providing a vanishing point. In both these models the upper portion of the ore body (400-510 RL) is not shown. The approximate location of the late reverse fault offsetting the ore body (section 3.3.4.2, Figure 5.3) is also shown in the second model.

These models allow several points to be made with regard to the geometry of the ore body prior to considering structural control on gold deposition:

- (1) The ore body has an irregular bulbous form (Figure 8.1) with several upward and downward terminating arms. This shape is consistent with the irregular nature of the permeability and porosity controlling gold deposition (section 8.2), but is also an artefact of the ore reserve model technique (10 m<sup>3</sup> blocks) and the contouring employed to construct the perspective model.
- (2) At the upper levels (300 and 400 RLs) the ore body consists of a wide region of irregular interconnecting ore zones. At lower levels the ore zones form en-echelon steeply dipping regions, comprising NE and SE trending segments (see section 8.4).

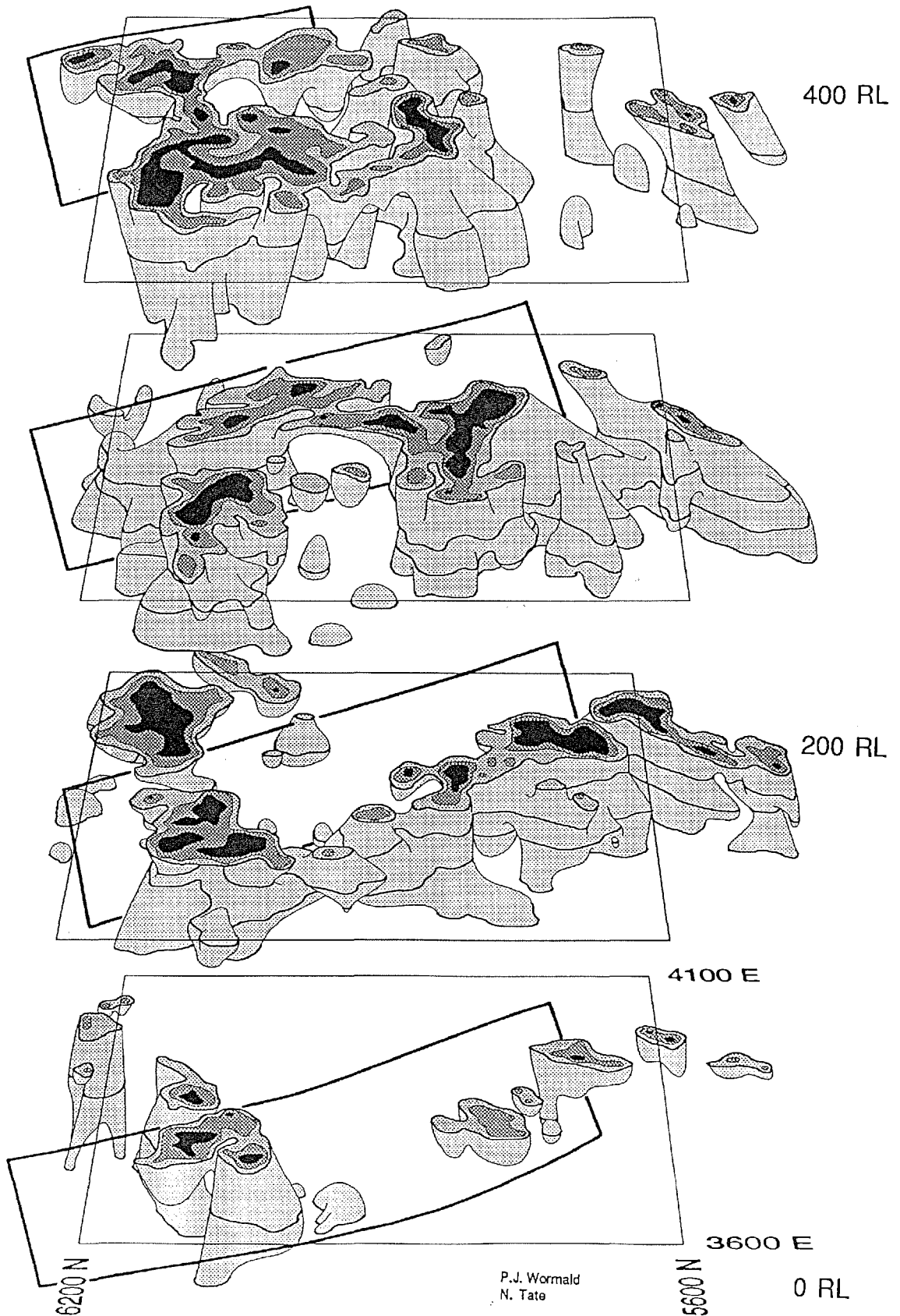


Figure 8.2: Perspective model of the Mt. Leyshon ore body, looking due east, showing the internal grade distribution at 100, 200, 300 and 400 RLs. Compiled from the mine bulk block model data, contours are approximately 0.96, 1.44, > 2.4 g/t gold. Dark lines indicate the form surface contours (0.96 g/t gold) from which the model was compiled. The late reverse fault off-setting the ore body is also shown. Note the linear, en-echelon geometry of the ore zones at lower levels. (In collaboration with N. Tate.)

- (3) Two separate "sill" ore zones are visible; one at 400 RL, the other at 200 RL.
- (4) The internal geometry of the ore zones (Figures 8.1 and 8.2), especially the high grade ore (>2.4 g/t), also indicates an en-echelon pattern. This is true of both steeply dipping ore zones and high grade ore within the "sill" zones.
- (5) The size and continuity of ore zones decreases below 100 RL.

Contoured assay plans constructed in this work were also used to assess the geometry of ore zones with respect to the geological framework established in Chapter 5. Two plans comparing ore distribution and rock units are shown in Figures 8.3 and 8.4. This work documents the well known primary control of Mt. Leyshon and Mt. Hope breccias on the location of the whole ore body (compare Figures 5.4 to 8.3 and 8.4). More importantly this work indicates neither the individual rock units or sub-facies within the Mt. Leyshon breccia control the geometry of gold bearing zones in the ore body. The en-echelon geometry of these zones has been noted above, and they do not directly relate to the geometry or distribution of the rock units.

#### 8.4 STRUCTURAL CONTROL ON GOLD MINERALISATION

The predominance of gold in rebrecciation sites in breccia cavities and veins has already been noted (section 8.2). When this is considered in conjunction with the geometry of the ore zones (section 8.3) they have implications for structural controls on gold mineralisation.

Irregular zones of rebrecciation and hydrothermal infill in the immediate vicinity of the Mt. Leyshon ore body have the same paragenesis as discrete planar veins in the ore body, and extensional and shear fibre veins noted in the competent lithologies (main pipe breccia and granite, sections 3.3.4.1 and 3.5). It is suggested (sections 3.6.2 and 7.4.2) these veins formed in response to fault reactivation under high fluid pressure conditions. It is likely rebrecciation of breccia cavities and veins in and around Mt. Leyshon breccia is also related to fault reactivation. The suborthogonal and en-echelon nature of the ore zones (Figures 8.2 and 8.4), becoming markedly linear in the lower portion of the ore body, supports this interpretation. The trend (NE and SE) of these ore segments is approximately parallel to the dominant fault orientations in the NW corner of the breccia complex (Figures 3.2 and 3.10E), which implies active strike slip fault control on gold mineralisation. The presence of distinct geometric anisotropy in the resource estimation zones of the Mt. Leyshon ore body (Gleeson, 1992) is consistent with structural control on their formation. According to mine drill hole data, the horizontal ore zones at 200 and 400 RL (Figure 8.2) partly coincide with late igneous sills, which could be interpreted as having trapped the gold bearing fluid. However, given the structural control discussed above, it is more likely these gently dipping mineralised zones formed by reactivation of dyke contacts or existing veins under high fluid pressure conditions. The expanded interconnected nature of the upper portion of the ore body (Figure 8.3) most likely results from one or a combination of the following:

- (1) A rheological control (section 3.5) - the granite and dolerite rich breccia (zone 4A, section 5.4) would re-break in a diffuse anastomosing manner, compared to the more brittle fracture

characteristic of main pipe breccia (dominant as fragments and blocks in lower portions of the breccia pipe).

(2) A structural control - strike slip faults observed in the pit have an upward branching geometry, it is probable that the fault system causing the late stage rebrecciation also had such a geometry.

The characteristics and trend of the ore zones suggest that at the regional scale the mineralisation is controlled by the same intersecting NE and SE trending regional wrench corridors (Chapter 3) implicated in the mechanical development of the whole complex (section 7.3.1).

## 8.5 IMPLICATIONS OF THE DYNAMIC GEOLOGICAL MODEL FOR GOLD MINERALISATION

Textural evidence presented in Chapter 4 indicates that gold and the bulk of base metal mineralisation at Mt. Leyshon post-date all coeval igneous emplacement and a considerable sequence of prograde to retrograde hydrothermal fluid evolution. Thus, evidence for a direct temporal or genetic relationship between gold and base metal mineralisation, and the magmatic system is lacking.

Based on O, C and S isotopes for quartz, calcite and pyrite (from a three stage mineral paragenesis), and fluid inclusion temperatures of 300 - 500 °C, Morrison et al. (1988) interpreted the mineralising fluids to be dominantly magmatic for all three stages, and to have undergone little if any mixing with other fluid types. Quartz molybdenite veins contain high salinity (30-50 wt % NaCl eq.) fluid inclusions, homogenising at temperatures of 450-500 °C, and with calculated oxygen isotope compositions of +5.2 to +6.2 per mil for the aqueous fluid (at this temperature range; Morrison et al., 1988). Quartz infill in the Mt. Leyshon breccia (second and third stages of Morrison et al., 1988), which are shown in this study to be paragenetically equivalent, have  $\delta^{18}\text{O}$  quartz of +9.1 to +11.2 and +7.9 to +13.4. Fluid inclusion temperatures for this quartz were estimated as 300 - 400 °C (Morrison et al., 1988), and a predominant fluid inclusion population of 300-400 °C but down to 160 °C for secondary inclusions (Uemoto et al., 1992). If a fluid temperature of 350 °C is assumed, the calculated oxygen isotope composition for water coexisting with cavity quartz is +3.1 to +5.2, and for vein quartz is +1.9 to +7.4 per mil (using the data of Taylor, 1979).

These data for the quartz molybdenite veins suggest they were dominantly derived from a magmatic fluid. However, the isotope data for cavity quartz and the lower limit for the vein quartz fall well outside the calculated "primary" magmatic water (+5.5 to +10 per mil; Taylor, 1979). In view of the geological evidence presented in this thesis (Chapters 4 and 7), these isotope data are better interpreted as indicating gold and base metal mineralisation and alteration in the Mt. Leyshon breccia was derived from variable mixing between a crustal pore water or meteoric water and a magmatic fluid. This evidence includes:

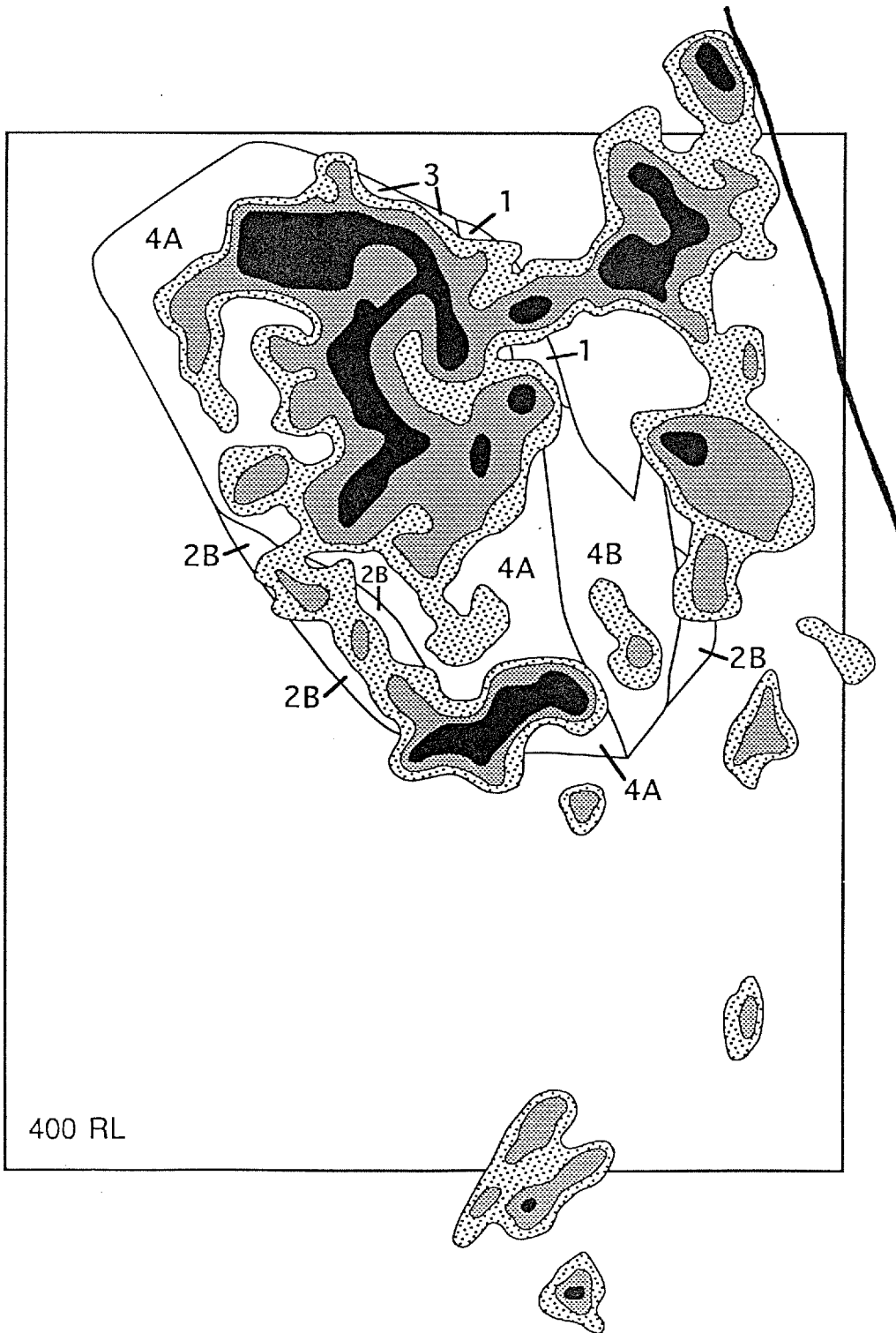


Figure 8.3: Comparison of gold distribution versus breccia facies of the Mt. Leyshon breccia pipe (400 RL; Mt. Hope geology not shown). Contours are approximately 0.96, 1.44, > 2.4 g/t gold. Late reverse fault is shown. Note the irregular interconnected nature of the ore zones at this level which cut across the Mt. Leyshon pipe facies (see Chapter 5). High grade zones (black) have an en-echelon pattern.

- (1) Paragenetic evidence for early low temperature argillic alteration, most likely derived from crustal pore water, overprinted by prograde high temperature alteration and by implication mixing of fluids.
- (2) The absence of coeval igneous emplacement during this period and the absence of high temperature alteration during igneous emplacement.
- (3) Repeated rebrecciation and fluid flow in the ore body, plausibly related to aftershock activity and stress / fluid pressure cycling, combined with liberation of trapped magmatic vapour (section 7.4.2). Richards (1992) has suggested that gold was precipitated in the Porgera gold deposit following tectonically induced fluid phase separation.
- (4) Secondary fluid inclusion temperatures down to 160 °C in quartz infill to the Mt. Leyshon breccia (Uemoto et al., 1992) is consistent with geological evidence which suggests lower temperature fluids were responsible for post-quartz base metal and gold mineralisation.
- (5) Recent work (BMR Research News Letter, 1991) suggests large scale hydrothermal fluid flow with a significant meteoric component has effected many of the igneous rocks at the northern end of the Bowen Basin.

Gold mineralisation, therefore, could equally well be genetically related to a crustal metamorphic fluid (eg. Goldfarb et al., 1991) or to a deep basinal fluid interacting with a meteoric component (eg. Werner, 1990), in either case driven by the thermal pulse associated with tectonic and/or igneous activity. Further work beyond the scope of this study is required to resolve these conflicts, for example, an investigation of the isotopic signature of fluids actually responsible for gold mineralisation (rather than of earlier alteration).

## **8.6 MODEL FOR GOLD MINERALISATION AT MT. LEYSHON**

In summary, analysis and discussion presented in this thesis suggests the following model (Figure 7.11) for gold mineralisation:

- The bulk of gold mineralisation is paragenetically very late and postdates all coeval igneous emplacement and a considerable sequence of prograde to retrograde hydrothermal evolution.
- At least three types of porosity provided sites for gold mineralisation in the host rocks:
  - (1) Primary porosity - reflecting the characteristics of the rock units.
  - (2) Secondary porosity - resulting from the formation of rebrecciation zones in the rocks.
  - (3) Tertiary porosity - resulting from dissolution of rock and previous alteration minerals by hydrothermal fluid.
- Overall the Mt. Leyshon ore body has an irregular, steeply dipping and bulbous form consistent with the irregular nature of the permeability and porosity controlling gold deposition. At lower levels the ore body consists of linear en-echelon segments, trending NE and SE but spreads out at upper levels to form a wide region of interconnecting ore zones. Two gently dipping, discontinuous ore zones also occur. The internal geometry of steeply and gently dipping high grade ore zones also indicates an en-echelon control on gold deposition.
- In view of the orientation of mineralised segments comprising the ore body, and the timing and distribution of gold in the host rock, gold deposition was likely controlled by fault reactivation

under high fluid pressure conditions. The expanded interconnected nature of the upper portion of the ore body most probably results from the fault geometry controlling re-brecciation and/or a rheological contrast between upper and lower ore body host rocks.

- The ore body characteristics suggest that secondary porosity and as a consequence gold mineralisation within the breccia complex, was controlled by the intersection of regional strike slip faults within the Mt. Leyshon and Mt. Dean corridors; rather than rock units or subfacies.
- In the context of the geologic and paragenetic data presented in this thesis, the existing isotopic and fluid inclusion data suggests that the gold bearing fluid was most likely derived from the mixing of a basinal or metamorphic fluid and/or magmatic fluid with a meteoric water. This mixing may have resulted from fluid diffusion and release of trapped magmatic vapour during after shocks following seismic rupture.

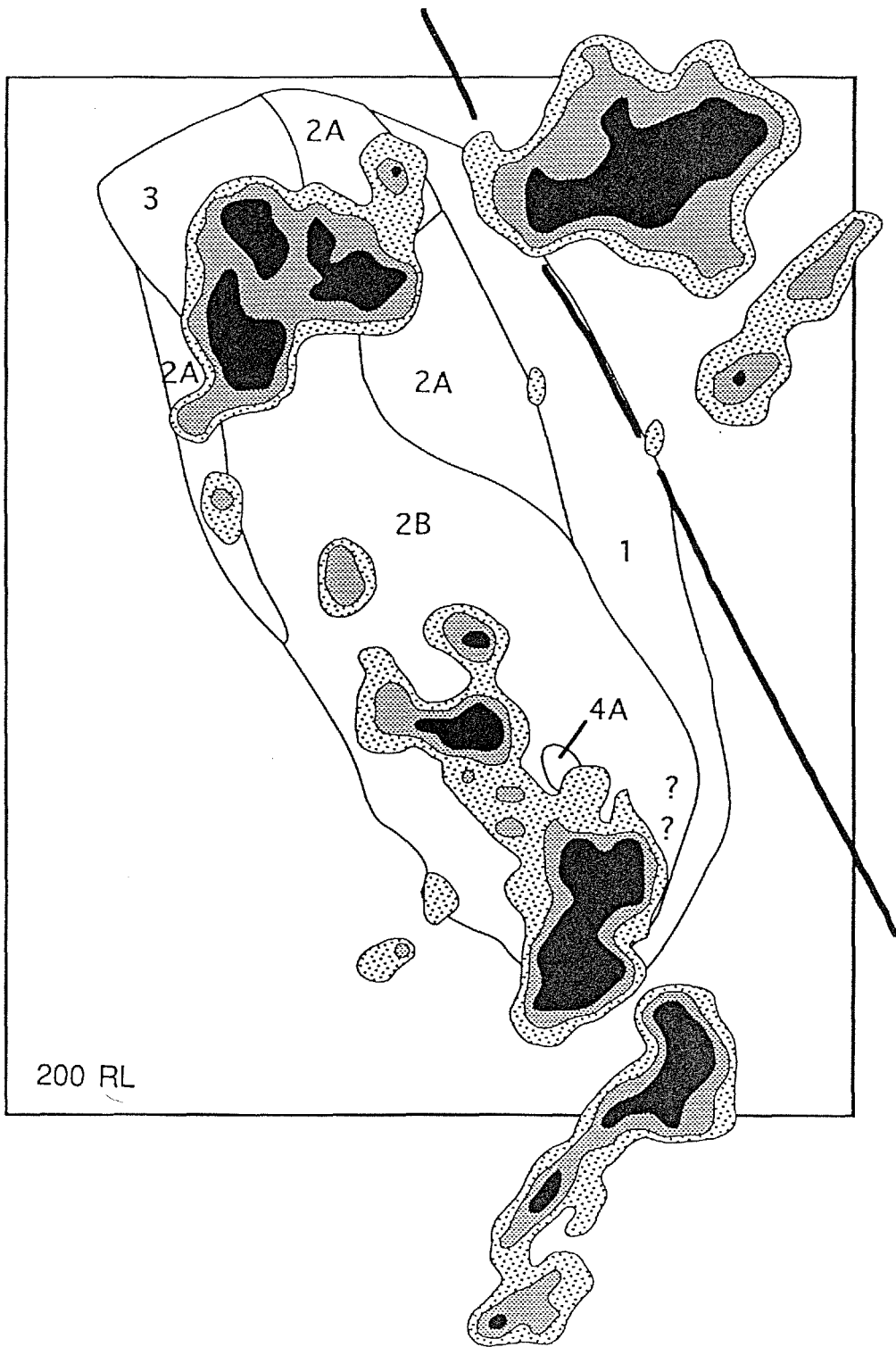


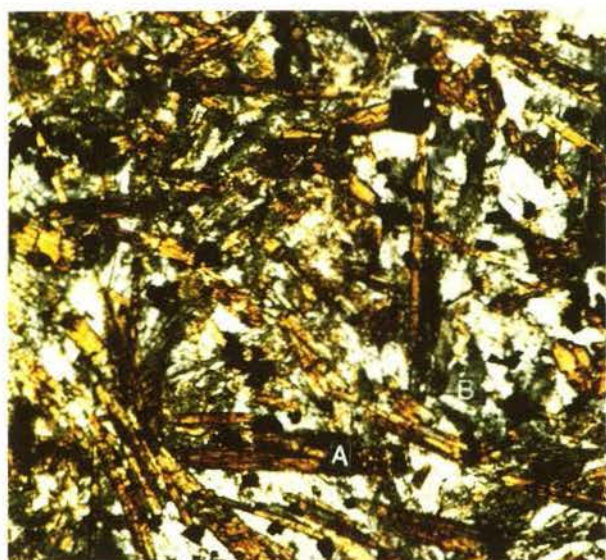
Figure 8.4: Comparison of gold distribution versus breccia facies of the Mt. Leyshon ore body (200 RL; Mt. Hope geology not shown). Late reverse fault is shown. Contours are approximately 0.96, 1.44, > 2.4 (black) g/t gold. Note the en-echelon linear ore segments which cut across the Mt. Leyshon pipe facies (see Chapter 5).

Plate 6.7: Basalt dyke. Groundmass is predominantly composed of acicular and radiate amphibole (A) and plagioclase (B), and an opaque mineral. (Photomicrograph, XPL, base of photo = 1.5 mm; Sample no. B/AD.)

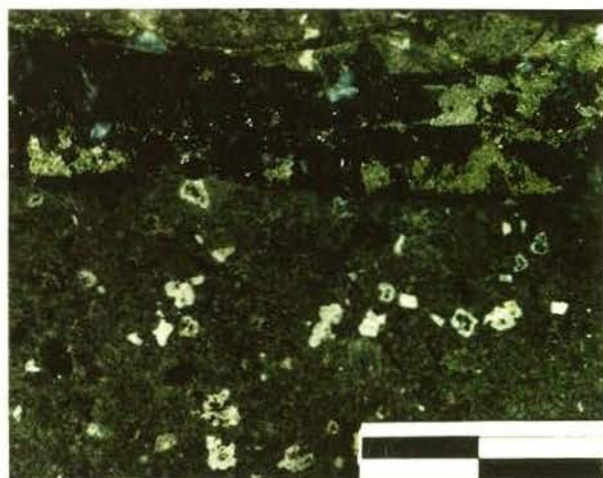
Plate 8.1: Polymetallic (sp-cpy-ga-gold) vein cutting DG dyke within Mt. Leyshon breccia pipe. Repeated reactivation has allowed sequential mineral development as follows, quartz, py, sp, cpy, gold (see Plate 4.16). (Polished drill core sample no. T/277/GV).

Plate 8.2: Scanning electron microscope (secondary electron) image of a pyrite grain in a fine tuffisite breccia dyke. Note, (1) the high porosity of the tuffisite dyke (A), (2) the bright particles of gold (g) attached to the pyrite surface (dull particles are illitic clay), and (3) the larger composite gold/illitic particle (B) in pocket on pyrite surface. (Sample no. 183/7.)

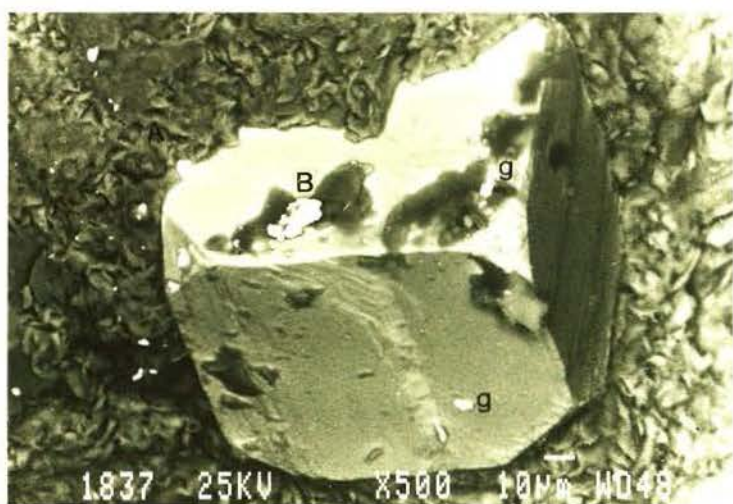
Plate 8.3: Detail of composite gold particle inside pocket on pyrite surface (Plate 8.2), back-scatter image. Photo shows delicate flake morphology of gold illite particle in porosity. (Sample no. 183/7.)



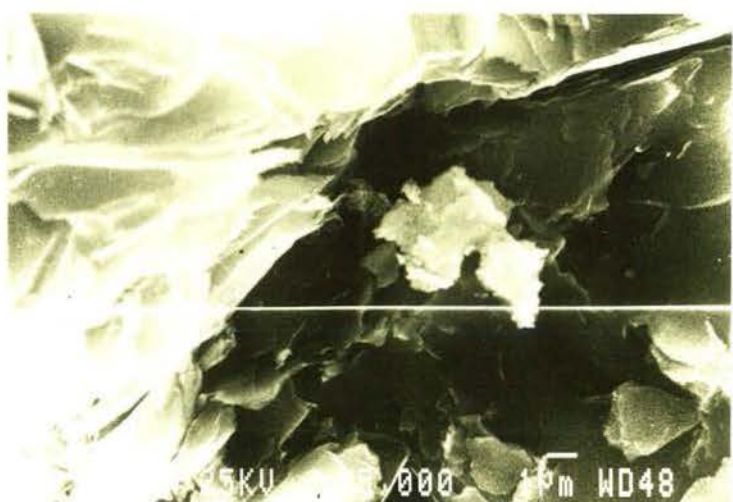
6.7



8.1



8.2



8.3

## Chapter 9

# CONCLUSIONS

---

Conflicting models for the setting of the Mt. Leyshon gold mine prompted this study on the geology and facies architecture of the Mt. Leyshon breccia complex. Systematic analysis of facies characteristics, structure, igneous geochemistry, mineral paragenesis and hydrothermal alteration studies, have implications for the genesis of the Mt. Leyshon breccia complex, controls on gold mineralisation and regional exploration for porphyry hosted mineral deposits. As a consequence of this integrated geological approach, the dynamic model presented in this thesis also has implications for breccia mechanisms and magmatic processes in actively deforming upper crust. A facies model for the complex is integrated with its structural and hydrothermal fluid evolution, which allows discussion of breccia pipe forming mechanisms, and controls on gold mineralisation.

### 9.1 A FACIES MODEL OF AN INTRUSIVE BRECCIA AND IGNEOUS COMPLEX

Detailed mapping and drill core analysis has determined the facies architecture of the Mt. Leyshon breccia complex, requiring its re-interpretation as a subvolcanic intrusive breccia and igneous complex. The rhombohedral shaped breccia complex is defined by the main pipe breccia which has an overall antler-like geometry and intrusive, inter-fingering contacts with basement; both at its margin and with blocks in the complex. Basement blocks within the complex have undergone only limited rotation and preserve evidence for two geometrically distinct (1st and 2nd order) fragmentation events. Rheological contrasts across the structurally offset granite-metasediment contact, and abundant dislocation points in the metasediment, controlled the location of the complex within regional wrench system. No unambiguous evidence for pyroclastic lithologies occurs in the complex, nor is there evidence the complex vented. The mobile/transported component (third order fragmentation) of breccia units have characteristics suggesting forceful injection into host rocks as a result of high pressure fluid discharge, rather than low pressure free discharge to the surface.

The main pipe breccia is composed of two distinct units (fine and coarse variants) which have gradational and steeply dipping contacts. Commonly these units are discrete or gradational from one to the other, but locally oscillate between fine and coarse variants over short distances. Accretionary structures (pellets) occurring predominantly in the fine variant suggest particle accretion during breccia formation. Their presence in the main pipe breccia indicates they are not necessarily diagnostic of pyroclastic lithologies. The facies characteristics of the main pipe breccia suggest it resulted from pervasively distributed host rock extension, combined with prolonged mobilisation and transport of fragments upwards along brittle faults, in the presence of a fluid phase. A juvenile igneous component has not been identified in the main pipe breccia, but the rare presence of non-vesiculated felsic and intermediate cognate igneous fragments suggest the existence of a magma system prior to complex formation.

Subsequent evolution of the Mt. Leyshon complex involved smaller scale brecciation at a higher level in the crust. An initially quiescent magmatic period (resulting in quartz-molybdenite mineralisation) evolved into a dynamic and interactive period, where a progressive increase in cognate and juvenile igneous fragments in breccias, and the implied digestion of the fragmental component of porphyry unit II by the magma, provides evidence for magma/breccia interaction.

The first brecciation event of the interactive period formed the Mt. Leyshon breccia pipe (the main gold-bearing unit), followed closely by the fragmental component of porphyry unit II, the Mt. Hope breccia and felsic igneous (porphyry unit II, III and IV) intrusions, which partly engulfed and reworked these last two breccia units. The facies characteristics of these breccia units suggest processes of pervasively distributed host rock extension controlled their formation, in conjunction with minor to moderate fluid release.

The final brecciation events formed tuffisite breccia dykes and late breccia dykes, which were focused into dyke- and sill-shaped bodies and contain abundant cognate and juvenile igneous particles. These breccias were preceded by intermediate igneous dyke and sill emplacement and overlapped with felsic dyke intrusion. The facies characteristics of the final breccia units suggest processes of prolonged fragment mobility/transport (gas-solids mobilisation and fluidisation) controlled their formation.

## 9.2 STRUCTURAL SETTING OF THE BRECCIA COMPLEX

The evolution of the Mt. Leyshon breccia complex was controlled by active strike slip faulting. The complex is localised at the intersection of two regional (NE and SE trending) sub-orthogonal strike slip corridors, defined by groups of linears and faults. Breccia complex strike slip faults, commonly expressed as brittle reactivation of ductile basement structures, link with the regional structures, suggesting the regional stress system controlled the structural development of the breccia complex. Late Palaeozoic deformation in basins within and abutting the Charters Towers Block is explained by linking of NE trending transfer faults with extensional, compressional and strike slip faults. In these basins, transfer faults were important in localising igneous emplacement and possibly gold mineralisation.

Distributed, extensional brittle strike slip faulting resulted in basement fault and fracture meshes (and extensional quartz veins) prior to intrusion of the main pipe breccia, which is consistent with limited data suggesting regional east-west extension at this time. Subsequent to hydrothermal lithification of the main pipe breccia, east-trending laminated quartz-molybdenite veins and oblique slip normal faults suggest a local change to east-west compression prior to Mt. Leyshon breccia formation. Inter-breccia shear zones at the western margin of the pipe indicate the strike slip fault system remained active during this time, and possibly resulted in the fracture mesh at the site of subsequent pipe formation. The orientation of breccia and igneous units together with the tendency for strike slip faults to reactivate earlier formed dyke contacts, veins and faults suggests the wrench system remained active during all periods of complex development. Extensional and

shear fibre veins of the same paragenetic stage suggest this is also true of hydrothermal fluid flow in the complex, which evolved during fluctuating high fluid pressures.

Late reverse faults (post dating gold mineralisation) in the complex indicate a change to dominantly compressional tectonics, probably related to regional east-west compression and Triassic inversion of the Bowen Basin. This change in stress system likely contributed to the complicated movement history of breccia complex strike slip faults.

### **9.3 INTEGRATED GEOLOGIC AND HYDROTHERMAL FLUID EVOLUTION**

The geologic and paragenetic studies on the Mt. Leyshon breccia complex define four main episodes of igneous emplacement, breccia generation and hydrothermal evolution. In the first episode, widespread extensional quartz veins (hydrothermal stage I) formed in host rock, and the emplacement at depth of a magmatic system probably contributed to main pipe breccia formation, which defines the Mt. Leyshon complex. Argillic I alteration was both the first hydrothermal event to effect the main pipe breccia and the first event of episode II, suggesting a significant time interval separated the formation of the breccia and subsequent high temperature alteration. Prograde potassic alteration was probably transitional to propylitic alteration, and formed during high temperature fluid flow that lithified the main pipe breccia. In the latter part of episode II, the emplacement of intermediate then felsic dykes preceded sericitic I alteration and quartz-molybdenite vein formation.

Episode III (interactive magma/breccia sequence) is characterised by periodic breccia and (intermediate and felsic) igneous emplacement, beginning with the Mt. Leyshon breccia. The interactive magma/breccia sequence was overprinted by argillic II alteration prior to high temperature alteration in episode IV. During this final period, widespread but structurally controlled alteration developed throughout the complex, in association with vein and fault style brecciation, in the absence of igneous emplacement. Hydrothermal fluid flow was channelled through intermittent re-brecciation zones, resulting in earlier quartz infill and sequentially later propylitic II, sericitic II, argillic III and kaolinite alteration. Minor gold mineralisation was probably deposited in association with pyrite during the later stages of this porphyry-style system.

Widespread manganosiderite and base metal mineralisation, again possibly with minor gold mineralisation, records a change in hydrothermal fluid character. The bulk of gold mineralisation in the Mt. Leyshon deposit formed as a late mineralising event in re-break zones (secondary porosity) within breccia cavities and veins, apparently in the absence of any associated host rock alteration.

### **9.4 FACIES MODEL OF THE MT. LEYSHON BRECCIA PIPE**

Examination of the relationship between host rock outside the pipe, blocks within the pipe and the smaller fragments provides the frame of reference for facies analysis investigating Mt. Leyshon

breccia pipe formation. With the aid of graphic analysis of drill core, the breccia pipe is divided into six facies based on fragmentation characteristics (fragmentation progressions, jigsaw fit textures), the proportion of mixed fragment zones and fragment types. On the basis of these facies characteristics, the six facies are interpreted to reflect variations in three fundamental mechanisms of pipe formation:

- (1) Host rock fragmentation.
- (2) Host rock expansion.
- (3) Fragment transport/mobility.

Facies characteristics (such as an increased sorting and a reduction in fragment size in transport zones) suggest the presence of a fluid phase during brecciation.

Much of the breccia pipe consists of variably *in situ* fragmented host rock. These regions and variation in dominant fragment type define a pre-pipe host rock stratigraphy. Portions of the pipe dominated by fragmentation progressions have characteristics and a geometry suggesting they formed by fault induced (first order) host rock fragmentation. Horizontal and vertical extension of the host rock during pipe formation is indicated by high matrix zones (with expanded fragments), jigsaw fit textures and the geometry of the whole pipe. Several stages in the dynamic evolution of the breccia pipe are preserved in the facies characteristics. As the degree of host rock fragmentation, expansion and transport/mobility in a given portion of the pipe increase, jigsaw fit textures and mixed fragment zones become dominant over fragmentation progression.

Zones of fragment transport occur in narrow regions of maximum extension throughout the pipe and in a steeply dipping irregular region at the northern end of the pipe; the probable focus of fluid release. Variation in host rock rheology influences the style of fragmentation and as a consequence facies characteristics. The style of deformation--extensional shear versus pure extension--may also be important.

## 9.5 EVOLUTION OF THE MAGMATIC SYSTEM

The geologic and petrographic relations of the Mt. Leyshon igneous units associated with breccia formation indicate magmatic evolution was complex, and the emplacement of igneous bodies was coeval with, and resulted in, breccia generation. Current models for magmatic evolution associated with porphyry style mineralised systems require modification to reflect the more realistic geologic situation.

Early magmatic evolution is poorly known; if a batholith was associated with the main pipe breccia formation it was likely several kilometres below the level of exposure. Cognate igneous fragments in the main pipe breccia, however, imply the early presence of magmatic cycles. Early post-main pipe breccia magmatic evolution was relatively quiescent and culminated in quartz-molybdenite mineralisation. This is consistent with the geologic and paragenetic evidence suggesting the main pipe breccia was only partially lithified, favouring aseismic events and encouraging a high degree of fractionation.

Subsequent breccia events occurred during a dynamic period of magmatic evolution (magma/breccia interaction) when simultaneously molten, fluidly mingled and chilled magma was spatially, temporally and genetically related to, and partially consumed, breccia units. Tectonically induced extension overlapped with this dynamic period, and brecciation resulted from the following repeated magmatic cycle: recharge of more basic magma to the felsic magma system, fractionation to felsic magma compositions, intrusive breccia generation during vapour release.

On the basis of their petrographic and geochemical characteristics the Mt. Leyshon igneous units are divided into a felsic and intermediate group. A petrogenetic model for the Mt. Leyshon igneous units proposes fractional crystallisation of the observed phenocryst phases controlled their evolution. However, periodic input of more basic magma induced minor magma mingling, implying volatile transfer, and possibly resulted in a zoned magma system, from which periodic igneous emplacement and volatile loss into the Mt. Leyshon complex occurred. The petrographic characteristics of the igneous rocks genetically related to brecciation, such as the presence of K-feldspar megacrysts, suggest they were not saturated with an aqueous fluid phase during emplacement. A fluid phase with an appreciable non-aqueous component (CO<sub>2</sub>, SO<sub>2</sub>, HCl, etc.) was likely present during brecciation.

Available data suggests the compositional variation of the regional igneous units was also due to fractional crystallisation. The Mt. Leyshon and regional suites are broadly calc-alkaline, although significant chemical differences between the two suites, such as the weakly alkaline character and the presence of an inflection in the Zr evolution trend for the Mt. Leyshon units, suggests they generally evolved as separate magma systems.

## 9.6 BRECCIA MECHANISMS

Variation in the rate and duration of the same fundamental processes (structural, fluid phase and magmatic) can produce a wide variety of breccia types without the need to resort to grossly different mechanisms or levels in the crust to explain their textural differences. Based on the geologic, paragenetic and geochemical evidence noted above, the three fundamental mechanisms of host rock brecciation (fragmentation, expansion and transport/mobilisation) defined in this thesis are examined in terms of current concepts regarding structural, fluid phase and magmatic processes.

A dynamic model for the Mt. Leyshon breccia complex reflects the evidence suggesting these geologic processes are complexly interdependent. Five breccia events are identified in the complex resulting from four geological cycles. Brecciation results from variable coupling of the same geological processes:

- (1) Brittle strike slip faulting and host rock extension interpreted to result from seismic rupture perturbation at dilational fault irregularities as a consequence of the earthquake (crustal/fluid pressure) cycle.

- (2) Magmatic vapour evolution as a consequence of fractional crystallisation, combined with periodic recharge of more basic magma and resultant volatile exsolution, and possible inter-system vapour transfer.
- (3) Explosively driven hydrofracture as a consequence of rapid magmatic vapour decompression (first boiling), evolving to time dependent vapour discharge, and as a result fragment transport/mobilisation in breccia pipes and dykes.
- (4) Fluid re-distribution in conjunction with after shock activity.

These interdependent processes may operate synchronously or stepwise and as a consequence the final breccia unit characteristics will reflect their complex interaction. As a consequence of the geological rate of these processes, they become variably decoupled and assume changing importance with time. A third aspect to breccia mechanisms is the time dependant nature of these processes, which in turn reflect the physical conditions (e.g. capacity of a magmatic system to allow inter-system vapour transfer).

The overall evolution of the Mt. Leyshon breccia complex records the passage of a magmatic system through the upper crust during transcurrent faulting. Three general mechanisms of brecciation are envisaged within this time-space framework:

- (1) Tectonic extension dominant (main pipe and Mt. Leyshon breccias).
- (2) Magma recharge and vapour evolution dominant (tuffisite breccia dykes and late breccia dykes).
- (3) A complex regime where both mechanisms interact (e.g. "porphyry" unit II).

As a consequence of differences in the rate of geological processes, therefore, the controlling mechanism may change with time.

## 9.7 MODEL FOR GOLD MINERALISATION

In terms of the geological cycles proposed in this thesis, gold mineralisation occurred in the Mt. Leyshon breccia complex at the end of an extended period where the evolution of the complex was dominated by fluid phase and structural processes (cycle IV). The geometry of the ore body, the orientation of the mineralised segments, and the timing and distribution of gold in the host rocks suggest gold mineralisation was controlled by fault reactivation under high fluid pressure conditions.

The bulk of gold mineralisation is paragenetically very late and postdates all coeval igneous emplacement and a considerable sequence of prograde to retrograde hydrothermal evolution. Gold occurs in at least three types of porosity within the host rocks:

- (1) Primary porosity reflecting the original characteristics of the brecciated rocks as exemplified by the Mt. Leyshon breccia.
- (2) Secondary porosity resulting from re-break zones cutting across rock units.
- (3) Tertiary porosity resulting from dissolution of rock and alteration minerals (especially tuffisite breccia dykes and porphyry unit IV).

The Mt. Leyshon ore body has an irregular, steeply dipping and bulbous geometry consistent with the control by the irregular nature of porosity and permeability on gold deposition. At lower levels the ore body consists of linear NE and SE trending en-echelon mineralised segments, interpreted to result from movement on similarly oriented strike slip faults. The expanded upper levels of the ore body probably resulted from an upward branching fault geometry and/or rheological contrast between upper (granite and dolerite rich) and lower (main pipe breccia rich) host rocks to the ore body.

These characteristics suggest that at the regional scale the location of the ore body within the Mt. Leyshon breccia complex was controlled by secondary porosity, resulting from the intersection of strike slip fault segments in the Mt. Leyshon and Mt. Dean corridors. The dynamic geological model suggests fluid mixing may have resulted from diffusion into dilated regions of the complex following seismic rupture, combined with release of trapped magmatic vapour during aftershocks. Gold bearing fluid(s) was possibly derived from the mixing of a crustal pore water with a deeper metamorphic fluid or basinal brine, and a magmatic fluid.

### **9.8 RECOMMENDATIONS FOR FUTURE WORK**

Existing work on the geochemistry of the Mt. Leyshon hydrothermal system is speculative. The dynamic geological model determined in this thesis provides the framework for subsequent detailed geochemical investigation of ore forming fluid(s).

At the local mine scale little is known about the kinematic and spatial significance of structures (secondary porosity) which probably controlled the distribution of gold mineralisation in the breccias. A different but related problem is the possible control of clay mineralogy on trap sites for gold precipitation in host rocks.

---

**References**

- Allegre, J. C., Treuil, M., Minster, J. F., and Albarede, F., 1977, Systematic use of trace elements in igneous processes. Part I: Fractional crystallisation processes in volcanic suites, *Contributions Mineralogy Petrology*, V. 60, p.57 - 75.
- Allen, R. L., 1988, False pyroclastic textures in altered silicic lavas, with implications for volcanic-associated mineralisation, *Economic Geology*, V. 83, p. 1424-1426.
- Anderson, E. M., 1951, *The Dynamics of Faulting and Dyke Formation with Applications to Britain*. Oliver and Boyd, Edinburgh.
- Anderson, W. B., 1975, Cooling history and uranium mineralisation of the Buckshot Ignimbrite, Presidio and Jeff Davis Counties, Texas, unpublished Masters Thesis, The University of Texas at Austin.
- Andrew, S. A., Morrison, G. W., Whitford, D. J., and Bird, M. I., Discussion of Scott, K. M. "Origin of alunite- and jarosite-group minerals in the Mt. Leyshon epithermal gold deposit, northeast Queensland, Australia".
- Bacon, R. C., 1986, Magmatic inclusions in silicic and intermediate volcanic rocks, *Journal of Geophysical Research*, V. 91, No. B6, p. 6091-6112.
- Baker, E. M., and Andrew, A. S., 1991, Geologic, Fluid Inclusions, and Stable Isotope Studies of the Gold-Bearing Breccia Pipe at Kidston, Queensland, Australia, *Economic Geology*, V. 86, p. 810-830.
- Baker, E. M., Kirwin, D. J., Taylor, R. G., 1986, Hydrothermal breccia pipes, Contributions of the Economic Geology Research Unit, No. 12, Geology Department, James Cook University, p. 45.
- Baker, R. M., 1987, Geologic and fluid inclusion study of breccia hosted gold mineralisation at Kidston, North Queensland, Australia, unpublished Ph.D Thesis, James Cook University of North Queensland, Townsville, Australia.
- Banks, N. G., 1976, Halogen contents of igneous minerals as indicators of magmatic evolution of rocks associated with the Ray porphyry copper deposit, Arizona, U.S. Geological Survey, *Journal Research*, V. 4, p. 91-117.
- Barrett, T. J. and MacLean, W. H., 1991, Chemical, mass, and oxygen isotope changes during extreme hydrothermal alteration of an Archean rhyolite, Noranda, Quebec, *Economic Geology*, V. 86, p. 406 - 414.
- Bird, M. I., Chivas, A. R., and McDougall, I., 1990, An isotopic study of surficial alunite in Australia. 2: potassium-argon geochronology, *Chemical Geology*, V.80, p.133-145.
- Blake, S., 1981, Eruption from zoned magma chambers, *Journal Geological Society London*, V. 138, p. 281-287.
- BMR Research Newsletter 1991, Regional oxygen-isotope patterns, Implications for epithermal gold exploration, *Geology and Geophysics*, Number 14, p. 1-2.
- Bradbury, J., 1988, The volcanic and shallow sub-volcanic component of the breccia hosted Olympic Dam U-Cu-Au deposit: implications for breccia pipe development, unpublished Honours Thesis, Department of Earth Sciences, Monash University.
- Bryant, D. G., 1968, Intrusive breccias associated with ore, Warren (Bisbee) mining district, Arizona, *Economic Geology*, V. 63, p.1-12.

- Bryner, L., 1961, Breccia and pebble columns associated with epigenetic ore deposits, *Economic Geology*, V. 56, p. 488-508.
- Bryner, L., 1968, Proposed terminology for hydrothermal breccias and conglomerates, *Economic Geology*, V. 63, p. 692 - 693.
- Burnham, C. W. and Ohmoto, H., 1980, Late stage processes of felsic magmatism. In: *Granitic magmatism and related mineralisation*, Eds. Ishihara, S., and Takenouchi, S., Society Mining Geologists Japan, Special Issue, No. 8, p. 1-11.
- Burnham, C. W., 1979, Magmas and hydrothermal fluids. In: *Geochemistry of hydrothermal ore deposits*, Barnes, H. L. (ed.), *Geochemistry of hydrothermal ore deposits*, Wiley, New York, p. 71-136.
- Burnham, C. W., 1985, Energy release in subvolcanic environments: implications for breccia formation, *Economic Geology*, V. 80, p. 1515-1522.
- Bussell, M. A., and McCourt, W. J., 1977, The Inglesia Irca intrusion and the role of gas brecciation in the emplacement of the coastal batholith of Peru, *Geological Magazine*, V. 114, p. 375-387.
- Byerlee, J. D., 1978, Friction of rocks, *Pure and Applied Geophysics*, V. 77, p. 691-693.
- Caldeira, K., and Rampino, M. R., 1992, Mount Etna CO<sub>2</sub> may affect climate, *Nature*, V. 355, p. 401 - 402.
- Candela P. A., and Holland H. D., 1986, A mass transfer model for copper and molybdenum in magmatic hydrothermal systems: the origin of porphyry-type ore deposits, *Economic Geology*, V. 81, p. 1 - 19.
- Candela, P. A., 1986, The evolution of aqueous vapour from silicate melts: Effects on oxygen fugacity, *Geochimica et Cosmochimica Acta*, V. 50, p. 1205 - 1211.
- Carrigan, C. R., Schubert, G., and Eichelberger, J. C., 1992, Thermal and dynamical regimes of single and two-phase magmatic flow in dykes, *Geophysical Abstracts in Press*, July 1992.
- Carten, R. B., Geraghty, E. P., Walker, B. M., and Shannon, J. R., 1988, Cyclic development of igneous features and their relation ship to high-temperature hydrothermal features in the Henderson Porphyry molybdenite deposit, Colorado, *Economic Geology*, V. 83, p. 266-296.
- Carter, F. W., 1969, The Cloudy Pass epizonal batholith and associated subvolcanic rocks, *Geological Society America Special Paper*, No. 116, p. 1-54.
- Cas, R. A. F., and Wright, J. V., 1987, *Volcanic Successions: modern and ancient*, Allen and Unwin, p. 528.
- Cathles, L. M., 1981, Fluid flow and genesis of hydrothermal ore deposits, *Economic Geology*, 75th Anniversary volume, p. 424-457.
- Cerny, P., Meintzer, R. E., and Anderson A. J., 1985, Extreme fractionation of rare-element granitic pegmatites: selected examples of data and mechanisms, *Canadian Mineralogist*, V. 23, p. 381-421.
- Clarke, D. E., 1971, *Geology of the Ravenswood 1-mile sheet area, Queensland*, Report Geological Survey, Queensland, V. 43.
- Clayton, W. F. 1991, *Structure and breccia development in the Mount Leyshon area, North Queensland*, Masters Thesis, Department of Geology, James Cook University of North Queensland, Australia.
- Cloos, H., 1941, Bau and tatigkeit von tuffschloten. Untersuchungen an den Schwabischen vulkan, *Geologische Rundschau*, V. 32, p. 709 - 800.
- Cocherie, A., 1986, Systematic use of trace element distribution patterns in log-log diagrams for plutonic suites, *Geochimica et Cosmochimica Acta*, V. 50, p. 2517-2522.

- Colley, H., Treloar, P. J., Shepherd, T. J., and Naden, J., 1991, Formation of San Pedro de Cachiyuyo breccia pipes, Inca de Oro, Chile, *Transactions IMM*, V. 100, p. B179-B191.
- Cornwall, H. R. 1982, Petrology and chemistry of igneous rocks: Ray Porphyry Copper District, Pinal County, Arizona. In: *Advances in the geology of porphyry copper deposits-southwestern North America*, Titley, S. R., Ed., The University of Arizona Press, Tuscon, Arizona.
- Cox, K. G., Bell, J. D., and Pankhurst, R. J., 1979, *The interpretation of igneous rocks*, George Allen and Unwin, London, p. 450.
- Daubrée, A., 1891, Recherches experimentales sur le rôle de gaz à hautes températures, dones de tres fortes pressions et animes d'un mouvement forte rapide divers phenomenes geoloiques, *Bull. Soc. Géol. France 3eSer.*, V. 19, p. 313-354.
- Dilles, J. H., 1987, Petrology of the Yerington Batholith, Nevada: Evidence for evolution of porphyry copper ore fluids, *Economic Geology*, V. 82, p. 1750 - 1789.
- Eberl, D. D., 1993, Three zones of illite formation during burial diagenesis and metamorphism, *Clays and Clay Minerals*, V. 41, p. 26-37.
- Eichelberger, J. C., 1975, Origin of andesite and dacite: evidence of mixing at Glass Mountain in California and at other Circum-Pacific volcanoes, *Geological Society America Bulletin*, V. 86, p. 1381-1391.
- Ernst, W. G., and Hall, C. A., 1975, Feldspathic Geodes near Black Mountain, Western San Luis Obispo County, California, *American Mineralogist*, V. 60, p. 1105-1112.
- Ewart, A., 1971, Chemical changes accompanying spherulitic crystallisation in rhyolitic lavas, Central Volcanic Region, New Zealand, *Mineralogy Magazine*, V. 38, p. 424-434.
- Ewers, G., MacKenzie, D., Oversby, B., and Wyborn, D., 1991, Regional oxygen-isotope patterns: Implications for epithermal gold exploration, *BMR Research Newsletter*, No. 14, April, p. 1-2.
- Eyles, N., Eyles, C. H., and Maill, A. D., 1983, Lithofacies types and vertical profile models; an alternative approach to the description and environmental interpretation of glacial diamict and diamictite sequences, *Sedimentology*, V. 30, p. 393 - 410.
- Floyd, P. A., and Winchester, J. A., 1978, Identification and discrimination of altered and metamorphosed volcanic rocks using immobile elements, *Chemical Geology* V.21, p. 291-306.
- Fyfe, W. S., Price, N. J., and Thompson, A. B., 1978, *Fluids in the earth's crust*, *Developments in Geochemistry*, 1, Elsevier, Amsterdam, p. 383.
- Gates, O., 1959, Breccia pipes in the Shoshone range, Nevada, *Economic Geology*, V. 54, p. 790-815.
- Geike, A., 1902, The geology of the Eastern Fife, *Memoirs Geol. Surv. Scotland*, No. 40a, 41, 48a, 49a, p. 520.
- Gerlach, T. M., 1986, Exsolution of H<sub>2</sub>O, CO<sub>2</sub>, and S during eruptive periods at Kilauea Volcano, Hawaii, *Journal Geophysical Research*, V. 19, p. 12177-12185.
- Gerlach, T. M., 1991, Present-day carbon dioxide emission from volcanos, *Earth in space*, V. 4, p. 5 and 14.
- Gerlach, T. M., and Taylor, B. E. 1990, carbon isotope constraints on degassing of carbon dioxide from Kilauea Volcano, *Geochemica et Cosmochimica Acta*, V. 54, No. 7, p. 2051-2058.
- Gibbs, A. D., 1984, Structural evolution of extensional basin margins, *Journal Geological Society London*, V. 141, p. 609-620.

- Giggenbach, W. F., 1987, Redox processes governing the chemistry of fumarolic gases from White island, New Zealand, *Applied Geochemistry*, V. 2, p. 143-161.
- Giggenbach, W. F., 1992, Magama degassing and mineral deposition in hydrothermal systems along convergent plate boundaries, *Economic Geology*, V. 87, p. 1927-1944.
- Giggenbach, W. F., Garcia P. N., Londono C. A., Rodriguez V. L., Rojas G. N., and Calvache V. M. L., 1990, The chemistry of fumarolic vapor and thermal-spring discharges from the Nevado del Ruiz volcanic-magmatic-hydrothermal system, Colombia, *Journal of Volcanology and Geothermal Research*, V. 42, p. 13 - 39.
- Glazner, A. F., 1991, Plutonism, oblique subduction, and continental growth: An example from the Mesozoic of California, *Geology*, V. 19, p. 789-786.
- Gleeson, P., 1992, Resource Estimation and 3 Dimensional Modelling of Gold Mineralisation at the Mt Leyshon Gold Mine NE Queensland, M.Sc. applied science thesis, University of Queensland, unpublished.
- Gleick, J., 1987, Chaos: making a new science, *Cardinal*, p. 352.
- Goellnicht, N. M., Groves, D. I., and McNaughton, N. J., 1991, Late proterozoic fractionated granitoids of the mineralised Telfer area, Paterson Province, Western Australia, *Precambrian Research*, V. 51, p. 375-391.
- Goldfarb, R. J., Snee, L. W., Miller, L. D., and Newberry, R. J., 1991, Rapid dewatering of the crust deduced from ages of mesothermal gold deposits, *Nature*, V. 354, p.296-298.
- Goodspeed, G. E., 1953, Rheomorphic breccias, *American Journal of Science*, V. 251, p. 453-469.
- Gustafson, L. B., and Hunt, J. P., 1975, The porphyry copper deposit at El Salvador, Chile, *Economic Geology*, V. 70, p. 857-912.
- Hammond, R., 1990, Modelling the Geological Structure of the Bowen Basin, present and future, Bowen Basin Symposium 1990, p. 7-9.
- Hartley, J. S., Peter, S. G., and Beams, S. D., 1989, Current developments in the Charters Towers geology and gold mineralisation, NQ Gold 1989 Conference, Townsville, Queensland, p. 7-14.
- Hazlitt, J. S., and Thompson, T. B., 1990, Breccia bodies in the Leadville District, with emphasis on occurrences in the Black Cloud Mine, Lake County, Colorado, *Economic Geology*, Monograph 7, p. 180-192.
- Hedenquist, J. W., and Henley, R. W., 1985, Hydrothermal eruptions in the Waiotapu geothermal system, New Zealand: Their origin, associated breccias, and relation to precious metal mineralisation, *Economic Geology*, V. 80, p. 1640-1668.
- Heinrich, C. A., Henley, R. W., and Seward, T. M., 1989, Hydrothermal Systems, Australian Mineral Foundation, Adelaide, p. 74.
- Heinrich, C., Mernagh, T., and Ryan, C., 1992, Metal segregation by magmatic gases - first results from new fluid inclusion technique, *BMR Research Newsletter*, V. 16, p. 12-13.
- Henderson, R. A., 1986, Geology of the Mt. Windsor Subprovince - a Lower Palaeozoic volcano-sedimentary terrane in the northern Tasman Orogenic Zone, *Australian Journal of Earth Sciences*, V. 33, p. 343-364.

- Henley, R. W., and Adams, D. P. M., 1992, Strike-slip reactivation as a control on epithermal vein-style gold mineralization, *Geology*, V. 20, p. 443-446.
- Henley, R. W., and McNabb, A., 1978, Magmatic vapor plumes and ground-water interaction in porphyry copper emplacement, *Economic Geology*, V. 73, p. 64-68.
- Hildreth, W., Grove, T. L., and Dungan, M. A., 1986, Introduction to special section on open magmatic systems, *Journal Geophysical Research*, V. 91, p. 5887-5889.
- Hill, D. P., 1977, A model for earthquake swarms, *Journal Geophysical Research*, V. 82, p. 1347-1352.
- Hill, D. P., and Thatcher, W., 1991, Fault orientations in extensional and conjugate strike-slip environments and their implications, *Geology*, V. 19, p. 1116-1120.
- Hoek, E., and Brown, E. J., 1980, *Underground excavations in rock*, Institute of Mining and Metallurgy, London, p. 527.
- Holloway, J. R., 1976, Fluids in the evolution of granitic magmas: Consequences of finite CO<sub>2</sub> solubility, *Geological Society of America Bulletin*, V. 87, p. 1513-1518.
- Horton, D. J., 1982, Porphyry-type copper and molybdenum mineralisation in eastern Queensland, Geological Survey of Queensland publication No. 378, p. 59.
- Huppert, H. E., and Sparks, R. S. J., 1988, The generation of granitic magma by intrusion of basalt into continental crust, *Journal of Petrology*, V. 29, p. 599-624.
- Huppert, H. E., Sparks, R. S. J., and Turner, J. S., 1982, Effects of volatiles on mixing in calc-alkaline magma systems, *Nature*, V. 297, p. 554-557.
- Hutton, D. H. W., and Reavy, R. J., 1992, Strike slip tectonics and granite petrogenesis, *Tectonics*, V. 11, p. 960-967.
- Hutton, L. J., Rienks, I. P., and Wyborn, D., 1990, A reinterpretation of the Ravenswood Batholith, North Queensland, Pacific Rim '90 Congress proceedings, AusI.M.M., Melbourne, p. 179-185.
- Jaeger J. C., and Cook, N. G., (Editors), 1979, *Fundamentals of rock Mechanics*, Chapman and Hall, London, p. 593.
- Johnson, S. E., and Henderson, R. A., 1991, Tectonic development of the Drummond Basin, eastern Australia: backarc extension and inversion in a late Palaeozoic activemargin setting, *Basin Research*, V. 3, p. 197-213.
- Jones, B. K., and Thompson, J. F. H., 1991, Application of empirical models to porphyry copper-gold exploration, Research Newsletter '91, Mineral Deposit Research Unit, Department of Geological Science, University British Columbia.
- Judd, J. W., 1873, The secondary rocks of Scotland, *Quart. J. Geol. Soc.*, V. 29, p. 97-197.
- Kennedy, A. K., Hart, S. R., and Frey, F. A., 1990, Composition and isotopic constraints on the petrogenesis of alkaline arc lavas: Lihir Is., Papua New Guinea, *Journal of Geophysical Research*, V. 95, No. B5, p. 6929-6942.
- Kents, P., 1964, Special breccias associated with hydrothermal developments in the Andes, *Economic Geology*, V. 59, p. 1551 - 1563.
- Knipe, S. W., Foster, R. P., and Stanley, C. J., 1992, Role of sulphide surfaces in sorption of precious metals from hydrothermal fluids, *Transaction IMM*, V. 101, p. B83-B88.

- Koyaguchi, T., 1986, Evidence for two stage mixing in magmatic inclusions and rhyolitic lava domes on Niijima Island, Japan, *Journal Volcanology and Geothermal Research*, V. 29, p. 71-98.
- Lacy, W. C., 1990, The breccia environment, 50-year retrospection, Pacific Rim '90 Conference Volume, AusIMM, Melbourne, p. 63-68.
- Lang, S. C., Gunther, L. M., and Rich, N., 1990, The Devonian-Carboniferous intracratonic Burdekin Basin, North Queensland:II Volcaniclastic continental facies of the Dotswood Group.Proceedings of the Pacific Rim '90 Congress, AusIMM, Brisbane, p. 631 - 637.
- Laznika, P., 1988, Breccias and coarse fragmentites: petrology, environments, associations, ores, developments in economic geology, 25, Elsevier, p. 832.
- Le Bas, M. J., Le Maitre, R. W., Streckeisen, A., and Zanettin, B., 1986, A chemical classification of volcanic rocks based on the total alkali-silica diagram, *Journal Petrology*, V. 27, p. 745-750.
- Lipman, P. W., Christiansen, R. L. and Van Alstine, R. E., 1969, Retention of alkalis by calc-alkalic rhyolites during crystallisation and hydration, *American Mineralogist*, V. 54, p. 286-291.
- Locke, A., 1926, The formation of certain ore bodies by mineralization stopping, *Economic Geology*, V. 21, p. 431-453.
- Lofgren, G., 1970, Experimental devitrification rate of rhyolite glass, *Geological Society America Bulletin*, V.81, p. 553-560.
- Lofgren, G., 1971a, Experimentally produced devitrification textures in natural rhyolite glass, *Geological Society America Bulletin*, V. 82, p. 111-124.
- Lofgren, G., 1971b, Spherulitic textures in glassy and crystalline rocks, *Journal of Geophysical Research*, V. 76, p. 5635-5648.
- Lorenz, V., 1975, Formation of phreatomagmatic maar-diatreme volcanoes and its relevance to kimberlite diatremes, *Physics Chemistry Earth*, V. 9, p. 17 - 27.
- Maaloe, S., and Wyllie, P. J., 1975, Water content of a granite magma deduced from the sequence of crystallization determined experimentally with water-undersaturated conditions, *Contribution Mineralogy Petrology*, V. 52, p. 175-191.
- MacLean, W. H., 1990, Mass change calculations in altered rock series, *Mineralium Deposita*, V. 25, p. 44-49.
- Mann, A. C., 1983, Trace element geochemistry of high alumina basalt - andesite - dacite - rhyodacite lavas of the main volcanic series of Santorini volcano, Greece, *Contributions to Mineralogy and Petrology*, V. 84, p. 43-57.
- Marshall, R. R., 1961, Devitrification of natural glass, *Geological Society America Bulletin*, V. 72, p. 1493-1520.
- Mason, D. R. and McDonald, J. A., 1978, Intrusive rocks and porphyry copper occurrences of the Papua New Guinea - Solomon Islands region, a reconnaissance study, *Economic Geology*, V. 73, p. 857-877.
- Mawer, C. K., and Williams, P. F., 1985, Crystalline rocks as possible paleoseismicity indicators, *Geology*, V. 13, 100-102.
- McCallum, M. E., 1985, Experimental evidence for fluidisation processes in breccia pipe formation, *Economic Geology*, V. 80, p.1523-1543.

- McKibben, M. A., and Elders, W. A., 1985, Fe-Zn-Cu-Pb Mineralization in the Salton Sea Geothermal system, Imperial Valley, California, *Economic Geology*, V. 80, p. 539-559.
- McKinstry, H. E., 1948, *Mining Geology*, Prentice-Hall, Englewood Cliffs, New Jersey, 677 p.
- McPhie, J., Black, L. P., Law, S. R., Mackenzie, D. E., Oversby, B. S., and Wyborn, D., 1990, Distribution, character, setting of mineralised Paleozoic volcanic sequences, Burdekin Falls region, North Queensland, *Australasian Institute of Mining and Metallurgy*, V. 2, p. 465-471.
- Meyer, J., and Foland, K. A., 1991, Magmatic-tectonic interaction during early Rio Grande rift extension at Questa, New Mexico, *Geological Society of America Bulletin*, V. 103, p. 993-1006.
- Middleton, G. V., 1990, Non-linear dynamics and chaos: potential applications in the earth sciences, *Geoscience Canada*, V. 17, p. 3 - 11.
- Mitcham, T. W., 1974, Origin of breccia pipes, *Economic Geology*, V. 69, p. 412-413.
- Miyashiro, A., 1974, Volcanic rock series in island arc and active continental margins, *American Journal Science*, V. 274, p. 321-355.
- Morrison, G. W., Teale, G. S., and Hodkinson, I., 1987, Geology and gold mineralisation at Mount Leyshon, North Queensland, *Proceedings of the PacRim Congress '87, AusIMM*, p. 777-780.
- Morrison, G. W., Teale, G. S., and Hodkinson, I., 1988, The Mount Leyshon gold deposit. In: *Epithermal and porphyry style gold deposits in North Queensland, Bicentennial Gold '88 excursion handbook*, Economic Geology Research Unit, Contribution 29, James Cook University, p. 43-55.
- Murphy, F. C., 1984, Fluidized breccias: A record of brittle transitions during ductile deformation, *Tectonophysics*, V. 104, p. 325-349.
- Murray, C. G., Fergusson, C. L., Flood, P. G., Whitaker, W. G., and Korsch, R. J., 1987, Plate tectonic model for the Carboniferous evolution of the New England Fold Belt. *Australian Journal of Earth Sciences*, V. 34, p. 213-236.
- Musselwhite, D. S., De Paolo, D. J., and McCurry, M., 1989, The evolution of a silicic magma system: isotopic and chemical evidence from the Woods Mountain Volcanic Center, Eastern California, *Contributions Mineralogy Petrology*, V. 101, p. 19-29.
- Myers, J. S., 1975, Cauldron subsidence and fluidization: mechanisms of intrusion of the coastal batholith of Peru into its own volcanic ejecta, *Geological Society of America Bulletin*, V. 86, p. 1209-1220.
- Mysen, B. O., Eggler, D. H., Seitz, M. G., and Holloway, J. R., 1976, Carbon dioxide in silicate melts and crystals, Part I. Solubility measurements, *American Journal of Science*, V. 27, p. 455-479.
- Nakano, T., and Urabe, T., 1989, Calculated compositions of fluids released from a crystallizing granitic melt: Importance of pressure on the genesis of ore forming fluid, *Geochemical Journal*, V. 23, p. 307-319.
- Naney, M. T., 1983, Phase equilibria of rock-forming ferromagnesian silicates in granite systems, *American Journal of Science*, V. 283, p. 993-1033.
- Nilson, R., Rimer, N., and Halda, E., 1991, Dynamic modeling of explosively driven hydrofracture, *Journal of Geophysical Research*, V. 96, B11, p. 18,081-18100.
- Nobel, D. C., 1967, Sodium, potassium and ferrous iron contents of some secondary hydrated natural silicic glasses, *American Mineralogist*, V. 52, p. 280-286.

- Noble, L. F., 1941, Structural features of the Virgin Spring area, Death Valley, California, *Geological Society America Bulletin*, V. 52, p. 941-999.
- Norman, D. I., and Sawkins, F. J., 1985, The Tribag breccia pipes: Precambrian Cu-Mo deposits, Batchawana Bay, Ontario, *Economic Geology*, V. 80, 1593-1621.
- Norman, D. K., Parry, W. T., and Bowman, J. R., 1991, Petrology and geochemistry of propylitic alteration at southwest Tintic, Utah, *Economic Geology*, V. 86, p. 13-28.
- Norton, D. L., and Cathles, L. M., 1973, Breccia pipes-products of exsolved vapour from magmas, *Economic Geology*, V. 68, p. 540-546.
- Norton, D., and Knight, J., 1977, Transport phenomena in hydrothermal systems: Cooling plutons, *American Journal Science*, V. 277, p. 937-981.
- Norton, W. H., 1917, Studies for students. A classification of breccias, *Journal Geology*, V. 25, p. 160-194.
- Novikov, L. A., and Slobodskoy, R. M., 1979, Mechanism of formation of diatremes, *Internat. Geology Rev.*, V. 21, no. 10, p. 1131-1139.
- Nur, A., and Brooker, J. R., 1972, Aftershocks caused by pore fluid flow ?, *Science*, V. 175, p. 885-887.
- O'Hara, M. J., and Mathews, R. E., 1981, Geochemical evolution in an advancing periodically replenished, periodically tapped, continuously fractionated magma chamber, *Journal Geological Society London*, V. 138, p. 237-277.
- Ord, A., and Oliver, N., 1992, Controls on fluid pumping during deformation, *Geological Society of Australia Abstracts Number 32*, Ballarat.
- Paull, P. L., Hodkinson, I. P., Morrison, G. W., and Teale, G. S., 1990, Mount Leyshon gold deposit. In: *Geology of mineral deposits of Australia and Papua New Guinea*, ed. Hughes, F. E., AusI. M. M., Melbourne, p. 1471-1481.
- Peters, S. G., 1990, Lode controls of the Charters Towers goldfield, northeast Queensland, *The AusIMM Proceedings*, V. 295, p. 51-60.
- Petford, N., and Atherton, M. P., 1992, Granitoid emplacement and deformation along a major crustal lineament: the Cordillera Blanca, *Tectonophysics*, V. 205, p. 171-185.
- Phillips, W. J., 1972, Hydraulic fracturing and mineralisation, *Journal Geological Society of London*, V. 128, p. 337-359.
- Pitcher, W. S., 1987, Granites and yet more granites forty years on, *Geologische Rundschau*, V. 76, p. 51-79.
- Pollard, P. J., Taylor, R. G., and Tate, N. M., 1989, Textural evidence for feldspar dissolution as a mechanism of formation for Maggs Pipe, Zaaipplaats tin mine, South Africa, *Mineralium Deposita*, V. 24, p. 210-218.
- Pollard, P. J., Taylor, R. G., and Tate, N. M., 1989, Textural evidence for quartz and feldspar dissolution as a mechanism of formation for Maggs Pipe, Zaaipplaats tin mine, South Africa, *Mineralium Deposita*, V. 24, p. 210-215.
- Porter, E. W., and Ripley, E., 1985, Petrologic and stable isotope study of the gold-bearing breccia pipe at the Golden Sunlight deposit, Montana, *Economic Geology*, V. 80, p. 1689-1706.
- Ramsay, J. G., and Huber, M. I., 1983, *Modern Structural Geology V. 1: strain analysis*, Academic Press, p. 307.

- Ramsay, J. G., and Huber, M. I., 1987, *Modern Structural Geology V. 2: folds and fractures*, Academic Press, p. 700.
- Reynolds, J. H., 1928, Breccias, *Geological Magazine*, V. 65, p. 97-107.
- Richards, J. P., 1992, Magmatic-epithermal transitions in alkalic systems: Porgera gold deposit, Papua New Guinea, *Geology*, V. 20, p. 547-550.
- Richards, J. P., Chappell, B. W., and McCulloch, M. T., 1990, Intraplate-type magmatism in a continent-island-arc collision zone: Porgera intrusive complex, Papua New Guinea, *Geology*, V. 18, p. 958-961.
- Roedder, E., 1972, Composition of fluid inclusions, in Fleischer, M. (ed.), *Data of geochemistry: U.S. Geological Survey Professional Paper*, 440-JJ, p. 165.
- Rogers, P., McPhail, D., and Ryan, J., 1993, Crizzling: a method to slow the ageing process affecting glass collections, *Spectrum*, *British Science News*, No. 228/1, p. 8-11.
- Rose, A. W., and Burt, D. M., 1979, Hydrothermal Alteration. In: *Geochemistry of Hydrothermal Ore Deposits*, 2nd edition, Ed. Barnes, H. L., p. 176-235.
- Rose, A. W., and Burt, D. M., 1979, Hydrothermal alteration. In: *Geochemistry of hydrothermal ore deposits*, Ed. Barnes, H. L., Wiley, New York, p. 173-235.
- Ross, C. S., and Smith, R. L., 1961, Ash flow tuffs: their origin, geologic relations, and identification, *U.S.G.S. Professional Paper* 366, p. 81.
- Rottura, A., Del Morro, A., Piranelli, L., Petrini, R., Peccerillo, A., Caggianelli, A., Bargossi, G. M., and Piccarreta, G., 1991, Relationship between intermediate and acidic rocks in orogenic granitoid suites: petrological, geochemical and isotopic (Sr, Nd, Pb) data from Capo Vaticano (Southern Calabria, Italy), *Chemical Geology*, V. 92, p. 153-176.
- Rutter, E. H., and Hadizadeh, J., 1991, On the influence of porosity on the low temperature transition in siliciclastic rocks, *Journal of Structural Geology*, V. 13, p. 609-614.
- Sander, M. V., and Einaudi, M. T., 1990, Epithermal deposition of gold during transition from propylitic to potassic alteration at Round Mountain, Nevada, *Economic Geology* V. 85, p. 285-311.
- Sawkins, F. J., 1969, Chemical brecciation, an unrecognized mechanism for breccia formation ?, *Economic Geology*, V. 64, p. 613-617.
- Scott, K. M., 1990, Origin of alunite- and jarosite-group minerals in the Mt. Leyshon epithermal gold deposit, northeast Queensland, Australia, *American Mineralogist*, V. 75, p. 1176-1181.
- Scott, R. B., 1971, Alkali exchange during devitrification and hydration of glasses in ignimbrite cooling units, *Journal Geology*, V. 79, p. 100-110.
- Segall, P., and Pollard, D. D., 1980, Mechanics of discontinuous faults, *Journal Geophysical Research*, V. 85, p. 4337-4350.
- Segall, P., and Pollard, D. D., 1983, Nucleation and growth of strike slip faults in granite, *Journal of Geophysical Research*, V. 88, p. 555-568.
- Sharp, J. E., 1978, A molybdenum mineralised breccia pipe complex, Redwell Basin, Colorado, *Economic Geology*, V. 73, p. 369-382.
- Shaw, H. R., 1980, The fracture mechanics of magma transport from the mantle to the surface. In: *Physics of magmatic processes*, Hargraves, R. B. (ed.), Princeton University Press, Princeton, p. 201-264.

- Shaw, H. R., 1988, Mathematical attractor theory and plutonic-volcanic episodicity. In: *Modelling of volcanic processes*, Chi-Yu King and Scarpa, R. (eds.), Friedr. Vieweg und Sohn, Braunschweig/Wiesbaden, p. 162-206.
- Sibson, R. H., 1981, Fluid flow accompanying faulting: field evidence and models. In: *Earthquake prediction, an international review*, Simpson, D. W., and Richards, P. G. (Eds.), American Geophysical Union, Maurice Ewing Volume, 4, p. 593-603.
- Sibson, R. H., 1985, Stopping of earthquake ruptures at dilational fault jogs, *Nature*, V. 316, 248-251.
- Sibson, R. H., 1986, Brecciation processes in fault zones: inferences from earthquake rupturing, *Pure and Applied Geophysics*, V. 124, p. 159-175.
- Sibson, R. H., 1987, Earthquake rupturing as a hydrothermal mineralising agent, *Geology*, V. 15, p. 701-704.
- Sibson, R. H., 1989a, Structure and mechanics of fault zones in relation to fault-hosted mineralisation, *Australian Mineral Foundation course book*, p. 66.
- Sibson, R. H., 1989b, Earthquake faulting as a structural process, *Journal of Structural Geology*, V.11, p. 1-14.
- Sibson, R.H., 1987, Earthquake rupturing as a hydrothermal mineralizing agent, *Geology*, V. 15, p. 701-704.
- Sillitoe, R. H., 1985, Ore-related breccias in volcanoplutonic arcs, *Economic Geology*, V. 80, p. 1467-1514.
- Sillitoe, R. H., 1990, Gold-rich porphyry copper deposits of the Circum-Pacific region - an updated overview. In: *Pacific Rim '90 congress proceedings*, p. 119-126.
- Sillitoe, R. H., and Sawkins, F. J., 1971, Geologic, mineralogic, and fluid inclusion studies relating to the origin of copper bearing tourmaline breccia pipes, Chile, *Economic Geology*, V. 66, p. 1028-1041.
- Sillitoe, R. H., Baker, E. M., and Brook, W. A., 1984, Gold deposits and hydrothermal eruption breccias associated with a maar volcano at Wau, Papua New Guinea, *Economic Geology*, V. 79, p. 638-655.
- Sillitoe, R. H., Halls, C., and Grant, J. N., 1975, Porphyry tin deposits of Bolivia, *Economic Geology*, V. 70, p. 913-927.
- Simons, F. S., 1962, Devitrification dykes and giant spherulites from Klondike, Arizona, *American Mineralogist*, V. 47, p. 871-885.
- So, C.-S., and Shelton, K. L., 1983, A sulphur isotopic and fluid inclusion study of the Cu-W-bearing tourmaline breccia pipe, Ilkwang mine, Republic of Korea, *Economic Geology*, V. 78, p. 326-332.
- Sparks, R. S. J., and Marshall, L. A., 1986, Thermal and mechanical constraints on mixing between mafic and silicic magmas, *Journal Volcanology and Geothermal Research*, V. 29, p. 99-124.
- Streckeisen, A., 1976, To each plutonic rock its proper name, *Earth Science Review*, V. 12, p. 1-35.
- Streckeisen, A., 1979, Classification and nomenclature of volcanic rocks, lamprophyres, carbonatites, and melilitic rocks: recommendations and suggestions of the IUGS Subcommittee on the systematics of igneous rocks, *Geology*, V. 7, p.331-335.
- Sugden, T. J., and K. C. Cross, 1991, Significance of overprinting fault systems in the Olympic Dam Breccia Complex, *Structural Geology in Mining and Exploration, Extended Abstracts*, Geology Department and University Extension, University of Western Australia, Publication No. 25.
- Sugden, T., 1989, Characteristics of fault at Olympic Dam and their possible relationship to regional lineaments, *Australian Tectonics, Specialist Group in Tectonics and Structural Geology, Kangaroo Island Conference, Geol. Soc. Aust. Abstract*, V. 24, p. 143-145.

- Swanson, S. E., 1979, The effect of CO<sub>2</sub> on phase equilibria and crystal growth in the system KAlSi<sub>3</sub>O<sub>8</sub>-NaAlSi<sub>3</sub>O<sub>8</sub>-CaAl<sub>2</sub>Si<sub>2</sub>O<sub>8</sub>-SiO<sub>2</sub>-H<sub>2</sub>O-CO<sub>2</sub> to 8000 bars, *American Journal of Science*, V. 279, p. 703-720.
- Takada, A., 1989, Magma transport and reservoir formation by a system of propagating cracks, *Bulletin of Volcanology*, V. 52, p. 118-126.
- Taylor, B. E., 1991, Degassing of Obsidian Dome rhyolite, Inyo volcanic chain, California. In *Stable isotope geochemistry: a tribute to Samuel Epstein*, Taylor, H. P. Jnr. (Ed.), Special publication - Geochemical Society V. 3 p. 339-353.
- Taylor, H. P., Jr., 1979, Oxygen and Hydrogen Isotope Relationships in Hydrothermal Mineral Deposits. In *Geochemistry of Hydrothermal Ore Deposits*, 2nd edition, Ed. Barnes, H. L., p. 236-272.
- Taylor, R. G., 1980, Geology of tin deposits, *Developments in Economic Geology*, V. 11, p. 543.
- Taylor, R. G., 1992, Ore textures; recognition and interpretation; I: Infill textures, James Cook University of North Queensland, p. 24.
- Taylor, S. T., 1965, The application of trace element data to problems in petrology. In: *Physics and chemistry of the earth*, Ahrens, L. H., Press, F., Runcorn, S. K., and Vrey, H. C. (Eds.), Pergamon Press, London, p. 133-213.
- Thompson, R. A., Dungan, M. A., Lipman, P. W., 1986, Multiple differentiation processes in early-rift calc-alkaline volcanics Northern Rio Grande Rift, New Mexico, *Journal of Geophysical Research*, V. 91, p. 6048-6058.
- Tikoff, B., and Teyssier, C., 1992, Crustal-scale, en echelon "P-shear" tensional bridges: A possible solution to the batholithic roomproblem, *Geology*, V. 20, p. 927-930.
- Titley, S. R. (Ed.), 1982, *Advances in Geology of the Porphyry Copper Deposits*, The University of Arizona Press / Tucson, Arizona, p. 560.
- Titley, S. R., 1990, Contrasting metallogenesis and regional settings of CircumPacific Cu-Au porphyry systems. In: *Pacific Rim '90 Congress proceedings*, p. 127-133.
- Trail, A. F., and Spera, F. J., 1990, Mechanisms for the generation of compositional heterogeneities in magma chambers, *Geological Society America Bulletin*, V.102, p. 353-367.
- Turner, J. S., Huppert, H. E., and Sparks, R. S. J., 1983, An experimental investigation of volatile exsolution in evolving magma chambers, *Journal of Volcanology and Geothermal Research*, V. 16, p. 263-277.
- Turner, W. S., 1982, A study of the wall rock alteration and devitrification zoning surrounding the Ben Lomond U-Mo deposit, North Queensland, unpublished Masters Thesis, James Cook University of North Queensland, Australia.
- Uemoto, T., Watanabe, M., Hoshino, K., Kagami, H., Hodkinson, I. P., and Orr, T. O. H., 1992, Geochemistry of gold mineralisation and related magmatic events at the Mt. Leyshon mine, Queensland, Australia, *Mining Geology*, V. 42, p. 361-378.
- Velde, B., Dubois, J., Moore, D., and Touchard, G., 1991, Fractal patterns of fractures in granites, *Earth and Planetary Science Letters*, V. 104, p. 25-35.
- Vernon, R. W., 1983, Restite, xenoliths and microgranitoid enclaves in granites, *Journal Proceedings Royal Society N.S.W.*, V. 116, p. 77-103.

- Vogel, T. A., Ryerson, F. J., Noble, D. C., and Younker, L. W., 1987, Limits to magma mixing based on chemistry and mineralogy of pumice fragments erupted from a chemically zoned magma body, *Journal of Geology*, V. 95, p. 659-670.
- Walker, R. G. (Ed.), 1984, *Facies Models*, second edition, Geoscience Canada, p. 317.
- Warnaars, F. J., Holmgren, C., and Barassi, S., 1985, Porphyry copper and tourmaline breccias at Los Bronces-Rio Blanco, Chile, *Economic Geology*, V. 80, p. 1544-1565.
- Waters, A. C., and Krauskopf, K., 1941, The protoclastic border of the Colville Batholith, *Bulletin Geological Society America*, V. 52, p. 1355-1418.
- Webb, A. W., 1969, Metallogenic epochs in eastern Queensland, *Proceedings AusI.M.M.*, V. 230, p. 29-37.
- Webster, J. D. and Holloway, J. R., 1990, Partitioning of F and Cl between magmatic hydrothermal fluids and highly evolved granitic magmas. In: *Ore-bearing granite systems; petrogenesis and mineralising processes*, Eds. Stein, W. J. and Hannah, J. L., Geological Society of America Special Paper 246, p. 1-10.
- Werner, W., 1990, Examples of structural control of hydrothermal mineralization: Fault zones in epicontinental sedimentary basins - A review, *Geologische Rundschau*, V. 79, p. 279-290.
- Wesnousky, S. G., 1988, Seismological and structural evolution of strike slip faults, *Nature*, V. 335, p.340-343.
- White, D. E., 1981, Active geothermal systems and hydrothermal ore deposits, *Economic Geology*, 75th Anniversary Volume, p. 392-423.
- White, D. L., 1991, Maar-diatreme phreatomagmatism at Hopi Buttes, Navajo Nation (Arizona), USA, *Bulletin of Volcanology*, V. 53, p. 239-258.
- Whitney, J. A., 1989, Origin and evolution of silicic magmas. In: *Ore Deposition Associated with Magmas*, Eds. Whitney, J. A. and Naldrett, A. J., *Reviews in Economic Geology*, V. 4, p. 183-201.
- Whitney, J. A., Dorias, M. J., Stormer, J. C., Jr., Kline, S. W., and Matty, D. J., 1988, Magmatic conditions and development of chemical zonation in the Carpenter Ridge Tuff, central San Juan volcanic field, Colorado, *American Journal of Science*, Wones Memorial Volume, V. 288-A, p. 16-44.
- Williams, P. J., 1991, Geology, alteration and mesothermal Au-Ag-mineralisation associated with a volcanic-intrusive complex at Mt. Shamrock-Mt. Ophir, SE Queensland, *Mineralium Deposita*, V. 26, p.11-17.
- Winchester, J. A., and Floyd, P. A., 1977, Geochemical discrimination of different magma series and their differentiation products using immobile elements, *Chemical Geology*, V. 80, p. 325-343.
- Wolfe, J. A., 1980, Fluidisation versus phreatomagmatic explosions in breccia pipes, *Economic Geology*, V. 75, p. 1105-1111.
- Wormald, P. J., Orr, T. O. H., and Hodkinson, I. P., 1991, The Mount Leyshon Gold Mine (NE Queensland), an intrusive breccia and igneous complex, *Proceedings World Gold '91 conference*, AusI.M.M., p. 223-232.
- Wright, A. E., Bowes, D. R., 1963, Classification of volcanic breccias: a discussion, *Geological Society American Bulletin*, V. 74, p. 79-86.
- Wright, A., 1983, The Ortiz gold deposit (Cunningham Hill)-Geology and exploration: Nevada, *Bureau Mines Geology Report* 36, p.42-51.

- 
- Wright, J. V., 1990, Basins and styles of basin, epithermal and other high crustal level mineralisation. In: Contributions of the Economic Geology Research Unit, Contribution 35, Geology Department, James Cook University, p. 158.
- Yerkes, R. F., Levine, P., and Wentworth, C. M., 1990, Abnormally high fluid pressures in the region of the Coalinga earthquake sequence and their significance, US. Geological Survey Professional Paper , no. 1487, p.235-357.
- Zorpi, M. J., Coulon, C., and Orsini, J. B., 1991, Hybridisation between felsic and mafic magmas in calc-alkaline granitoids - a case study in Northern Sardinia, Italy, *Chemical Geology*, V. 92, p. 45-86.

APPENDIX 1: Selected microprobe analyses of igneous phenocryst and hydrothermal alteration minerals.

	Clay	musc.	musc.	musc.	mica	musc.	musc.	musc.	musc.	musc.	musc.	musc.	illite
	S14BAM	DG200CM	DG200CM	DG200FM	236/22mica	2373M1	2373M2	2373M3	2373M4	23616bM1	23616bM2	23616bM3	236 16b11
SiO <sub>2</sub>	58.36	50.93	48.00	50.93	61.31	46.39	47.62	48.57	48.41	44.66	45.42	44.6	40.07
TiO <sub>2</sub>	0.00	0.22	0.22	0.19	0.08	0.48	0.31	1.21	0.34	0.47	0.29	0.39	0.06
Al <sub>2</sub> O <sub>3</sub>	22.73	33.31	32.46	33.49	22.14	33.40	34.01	32.85	33.20	33.23	33.79	33.47	28.27
FeO	1.70	3.16	2.99	3.02	0.54	0.80	0.63	0.62	0.58	2.73	2.01	2.86	7.3
MnO	0.00	0.00	0.00	0.14	0.00	0.07	0.00	0.00	0.00	0.12	0.15	0	0.74
MgO	3.42	1.33	1.02	1.37	0.82	2.23	1.90	1.66	1.68	1.68	1.26	1.15	7.17
CaO	0.89	0.00	0.00	0.00	0.25	0.00	0.06	0.08	0.06	0.1	0.09	0.08	0.15
Na <sub>2</sub> O	0.16	0.09	0.14	0.11	0.51	0.43	0.48	0.31	0.32	0.33	0.41	0.25	0
K <sub>2</sub> O	0.59	8.98	9.77	9.48	10.40	10.52	10.03	9.02	9.56	10.5	10.2	10.86	5.15
Total	87.85	98.02	94.59	98.72	96.04	94.32	95.05	94.32	94.13	93.83	93.62	93.66	88.93
Number of ions on the basis of 22 (O)													
Si(iv)	7.785	6.532	6.434	6.506	7.890	6.233	6.306	6.430	6.435	6.110	6.179	6.120	5.835
Al(iv)	0.215	1.468	1.566	1.494	0.110	1.767	1.694	1.570	1.565	1.890	1.821	1.880	2.165
Ti	0.000	0.021	0.022	0.018	0.008	0.049	0.031	0.120	0.034	0.048	0.030	0.040	0.007
Al(vi)	3.360	3.568	3.564	3.550	3.248	3.523	3.615	3.557	3.638	3.470	3.598	3.534	2.688
Fe	0.190	0.339	0.335	0.323	0.058	0.090	0.070	0.069	0.064	0.312	0.229	0.328	0.889
Mn	0.000	0.000	0.000	0.015	0.000	0.008	0.000	0.000	0.000	0.014	0.017	0.000	0.091
Ca	0.127	0.000	0.000	0.000	0.034	0.000	0.009	0.011	0.009	0.015	0.013	0.012	0.023
Mg	0.680	0.254	0.204	0.261	0.157	0.447	0.375	0.328	0.333	0.343	0.255	0.235	1.556
Na	0.041	0.022	0.036	0.027	0.127	0.112	0.123	0.080	0.082	0.088	0.108	0.067	0.000
K	0.100	1.469	1.671	1.545	1.707	1.803	1.695	1.523	1.621	1.833	1.770	1.901	0.957







APPENDIX 2: Mt. Leyshon igneous units

Sample No.	unit	SiO2	TiO2	Al2O3	Fe2O3	MnO	MgO	CaO	Na2O	K2O	P2O5	SUM	LOI	TOTAL	As	Pb	Rb	Sr	Y	Zr	Nb
DST230	I	60.80	0.60	16.29	5.47	0.12	2.02	3.11	5.40	1.51	0.29	95.61	3.65	99.26	4	18	89	393	23	110	12
DX230	I	62.49	0.58	16.31	5.57	0.16	2.02	2.90	4.92	1.62	0.28	96.84	2.58	99.42	5	21	71	424	21	112	11
D230	I	62.01	0.60	16.16	5.86	0.09	2.09	2.86	4.98	1.26	0.27	96.17	3.17	99.34	5	20	60	396	21	113	11
EP166*	EP	64.12	0.48	14.90	3.45	0.27	2.05	1.23	1.70	7.85	0.14	96.19	1.51	97.70	3	22	298	193	9	131	11
ED227	ED	72.54	0.17	13.57	0.92	0.09	0.71	1.30	1.53	6.47	0.06	97.36	2.97	100.33	3	108	185	134	10	89	15
ED75	ED	70.78	0.19	13.37	2.27	0.12	0.69	0.95	0.92	6.09	0.07	95.44	2.30	97.74	2	26	157	57	12	101	14
OT230	III	69.84	0.21	13.87	2.06	0.11	0.62	1.57	3.77	3.20	0.08	95.33	3.02	98.35	2	10	118	182	13	121	13
OST230	III	69.92	0.22	13.68	2.03	0.09	0.66	1.26	3.48	3.30	0.09	94.72	2.97	97.69	2	11	117	106	13	127	14
WI7*	III	73.58	0.16	13.83	1.49	0.04	0.43	0.42	1.86	6.08	0.06	97.96	1.95	99.91	4	11	109	227	15	122	13
TP201	IV	75.58	0.11	12.71	1.00	0.12	0.36	1.18	0.26	6.26	0.03	97.62	2.48	100.10	10	40	269	39	12	50	16
PP230	IV	74.26	0.12	13.51	1.49	0.05	0.47	0.42	0.79	6.24	0.04	97.40	2.78	100.18	2	21	256	78	13	60	16
FP230	IV	73.84	0.16	13.78	1.52	0.05	0.40	0.21	2.21	5.27	0.06	97.51	2.16	99.67	3	25	186	124	12	93	17
F230	IV	70.75	0.22	14.52	2.23	0.03	0.44	0.69	4.72	3.79	0.10	97.49	1.95	99.44	10	16	209	135	13	90	17
P231	IV	74.59	0.13	13.29	1.03	0.09	0.26	1.40	6.01	0.97	0.04	97.81	1.77	99.58	2	11	26	128	8	60	11
WI1	IV	73.28	0.12	13.49	1.21	0.05	0.34	0.56	4.27	4.41	0.05	97.77	1.76	99.53	2	23	85	184	12	59	16
SILL*	SILL	61.77	0.52	15.13	3.93	0.59	2.31	4.68	0.38	4.04	0.15	93.50	6.16	99.66	9	21	156	76	9	141	9
22/211	22	67.91	0.28	14.24	2.76	0.13	1.06	1.46	3.41	4.87	0.09	96.21	3.48	99.69	7	56	130	169	10	113	12
22/254	22	67.79	0.29	14.30	2.29	0.10	1.13	1.93	2.81	4.84	0.10	95.59	3.16	98.75	2	21	143	196	11	112	12
WI4X	XEN	65.84	0.56	15.82	3.88	0.23	1.75	3.08	4.57	3.15	0.21	99.09	1.18	100.27	5	200	99	372	13	140	9
CPT230	12	67.12	0.36	14.15	2.90	0.10	1.33	1.93	4.42	2.99	0.11	95.40	2.46	97.85	5	20	88	261	13	93	12
WI2*	12	70.61	0.31	14.33	2.26	0.13	1.09	1.94	3.78	3.31	0.11	97.89	2.12	100.01	4	29	100	354	17	95	12
WI3*	12	68.83	0.32	14.20	2.34	0.11	1.12	2.09	4.22	3.06	0.11	96.39	3.20	99.59	4	30	97	322	31	90	13
WI4	12	68.58	0.33	14.41	2.49	0.18	1.31	2.29	4.06	3.16	0.12	96.93	3.12	100.05	3	37	98	275	12	96	12
12/200	12	68.60	0.32	13.80	2.39	0.38	1.03	2.65	1.53	4.53	0.11	95.34	4.19	99.53	3	39	180	128	12	91	13
DG166	DG	63.68	0.53	15.34	7.44	0.59	2.63	0.61	0.17	4.72	0.17	95.88	3.84	99.72	6	172	210	25	13	147	10
FDG173	DG	61.63	0.52	15.32	10.49	0.56	2.45	0.30	0.20	3.39	0.16	95.01	4.22	99.24	25	102	130	8	10	147	10
LD211	DG	61.23	0.47	14.63	9.45	0.21	2.44	0.36	0.30	4.97	0.14	94.19	5.11	99.30	10	119	168	33	13	131	9
LDG200	DG	57.37	0.52	15.46	11.89	0.81	2.02	0.40	0.21	3.44	0.16	92.29	6.74	99.03	13	41	123	12	11	142	10
LD200	DG	61.18	0.42	14.05	10.24	0.52	1.44	0.38	0.17	3.23	0.13	91.76	7.60	99.36	39	18	112	9	9	132	10
FLD219	DG	60.07	0.41	13.64	9.91	0.33	1.32	0.32	0.26	3.38	0.12	89.76	9.21	98.98	22	115	124	14	8	133	10
STD101	SLD	68.36	0.28	14.34	1.91	0.23	0.91	2.42	2.48	4.64	0.10	95.67	4.39	100.06	2	19	176	167	14	158	13
STD161	SLD	69.54	0.28	14.43	3.39	0.22	0.78	0.36	3.01	4.47	0.10	96.59	2.81	99.39	3	13	200	185	13	159	13
TA383	Basalt	44.95	1.80	15.33	10.02	0.17	7.19	7.74	3.03	2.59	0.83	93.65	4.41	98.06	1	13	34	1285	17	138	12
TA390	Basalt	44.18	1.74	15.13	9.78	0.27	5.07	10.44	2.26	3.04	0.81	92.72	8.83	101.54	2	13	50	860	15	140	12
XFTA	Basalt	43.96	1.73	14.90	8.98	0.21	5.40	8.59	2.10	2.75	0.78	89.41	8.87	98.29	2	14	36	688	16	157	13
FTS236	FineTS	68.65	0.28	14.48	2.62	0.09	0.85	1.25	1.86	6.59	0.08	96.74	2.52	99.26	3	111	200	125	12	121	13

APPENDIX 3: CIPW norm data for the Mt. Leyshon igneous units.

Sample No.	Q	C	or	ab	an	ne	di	hy	ol	mt	il	ap	TOTAL
DST230	11.84	0.74	8.92	45.70	13.72	0.00	0.00	11.24	0.00	1.21	1.14	0.69	95.20
DX230	16.22	1.79	9.57	41.63	12.74	0.00	0.00	11.47	0.00	1.23	1.10	0.66	96.43
D230	16.63	1.99	7.45	42.14	12.60	0.00	0.00	11.85	0.00	1.30	1.14	0.64	95.73
EP166	16.98	1.67	46.39	14.39	5.28	0.00	0.00	9.21	0.00	0.76	0.91	0.33	95.93
ED227	34.70	1.82	38.24	12.95	6.10	0.00	0.00	2.83	0.00	0.20	0.32	0.14	97.29
ED75	37.96	3.69	35.99	7.79	4.30	0.00	0.00	4.52	0.00	0.50	0.36	0.17	95.27
OT230	30.45	1.52	18.91	31.90	7.32	0.00	0.00	4.03	0.00	0.46	0.40	0.19	95.17
OST230	32.50	2.29	19.50	29.45	5.72	0.00	0.00	4.04	0.00	0.45	0.42	0.21	94.58
WI7	37.32	3.56	35.93	15.74	1.73	0.00	0.00	2.78	0.00	0.33	0.30	0.14	97.84
WTP201	46.52	3.43	37.00	2.20	5.68	0.00	0.00	2.21	0.00	0.22	0.21	0.07	97.53
PP230	43.47	4.78	36.88	6.69	1.85	0.00	0.00	2.96	0.00	0.33	0.23	0.09	97.27
FP230	39.12	4.19	31.14	18.70	0.69	0.00	0.00	2.76	0.00	0.34	0.30	0.14	97.38
P231	32.12	0.00	5.73	50.86	6.42	0.00	0.24	1.79	0.00	0.23	0.25	0.09	97.73
F230	25.75	1.61	22.40	39.94	2.84	0.00	0.00	3.63	0.00	0.49	0.42	0.24	97.32
WI1	29.33	0.78	26.06	36.13	2.48	0.00	0.00	2.28	0.00	0.27	0.23	0.12	97.69
SILL	28.61	1.95	23.88	3.22	22.34	0.00	0.00	11.00	0.00	0.87	0.99	0.36	93.20
22/211	23.45	0.90	28.78	28.86	6.71	0.00	0.00	5.94	0.00	0.61	0.53	0.21	95.99
22/254	26.16	1.15	28.60	23.78	8.99	0.00	0.00	5.44	0.00	0.51	0.55	0.24	95.41
WI4X	16.65	0.00	18.62	38.67	13.35	0.00	0.58	8.52	0.00	0.86	1.06	0.50	98.80
CPT230	22.63	0.37	17.67	37.40	8.93	0.00	0.00	6.60	0.00	0.64	0.68	0.26	95.19
WI2	29.26	1.24	19.56	31.99	8.98	0.00	0.00	5.33	0.00	0.50	0.59	0.26	97.70
WI3	25.49	0.38	18.08	35.71	9.72	0.00	0.00	5.45	0.00	0.52	0.61	0.26	96.22
WI4	24.96	0.41	18.67	34.36	10.66	0.00	0.00	6.23	0.00	0.55	0.63	0.28	96.74
22/200	33.96	1.80	26.77	12.95	12.50	0.00	0.00	5.79	0.00	0.53	0.61	0.26	95.16
DG166	35.41	9.21	27.89	1.44	2.03	0.00	0.00	16.25	0.00	1.65	1.01	0.40	95.29
FDG173	37.43	11.12	20.03	1.69	0.55	0.00	0.00	19.65	0.00	2.32	0.99	0.38	94.17
LD211	31.10	8.40	29.37	2.54	0.96	0.00	0.00	17.74	0.00	2.09	0.89	0.33	93.43
LD200	39.13	9.86	19.09	1.44	1.12	0.00	0.00	16.91	0.00	2.26	0.80	0.31	90.92
LDG200	32.32	11.01	20.33	1.78	1.04	0.00	0.00	20.83	0.00	2.63	0.99	0.38	91.31
LD219	37.55	9.23	19.98	2.20	0.88	0.00	0.00	15.85	0.00	2.19	0.78	0.28	88.95
STD101	28.79	1.05	27.42	20.99	11.42	0.00	0.00	4.67	0.00	0.42	0.53	0.24	95.53
STD161	31.30	4.20	26.42	25.47	1.20	0.00	0.00	6.21	0.00	0.75	0.53	0.24	96.31
TA383	0.00	0.00	15.31	18.37	20.58	3.94	10.51	0.00	16.65	2.22	3.42	1.97	92.95
TA390	0.00	0.00	17.97	9.72	22.16	5.09	20.42	0.00	9.29	2.16	3.30	1.92	92.04
XFTA	0.00	0.00	16.25	17.77	23.11	0.00	12.18	1.23	11.12	1.99	3.29	1.85	88.78

APPENDIX 4: Atomic % data for the Mt. Leyshon igneous units

Sample	Atom% Si	Atom% Al	Atom% Na	Atom% K
DST230A	24.34	12.53	3.54	1.68
DX230A	24.71	12.39	3.18	1.78
D230AA	24.63	12.34	3.24	1.39
EP166	25.75	11.50	1.12	8.78
ED227A	30.32	10.90	1.04	7.52
ED75	29.58	10.74	0.63	7.08
OT230A	29.63	11.31	2.62	3.78
OST230	29.86	11.23	2.43	3.92
WI7	30.30	10.95	1.26	6.97
WTP201A	31.67	10.24	0.18	7.30
PP230A	30.79	10.77	0.54	7.21
FP230A	30.64	10.99	1.50	6.08
P231A	31.87	10.91	4.21	1.16
FF230	29.12	11.49	3.18	4.34
WI1	30.66	10.85	2.92	5.13
SILLA	25.73	12.11	0.26	4.68
22/211A	28.01	11.29	2.30	5.59
22/254A	28.33	11.48	1.92	5.63
WI4X	26.05	12.03	2.96	3.47
CPT230	28.12	11.39	3.03	3.49
WI2	29.12	11.36	2.55	3.80
WI3	28.79	11.42	2.89	3.56
WI4	28.45	11.49	2.76	3.65
22/200A	28.81	11.14	1.05	5.29
DG166A	24.57	11.37	0.10	5.07
DG173A	23.12	11.04	0.12	3.54
LD211A	23.39	10.74	0.19	5.28
ALD200A	23.79	10.50	0.11	3.50
LDG200A	21.54	11.15	0.13	3.59
LD219	23.90	10.43	0.17	3.74
STD101A	28.71	11.58	1.71	5.42
STD161A	28.31	11.29	2.00	5.07
Orthoclase	24.48	14.18	0.27	16.46
Muscovite	18.03	22.66	0.05	8.85
Albite	27.04	16.94	6.16	0.00
Clay	25.70	19.24	0.12	0.72
Andesite	22.00	11.96	2.22	2.25
Granodiorite	24.69	11.60	2.29	3.26
Granite	31.66	10.31	1.97	5.88

APPENDIX 5: Regional Permo-Carboniferous igneous geochemical data.

Sample No.	Igneous Unit	SiO2	TiO2	Al2O3	Fe2O3	FeO	MnO	MgO	CaO	Na2O	K2O	P2O5	LOI	TOTAL	Rb	Sr	Pb	Zr	Nb	Y
86302066 T	Qmonzodiorite	57.96	1.16	16.52	2.61	4.50	0.12	3.44	6.35	3.64	2.14	0.32	0.61	99.32	59.00	530.00	10.00	227.00	9.00	23.00
86302067 T	andesite	56.09	1.21	16.81	4.07	4.00	0.26	3.55	6.76	3.23	2.48	0.40	1.27	100.13	95.00	541.00	11.00	179.00	9.00	25.00
86302068 T	granodiorite	62.04	0.87	15.95	2.65	2.84	0.11	2.40	4.74	4.23	2.59	0.26	1.12	99.75	60.00	445.00	10.00	247.00	10.00	23.00
86302070 T	andesite	58.47	1.06	16.54	3.51	3.78	0.17	3.07	6.06	3.60	2.15	0.36	0.85	99.58	66.00	502.00	5.00	192.00	9.00	25.00
86302073 T	granodiorite	62.44	0.86	15.97	2.11	3.12	0.10	2.32	4.60	4.23	2.64	0.26	0.68	99.23	61.00	438.00	15.00	236.00	9.00	23.00
86302075 T	granodiorite	58.06	1.14	16.49	2.83	4.11	0.12	3.24	6.17	3.55	2.28	0.30	1.19	99.43	60.00	517.00	9.00	226.00	9.00	23.00
86302083 T	tonalite	58.81	0.99	16.43	2.94	3.77	0.11	3.20	6.00	3.79	1.88	0.31	1.36	99.59	52.00	525.00	11.00	197.00	8.00	22.00
88302107 T	quartzdiorite	53.28	1.47	16.92	3.80	5.04	0.15	4.48	7.81	3.58	1.47	0.39	1.43	99.82	52.00	623.00	11.00	155.00	10.00	26.00
88302108 T	granodiorite	63.26	0.81	15.53	2.89	2.41	0.10	2.27	4.51	3.58	3.09	0.19	0.86	99.50	99.00	406.00	15.00	243.00	10.00	25.00
RBR196 T	diorite	55.00	1.22	16.90	3.80	4.70	0.13	4.10	7.60	3.40	1.54	0.32	0.54	99.32	38.00	620.00	5.00	135.00	6.00	17.00
RBR199 T	granodiorite	63.40	0.80	15.50	2.10	3.10	0.09	2.20	4.40	3.60	3.01	0.21	0.66	99.09	90.00	435.00	11.00	230.00	10.00	23.00
88302112 B	granodiorite	62.91	0.77	15.46	2.33	2.70	0.09	2.27	4.55	3.47	3.24	0.18	1.30	99.27	119.00	427.00	10.00	247.00	9.00	25.00
RBR281 B	ademelite	62.20	0.78	16.10	2.30	3.10	0.11	2.40	4.90	3.50	3.03	0.20	0.75	99.36	115.00	470.00	10.00	250.00	7.00	22.00
RBR299B B	diorite	55.10	1.24	18.30	2.50	5.00	0.12	3.20	7.70	3.60	1.65	0.44	0.54	99.38	50.00	690.00	10.00	160.00	6.00	21.00
RBR321 B	granite	76.10	0.07	12.90	0.60	0.20	0.03	0.14	1.10	2.90	5.08	0.02	0.76	99.92	145.00	90.00	19.00	70.00	8.00	18.00
RBR322 B	granodiorite	57.60	1.02	16.50	2.40	4.90	0.12	3.90	6.80	3.20	2.22	0.27	0.41	99.35	80.00	550.00	8.00	150.00	7.00	23.00
RBR496 F	diorite	54.40	1.57	17.50	2.60	5.10	0.10	4.20	7.50	4.00	1.37	0.49	0.41	99.23	37.00	1020.00	7.00	105.00	7.00	14.00
RBR490 F	granodiorite	60.30	0.97	16.10	2.10	4.00	0.12	2.80	5.40	3.80	2.57	0.27	0.99	99.44	95.00	435.00	11.00	195.00	10.00	31.00
RBR492 F	tonalite	58.20	1.09	16.60	2.10	4.80	0.11	3.30	6.30	3.60	2.22	0.28	0.84	99.45	75.00	530.00	11.00	135.00	8.00	23.00

DATA SOURCE: Numbers starting with RBR.. are from D. Wybourne, BMR. Those starting with 8.. are from I. Rienks, DRI.

DATA SOURCE: Numbers starting with RBR.. are from D. Wybourne, BMR. Those starting with 8.. are from I. Rienks, DRI.

## **APPENDIX 6:** Methodology and sample collection for geochemical analysis.

Rock samples greater than 0.5 kilograms were crushed for each rock type to minimise the effects of phenocryst distribution on analyses. Where possible samples were taken from drill-core that are least effected by hydrothermal alteration, although as described in Chapter 4, all samples show variable alteration effects. A split sample taken from this bulk sample was used for each analysis, and duplicate samples were run. All samples were crushed in a tungsten carbide tima mill and analyses were run in the James Cook University instrument centre by Alan Chappel. Trace and major elements were by XRF analyses of pressed powders and fused discs. Analyses for each sample are presented in appendix 2 as unnormalised values with their loss on ignition.

The James cook university instrumentation centre quotes the following values of precision (at 3 sigma) for XRF analyses (ppm):

As-0.9, Pb-2.4, Rb-2.1, Sr-28.5, Y-0.9, Zr-7.5, Nb-2.4.

APPENDIX 7: Essential paragenetic and geochemical samples for this study, housed in the geology department rock collection.

JCU no.	Sample no	Rock type	Location	S	T	P
37287	156/29	MPB	MLD 156, 195.25	*	*	
37288	157/16	PU IV	MLD 157, 88.9 m	*	*	
37289	183/7	FTS	MLD 183, 160 m	*	*	
37290	230/12	MLB	MLD 230, 130 m	*	*	
37291	236/1	MPB	MLD 236, 195 m	*	*	
37292	T1/5A	MLB	Open pit	*	*	
37293	237/1	MPB	MLD 237, 217.70 m	*	*	
37294	237/3	MPB	MLD 237, 27.80 m	*	*	
37295	B/AD	Basalt dyke	Open pit	*	*	
37296	D/168/392	MLB	MLD 168, 392 m	*	*	
37300	T/156/34	MPB	MLD 156, 210.36m		*	
37301	T/161/3	LBD	MLD 161, 46.66 m		*	
37302	T/236/16	FTS	MLD 236, 403.80 m		*	
37303	T/277/GV	DG dyke	MLD277, 266.3 m	*		
37304	T1/2	MLB	Open pit		*	
37305	T1/2A	MLB	Open pit	*	*	
37306	T1/2B	MLB	Open pit	*	*	
37307	T1/4B	MLB	Open pit		*	
37308	DST230	PU I	MLD 230, 25m			*
37309	DX230	PU I	MLD 230, 23.7m			*
37310	D230	PU I	MLD 230, 83.05m			*
37311	EP166	EP dyke	MLD 166, 218.1m			*
37312	ED227	Early dyke	MLD 227,136.5m			*
37313	ED75	Early dyke	MLD 75, 141.8 m			*
37314	OT230	PU III	MLD 230, 169.65m			*
37315	OST230	PU III	MLD 230, 83.05m			*
37316	I7	PU III	5170 N 4035 E		*	*
37317	TP201	PU IV	MLD 201, 256m			*
37318	PP230	PU IV	MLD 230, 263m			*
37319	FP230	PU IV	MLD 230, 208.5m			*
37320	P231	PU IV	MLD 231, 101.5m	*	*	*
37321	F230	PU IV	MLD 230, 220.5m			*
37322	I1	PU IV	5390 N 4060 E			*
37323	SILL	Sill	430 RL, main pit			*
37324	22/211	22 dyke	MLD 211, 343m			*
37325	22/254	22 dyke	MLD 254, 310.6m	*	*	*
37326	I4X	Enclave (12)	5215 N 4000 E	*	*	*
37327	CPT230	12 dyke	MLD 230, 64.5m			*
37328	I2	12 dyke	5490 N 4035 E			*
37329	I3	12 dyke	5250 N 4020 E			*
37330	I4	12 dyke	5215 N 4000 E			*
37331	22/200	12 dyke	MLD 200, 190m			*
37332	DG166	DG dyke	MLD 166, 62.1m	*	*	*
37333	DG173	DG dyke	MLD 173, 109.7m			*
37334	LD211	DG dyke	MLD 211, 518.2m			*
37335	LD200	DG dyke	MLD 200, 194m			*
37336	LDG200	DG dyke	MLD 200, 194.9m			*
37337	LD219	DG dyke	MLD 219, 267.1m			*
37338	STD101	FLD	MLD 101, 173.5m			*
37339	STD161	FLD	MLD 161, 56.9m	*	*	*
37340	TA383	Basalt dyke	open pit			*
37341	TA390	Basalt dyke	open pit			*
37342	XFTA	Basalt dyke	open pit			*

S=Rock sample, T=thin section, P=powder.

Abbreviations: MPB-main pipe breccia, FTS-fine tuffisite breccia dyke, MLB-Mt. Leyshon breccia, LBD-late breccia dyke, FLD-fine late dyke, PU I-PU IV - porphyry unit I-IV.